

Multi-Contact Protocol-Constrained Collision Avoidance for Autonomous Marine Vehicles

by
Kyle Woerner

B.S., Washington University in St. Louis (2004)

M.E.M., Old Dominion University (2008)

S.M., Massachusetts Institute of Technology (2014)

Naval Engineer, Massachusetts Institute of Technology (2014)

Submitted to the Department of Mechanical Engineering
in partial fulfillment of the requirements for the degree of

Doctor of Philosophy


at the


MASSACHUSETTS INSTITUTE OF TECHNOLOGY


June 2016


© Kyle Woerner, MMXVI. All rights reserved.

The author hereby grants to MIT permission to reproduce and to distribute publicly paper and electronic copies of this thesis document in whole or in part in any medium now known or hereafter created.

Author 
Department of Mechanical Engineering
May 09, 2016

Certified by 
John J. Leonard
Samuel C. Collins Professor of Mechanical and Ocean Engineering
Thesis Supervisor

Certified by 
Michael R. Benjamin
Research Scientist, Department of Mechanical Engineering
Thesis Supervisor

Accepted by ... 
Professor Rohan Abeyaratne
Chairman, Department Committee on Graduate Students

Multi-Contact Protocol-Constrained Collision Avoidance for Autonomous Marine Vehicles

by

Kyle Woerner

Submitted to the Department of Mechanical Engineering on May 09, 2016, in partial fulfillment of the requirements for the degree of Doctor of Philosophy

Abstract

The field of autonomous collision avoidance has continued to advance in many areas including sensory and perception, navigation, payload integration, and collision avoidance. The advances in collision avoidance, however, have largely focused on iterative changes to the velocity obstacle – an algorithm that inherently loses important collision avoidance information key to replicating a human-like decision space. This thesis examines algorithms that generalize the traditional velocity obstacle into a multi-threshold based approach that more realistically represent and evaluate human ship driving practices. Novel protocol-constrained collision avoidance evaluation algorithms are proposed including the ability to perform both on-line and post-mission analysis of both robots and humans. These algorithms become especially important when considering complex missions of competing objectives in a contact-dense, protocol-constrained collision avoidance environment. Introduction of competing performance metrics consistent with human ship driving practices allows autonomous collision avoidance algorithm designers to consider previously unexplored tradespaces. On-water results of up to five simultaneously interacting autonomous vessels validate the collision avoidance algorithms using four key areas of evaluation: spatial efficiency, temporal efficiency, protocol compliance, and safety. Testing of 10 complex scenarios totaled over 6,150 vehicle-pair on-water encounters. Human-robot field experimentation demonstrated autonomous collision avoidance performance under conflicting protocol requirements of COLREGS while interacting with human-driven vessels. An autonomous collision avoidance “road test” framework is proposed to incorporate testing of arbitrary collision avoidance algorithms both in the field and in simulation.

Thesis Supervisor: John J. Leonard

Title: Samuel C. Collins Professor of Mechanical and Ocean Engineering

Thesis Supervisor: Michael R. Benjamin

Title: Research Scientist, Department of Mechanical Engineering

Acknowledgments

The work contained in this thesis would not have been possible without my colleagues, friends, and family who supported me each day. To the United States Navy and the Office of Naval Research (Code 33) for continued funding and support, particularly Dr. Robert Brizzolara, thank you. To Battelle, thank you for supporting a tremendous laboratory and for your support of the MIT autonomy community more generally.

My efforts would not have been possible without the support of my colleagues on the staff of the Chief of Naval Operations as well as the Secretary of the Navy's Advisory Panel. Your continued words of encouragement were key to my success.

To the staff of the MIT Sailing Pavilion, thank you for the continued use of your equipment at all hours of the day and night. To the MIT Police and Massachusetts State Police, thank you for your continued patience and understanding as we tested throughout the late nights on the Charles River.

To my colleagues in the Marine Robotics Group and the Laboratory for Autonomous Marine Sensing Systems, you proved invaluable at every turn in the work. Your continued support both professionally and personally has been unforgettable. The conversations we had greatly influenced my approach and thinking in the world of autonomy. I especially thank Alon Yaari and Hugh Dougherty for support with on-water experimentation. To Misha Novitzky, thank you for your countless hours on the water and in the lab as well as your friendship throughout the entire process.

To my committee (John Leonard, Henrik Schmidt, Jonathan How, and Michael Benjamin), I thank you for your guidance, expertise, and patience throughout all of my studies and research. A very special thank you to Mike Benjamin for his continuous enthusiasm and close friendship throughout this work. Without you, this work would not have been possible.

A final thank you for the undying support of my wife, Daniela, and her never ending patience with my long hours of work, mistakenly missed meals, and seemingly never ending stories about those listed above.

THIS PAGE INTENTIONALLY LEFT BLANK

Contents

1	Introduction	25
1.1	Motivation	26
1.2	Contributions of this Research	27
1.2.1	Primary Contributions	27
1.2.2	Attributes Supporting the Primary Contributions	28
1.3	Formal Problem Statements	29
1.3.1	Reduction of Collisions	29
1.3.2	Identification of Non-Compliant Vessels from Track Data	29
1.3.3	Reduction of Performance in Alternative Scenarios	30
1.4	Assumptions and Scope	30
1.5	Thesis Overview	32
2	Literature Review: State of the Art	33
2.1	Motivation	34
2.2	Global Path Planning	36
2.3	Local Reactive Path Planning for Collision Avoidance	42
2.3.1	Target Following	47
2.3.2	Assessing Collision Risk	47
2.3.3	Collision Avoidance Utility Functions	51
2.4	Collision Avoidance Testing and Evaluation	53
2.5	Velocity Obstacle Collision Avoidance Algorithms	55
2.5.1	Traditional Velocity Obstacles	55
2.5.2	Generalized Velocity Obstacles	58

2.5.3	Reciprocal Velocity Obstacles	59
2.5.4	Generalized Reciprocal Velocity Obstacles	60
2.5.5	Hybrid Reciprocal Velocity Obstacles	61
2.6	Velocity Obstacle Techniques in Practice	63
2.7	Closest Point of Approach (CPA) Collision Avoidance Algorithms . .	65
2.7.1	Real-Time, Non-Brute Force Methods: Interval Programming (IvP)	66
2.8	CPA Techniques in Practice	69
2.9	COLREGS Compliance in the Literature	70
2.10	Protocol Evaluation	73
2.11	Summary of Collision Avoidance Testing	74
3	Protocol-Constrained Collision Avoidance Objective Functions	77
3.1	Objective Function Construct	77
3.1.1	Multi-Objective Optimization	78
3.1.2	Marine Autonomy Objective Function Construct	79
3.2	Closest Point of Approach	85
3.3	Full CPA Quantification Algorithm	91
3.3.1	Velocity Obstacle	92
3.3.2	Collision Avoidance Utility Mapping	96
3.3.3	Formal Description of Algorithm	104
3.3.4	Generalization of the Velocity Obstacle	106
3.3.5	Application to Protocol Collision Avoidance Constraints . . .	107
3.4	Techniques to Improve Computational Efficiency	113
3.4.1	Sampling Size	113
3.4.2	Smart Refinement	113
3.5	Sampling Algorithms Applied to Collision Avoidance	115
3.6	Designing for Patience	123
3.6.1	Course-Speed Design Ratio	124
3.6.2	Patience Parameter	126

3.7	Conclusions	127
4	Collision Avoidance Metrics and Evaluation	129
4.1	The Tradespace of Safety, Efficiency, and Protocol Compliance	130
4.2	Efficiency and Mission Performance	131
4.2.1	Spatial Efficiency	132
4.2.2	Temporal Efficiency	133
4.3	Evaluating Protocol Compliance: Quantifying the Rules	134
4.3.1	Categories for COLREGS Scope	135
4.3.2	Approach	137
4.4	Evaluating Safety Using CPA Range and Pose	138
4.5	Rule-Specific Algorithms and Considerations	142
4.5.1	Vessel Encounters in Sight of One Another	144
4.5.2	Responsibilities of Vessels within Sight: Rules 11, 18	165
4.5.3	General Rules (Rules 1-3)	166
4.5.4	General Conduct of Vessels and Special Traffic Schemes (Rules 4-10)	168
4.5.5	Sailing in Sight of Another Sailing Vessel (Rule 12)	170
4.5.6	Restricted Visibility (Rule 19)	171
4.5.7	Lights and Shapes (Rules 20-31)	171
4.5.8	Sound and Light Signals (Rules 32-37)	172
4.6	COLREGS Testing and Evaluation	172
4.6.1	Evaluation Library	173
4.6.2	Real-Time Analysis	176
4.6.3	Post-Mission Analysis	178
4.7	Validation of Protocol Evaluation Algorithms	180
4.7.1	Validation of Protocol Agnostic Vehicle	180
4.7.2	Validation of Collision Agnostic Vehicle	184
4.7.3	Significance Testing for Compliance Detection	184
4.7.4	Human Agreement with Evaluation Results	187

4.8	Conclusions	190
5	Performance Testing and Simulation Methods	191
5.1	Performance Curves of the Objective Tradespace	193
5.2	Default Safety Maneuvers	196
5.3	Egregiousness	197
5.3.1	Blame	199
5.4	Iterative Geometric Testing	200
5.5	Case Study on High-Speed Vessels	204
5.5.1	Experimental Setup	205
5.5.2	Example Encounter Analysis	208
5.5.3	Case Study Analysis	210
5.5.4	Limiting Range and Safety Analysis	212
5.6	Integrating Autonomous Systems with Humans	217
5.7	Conclusions	218
6	On-Water Experimentation and Results	221
6.1	Extended Scenarios and Evaluation Techniques	221
6.1.1	Algorithm Comparison (Scenarios A & B)	223
6.1.2	Traffic-Constrained Monitoring Missions (Scenario C)	226
6.1.3	Testing Human Integration (Scenario D)	227
6.1.4	Non-Compliant and Unresponsive Vehicles (Scenarios E - G)	229
6.1.5	Navigationally-Constrained Environment (Scenarios H - J)	230
6.2	On-Water Experimentation Setup	231
6.2.1	Vehicles	231
6.2.2	Experimentation Field	231
6.3	On-Water Experimentation Results	236
6.3.1	Scenario A & B Results	239
6.3.2	Scenarios C - J Results	245
6.4	Conclusions	250

7	Conclusions and Future Work	253
7.1	Conclusions	253
7.2	Future Work	254
7.2.1	Collision Avoidance Road Test	256
7.2.2	Incorporating the Human Factor	257
7.3	Final Thoughts	259
A	COLREGS Reference	261
A.1	Collision Regulations for Power-Driven Vessels in Sight	262
A.2	Example Collision Avoidance Geometries	266
B	Lexicon and Notation	267
B.1	Lexicon	268
B.2	Notation	270
C	Computational Loading	273
C.1	Computational Loading	274
D	Validation of Evaluation Algorithms	279
D.1	Experience Question	280
D.2	Scenario Questions	280
D.2.1	Scenario 1	280
D.2.2	Scenario 2	281
D.2.3	Scenario 3	282
D.2.4	Scenario 4	284
D.2.5	Scenario 5	284
D.2.6	Scenario 6	285
D.2.7	Scenario 7	286
D.2.8	Scenario 8	287
D.2.9	Scenario 9	288
D.3	Studies Conducted in the Literature	292

THIS PAGE INTENTIONALLY LEFT BLANK

List of Figures

2-1	Larson’s Local Reactive Path Planning	42
2-2	Tam’s Safety Area-Based Geometry	50
2-3	Example Collision Risk	51
	a Kim’s Minimum Range Requirement	51
	b Kuwata’s Minkowski Sum	51
2-4	Velocity Obstacle Utility	57
2-5	Velocity Obstacle Polar Utility	58
2-6	Velocity Obstacle Sketch	62
	a Velocity Obstacles	62
	b Generalized Velocity Obstacles	62
2-7	Kuwata’s Velocity Obstacle with Protocol Exclusion	63
2-8	Choi’s Safety Boundary	69
3-1	Collision Avoidance Geometry	95
	a Initial Geometry	95
	b Candidate Maneuver Geometry	95
3-2	Velocity Obstacle Utility Function	96
3-3	Velocity Obstacle Algorithm	97
3-4	Multi-Threshold CPA-Based Utility Functions	100
	a Step Utility	100
	b Linear Utility	100
	c Quadratic Utility	100
	d Arbitrary Utility	100

3-5	Multi-Threshold Priority Weight Functions	101
a	Step Priority Weight	101
b	Linear Priority Weight	101
c	Quadratic Priority Weight	101
d	Arbitrary Priority Weight Function	101
3-6	Full CPA Quantification Algorithm	106
3-8	Polar Plot of Raw CPA Range	110
3-9	Velocity Obstacle Representations in Polar Form	111
a	Velocity Obstacle	111
b	Velocity Obstacle with COLREGS	111
3-10	Full CPA Quantification Algorithm in Polar Form	112
a	Full CPA	112
b	Full CPA with COLREGS	112
3-11	Sampling Size of IvP Functions	114
a	64 pieces	114
b	512 pieces	114
c	1000 pieces	114
d	4000 pieces	114
e	Underlying Objective Function	114
3-12	Smart Refinement of IvP Functions	116
a	100 pieces	116
b	200 pieces	116
c	500 pieces	116
d	750 pieces	116
e	Underlying Objective Function	116
3-13	Sampling Size of IvP Functions for Collision Avoidance	118
a	64 pieces	118
b	500 pieces	118
c	1000 pieces	118
d	4000 pieces	118

e	Underlying Objective Function	118
3-14	Smart Sampling Size of IvP Functions	119
a	100 pieces	119
b	200 pieces	119
c	500 pieces	119
d	750 pieces	119
e	1000 pieces	119
f	2000 pieces	119
g	Underlying Objective Function	119
3-15	Bisecting of Collision Avoidance Objective Functions	121
a	Bisected Objective Function of Figure 3-11e	121
b	Bisecting Objective Function of Figure 3-13e	121
3-16	Bisecting of Complex Collision Avoidance Objective Functions	122
a	Underlying Function – Top View	122
b	Underlying Function	122
c	Bisected Objective Function at $z = R_{min}$	122
d	Bisected Objective Function at $z > R_{min}$	122
3-17	Patience Parameter	125
a	$\pi_{\theta} = 30\%$	125
b	$\pi_{\theta} = 70\%$	125
4-1	Spatial and Temporal Efficiencies	133
a	High Spatial Efficiency	133
b	High Temporal Efficiency	133
4-2	Influence of Pose at CPA on Safety	146
a	Perpendicular CPA	146
b	Parallel CPA	146
4-3	Relative Bearing, Contact Angle, and Pose	147
a	Initial Pose (Θ_0)	147
b	Arbitrary Pose at CPA (Θ_{cpa})	147

4-4	Importance of Pose at CPA	148
	a Bow-Crossing Pose at CPA	148
	b Stern-Crossing Pose at CPA	148
4-5	Non-Stepwise Safety Scoring	148
4-6	Example Pose Reward Function	149
4-7	COLREGS Entry Criteria	151
	a Overtaking	151
	b Head-on	151
	c Crossing	151
	d Crossing (edge case)	151
4-8	Overtaking Encounter	152
	a Initial Overtaking Geometry	152
	b Overtaking Astern of Contact	152
4-9	Head-on Encounter	156
	a Near-Canonical Encounter	156
	b Result of Delayed Action	156
4-10	Rule 14 Protocol Evaluation Function	158
	a Top-Down Plot	158
	b Polar Plot	158
4-11	Alternative Rule 14 Protocol Evaluation Function	159
	a Top-Down Plot	159
	b Polar Plot	159
4-12	Example COLREGS Evaluation Encounter Scenario	174
4-13	Example COLREGS Evaluation Report by Categories	175
4-14	COLREGS Real-Time Evaluation Program	178
4-15	Safety Range Violation Visual Indicator	179
	a Minimum Desired Range Violation	179
	b Near-Miss Range Violation	179
	c Collision Range Violation	179
	d COLREGS Violation	179

4-16	Validation of Evaluation Algorithm	181
4-17	Validation of Protocol Agnostic Identification	182
4-18	Summary of Protocol Agnostic Identification	183
4-19	Validation of Collision Agnostic Identification	185
4-20	Summary of Collision Agnostic Identification	186
4-21	Human Survey Validation of Evaluation Results	189
5-1	2D Performance Curves	194
	a Mission vs. Safety	194
	b Protocol Compliance vs. Mission	194
	c Protocol Compliance vs. Safety	194
5-2	Egregiousness	198
5-3	Visual Indicators for On-Water Evaluation Results	199
	a COLREGS Violation	199
	b Safety Violation	199
5-4	Iterative Geometric Testing	203
	a Initial Positions	203
	b Positions with Noise and Ownship Iterations	203
5-5	Eight-Step Iterative Geometry	206
5-6	Instantaneous Relative Geometries	209
5-7	Resulting Objective Functions as Function of Patience	210
5-8	High-Speed Efficiency Results	211
	a Initial Positions	211
	b Initial Positions	211
5-9	High-Speed Vehicle Case Study Results	213
5-10	Minimum Safety Scores	216
6-1	Experimental Geometry: 5-Vehicle 5-Track	224
6-2	Experimental Geometry: 5-Vehicle 3-Track	225
6-3	Waypoint Objective Function	226
6-4	Traffic-Constrained Monitoring Scenario	228

a	Experimental Geometry	228
b	On-Water Testing	228
6-5	Nominal On-Water Testing Geometry with Humans	229
6-6	Navigationally Constrained Encounter Scenario	230
6-7	On-Water Testing Vehicles	232
a	Vehicles in Shoreside Lab	232
b	Vehicles on Dock	232
c	M200 Autonomous Catamarans	232
6-8	Daytime Testing Range	233
6-9	Night Testing Range	234
6-10	On-Water Testing After Perturbations	235
6-11	Track Data from Long Duration Experiment	239
6-12	On-Water Results	240
6-13	Objective Functions from On-Water Results	241
6-14	Minimum Acceptable CPA Violations	242
6-15	Mean Protocol Scores	246
6-16	Mean Safety Results	248
C-1	High Speed CPU Load	275
C-2	Slow A CPU Load	276
C-3	Slow B CPU Load	277
D-1	Scenario 1	281
D-2	Scenario 2	282
D-3	Scenario 3	283
D-4	Scenario 4	285
D-5	Scenario 5	286
D-6	Scenario 6	287
D-7	Scenario 7	288
D-8	Scenario 8	289
D-9	Scenario 9	290

D-10 Percent Correct Answers on Exams 292
D-11 Collision Factors 293
D-12 Reasons Drivers Failed to Obey COLREGS 293

THIS PAGE INTENTIONALLY LEFT BLANK

List of Tables

2.1	Summary of Literature Attributes Relative to this Thesis	76
4.1	Categories of Scope for Evaluation of COLREGS Compliance	137
4.2	Significance Testing for Compliance Detection	187
4.3	Significance Testing: t-Test Values	188
4.4	Significance Testing: Degrees of Freedom	188
5.1	Iterative Geometric Testing Attributes	204
5.2	Iterative Geometry Experimentation Configuration	207
6.1	Scenarios for On-Water Experimentation	222
6.2	Number of On-Water Encounters Observed per Scenario	236
6.3	Summary of On-Water Experiments	237
6.4	Mean CPA Range Normalized to Desired CPA for 5-Vehicle Scenarios	242
6.5	Number of On-Water Experiments Performed for 5-Vehicle Scenarios	243
6.6	Percent of $r_{cpa} < R_{min}$ Events for Scenario A & B 5-Vehicle On-Water Collision Avoidance Encounters	243
6.7	Mean Spatial Efficiency for Scenario A & B 5-Vehicle On-Water Colli- sion Avoidance Encounters	243
6.8	Mean Temporal Efficiency for Scenario A & B 5-Vehicle On-Water Collision Avoidance Encounters	244
6.9	Standard Deviation of Spatial Efficiency for Table 6.7	244
6.10	Standard Deviation of Temporal Efficiency for Table 6.8	244
6.11	Mean Protocol Score	247

6.12	Standard Deviation of Protocol Score	247
6.13	Mean Safety Score	249
6.14	Standard Deviation of Safety Score	249
7.1	Road Test Performance Areas	258
7.2	Road Test Attributes	259
B.1	Table of Definitions	268
B.2	Table of Definitions	269
B.3	Table of Notation	270
B.4	Table of Notation	271
B.5	Table of Notation	272
D.1	Individual Respondent Data Before Controlling for Percent of Blame	291

List of Algorithms

1	Full CPA Quantification Algorithm	107
2	Full CPA Algorithm with Range-Only Discrimination	108
3	General Approach of Safety Evaluation	142
4	General Approach of Evaluation Technique	143
5	COLREGS Entry Criteria: Determining the Appropriate Rule Set . .	145
6	Rule 13/16: Overtaking Vessels	153
7	Rule 13/17: Overtaken Vessels	154
8	Rule 14: Head-on Vessels	157
9	Rule 15: Power-Driven Crossing	161
10	Rule 16: Give-way Vessels	162
11	Rule 17: Stand-on Vessels	163
12	Penalize for Delayed Action	164
13	Penalize for Non-Readily Apparent Maneuver	164
14	Check for Non-Readily Apparent Course Change	164
15	Check for Non-Readily Apparent Speed Change	165
16	Penalize Course Change	165
17	Penalize Speed Change	166
18	Iterative Geometry Generation	202

THIS PAGE INTENTIONALLY LEFT BLANK

Chapter 1

Introduction

The field of marine robotics has continued to advance in many areas including sensing and perception, navigation, payload integration, and collision avoidance. The advances in collision avoidance, however, have largely focused on iterative advances to the velocity obstacle algorithm – a technique that creates binary decision regions where results are said to either result in or not result in a collision. Velocity obstacle-based methods inherently lose key encounter information that humans use in their decision making.

This thesis investigates and expands collision avoidance algorithms that generalize the velocity obstacle into a multi-threshold based approach that more realistically represents human ship driving practices. These algorithms become especially important when considering complex missions of competing objectives in protocol-constrained, contact-dense environments. On-water testing of up to five autonomous vessels under the protocol constraints of COLREGS demonstrates superior performance of these collision avoidance algorithms compared to the velocity obstacle of the current state of the art.

Introduction of performance metrics consistent with human ship driving practices allows new tradespaces for autonomous collision avoidance designers and evaluators. Collision avoidance protocol metrics and evaluation algorithms enable evaluators to perform both on-line and post-mission analysis using a configurable protocol evaluation library. These evaluation algorithms can be applied to both autonomous and

human-operated vehicle track data independent of the underlying collision avoidance algorithm.

Extensive on-water experimentation results demonstrate improvement in performance metrics when comparing the algorithms of this thesis to the velocity obstacle approach in four key performance areas: spatial efficiency, temporal efficiency, protocol compliance, and safety. These on-water experiments included complex and often competing COLREGS¹ requirements in which vehicles were either autonomous or human-operated. A proposed autonomous collision avoidance road test framework incorporates testing of arbitrary collision avoidance algorithms both in the field and in simulation to a standardized level of performance. The road test framework extends naturally to test human operators to the same criteria of autonomous robots thereby advancing evaluation transparency, trust of autonomous systems, and ease of transition to human-machine teaming in protocol-constrained environments. Combining the proposed performance metrics, evaluation techniques, testing procedures, and improved collision avoidance algorithm results in more human-like autonomy as demonstrated by over 6,150 on-water encounters.

1.1 Motivation

As vehicles with varying degrees of autonomy become increasingly present in human-dominated environments, the ability for humans and robots to safely and efficiently interact becomes paramount. Autonomous collision avoidance algorithms exist in many physical domains including land, air, undersea, and sea surface (“surface”). To enable right-of-way and offer decentralized governance without communication, certain governing bodies adopted rules that codify collision avoidance protocols for specific physical domains. Many civilian ground transportation governance bodies, for

¹COLREGS refers to international rules as formalized at the Convention on the International Rules for Preventing Collisions at Sea, developed by the International Maritime Organization, and ratified as an international treaty by Congress. These rules were further formalized by the U.S. International Navigational Rules Act of 1977 [84], and are sometimes referred to as the Collision Regulations outside the United States. Additional information is presented for reference in Appendix A.

example, give right-of-way to a particular ground vehicle when two or more vehicles simultaneously arrive at an intersection controlled by a stop sign.

In the air, rules instruct aviators as to required altitude changes and course maneuvers. The rules governing collision avoidance of surface ships allows any two vessels to know their required role and order of precedence based only on the type of vessels involved, relative geometry, and relative speed. These collision avoidance rules comprise a subset of the COLREGS and increasingly have been the focus of research in the field of marine autonomy. The rules reflect intentionally vague language and do not account for all marine customs and traditions. Further, case law and maritime navigational experience greatly influence the humanistic reality of the rules in practice.

To enable autonomous vehicles to emulate human behavior in collision avoidance scenarios, this thesis introduces techniques to replicate the human decision making process including metrics to articulate the active tradespace. Practical application can be seen beyond the realm of algorithm design and testing. Insurance companies, safety regulators, acquisition authorities, and litigation courts may greatly benefit from the standardized, repeatable, and quantifiable means to evaluate performance described in this thesis.

1.2 Contributions of this Research

1.2.1 Primary Contributions

Three primary contributions of this research combine to yield more human-like behavior than the current state of the art in autonomy and marine robotics including: 1) demonstration that a range-, time-, and pose-informed CPA-based collision avoidance algorithm generalizes and outperforms the velocity obstacle, 2) development of protocol-based collision avoidance evaluation metrics, algorithms, and testing techniques, and 3) performance of over 6,150 on-water experiments spanning 10 complex multi-contact scenarios validating the claims of Section 1.3 and techniques of Chap-

ters 4 and 5.

1.2.2 Attributes Supporting the Primary Contributions

Several attributes of this thesis contributed to the above primary contributions as articulated in the following sections:

- demonstration that CPA-based collision avoidance algorithms generalize the literature-standard velocity obstacle to multiple range thresholds (Section 3.3.4)
- introduction of the patience parameter for autonomous primary missions (Section 3.6)
- first to measure, evaluate, and design for efficiency & safety as a tradespace (Sections 4.2 and 4.4)
- first to quantify and subsequently assess performance with respect to protocol compliance (Section 4.3)
- first known rigorous analysis of entry and exit criteria of protocol-constrained collision avoidance rules for autonomous vessels (Section 4.5.1)
- first to develop a collision avoidance protocol evaluation library with real-time and post-mission tools (Section 4.6)
- development of iterative geometric testing algorithms for autonomous collision avoidance robustness testing and sensitivity analysis (Section 5.4)
- development of the first known “road test” framework for autonomous collision avoidance algorithms (Section 5.6)
- demonstration of significant² on-water testing involving over 6,150 on-water vehicle-pair encounters using 5-vehicle interactions in 10 collision avoidance scenarios (Chapter 6) including:

²This represents a greater number of simultaneous rule combinations, on-water vehicles, and total vehicles encounters than any work in the current literature.

- 5+ vehicle conflicting traffic patterns (Section 6.1.1)
- UUV track & trail scenario in congested traffic (Section 6.1.2)
- human-robot interactions in which a vessel was human operated among a field of autonomous vehicles (Section 6.1.3)
- high-speed interactions (case study in simulation: Section 5.5; on-water results: Section 6.1.3)
- non-compliant actor scenarios (protocol agnostic, collision agnostic, & dead in the water) (Section 6.1.4)
- navigationally constrained & congested harbor scenarios (Section 6.1.5)

1.3 Formal Problem Statements

1.3.1 Reduction of Collisions

For a vessel with current state $\langle x, y, \theta, v \rangle$ and limited kinematic prediction, find the solution course-speed vector $\langle \theta^*, v^* \rangle$ satisfying conflicting protocol collision avoidance constraints with human-realistic behavior that optimizes trades between safety, collision avoidance protocol requirements, and mission performance efficiencies.

Assertion: Development of a continuous utility function to generalize the velocity obstacle improves safety and efficiency in complex, multi-contact collision avoidance encounters under the protocol constraints of COLREGS.

Chapter 3 presents material to define the solution space. Chapter 4 defines the metrics for safety, protocol compliance, and efficiencies. Chapter 6 demonstrates results to validate the assertion of this problem statement.

1.3.2 Identification of Non-Compliant Vessels from Track Data

Using only track data (position-heading tuples), identify, quantify, and assess protocol requirements and compliance.

Assertion: Evaluation algorithms can identify a vehicle not complying with the rules (protocol agnostic or collision agnostic) using only track data.

Chapter 4 introduces the algorithms and techniques for evaluation. Section 4.7 demonstrates validation for identification algorithms.

1.3.3 Reduction of Performance in Alternative Scenarios

Using only track data (position-heading tuples), demonstrate the reduction of performance throughout various on-water experimentation scenarios.

Assertion: Testing of collision avoidance algorithms within a limited scope of mission scenarios insufficiently bounds performance under alternative mission scenarios.

Chapter 4 introduces the algorithms and techniques for evaluation. Chapter 5 demonstrates reduction of performance based on initial contact geometry and patience pairs. Chapter 6 demonstrates reduction of performance for various on-water mission scenarios.

1.4 Assumptions and Scope

1. Vessels assumed other agents followed a linear track at constant speed for their current instantaneous state. Contacts were not necessarily assumed to adhere to protocol requirements any more than a human-operated contact in the high seas would be assumed to do so. No explicit communication verified intent of a contact prior to commencement of a compliant maneuver in real time. Updates of instantaneous state at a $4Hz$ frequency allowed for real-time evaluation of a contact's intent consistent with a human watch stander³. Communication remained limited to state data $\langle x, y, \theta, v \rangle$ consistent with visual observations by a human watch stander.
2. Perfect sensing was assumed using GPS position reports of all agents via a shared communication link occurring within a sufficient time interval. While

³The term watch stander denotes the person responsible for a particular function(s) of a vessel's safe operations.

real-ships operate using the Automated Information System (AIS,[81]), they are required to have and operate onboard sensors (visual, auditory, and radar). This thesis focused on the collision avoidance algorithms and protocol evaluation techniques while assuming perfect contact sensing and sensor fusion consistent with the communication limitations of Assumption 1.

3. To model realistic sensing limitations, position information was only made available to other agents who were within a reasonable range to be considered detected visually. Unless specifically annotated, detection ranges were assumed to be approximately twice the preferred range at closest point of approach.
4. Discussion and modeling of protocol-based collision avoidance was limited to the international COLREGS, specifically as they govern interactions between power-driven vessels unless otherwise specified. The methods of this thesis naturally extend to other collision avoidance protocols of other physical domains such as the “Rules of the Air”.

Within the context of this thesis, multi-objective optimization refers to the “subclass of single-objective optimization problems where the single objective function to be optimized is composed of components that are themselves meaningful objective functions” unless otherwise annotated [3]. The problem described in Chapter 3 focuses on the selection of an optimal solution within the set of admissible values of the decision variables without necessarily exploring alternative solutions in the objective tradespace. While this usage of the term multi-objective optimization in this context is consistent with published literature [3–5], the distinction is articulated to avoid confusion.

Four specific objective tradespace metrics considered in this thesis are temporal efficiency, spatial efficiency, safety, and protocol compliance using variations of the patience parameter described in Section 3.6. These four objective tradespace quantities – with efficiencies acting as a surrogate for any specific mission performance requirements – constitute the primary values that a human operator might reason

about when making maneuvering decisions. True multi-objective optimization becomes relevant when assigning a value of importance to these objective space metrics relative to each other, as discussed in Chapters 4-6.

1.5 Thesis Overview

Chapter 2 provides a review of relevant literature and the current state of the art including autonomous collision avoidance algorithms, path planning algorithms, and collision risk metrics. Chapter 3 introduces the full (range-, time-, and pose-informed) CPA quantification algorithms including the generalization of the velocity obstacle. Chapter 4 presents evaluation techniques and metrics for autonomous collision avoidance. Chapter 5 presents techniques to robustly test non-canonical encounter geometries in statistically significant ways using a design of experiments. Chapter 5 further presents testing techniques for robustness and sensitivity analysis of collision avoidance algorithms. Results in Chapter 6 validate the claims of Section 1.3 and demonstrate meaningful improvements over the current state of the art. Chapter 7 presents conclusions and opportunities for future work including the autonomous road test framework.

Appendix A presents a brief overview of the relevant sections of COLREGS for power-driven vessels. Appendix B presents lexicon and notation found throughout this thesis. Appendix C provides verification of ample CPU loading margin during computation of multi-contact collision avoidance encounters. Appendix D provides details of the validation of the evaluation algorithms of Chapter 4 using human operator surveys.

Chapter 2

Literature Review: The State of the Art

Recent literature demonstrates considerable interest in solving practical autonomous collision avoidance problems where a vehicle either knows or senses an obstacle's course and speed. Ultimately, the final decision of an autonomous decision maker must be to select an appropriate velocity vector. Velocity obstacles and closest point of approach (CPA) methods encompass the two most commonly developed types of algorithms for determining if a candidate decision vector (course and speed) results in a collision free path. Local reactive path planning literature for collision avoidance focuses on finding a safe, collision-free trajectory that achieves the primary mission needs using only on-board sensing and knowledge.

Local reactive path planning is a subset of global path planning literature. The area of local reactive path planning focusing on interactions with newly detected static obstacles has dominated replanning algorithms for global path planning for some time. Advances were then made toward local replanning for dynamic obstacles including collision avoidance with other vessels. This set of literature is then further refined to include local replanning for dynamic obstacles with the constraints of a protocol-based collision avoidance rule set. To fully appreciate the scope of literature involved, a review of more general global path planning literature is first introduced. A sampling of literature for system identification and how it informs global path plan-

ning is discussed. This review then zooms into the section of path planning literature involved in localized reactive path planning dealing with collision avoidance. The notion of collision risk is discussed including the necessary creation of collision avoidance utility functions to reason about various deviations from the primary mission objective. The primary collision avoidance algorithms for determination of collision risk (velocity obstacles and explicit closest point of approach techniques) are reviewed and analyzed in the context of quantifying collision risk to inform local path planning utility functions. A subsequent discussion of literature for evaluation of protocols to quantify the notion of protocol “compliance” is addressed. Testing and evaluation frameworks are reviewed to include geometry configurations, simulations, and on-water experimentation. After a review of the literature, a brief introduction of its applicability to this research is given.

2.1 Motivation

Global path planning literature often focuses on moving a vehicle from a starting point to a destination with regard only to fixed obstacles and navigation constraints rather than collision avoidance of other vessels. Those authors who focus on collision avoidance of other vessels often do so from a non-path planning stance where evasive maneuvers will be taken before returning to a predefined-defined track. Many collision avoidance techniques disregard the triad of competing objectives when planning and constructing a path for traversal. The triad of competing objectives include:

- desires and goals of the mission(s)¹
- navigational and obstacle² avoidance requirements

¹Mission in this context refers to the reason(s) that a vessel is underway. This might include a simple transit of waypoints across a body of water or might include more intricate mission path planning and constraints for objectives that are more sensitive to changes of course or speed such as bottom mapping with a side-scan or towed sonar array.

²The literature is inconsistent with reference to obstacle and collision avoidance. In maritime operations, the lexicon differentiates allisions and collisions. The former is the striking of a static object or vessel with ownship. The latter involves two vessels which are both underway colliding. To differentiate between the two within the scope of this document, “obstacle avoidance” refers to decision making and maneuvers required to avoid an allision while “collision avoidance” refers to

- collision avoidance requirements

These three objectives are in no priority order until the designer of an autonomous mission assigns a priority weight to each component. This assignment of importance in most literature comes in the form of a binary representation where one of two primary modes is active while the other is precluded from the decision space. The two primary modes of most autonomous marine vehicle literature include:

- a path planning algorithm that constructs a path based on obstacles and navigation constraints while meeting the overall mission objective
- a collision avoidance algorithm that allows a vessel to deviate from the planned path to perform collision avoidance for another vessel or unexpected moving obstacle³

In operating under this binary mode scheme, the mission seems somewhat static with reasonably predictable obstacles and navigation constraints such as navigational markers, geographic features, and traffic control schemes. This predictable path planning is continued by most autonomous platforms until faced with a collision scenario; then, planners typically disregard mission requirements to perform collision avoidance for another vessel or avoid a newly discovered static obstacle. That is, most literature that addresses maritime collision avoidance will forego seeking some balanced weighting to continue achieving the mission while simultaneously avoiding collisions with other vessels. By incorporating a means of evaluating weighted priorities for each component of the mission, navigation, and collision avoidance constraints, a tradeoff can be continuously made that allows for selection of an appropriate course and speed combination with due consideration of mission efficiency, safety, and compliance with the governing protocol. The literature that attempt to balance the competing objectives predominantly seeks the least cost deviation from the *a priori* determined path

decision making and maneuvers required to avoid a collision. Allisions, and therefore obstacle avoidance, often involve navigation constraints such as buoys, day markers, piers, geographic features, and other static hindrances.

³This deviation often correctly considers navigational constraints but neglects the primary mission and the next track waypoint.

that is collision free. Little to no consideration is given to the overall effects (mission efficiency and safety) of incorporation of collision avoidance constraints into selection of the desired velocity vector. However, it has been shown that collision avoidance can greatly influence mission safety and efficiency [93]. Incorporating collision avoidance in the determination of the desired velocity vector is therefore a worthwhile consideration rather than as a heuristic to minimize deviation from a mission-only informed decision.

This balance must be made between computational expense, precision, and accuracy. The “good enough” standard for marine autonomy missions will vary for each designer and end user. A tradespace does exist for computational expense and solution refinement. When considering a collision avoidance protocol such as COLREGS with sufficient stand off ranges, obstacles avoidance, and general navigation, the problem seems readily achievable. By inserting multiple concurrent contact vessels operating under geometries resulting in multiple and often conflicting COLREGS rules, the problem grows more complicated. After cluttering the environment with navigational and obstacle constraints, a clear need exists for computationally efficient algorithms that are able to accurately predict compliant maneuvers without unnecessarily compromising overall efficiency or safety.

2.2 Global Path Planning

Motion planning is “widely studied in robotic navigation research” and mostly solved for land based problems [78]. Motion planning remains an open problem for surface vessels likely due to the sole culpability lying with the master of the vessel and political inertia preventing movement toward non-human, autonomous control. Insurance companies are also less likely to sponsor a vessel without a human master, though recent highlights in the media [56, 91] may help facilitate forward momentum.

Lekkas detailed the purpose of a continuous-curvature path for path planning in [53]. The two main categories discussed for connecting points were: 1) combining straight lines and arc segments, and 2) using splines. The former method is

inherent to Dubins path generation where the allowance is zero [23]. The latter category connects waypoints using splines but is mostly focused in the field of computer graphics [53]. The spline methods include clothoids, cubic Hermite spline interpolation, natural cubic splines, and Pythagorean-hodograph curves. As Lekkas describes, Pythagorean-hodographs do not guarantee curvature continuity. Curvature discontinuity is indicative of discontinuity in desired lateral acceleration which ultimately affects the heading controller as described in [83]. This is more relevant to autonomy focused on aerial systems, though the discussion of path smoothing is relevant for fitting techniques of trajectories. Lekkas described this technique of using an arc as a shortcut to reaching all waypoints by accepting some allowance [53].

Care should be taken though to consider scenarios where track deviation must be reduced or even eliminated to achieve each waypoint. Consideration is due at the time of mission planning as to whether these allowances can be tolerated or whether they could ultimately change the modeling style for macro level path planning. Allowance is therefore a topic of importance to the mission designer. Lekkas [51] introduced the principle of allowance which is discussed in more detail by [19]. Allowance is defined to be the deviation of the arc from the initial piecewise linear path. The allowance can be translated to other literature which refers to a “capture radius” of a waypoint [6], or in other words, how close a vehicle must be to its originally designed waypoint to be able to rightfully declare completion of that leg. The degree of precision of any waypoint capture is of considerable design consequence and depends greatly on the mission at hand. Many authors discuss the question of capture radius and the sensitivity thereof. There is often assumed no loss of utility for an arbitrarily large capture which may not be appropriate for an autonomous marine vehicle application such as bottom mapping where tolerance is low for missed waypoints. There is also little discussion in literature of error tolerances for waypoint capture radius, the needs of the mission, the effects on piloting, or similar affects which are important to marine navigation.

The definition of allowance can be expanded to show the comparison of errors between circular smoothing, Fermat smoothing, and clothoid smoothing. Each of

these may result in large errors which may not be appropriate for a given mission; again, the sensitivity to a given mission must be understood by the designer. Similar to allowance for given waypoints, track deviations between waypoints may also be adverse to the mission's needs especially in tracks requiring strict adherence such as towed sonar applications or side scan sonar where unnecessary course deviations can severely affect data quality. To this point, an incorporation of tolerance for allowance should be considered for certain missions. Another example is piloting in the vicinity of a buoy where passage to a particular side of the waypoint must be further understood beyond the scope of this study. Another example might include considering a piloting channel where a waypoint might represent the center of a buoy channel. While this example considers the risk of allision where obstacle avoidance techniques might supersede the discussion of allowance, other open-ocean scenarios without risk of allision might entail the same degree of importance of staying on track and achieving waypoints. A general note is made as to possible undesired effects of passing between waypoints in [52].

Lekkas's contributions in [51] were: 1) to use Fermat's spiral as a means of path smoothing to ensure continuous curvature by extending other research to remove a speed singularity at the origin, 2) to present a more thorough analysis of Fermat spiral arc length, and 3) to show that the Fermat spiral could be used in combination with circular arcs to produce Dubins paths with Fermat spiral transitions. The main motivation was to construct paths of simple geometry (straight lines and arc segments) which avoid the curvature discontinuity of Dubins paths and computational intensity of clothoids [53]. Rather than using clothoids, Lekkas used Fermat's spiral to cut down significantly on computation time. Two main categories of path planning with waypoints are discussed including the use of splines as well as combinations of straight lines and arc segments. Splines are discussed in the context of computer graphics including the cubic Hermite spline interpolation (CHSI) to achieve continuous velocity paths and eliminating wiggle. Lekkas points to other literature to discuss the spline method not necessarily having paths with continuous curvature.

The use of straight lines and arc segments is shown to be an extension of a Dubins

path which in its most general sense does not invoke continuous curvature at transition points between piecewise components. Tsourdos [83] is often cross referenced as a more rigorous discussion of the main disadvantage of the curvature discontinuity, while discussing that this curvature discontinuity yields a discontinuity in the desired lateral acceleration. The governing equation for this discussion is Equation (2.1) where a is lateral acceleration, v is the velocity vector, and κ is curvature using the notation of [83].

$$|a| = |v|^2 \cdot \kappa \quad (2.1)$$

Some authors recommend the use of a clothoid arc between a straight line and circular arc to achieve continuity of curvature. Clothoids are often called Euler spirals, Cornu spirals, or spiros and are advantageous due to their curvature being a linear function of arc length. Lekkas points out that a major disadvantage of the clothoid approach is that they require computation of the Fresnel integrals which can be costly due to lacking a closed-form solution. Two uses for clothoids are shown, namely to replace the arc that connects two line segments with two smoothing clothoids, or to use a clothoid to transition between a line segment and its adjoining arc segment. While clothoids provide a rather attractive feature for curvature, their computational time is poor compared to Fermat's spiral. Fermat's spiral however has a velocity and acceleration which are undefined at the ends until reparameterized [53].

Two types of curves are discussed for fitting in [51, 53], namely interpolating curves which pass through all given points and approximating curves which do not pass through all given points. The interpolating and approximating curves are therefore mutually exclusive for a given curve and set of points, that is, each curve can be interpolating or approximating, but not both by these definitions. Lekkas showed that the path tangential angle is discontinuous with undefined curvature at waypoints when only using linear segments resulting in a path that cannot be followed by under-actuated vehicles. Mission designers must also consider the true error resulting from attempting to follow such a piecewise linear path using an under-actuated

vehicle and determine if the resulting path deviation is of significant consequence. Further this assumes generation of a path without consideration of a vehicle's own maneuvering characteristics. If a piecewise linear path is constructed using a known feasible trajectory with sufficient resolution of waypoints, then the computationally heavy path construction that explicitly enforces curvature constraints is no longer necessary. For example, a small maximum error in track may not be important for most to all missions of a specified platform. If this is the case, it is possible to consider that the addition of functions to achieve constant curvature may in the end be unnecessary calculations which take computational resources from more important onboard processing especially when considering multiple simultaneous collision avoidance scenarios. The Lekkas study assumed constant external disturbances such as current acting on the vehicle rather than focusing on a purely geometric perspective. The lack of environmental considerations is consistent with many path planning algorithms in recent literature [78].

Smoothness is an important feature to consider in global path planning but takes multiple meanings. Lekkas describes two meanings of path smoothness, namely parametric and geometric continuity. Parametric continuity is defined as the combination of orientation and speed whereas geometric continuity removes the speed component. For a detailed discussion of their differences, see [51]. An automated procedure for determining waypoint locations is described in [51] as follows:

- define the obstacles on a given map [chart] and specify the clearance constraint (the shortest safe range that a vehicle should maintain from any given obstacle)
- generate a feasible set of ordered waypoints using the Voronoi diagrams to respect the clearance constraints
- design a path with allowance equal or lower than the clearance constraint

The property of tractability is afforded two main components: practicality of the overall shape of the path and shape control of the path [51]. The latter is concerned with the affect on the total path if one waypoint location is modified or added; this

applies more to macro path planning rather than reactive localized path planning for collision avoidance. Lekkas confirms the distinction when offering that a user can “tolerate a relatively short cross-track error at the curvature continuity locations” for the purpose of collision avoidance. In [51], obstacle avoidance is defined as being the collision free path resulting from consideration of static, fixed obstacles commonly seen in the literature as navigation constraints including land formations and buoys. An acceptable clearance range is considered as well as curvature constraints by means of Voronoi diagrams.

Comparing paths can be objectified using the several criteria below with a more detailed discussion of this concept is given in [53]:

- length
- allowance
- tractability
- algorithm complexity

While some authors prefer Voronoi diagrams for their $O(n)$ complexity, a balance must be reached to ensure a desired answer is produced. Voronoi diagrams translate a problem of obstacle avoidance into a geometric space such that the borders of the regions are maximally distant from all the obstacles in the environment. For example, classic Voronoi diagrams for navigating a buoy channel would yield a solution that places a vessel at the center of an allision free path, or in this case, the center of the buoy channel. This directly conflicts with ship driving practice and international law.

The assumptions required for far field planning, however, are not achievable for contact avoidance requiring decentralized, protocol-based decisions [47]. The far field marine collision avoidance problem requires reliable and complete contact input from sources such as the Automated Information System (AIS). AIS cannot be relied upon for information about all vessels. Rather, onboard sensors are required to ensure a complete contact picture. Raw radar, vision, and auditory sensors are required for

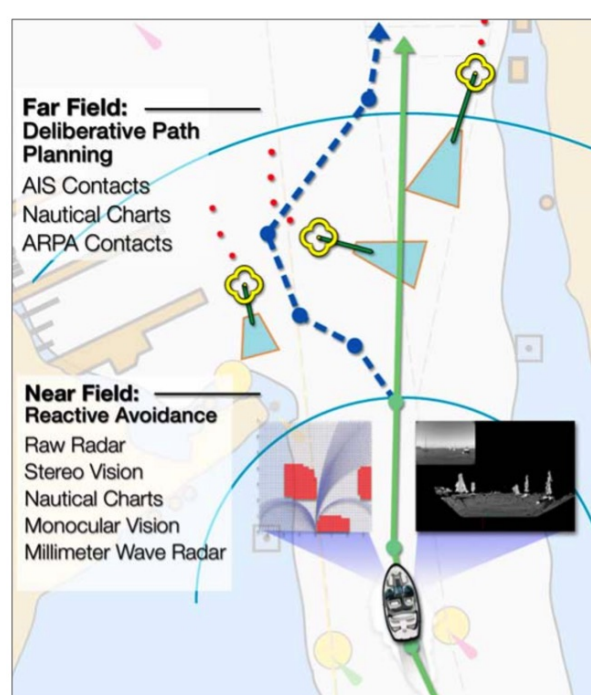


Figure 2-1 Larson showed that the COLREGS collision avoidance problem was distinctly reactive in [47]. Image is Figure 3 from [47].

onboard sensing and place any contacts detected by those means in the realm of local reactive path planning as shown in Figure 2-1.

2.3 Local Reactive Path Planning for Collision Avoidance

A comprehensive review of collision avoidance and path planning literature was completed by Tam [78]. Tam particularly focused on the collision avoidance evolution for marine environments. Path planning algorithms are traditionally focused on land-based robotic navigation (e.g., rule-based expert systems or combinatorial motion planning) and iterative non-deterministic optimization algorithms. Tam notes that these are difficult to adapt to COLREGS compliant schemes or other schemes in-

volving the “practice of seamanship.” Tam further notes that besides the protocol of COLREGS, vessel dynamics including different hull forms make the problem much harder than a land based system.

Collision avoidance techniques have increasingly focused on the use of velocity obstacles for ease of both computation and implementation. By their nature, velocity obstacles transform a single dynamic planning problem into m static problems [26, 27] where each static problem holds a binary value of safe or unsafe for each candidate maneuver (course and speed) in velocity space. In order to accomplish this transformation out of the dynamic environment, the range at which a collision is said to occur as well as the shape of all vehicles involved requires assumptions. Additional discussion of the traditional velocity obstacle may be found in Section 2.5.

Before entering the “harder” areas of collision avoidance, many authors have examined vehicle following in dynamic environments [71, 73, 74]. Campbell accurately captures this in a review of improving autonomy of unmanned surface vehicles through intelligent collision avoidance: “It should be stressed that motion planning for marine vehicles has been investigated in detail, however little attention is paid to COLREGS compliance” [12].

While velocity obstacle and CPA-based methods dominate the collision avoidance-informed local path planning literature, several other techniques have been examined in the literature. Fuzzy logic was used in [32, 36, 38, 43, 50, 60, 61, 98, 101] to allow for fuzzy reasoning about collision avoidance states. Genetic and evolutionary algorithms [37, 41, 69, 72, 76, 79] allowed for alternative methods for constructing collision free paths. Grid-based algorithms [59, 65, 75] used the traditional technique of populating an occupancy grid and searching for a collision free path, usually by an algorithm such as A*. Linear temporal logic [44] attempted to formalized the rules and entry criteria using a series of states including wind conditions. Maze routing [13] was attempted but was unable to overcome the reactive nature of onboard sensing requirements. Potential field [97] methods allowed attractive and repulsive forces though were unable to account for the necessity of apparent maneuvers. Rapidly-exploring random trees (RRTs) [2, 31, 48, 55, 63, 80] are promising for deliberative

planning problems. Using a more advanced means of determining collision risk such as the methods of Chapter 3, RRTs may prove promising once over-the-horizon collision avoidance information become available to ships via satellite feeds in the future. However, onboard sensors (and therefore reactive methods) will remain necessary for vessels undetected by methods such as shared position information. A local reactive RRT could become more realistic to the protocol-constrained maritime problem by reasoning about collision states and risk using the quantification techniques of this thesis. Voronoi diagrams [19, 51, 53, 83] provide a means staying clear of known obstacles, however are inconsistent with some protocol requirements including ensuring a bias toward a particular side of an obstacle (e.g., traffic separation scheme).

Global path planning approaches remain insufficient for cases of collision avoidance requiring rapid local re-planning and often focus on scenarios of piloting where navigational constraints are more numerous than collision avoidance constraints. Chang *et al.* [13] investigated Lee’s maze-routing algorithm using velocity vector advances and grid cell comparison to prevent any two ships from occupying the same cell simultaneously. This method does not neglect COLREGS entirely as alluded to in [78] but does only focus on Rule 8. Environmental conditions were entirely neglected and a weighted ship domain is considered which is mapped to the grid-maze. Szlapczynski [75] used a maze-routing method similar to Chang though incorporated additional turn penalties by increasing arrival time, time-dependent forbidden zone to alleviate risk of narrow passage diversion, and speed reduction ability in the case that course alteration alone was insufficient. This speed reduction was a linear function of range to the forbidden zone and accounted for discrete engine speeds. A binary search algorithm was used to find the minimum speed reduction necessary to avoid a collision scenario. Tam asserts that this lacked optimization with respect to environmental conditions and is only capable of handling ownship speed reduction [78]. Szlapczynski does however correctly consider that an examination is required to determine if slowing rather than turning is advantageous for “economical reasons.” This alludes to the determination of a balance of mission efficiency and collision avoidance though was focused on the assumption of maintaining course and speed to achieve the current

mission.

A Chebyshev problem of optimal control by solving the sequential gradient restoration algorithm was studied by Miele *et al.* [57]. Only two ships were considered and a safety range of zero was used. While interesting academically, no practical navigator would consider bringing a vessel this close in a collision avoidance scenario rendering Miele's work incompatible with real world modeling. Convex set theory was considered by Hong *et al.* [36] by creating triangular regions from the decomposition of obstacle-free regions. These were then used similar to a Voronoi diagram to identify a feasible collision-free path.

Schuster presented an interesting method of coupling a low-cost radar sensor model with a collision avoidance technique relying on three main models of a contact's trajectory [65]. Schuster quantified the likelihood of each of the three trajectory models being accurate. These three models consisted of constant velocity, constant turn rate with constant velocity, and constant acceleration. The constant turn rate with constant velocity model used a circular arc while relying on an interacting multi-model filter for obstacle detection. The contact data gathered was then used to find a safe path in close range encounters. Curvature was kept continuous by using Bezier splines to connect waypoints. A grid was then populated and an A* algorithm search algorithm was used to find a collision free path. To incorporate ship's kinematics, a T-shape neighborhood is enforced in the grid search to consider only grid cells that are reachable by the vessel's current state. COLREGS was attempted using a ship domain approach where the A* algorithm coupled with the grid allowed for a real-time capability of a waypoint search. Monte Carlo testing was performed to consider the error between GPS track and sensor data.

Schuster's results showed that the constant velocity model and the constant turn rate with constant velocity model had very similar likelihoods of accuracy during straight line vessel motion. This calls into question the need to suppress the constant turn rate with constant velocity during known straight line trajectories. An introduction of this type of logic to determine whether a non-zero yaw rate is expected should improve the accuracy of both models. Schuster claimed that this was likely

due to small yaw rates. Consideration should be given to an appropriate filter to remove small course corrections and noise that do not necessarily map to a change of ordered course. Bezier splines were used to generate a smooth path navigable by the vessel. On-water results with one dynamic obstacle were used to validate Monte Carlo simulations. Schuster discusses that while the absolute position accuracy was observably low, positions relative to ownship were satisfactory and often more important. This importance of relative position may be true for the case studied, but improved absolute position accuracy should be addressed more thoroughly for scaled applications such as multiple concurrent collision risks while simultaneously considering navigational constraints such as shoals, which are often addressed using absolute position. Schuster’s study considered a maximum range of 800m, which is perhaps appropriate for the small craft used in this study. Scalability for larger craft using Schuster’s approach would be a worthwhile extension of [65].

Smierzchalski [69] used an evolutionary algorithm for trajectory planning by altering ownship speed after first establishing polygon-shaped domains. Feasible navigation paths were used to seed randomly populated initialization genes before solving for the cost functions considering spatial, temporal, and trajectory smoothness factors. To impose COLREGS, the ship domain shape was modified to have ownship moved within the polygon depending on the particular COLREGS scenario. This approach also lacked environmental considerations.

Another genetic algorithm was used by Ito *et al.* [41] to compute the collision avoidance navigation path by first defining a ship domain as a danger zone to find the optimal configuration of passing points. Cost functions in this study were the level of danger, length of avoiding path, straightness of the avoiding course, and loss of energy. An optimum course was considered from the output of 100 iterations. COLREGS was not used as a part of the algorithm’s decision making scheme. The straightness consideration is a primitive example of a need to consider track efficiency as part of the collision avoidance decision making process.

2.3.1 Target Following

Target following has been studied to achieve proper compliance with COLREGS in many cases. A model predictive planner which included modeling of hydrodynamic coefficients was studied in [73]. This used a least-cost heuristic, weighted A* algorithm to find a trajectory to complete target following while avoiding dynamic obstacles and claiming COLREGS compliance. Because of the uncertainty in possible future states, worst case models were used for computations of range to CPA. In the event that a COLREGS-compliant action was not found in time, Svec [73] allowed vessels to violate COLREGS. Candidate trajectories were designated as being feasible, violating COLREGS, or violating a collision region that indicated a collision would eventually occur. However, [73] did not consider taking way off the vessel as a compliant and often safe alternative to proceeding with a maneuver known to violate the Rules. Taking way off the ship is often a safe alternative to a maneuver so long as there are no complicating vessels such as when traveling in a convoy formation. No extension to non-following scenarios was discussed.

Svec *et al.* [71] provide a method for achieving target following using a generalized velocity obstacle (Section 2.5) approach while accounting for the differences in vehicle dynamics of the target vehicle and the unmanned surface vessel follower. The work allows for dynamic targets to follow while considering “the risk of losing the target boat, trajectory length, risk of collision with obstacles, violation of COLREGS, and execution of avoidance maneuvers against boats that do not follow COLREGS.”

2.3.2 Assessing Collision Risk

Tam investigated the development of collision risk assessment for stand on vessels in close-range encounters [77]. This work was limited to analyzing the suitability of the navigation plan and did not go so far as to provide reasoning for a suitable evasive maneuver. For discovering a head on scenario, the study used a heading difference angle of $\pi/8$ radians. Tam used heading regions to categorize the obstacles and what rules might be required. An encounter safety area is created based on both

forward and aft considerations with a powerful way of visual realization using a polar plot. By incorporating the collision risk factor into the calculations, Tam removes the traditional safety offsets that other algorithms build around their target (contact) vessels due to uncertainty.

Collision risk assessment for ships at sea was investigated in [78]. Many of these methods for assessing collision risk were based entirely on range at CPA. Most path planning algorithms studied assumed a safety region around each obstacle that indicates the risk of collision as cited first by Fujii and Tanaka [29]. Fuji and Tanaka's study is often considered the basis for modern approaches of ellipsoidal shapes with ownship at center [78].

Iijima and Hagiwara [39] used a breadth-first heuristic search to perform autonomous collision avoidance including judgment of collision risk and maneuvering control. They evaluated collision danger by circular ship domain, shortest track, least rudder angle, and COLREGS conformity based on "knowledge-base rules" on a 10 second frequency while neglecting environmental factors. This evaluation of shortest track is one of the few instances where a collision avoidance algorithm gives any consideration to track efficiency of a candidate maneuver. This work, however, allowed turns to port in direct conflict with the protocol restrictions of COLREGS.

Fuzzy set theory has been used to model collision avoidance maneuvers. Hwang [38] used this method in conjunction with circular ship safety domains with useful graphical representations of the fuzzy inferences. A discussion of how the final output was not guaranteed to be optimal can be found in [78]. Additional fuzzy reasoning for collision risk was studied by Lee and Rhee where a collision avoidance module was activated and an A* search algorithm was used to find feasible safe actions at minimal cost. Lee and Rhee used both time and range to CPA in their analysis of collision risk. Of note, their examples violate COLREGS by allowing the stand on vessel to unnecessarily deviate from course when no imminent collision exists. Lee and Kim [50] used a fuzzy relational product to identify candidate sectors of a standard polar velocity plot then compared "safe" sectors against COLREGS based on an action table; Lee and Kim however only considered a single vehicle. Lee and Kim chose a six degree

offset from the bow for declaring a head on situation. This reflects a design choice that is not usually published but is reasonably consistent with real-world ship driving. Liu and Shi [98] used fuzzy set theory and a neural network with three subnets to monitor the 1) encounter type and output collision avoidance action, 2) speed ratio based on fuzzified terms, and 3) alteration action with the magnitude and direction. Liu and Shi only could account for the contact with highest collision risk.

Tam accurately notes that most studies make highly simplifying assumptions before addressing COLREGS related models [78]. Traffic management schemes were developed through iterations of local jurisdictions experimenting with marine navigation to reduce collisions. West Germany, France, and the United Kingdom were the first to impose a one-way traffic separation scheme similar to that used on land. With the success of this limited implementation of marine traffic separation in Europe, the International Maritime Organization supported the expansion of marine traffic separation schemes in other locations. The Dover Strait mandated the use of a similar scheme in 1967. Tam notes that this resulted in a significant reduction of the observed number of collisions in head on geometry [78].

The challenge with traffic separation of marine vessels compared to their aerial counterparts is that altitude separation is possible in the air. By removing the third dimension, only uni- and bi-directional schemes are possible without the introduction of crossing tracks [78]. For non-parallel geometries and all geometries outside of traffic separation schemes, a protocol such as COLREGS must be used to manage both safety and efficiency.

Geometry for Safety Buffers

With the introduction of Fiorini's velocity obstacles, disc shapes were assumed for both contacts and ownship [26, 27]. The radius of the ship was determined based on the dimensions of the vessels and various uncertainties. This is later generalized to spheres of arbitrary size for three dimensional collision avoidance. Disc shapes for collision avoidance are found in both maritime and aerial literature [68, 71, 96].

Tam [77] considered dividing a ship into fore and aft sections with different half-

elliptical areas based on ship parameters. Tam’s area-based ship domain concept was defined for both ownship and obstacles. Tam used these geometry offsets to reduce the safety margins built into more traditional disc shapes due to uncertainty in vehicle shape and other uncertainties. Tam’s original graphic from [77] is shown in Figure 2-2.

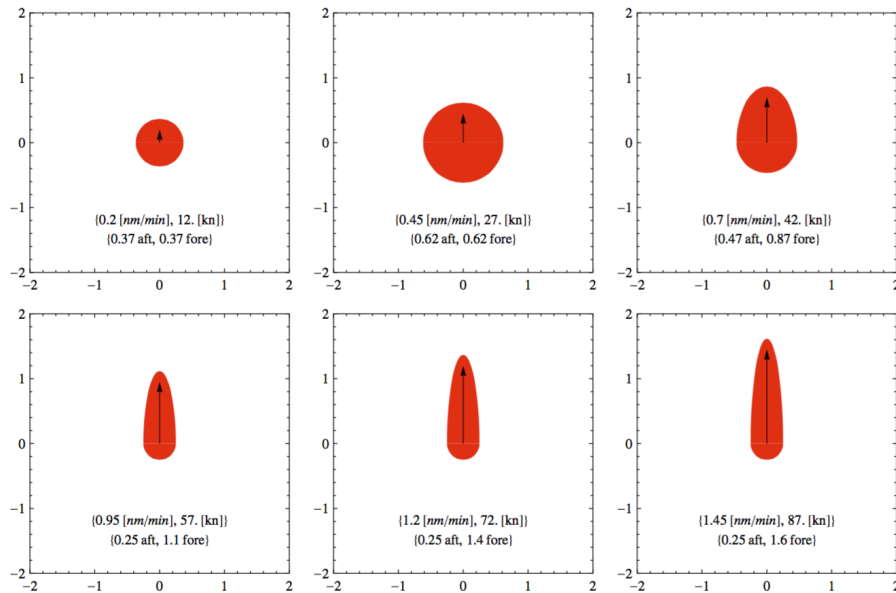


Figure 2-2 Tam introduced varying safety areas based on ownship and obstacle parameters using a fore and aft half-elliptical model. Image is Figure 6 from [77].

Kim *et al.* [43] introduce the concept of Minimum Range Requirement to account for pose, position, and velocity in a collision risk calculation, i.e., the drawing of a “collision shape” around a vessel. Pose in the context of [43] was limited to a binary value: orthogonal or parallel track to ownship. MRR effectively calculates center-of-body ranges for given poses to determine if actual vehicle shapes collide by determining rectangular outlines of vessels based on ship geometric parameters. Kim’s work effectively reduces the “collision” range for head-on like objects as the pose of detection to account for their narrow aspect.

Many authors have chosen simple geometries to bound the vessels for computational ease while others have computed the Minkowski sum of the vehicle shapes to form a collision region of arbitrary shape that facilitates computation of the velocity obstacle [45, 46]. This technique uses a fixed range for each side and projects the

bounding boxes of each vehicle to create a polygon of exclusion for candidate velocities rather than the disc originally used by Fiorini [26]. In cases using a bounding box such as this (e.g., Minkowski sum of shapes), an effective collision disc may be realized using the range of the contact and the circular shape that properly fits inside the velocity obstacle. Figure 2-3 shows examples of two collision risk methods from the literature.

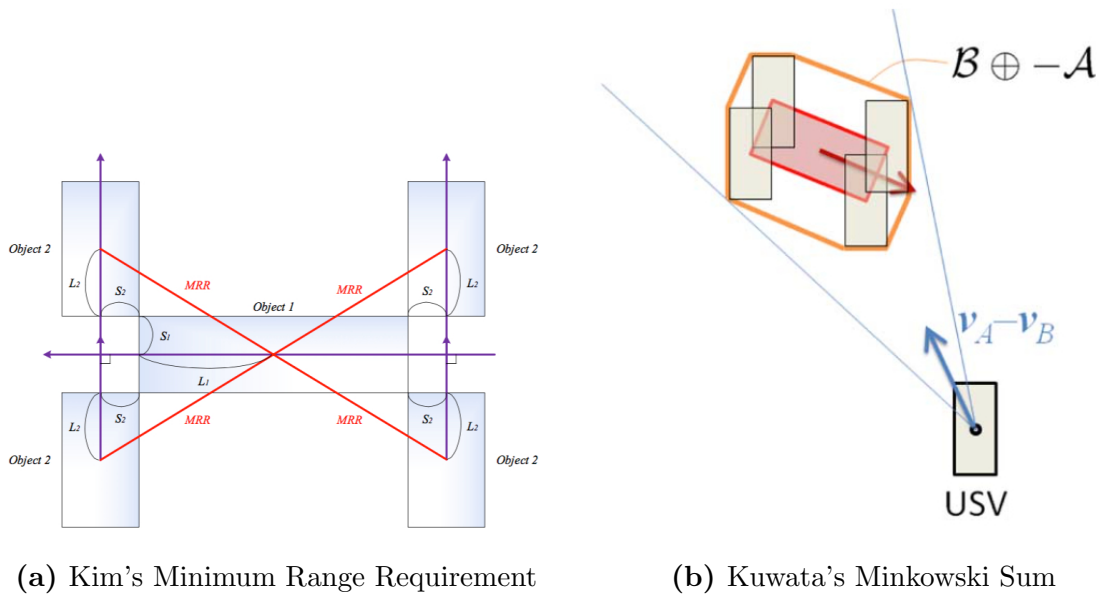


Figure 2-3 Kim introduced the minimum range requirement to produce a range to center line of a contact. Image (a) is Figure 3 from [43]. Kuwata used a Minkowski sum to create a collision boundary around a contact. Image (b) is Figure 3 from [45].

2.3.3 Collision Avoidance Utility Functions

Similar to creating utility functions to describe the attractiveness of any candidate velocity vector for the primary mission, collision avoidance behaviors can also be described using utility functions for the candidate velocity vector with respect to an obstacle. Rather than describing the utility of obtaining, for example, the best course and speed to track a submerged contact, the collision avoidance utility function determines if the candidate velocity vector results in a maneuver that is safe with respect to certain metrics for ownship and the given obstacle. The obstacle in this context is a

contact vessel. Similar to objective functions for the primary mission and navigational constraints, collision avoidance utility functions can be weighted to reflect the relative importance of the collision avoidance pair with respect to the safety of ship. For the case of protocol-constrained collision avoidance, metrics expressing compliance with the rules can further be incorporated. Multiple styles of utility function design for collision avoidance behaviors exist. The primary two methods are velocity obstacles and explicit quantification algorithms. As seen in Section 3.3.1, velocity obstacle based algorithms result in a binary decision: the maneuver is either safe or unsafe, or in utility function vernacular, 0 or 1. Explicit quantification algorithms can return utility values that are continuous between 0 and 1. Based on the weighting scheme, the importance of the overall objective function can be properly balanced with competing objectives. In the case of velocity obstacles, the collision avoidance utility function acts as a filter of *a priori* determined mission-preferred velocity vectors. However, explicit quantification algorithms can reflect varying degrees of safety to be reasoned about when considering candidate velocity vectors without using heuristic schemes. The resulting objective functions can then be used in conjunction with an optimal solver to determine the resulting course-speed pair of highest overall utility to ownship.

A simple weighted collision avoidance behavior with objective function $f_i = avd_i$ with priority weight w_i might define utility (Equation (2.2)) at each sampled candidate velocity vector $\vec{x} = \langle v, \theta \rangle$ as a function of CPA range (r_{cpa}), pose at CPA, or time until CPA. This collision avoidance objective function might have a priority weight as some function of current range to the contact (r), time at CPA (t_{cpa}) on current course and speed, pose at CPA (Θ_{cpa}), and/or range rate \dot{r}). Equation (2.3) demonstrates three example priority weight functions that a designer might choose for a collision avoidance priority weight depending on the overall mission profile considerations. More detailed collision avoidance design considerations may be found in Chapter 3. Consistent with marine autonomy literature, the specific modeling of lower order actuators and controllers is omitted. The decision space is limited to what a watch officer might consider on the bridge of a vessel as orders for driving the

ship: deciding on a course and speed pair within the limitations of a Dubins-like turn radius limitation. Collision avoidance algorithms using a maneuvering approximation such as the Dubins car model can be found in [19, 21, 22, 30, 34, 42, 64].

$$avd = avd(r_{cpa}) \tag{2.2}$$

$$avd = avd(\Theta_{cpa})$$

$$avd = avd(t_{cpa})$$

$$avd = avd(r_{cpa}, \Theta_{cpa}, t_{cpa})$$

$$w = w(r) \tag{2.3}$$

$$w = w(t_{cpa})$$

$$w = w(\Theta_{cpa})$$

$$w = w(\dot{r})$$

$$w = w(r, t_{cpa}, \Theta_{cpa}, \dot{r})$$

2.4 Collision Avoidance Testing and Evaluation

Canonical geometries for testing collision avoidance techniques are worthwhile in academic environments to improve algorithms and verify test cases, but they offer limited value in practical real-world vessel encounters. Less predictable encounter geometries occur in manned vessels environments where complex interrelations and less predictable initial geometries are present. Many factors can contribute to the less orderly encounter geometry. Some of the reasons that canonical geometries are insufficient are amplified by the following considerations:

- unique missions
- differing end points of each local vessel’s track
- unique maneuvering characteristics and capabilities of each vessel
- complicating characteristics of each encountered vessel including, for example, towed bodies, nets, or appendages
- tracks falling near transitions of traffic separation schemes
- ranges of stability in various sea states and environmental conditions forcing certain courses to be driven
- proficiency and awareness of the crews of manned vessels or sensing capabilities of their autonomous or remotely operated counterparts

Several examples of protocol based collision avoidance are found in the literature. Many of these authors [49, 50, 60–62] studied single vehicle pairs at any given time. Of those studies examining multiple vehicles, the scenarios often appear in sequential single vehicle pairs such as a vessel crossing a wide sea-lane. Several simulation-based protocol tests have also been conducted recently though many are limited in their scope to near-canonical encounter geometries and limited simultaneous, multi-contact encounters. These geometrically canonical or otherwise constrained encounters often evaluate either orthogonal or parallel tracks. In most recent literature, these “multi-contact” tests occur in succession rather than simultaneous fashion, thus limiting the utility of rigorously testing the underlying collision avoidance algorithms. More interesting results occur when the algorithms are stressed with competing constraints of both protocol and operational importance simultaneously.

2.5 Velocity Obstacle Collision Avoidance Algorithms

Since first introduced, the velocity obstacle has been widely used as a technique to eliminate course-speed pairs that would cause a collision. The velocity obstacle family of algorithms has developed to include many novel improvements to the underlying velocity obstacle algorithm. The velocity obstacle family is introduced and its evolutionary results are discussed.

2.5.1 Traditional Velocity Obstacles

The velocity obstacle family includes several variations of the original algorithm. Velocity obstacles were first introduced by Fiorini to allow for a transformation of a single dynamic planning problem into m static problem by introducing circular or more complex geometric objects in velocity space and projecting their motion in finite time along a linear path [26, 27]. Fiorini found that an efficient algorithm was needed as an alternative to explicitly solving the complicated dynamic problems associated with collision avoidance of an object and the obstacles it may encounter. By transforming the collision problems to velocity space, vector transformation was possible to scale the technique to multiple concurrent collision avoidance instances. Using Fiorini's notation in [26, 27], relative velocity is defined by $V_{0,i} = V_o - V_i$ for ownship (object) obj_o and any contact (obstacle) obs_i . The relative trajectory is defined by $trj_{0,i} = \{(x, \dot{x}) | \dot{x}(t_0) = V_{0,i}, x(t_0) = x_o\}$, and a collision exists in velocity obstacle problems if $trj_{0,i} \cap obs_i \neq \emptyset$. A collision cone is generated based on the relative trajectories $trj_{0,i}$ of the object obj_o and obstacles obs_i , and a translation can be made to obtain the absolute collision cone $CC_0(t_0)$ and thus the absolute velocities causing such a collision as shown in Equation (2.4) using the notation of [26]⁴. It is this absolute collision cone that Fiorini calls the Velocity Obstacle for a prescribed shape and size of collision shape. The selection of the shape including its size is a

⁴The notation shifted in [27] such that relative trajectory $\lambda \equiv trj_{0,i}$. The remainder of this thesis will refer to λ .

design choice that defines the effective “collision distance” of an object with respect to one or more obstacles.

$$\begin{aligned}
 v_0 &\in \overline{CC_0(t_0)} & (2.4) \\
 CC_0(t_0) &= \{v_0 | trj_{0,i} \in CC_0(t_0)\}
 \end{aligned}$$

Velocity obstacles reduced complicated brute force calculations of closest point of approach to a more manageable decision space of “allowed/excluded” regions by linearly projecting instantaneous velocities in time and determining if a single, fixed collision range threshold was violated. Collision discs of fixed ranges were traditionally used for both the object and the several obstacles to determine a superimposed region of excluded velocity vectors deemed to result in a “collision” within the velocity space. Here a collision implies a violation of the range threshold of one or more obstacles; however, with the additional margins built into the designer’s selection of a collision disc radius, a collision would not necessarily result in physical contact of two bodies.

The summation of the various velocity obstacle wedges in polar space (radius = speed, angle = course) resulted in a set of feasible solution space from which the course-speed decision could be made. Velocity obstacles create a first-order approximation of a vehicle’s velocities that would cause a collision within a finite time horizon but do not offer further information beyond whether a collision will or will not result [27]. Consideration is given to vehicle dynamics to determine the set of reachable (feasible) avoidance velocities [27]. Fiorini introduced several heuristics for consideration including choosing the highest avoidance velocity along the path of the goal, selection of the maximum avoidance velocity within some allowed deviation angle from the goal, and selection of a velocity that avoids the obstacles as ranked by their perceived risk. The first two heuristics assume an *a priori* known goal direction implying prior calculation of the optimal solution without regard to obstacles. The third heuristic chooses the “velocity that avoids that obstacles according to their perceived

risk” though no further details are given [27].

Using the utility function concept of Section 2.3.3, the binary state of velocity obstacles result in a safe or unsafe value and can therefore be mapped to a uniform stepwise function with values $\in \{0, 1\}$. A nominal velocity obstacle utility function mapping is shown in Figure 2-4 where the independent axis shows “collision range” and the dependent axis shows resulting utility. Note that the function has a stepwise increase to a safe value at the only range of concern: collision range. Using the family of velocity obstacle techniques, this collision range must account for ownship dimensions, contact ship dimensions, uncertainty standoffs, and a buffer range for peace of mind to the operator. Using a polar heat map (red = safe, blue = unsafe) shown in Figure 2-5, candidate velocity vectors can be mapped to a polar stepwise function representing the maneuvers determined to be safe for a contact.

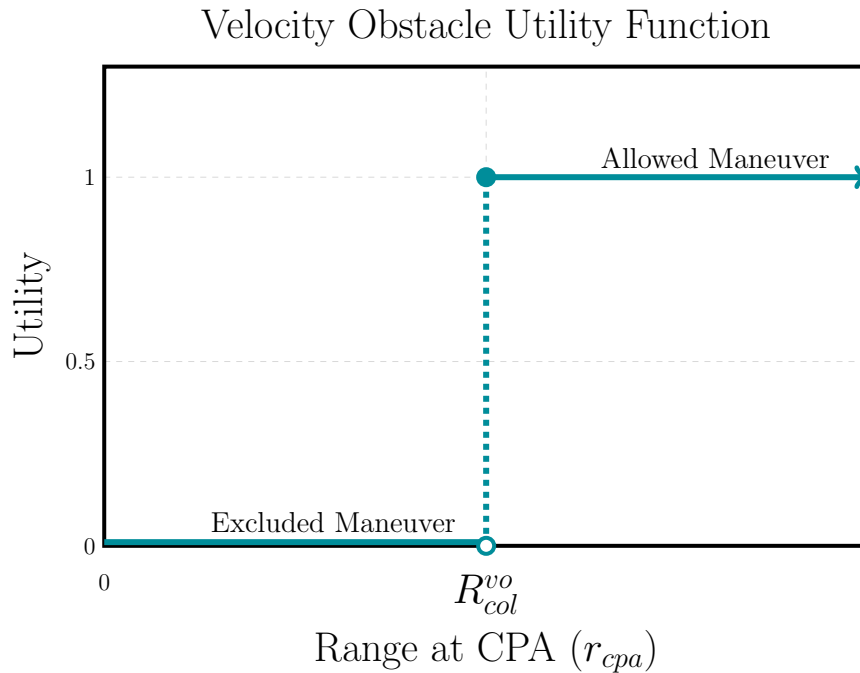


Figure 2-4 A nominal velocity obstacle utility function is shown representing the stepwise increase in safety as a resulting maneuver’s range crosses the *a priori* determined collision range.

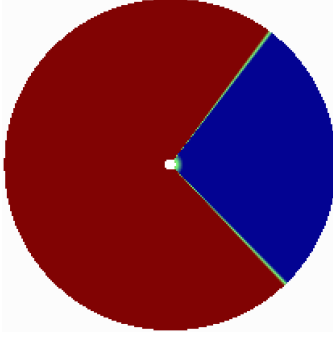


Figure 2-5 The aggregate of utility values for all candidate course-speed pairs is shown in a polar heat map where red is desirable (safe) and blue is undesirable (unsafe).

2.5.2 Generalized Velocity Obstacles

Wilkie *et al.* expanded on Fiorini’s work to define the generalized velocity obstacle [92]. The generalized velocity obstacle takes into account constraints of car-like robots that are then able to use a velocity obstacle-like approach. To achieve this, feasible control solution sets must be sampled for all controls on each iteration. By allowing kinematically constrained agents to consider a velocity obstacle-like approach, Wilkie *et al.* found that it was possible for their circularly shaped objects to, in some cases, determine an explicit equation for the velocity obstacle itself. Wilkie’s definition of the generalized velocity obstacle in the notation of [92] is shown in Equation (2.5) for object A with size $radius = r_A$ of control input u opposing obstacle B of size $radius = r_B$ for time t . This method admittedly has limitations including numerical inaccuracies requiring a safety buffer, high sensitivity to measured noise, low suitability for complex environments with local minima, and no guarantee to find a feasible solution even if one exists [92].

$$\{u|\exists t > 0 :: \|A(t, u) - B(t)\| < r_A + r_B\} \quad (2.5)$$

2.5.3 Reciprocal Velocity Obstacles

Reciprocal velocity obstacles for real-time multi-agent navigation were introduced by van den Berg to consider multiple dynamic obstacles as an extension of the traditional velocity obstacle. The work of van den Berg *et al.* introduces the reciprocal velocity obstacle which “implicitly assumes that the other agents make a similar collision-avoidance reasoning [90].” This algorithm therefore accounts for the assumed collision avoidance reaction of the opposing vessel. The oscillatory behavior is avoided by selecting velocities based on the mean of its current velocity and a velocity lying outside the other agent’s velocity obstacle. By invoking the assumption, the reciprocal velocity obstacle guarantees an oscillation-free collision avoidance decision with respect to which side of the contact ownership will pass. The work of van den Berg *et al.* advanced Fiorini’s work while adding a method to counter the oscillations often seen in multi-agent navigation [90]. The original representation of the reciprocal velocity obstacle is shown in Equation (2.6) where object A encounters obstacle B .

While 2D space was assumed, this could easily be translated to 3D geometries. The contact’s position and velocity are again required (as in the traditional velocity obstacles) and some assumption or acquired data about the shape of the obstacle is required. Each of the obstacles is kinematically and dynamically constrained as appropriate including maximum speed and maximum acceleration. In the event of a multi-agent candidate decision space that is wholly precluded by reciprocal velocity obstacles, van den Berg allows for violation of the reciprocal velocity obstacles while assessing a weighted penalty based on the expected time of collision and the deviation from the *a priori* preferred mission velocity vector. A limitation of the reciprocal velocity obstacle in practice is thrashing when two agents are unable to “agree” on which side to pass each other [70].

$$RVO_B^A(v_B, v_A) = \{v'_A | 2v'_A - v_a \in VO_B^A(v_B)\} \quad (2.6)$$

2.5.4 Generalized Reciprocal Velocity Obstacles

The reciprocal velocity obstacle is then generalized by van den Berg to create the generalized reciprocal velocity obstacle that assumes a linear weighting scheme to select a velocity between the current velocity and the candidate velocity that lies outside the velocity obstacle. By choosing the weight of the current velocity to be zero, the generalized reciprocal velocity obstacle recovers Fiorini’s traditional velocity obstacle. Geometrically, van den Berg shows that this is similar to a translation of the velocity obstacle apex to $(1 - \alpha_B^A)v_A + \alpha_B^A v_B$ for the share of effort A avoids B, α_B^A . Much like with other velocity obstacle algorithms, this approach allows for the combination of multi-agent collision avoidance constraints by summing the excluded regions to form a combined reciprocal velocity obstacle. Also similar to other related velocity obstacle techniques, selection of the final velocity vector using the reciprocal velocity obstacle relies on a technique of exclusion rather than preference. The generalized reciprocal velocity obstacle is shown in Equation (2.7) using the original notation of [90].

A preferred velocity vector without regard to potential collisions must be selected then the reciprocal velocity obstacle constraints applied. In cases where the preferred velocity vector is excluded by one or more reciprocal velocity obstacles, the velocity vector closest to the preferred velocity but outside the combined reciprocal velocity obstacle (and therefore inside the admissible velocity space) is chosen [90]. In the case of a fully excluded velocity decision space due to a combined reciprocal velocity obstacle that fully fills the set of admissible velocities, van den Berg allows selection of a velocity vector inside the excluded reciprocal velocity obstacle space (Equation (2.7)) while assigning a penalty dependent on the “distance” to the preferred velocity vector as measured by a vector norm plus a weighted time-to-collision factor. Then the velocity with the minimal penalty is selected as the new velocity. The penalty scheme is shown in Equation (2.8) using van den Berg’s notation with weight w_i to “reflect difference in aggressiveness and sluggishness [90]” to select the final velocity as that with the smallest penalty value as shown in van den Berg’s notation in Equation (2.9).

$$RVO_B^A(v_B, v_A, \alpha_B^A) = \{v'_A | \frac{1}{\alpha_B^A}v'_A + (1 - \frac{1}{\alpha_B^A})v_a \in VO_B^A(v_B)\} \quad (2.7)$$

$$penalty_i(v'_i) = w_i \frac{1}{tc_i(v'_i)} + \|v_i^{pref} - v'_i\| \quad (2.8)$$

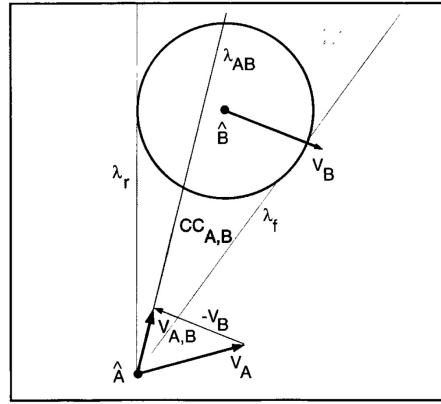
$$v'_i = \underset{v''_i \in AV^i}{\operatorname{argmin}} penalty_i(v''_i) \quad (2.9)$$

2.5.5 Hybrid Reciprocal Velocity Obstacles

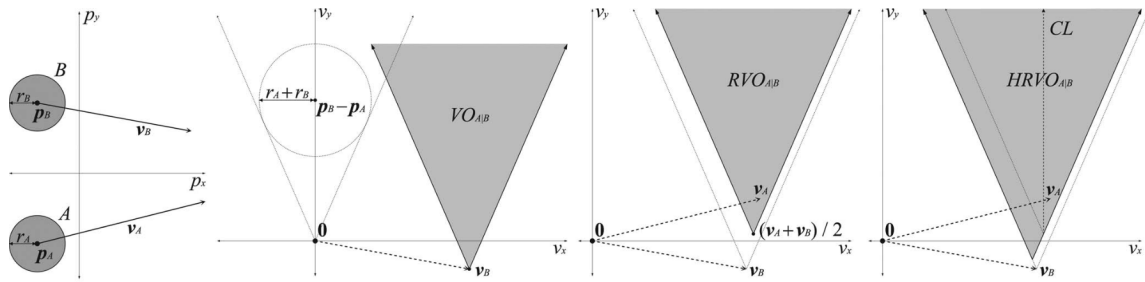
One limitation of the reciprocal velocity obstacle is that it can often enter a “reciprocal dance” when unable to reach agreement on which side to pass due to the implicit assumption of similarity in collision avoidance reasoning. The effective lock into an oscillatory pattern is addressed by Snape *et al.* using the hybrid reciprocal velocity obstacle [70]. Snape presented the hybrid reciprocal velocity obstacle which, as its name implies, is a hybrid of the velocity obstacle and the reciprocal velocity obstacle [70]. With a hybrid velocity obstacle, thrashing is reduced by yielding priority to the other agent if its first solution incorrectly assumed the side that would be passed in effect resulting in a traditional velocity obstacle. If the correct passing side was chosen, then cooperation with the other agent is assumed and actions continue with the benefits of the reciprocal velocity obstacle. If a vehicle incorrectly assumes the best side to pass another vehicle, then the hybrid reciprocal velocity obstacle forces ownership to yield full priority to the other vehicle. When both vehicles choose the “correct” side, then their cooperative nature is rewarded by retaining an equal priority similar to the reciprocal velocity obstacle [70]. Similar to other velocity obstacle techniques, the candidate velocities are prioritized by determining the closest non-excluded velocity to the *a priori* determined preferred velocity vector. As with other velocity obstacle techniques, the hybrid reciprocal velocity obstacle relies on an *a*

priori known “preferred velocity” $v_{A_i}^{pref}$ as shown in Equation (2.10) and expressed in the original notation of [70]. Figure 2-6 demonstrates the traditional velocity obstacle and its evolution in recent literature.

$$v_{A_i}^{new} = \underset{v \notin HRVO_{A_i}}{\operatorname{argmin}} \|v - v_{A_i}^{pref}\|_2 \quad (2.10)$$



(a) Velocity Obstacles



(b) Generalized Velocity Obstacles

Figure 2-6 Fiorini’s relative velocity $v_{A,B}$ and collision cone $CC_{A,B}$ are shown in (a). Image (a) is Figure 2 from [27]. Example sketches of different forms of velocity obstacles (b) shows the evolution of the velocity obstacle, reciprocal velocity obstacle, and hybrid reciprocal velocity obstacle. Image (b) is Figure 1 from [70].

2.6 Velocity Obstacle Techniques in Practice

Kuwata *et al.* employed velocity obstacles to demonstrate COLREGS-based collision avoidance with a single fixed threshold value of collision range including an additional safety margin offset [45] (Figure 2-7). Maneuvers resulting in COLREGS violations were superimposed on the velocity obstacle to further restrict the velocity vector decision space. The safety margin offset was just slightly larger than the actual velocity obstacle and used to account for worst case uncertainty resulting from “noise and state estimation errors for the tracked traffic boat.” Relaxation of the safety margin offset was possible for very distant contacts (as determined by time to CPA) whose sensor noise was irrelevant. Candidate solutions that were still admissible after velocity obstacle and COLREGS pruning then received a cost value based on time to collision and deviation from the mission-preferred velocity vector. On-water experimental results demonstrated a successful maneuver for a head-on contact pair detected using onboard sensors.

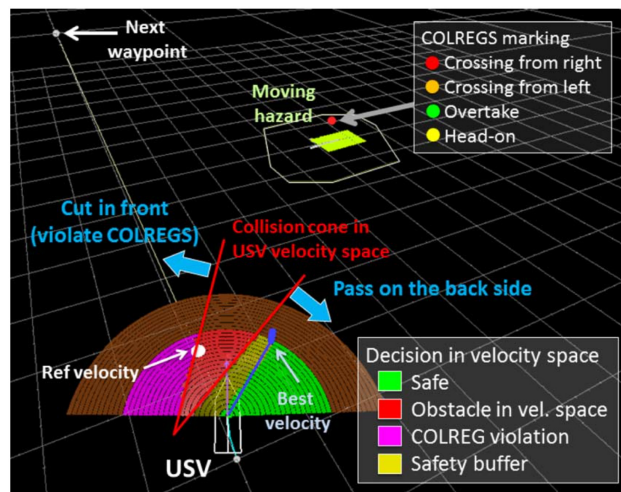


Figure 2-7 Kuwata applied the traditional velocity obstacle with an additional exclusion range for maneuvers that were said to be non-compliant with COLREGS. Image is Figure 10 from [45].

Shah [66] used a model-predictive trajectory planner with A^* and velocity obstacles in a “5D” state space (X,Y, speed, heading, time) to find a feasible control space as well as a contingency control space for emergency reactions in case of a non-compliant

vessel. This approach looked for the least cost from a given weighting scheme and used adaptive control action primitives with velocity obstacles. Shah further claimed “it may be in the USV’s best interest to actually breach COLREGS by turning left to avoid a collision.” The necessity to avoid a turn to port when at risk of collision with another vessel cannot be overemphasized. To characterize this breach of the Rules as a best interest reflects an absence of real-world experience navigating the nuances of Rules. Other authors continue to develop different algorithms for COLREGS-based collision avoidance using velocity obstacles as the underlying collision checker. Leng used velocity obstacles with mixed integer linear programming though a further computation was used to include CPA range and time [54]. This additional calculation was based on a single value for range discrimination. Future work from this author claims to look at the environmental factors and increased algorithm efficiency. Shah claims that this study resulted in improved planner performance and lower incidence of collisions compared Kuwata’s velocity obstacle-based COLREGS planner [45, 46].

Specifically, Shah claims that the deliberative planner has significantly fewer collisions than Kuwata’s velocity obstacle-based planner primarily due to the lack of consideration of vehicle dynamics and motion of contact vessels. To make this statement definitively, however, consideration must be given to the objective construction of experiments to remove other variables. The only variable that was consistent seemed to be the number of vehicles interacting. There was no consistency shown for any other variables including geometry of encounters, speed of encounters, applicable COLREGS rules at the time of interaction, range until first action, range of required action, and priority of collision avoidance with respect to other mission parameters. A more in depth analysis of these variables and their affects on both track efficiency and collision percentage is detailed in [93] using a CPA-based approach rather than velocity obstacles. Shah [67] later expands this to adaptively scale motion primitives during the search for a trajectory based on a traffic congestion metric.

2.7 Closest Point of Approach (CPA) Collision Avoidance Algorithms

Explicit CPA calculations were used to demonstrate COLREGS-based collision avoidance by Benjamin *et al.* using on-water autonomous testing [4, 5]. Benjamin’s work avoided brute force CPA calculations by invoking interval programming to sample the underlying decision space [3]. Further testing using explicit CPA calculations was demonstrated for an ocean-going catamaran in [24]. Choi *et al.* used a CPA range based algorithm to determine collision likelihood for a single fixed collision range threshold with multiple unmanned aerial vehicles [14]. Adherence to the Rules of the Air protocol was not addressed.

Rather than “transform[ing] a single dynamic planning problem into m static problems,[27]” explicit quantification techniques maintain the single dynamic problem for each contact pair. With the advances of computational power and sampling algorithms [7] since Fiorini introduced velocity obstacles, use of these more informative techniques are now available to onboard payload computers in real time.

Closest point of approach (CPA) based continuous decision space methods maintain the problem in the dynamic domain for computation of an exact value of CPA range, time, pose, and other desired information for each contact for each point of interest in the velocity space. By reasoning about exact numeric values rather than a boolean, the CPA method allows for consideration of a more decision-rich velocity vector space. When entering a multi-contact collision avoidance situation possibly with multiple competing mission objectives, known values of utility and risk can be incorporated to allow for more informed determination of the velocity vector.

Velocity obstacles are excellent for path following scenarios where the objective is to “follow a pre-defined path, which only involves a spatial constraint [11].” Using RRTs, several authors have achieved path tracking where the objective includes temporal data along the pre-defined path. For missions that are more complex than successive waypoint traversal, real-time path creation is necessary often with multiple competing inputs. One example of a real-time path creation problem for an

autonomous surface vessel is acoustic-based target tracking of a submerged contact. Based on the complex nature of localization and tracking of an underwater target coupled with the inherently uncooperative relationship and additional complications of honoring the protocol constraints of collision avoidance with other surface vessels, a waypoint traversal of global path planning is infeasible. When considering the use of evolving tactics, “a combination of deliberative, reactive, and reflexive path planning is required [9].” Rather, real-time local path planning that can appropriately account for all mission, navigation, and protocol-based collision avoidance constraints has lagged in the literature.

2.7.1 Real-Time, Non-Brute Force Methods: Interval Programming (IvP)

CPA-based collision avoidance algorithms are possible because of sufficient advances in sampling techniques within the last decade. Representing the entire decision space using brute force calculations rather than an intelligent sampling algorithm would result in extreme inefficiencies. Interval programming (IvP) provides an algorithmic approach to appropriately sample a decision space without the inefficiencies of brute force techniques. This sampling of the underlying decision space allows the expanded state space precision without sacrificing computational capabilities.

IvP constructs a set of piecewise linearly defined IvP pieces that represent the portion of the objective function that underlies each piece. By adjusting the coarseness of the overall sample, efficiency can be gained. By locally refining pieces of insufficient fit by constructing additional pieces from further sampling, a more accurate approximation to the underlying function is realized without compromising the efficiency gains.

The interval programming (IvP) model uses piecewise linearly defined objective functions that may represent only an approximation of an underlying objective function [3]. These functions are then searched through the combination space of pieces rather than through the actual decision space thus freeing the algorithm from form

assumptions and guaranteeing global optimality within the limitations of any approximation errors during formation. Techniques to produce accurate and efficient piecewise linear approximations for objective functions are more thoroughly discussed in [3–5, 8].

The interval programming model assumes that each decision variable within the decision space is finite, uniformly discrete, and consists of known upper and lower bounds. For the course-speed decision space of collision avoidance, this model fits well: upper and lower bounds of both decision variables are known ($\theta \in [0^\circ, 360^\circ]$ and $v \in [0, v_{max}]$); the decision space can be considered uniformly discrete (e.g., courses resolved to 0.5° precision); and, the decision space for each decision variable is therefore finite. The overall multi-variable decision space is also therefore finite and uniformly discrete. Little to no loss is assumed in the fidelity of the problem by assuming these uniformly discrete decision steps within each variable: to order a course or speed of greater precision is both unnecessary and wasteful of computational resources [3].

A proper IvP problem requires two components: IvP pieces and IvP functions. IvP piece construction uses the techniques shown in Equation (2.11) for rectilinear pieces where edges are parallel to the variable axes. IvP allows non-rectilinear pieces to be used as well by including the evaluation of some function $f(x, y)$, for example, as part of the interior function as shown in Equation (2.12). Each IvP piece is defined by upper and lower bounds for each decision variable and an interior function using the notation first described in [8].

As detailed in [3, 8], an IvP function has several representational restrictions including: each point in the decision space is contained in at most one piece, each piece is given by one set of boundary intervals for each decision variable, and each piece has a linear interior function used to evaluate each point in that piece. Any point not contained in a piece is considered infeasible. The assumption of a uniformly spaced decision space does not imply uniform distribution of pieces nor uniform shape of pieces [3].

$$\text{rect}(i) = m_{x_i}x + m_{y_i}y + c_i \quad (2.11)$$

$$x_i^- \leq x \leq x_i^+$$

$$y_i^- \leq y \leq y_i^+$$

$$\text{nonrect}(i) = m_{x_i}x + m_{y_i}y + m_{f_i}f + c_i \quad (2.12)$$

$$x_i^- \leq x \leq x_i^+$$

$$y_i^- \leq y \leq y_i^+$$

$$f_i^- \leq f(x, y) \leq f_i^+$$

An IvP problem is then formed by a collection of IvP functions (one per objective function) and their associated priority weights. The IvP functions reflect the design intentions that best realize the desired outcome of the behavior over each course-speed pair while the priority weight accounts for each function's relative importance to the vehicle's overall goal with account for appropriate state and environmental context.

The IvP model can lead to a natural tendency to discuss brute force techniques to exhaustively search a decision space for a globally optimal solution. These methods however do not scale especially when considering the multi-contact collision avoidance problem without leveraging computing power disproportionate to the vessel's appropriate outfitting. IvP, however, has guaranteed global optimality while balancing accuracy, speed, and flexibility [8]. While full brute force methods fall short in speed, simplified brute force methods fall short in accuracy, and analytical methods fall short in flexibility, IvP offers an appropriate balance of accuracy, speed, and flexibility. To achieve this balance, IvP problems must be accurate and efficient for both creation and solution phases. Additional details on these properties and the techniques used

to efficiently solve IvP problems are found in [8].

2.8 CPA Techniques in Practice

Choi examined reactive collision avoidance for multiple mid-air UAVs using a CPA-based collision avoidance algorithm [14]. Choi described this work as a reactive navigation method to inform the previously planned path. Choi’s collision avoidance utility function was designed based on a single range threshold. Choi used a mid-air collision “miss distance” to determine his proximity to the *a priori* defined safety radius as shown in Figure 2-8. Choi used disc geometry for all aircraft and neglected the protocol requirements for aerial vehicles (Rules of the Air). Multiple vehicles were considered simultaneously using weighted cost objective functions. Numerical simulations were performed for various 1-on-1 and 2-on-1 encounters showed positive results. A simulation of up to 8 simultaneous simulated aircraft demonstrated a star-like pattern was possible without collision or altitude separation, though protocol constraints were not invoked.

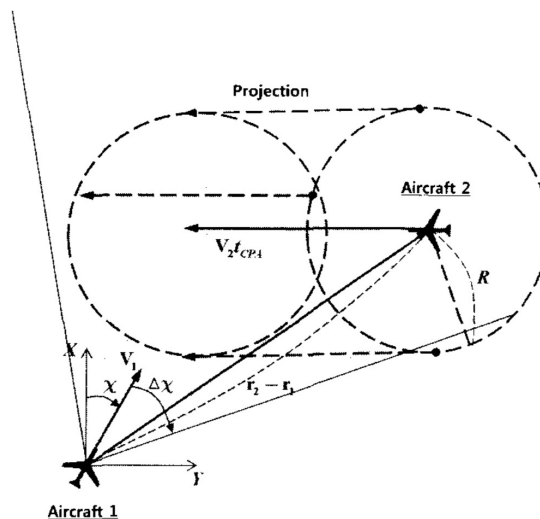


Figure 2-8 Choi used a safety area based on fixed range of ownship (airplane). Image is Figure 2 from [14].

Benjamin *et al.* first demonstrated on-water experimentation with CPA-based techniques under protocol constraints [4, 5]. Two vehicles were simultaneously un-

derway for waypoint-driven missions when they encountered each other. Benjamin demonstrated successful maneuvers that honored the protocol requirements of COLREGS. These single contact interactions were demonstrated with up to five on-water encounters while obeying COLREGS in [93]. Use of explicit quantification of CPA to examine safety and efficiency of the resulting maneuvers was described in [95]. This study of safety and efficiency was the first to give design effects based on input parameters for safety and efficiency while obeying a protocol constraint.

CPA-based collision avoidance techniques such as that used in [4, 5] rely on range calculations in the dynamic planning space based on geometric projection of all vehicles in time. The CPA ranges for each candidate course-speed pair are retained for each contact with which ownship has a potential interaction within a finite and prescribed look ahead time.

2.9 COLREGS Compliance in the Literature

Non-protocol based methods of collision avoidance are inconsistent with international law and are therefore insufficient as advances in marine autonomy intended for inclusion in human-present vessel environments that operate exclusively under protocol-based rules. These non-protocol based methods might be useful in specific conditions which are isolated from interactions with the general human-present marine environment but are inherently unable to be applied in human-present ocean-going collision avoidance applications where the COLREGS prevail. They therefore do not contribute to the human-robot integration of autonomous collision avoidance in a general practical sense, but rather add value to components that may be used by COLREGS-based solutions. Further, [93] showed that protocol constraints result in more safe, efficient, and predictable maneuvers than non-protocol constrained collision avoidance.

Other studies claim to be “COLREGS-compliant” but suggest allowing explicit violations of the Rules in certain scenarios. Violations of the Rules such as turning to port when a risk of collision exists [66] call into serious question the validity of

the study’s underlying collision avoidance algorithms and the researcher’s experience with the Rules. Experienced mariners would be highly unwilling to turn to port when a risk of collision exists especially in a more complex multi-interaction scenario where a turn to port sets into motion a cascade of reactions by other vessels. Proper action when a turn to port seems attractive is often to slow or back down rather than alter course to port. This decision to slow a vessel’s forward speed is also prudent for more complex situations such as multiple rules being concurrently relevant where direct communication is unavailable to resolve other vessels’ intentions or more time to analyze a situation might reduce the risk of a hasty and dangerous maneuver. Few authors have examined the tradespace of taking way off a vessel rather than finding a least-cost deviation from the mission preferred velocity vector.

Many collision avoidance algorithms have been designed for autonomous marine decision making by those with little real-world ship driving experience. The Rules are complex, vague, and full of nuances that must be considered; however, the true intuition required to appropriately invoke the Rules requires not only science but an art learned from proper application of these more nuanced scenarios while participating in real-world ship driving.

Collision avoidance protocols are prevalent in many physical domains where explicit negotiation or communication is either impractical or infeasible. In common practice, these protocols are often communicated simply as having “right of way.” In ground transit, drivers are taught to yield to the driver on the right when arriving simultaneously at an intersection with stop signs [18]. Airplanes use the Rules of the Air to determine right of way and appropriate maneuvers when not under active control of an air traffic controller [40]. Surface vessels similarly abide by the COLREGS to determine right of way and appropriate maneuvers without explicit communication [84]. Special rules within each protocol have evolved from real-world feedback; one such example is the traffic separation schemes of COLREGS when entering or exiting a harbor [17, 82]. While the Rules of the Air and COLREGS are largely similar, differences in the physical domains manifest as differences between the collision avoidance protocol requirements such as maintaining altitude separation.

Collision avoidance using COLREGS has been incorporated on autonomous vessels using various approaches since first introduced in [5]. Throughout maritime literature discussing COLREGS, the term “compliance” arises in varying context and meaning. Power-driven collision avoidance implementations of COLREGS (Rules 13-18) dominate the COLREGS-related literature. Other non-collision avoidance rules of COLREGS arise as being compliant within the literature when discussing acoustic detection and light configurations [20, 28].

Testing to date in the literature does not demonstrate what the term compliance means in any quantifiable fashion. Several authors claim compliance with these protocols without specifying the degree or scope of compliance [45, 66, 93]. In [45], the head-on rule was shown to appropriately eliminate all turns to port. It did not, however, appear to prefer courses that were “readily apparent” (COLREGS Rule 8) when finding a turn to starboard. Case law defines apparent course maneuvers to consist of a minimum of 35° turn while common practice often requires no less than 30° of heading change [1, 17, 85, 86]. Courts have found that head-on maneuvers with insufficient turns (i.e., not readily apparent) are in fact non-compliant and, when a collision occurs, partly to blame. The concern with readily apparent maneuvers rests with the ambiguity of a series of successive subtle (i.e., small) course maneuvers that are not easily recognized by other vessel operators. Therefore course maneuvers are required to be large enough to be easily recognized and allow for response by other vessels in vicinity. With velocity vector cost functions that favor maintaining course and speed [45, 90], improper selection of costing weights may easily result in less than apparent course changes. Other authors consider breaches of COLREGS that “may be in the USV’s best interest” such as turning to port to avoid a collision when explicitly prohibited by the COLREGS [66]. Many authors such as [93] simply claimed COLREGS compliance without any quantification or definition of scope.

Case law and common practice greatly influence the requirements of COLREGS despite not being found anywhere within the written rules. Examples of on-water collisions and case law provide relevant insight into nuances of the COLREGS and their evolution over the years. Areas for increased scrutiny in autonomous collision avoid-

ance solutions can be derived from problematic past encounters of human ship drivers. The intentional vagueness of the COLREGS including their underlying meaning as derived from the evolution of protocol-constrained collision avoidance in maritime environments, analysis of real-world examples, critiques of experienced mariners, and relevant rulings from Courts of Admiralty are presented in detail in [1, 17, 33, 82, 100] with examples presented as appropriate in this thesis.

2.10 Protocol Evaluation

The literature in general currently lacks any means of objectively quantifying a degree of compliance a vessel has with COLREGS. The Rules give guidance and requirements under many situations, though they are intentionally written quite vaguely to capture the human component of ship driving and to allow the master of a vessel to make his or her best judgment as to the appropriate maneuver. However, the master's intuition does not always succeed and collisions inevitably occur. There is no scorecard or other means of determining a numeric value to relate a vessel's actions with how consistent a maneuver or series of maneuvers is with respect to the intention of the Rules. That is, there is currently no means of scoring other than whether a vessel was or was not in a collision – simply a 0 or 1.

However, the majority of literature that includes collision avoidance often deviates from track to mitigate a collision risk then either returns to the *a priori* determined path or computes a new path to the objective end point once the collision risk has passed. There is no existing standard for evaluation or reasoning about higher order requirements that consider collision avoidance in the larger local reactive path planning optimization problem.

A certification scheme for protocol-based collision avoidance currently does not exist. This requires several components to evaluate rule compliance, safety, and efficiency. A means to allocate a numerical grade to the performance of a vehicle's compliance with the rules is necessary. A means to determine the degree to which the vehicle operated safely must be determined and incorporated into this score. Taking

excessive liberty to stretch the intention of the rules should not be rewarded; likewise, making overly conservative maneuvers that might delay or possibly increase risk to other vessels must also be avoided. While perhaps not an explicit violation of any rule, certain behaviors are inconsistent with normal maritime operations and must be penalized in order to allow a timely, safe, and natural evolution of autonomously controlled vehicles into the human-present marine domain.

2.11 Summary of Collision Avoidance Testing

Much of the collision avoidance testing in the literature can be categorized as preliminary steps toward autonomous vessel interactions using one or more of the following:

- experiments are limited to single vehicle pair interactions (this includes contacts that may be lumped into being effectively one contact)
- canonical encounter geometries are the norm with nearly parallel or perpendicular tracks
- opposing vessels are often predictably compliant or simply maintain course and speed
- non-protocol based methods are used with disregard to established protocols such as COLREGS
- human interactions and emulation are the exception and rarely mentioned

Many studies perform testing exclusively in simulated environments without validating their results with on-water testing. On-water testing is key to demonstrating that laboratory results will be realizable in real-world environments. Further complicating the literature is the absence of an objective method or algorithm to evaluate COLREGS with quantifiable output.

A more broad comparison of literature can be summarized in Table 2.1. CPA methods and “state of the art” velocity obstacle methods generally refer to marine literature. UAV collision avoidance methods in the literature predominantly rely on

velocity obstacle techniques while largely ignoring their protocol requirements of [40]. Similarly, the Google Car provides an example of in-field experimentation performed on autonomous ground vehicles with human interaction.

Table 2.1 Summary of Literature Attributes Relative to this Thesis

Previous Work	Physical Domain	Number ‡ of Vehicles	In-Field Experiments	Avoidance Algorithm	Protocol Constraints	Compliance Claimed	Human Interaction
Benjamin (CPA Methods)	Marine Surface	2 + 0	On-Water	CPA	COLREGS	Qualitative	No
Choi (UAVs)	Aerial	8 + 0	Simulated Only	CPA	None	N/A	No
Google Car	Ground	varies	On Road	Proprietary	Car Rules	N/A	Yes
Kuwata (State of the Art)	Marine Surface	1 + 3	On-Water	Velocity Obstacles	COLREGS	Qualitative	Yes
Shah	Marine Surface	5 + 0	Simulated Only	Velocity Obstacles	COLREGS (limited and violated)	Qualitative	No
Svec	Marine Surface	2 + 1 (following only)	On-Water	Velocity Obstacles	COLREGS (following)	Qualitative	Yes
This Thesis	Marine Surface	5+1	On-Water	Full CPA (w/ Pose)	COLREGS	Quantitative	Yes

‡ number of vehicles displayed as autonomous + human-operated

Chapter 3

Protocol-Constrained Collision Avoidance Objective Functions

This chapter¹ examines autonomous collision avoidance algorithms² and shows the generalization of the velocity obstacle using CPA-based methods. Section 3.1 describes multi-objective optimization formulation including the direct application to marine autonomy. Section 3.2 describes the closest point of approach method. Section 3.3 introduces the full CPA quantification algorithm and mathematically shows its generalization of the velocity obstacle currently used in state of the art systems. Section 3.6 introduces the course-speed decision ratio and the patience parameter to adapt primary mission objective function designs under collision avoidance constraints to maximize the performance metrics of Section 4.1. The concepts presented in this chapter create a foundation for the evaluation construct presented in Chapter 4.

3.1 Objective Function Construct

The construct of multi-objective optimization applies naturally to multi-contact, complex mission scenarios in marine autonomy. Each of a vehicle's several mission and navigation constraints maps to its own objective function. Similarly, each collision

¹Portions of this chapter first appeared in [93].

²Appendix B describes the notation used throughout this chapter.

avoidance vehicle pair maps to a unique objective function designed to adhere to the appropriate protocol constraints. This section describes the application of multi-objective optimization and objective function design. This section further describes the design of the protocol-constrained collision avoidance objective functions including their utility and priority weight functions within the context of the larger multi-objective optimization problem.

3.1.1 Multi-Objective Optimization

Multi-objective optimization seeks a globally optimal solution allowing autonomous decision makers to balance the many competing mission, navigation, and collision avoidance objectives. Each instantiation of a behavior forms its own objective function that expresses the designer’s³ intentions while accounting for real-time environmental and state conditions. Each objective function in turn has a priority weight that mathematically represents its relative importance to the overall decision scheme. A mathematical solver then finds the globally optimal solution vector that maximizes the combined weighted utilities over the collective domain of each decision variable according to the assigned priority weights.

The multi-objective optimization problem defined by Equation (3.1) determines a globally optimal solution for the given objective functions. Each $f_i(x_1, \dots, x_n)$ defines the objective function for the i^{th} of k active behaviors. The vector \vec{x} represents a candidate decision vector within the decision space. The vector \vec{x}^* represents the globally optimal solution of Equation (3.1). The evaluation of each f_i at some candidate \vec{x} gives a value for the candidate vector’s utility. The set of utility values over the decision space defines the surface of each objective function. Each objective function receives a priority weight w_i ($w_i \geq 0$) that represents the relative importance of the i^{th} behavior with respect to the overall system. Priority weights receive their values from current environmental and state variables according to the designer’s poli-

³Throughout this thesis, the term designer refers generally to both the person creating the software and the operator configuring a vehicle for deployment. Both of these entities make decisions that directly affect the decisions of the underlying autonomy.

cies. A behavior in this context represents any one of the many competing priorities of a vehicle; a behavior may also have multiple simultaneous instantiations. Each instantiation then becomes active once its priority weight w_i becomes positive.

$$\vec{x}^* = \underset{\vec{x}}{\operatorname{argmax}} \sum_{i=1}^k (w_i \cdot f_i(\vec{x})) \quad (3.1)$$

3.1.2 Marine Autonomy Objective Function Construct

Three primary decision areas are relevant to a human ship driver: mission, navigation, and collision avoidance. These three decision areas comprise the primary objective function types and allow expansion of Equation (3.1) to take the form of Equation (3.2) with utility functions $f_i = \{msn_i, nav_i, avd_i\}$, respectively. Each of c collision avoidance objective functions combines with objective functions for the m missions and n navigational constraints to determine the optimal \vec{x}^* . Each type of objective function requires specific consideration in design. Collision avoidance behaviors may rely on range at CPA (r_{cpa}), time until CPA (t_{cpa}), and contact pose (Θ) to determine utility (Section 3.2).

$$\begin{aligned} \vec{x}^* &= \underset{\vec{x}}{\operatorname{argmax}} \left(\sum_{i=1}^k (w_i \cdot f_i(\vec{x})) \right) \\ &= \underset{\vec{x}}{\operatorname{argmax}} \left(\sum_{i=1}^m (w_i^{msn} \cdot msn_i(\vec{x})) \right. \\ &\quad \left. + \sum_{i=1}^n (w_i^{nav} \cdot nav_i(\vec{x})) \right. \\ &\quad \left. + \sum_{i=1}^c (w_i^{avd} \cdot avd_i(\vec{x})) \right) \end{aligned} \quad (3.2)$$

Decision Variables

Autonomous surface vessels require course and speed input resulting from a weighted combination of objective functions. Each objective function may reason about one or both of these variables. For other physical domains, altitude or depth decisions are

made as appropriate. The course-speed pair forms a velocity vector $\vec{x} = \langle \theta, v \rangle$ that represents candidate decisions within the decision space of the multi-objective optimization problem. The vector $\vec{x}^* = \langle \theta^*, v^* \rangle$ represents the globally optimal solution of Equation (3.2). With each iteration of the solver, the globally optimal velocity vector passes \vec{x}^* to the front-seat controller to drive the vehicle. With an appropriate frequency of calculation⁴, the front-seat receives sufficiently updated orders allowing for timely maneuvering and calculation for complex multi-contact scenarios. In the case of autonomous surface vessels, the decision space \vec{x} is defined as the combination of feasible headings and speeds⁵, *viz* $\theta \in [0^\circ, 360^\circ), v \in [0, v_{max}]$, respectively. The optimal \vec{x} results in the highest utility of the combined weighted objective functions and becomes the preferred vehicle maneuver \vec{x}^* .

Primary Mission Objective Functions

A mission behavior represents the overall primary purpose of a vessel's actions less any navigation or collision avoidance constraints. The utility function of each mission takes the form of Equation (3.2) where $f_i = msn_i(\theta, v)$ with some priority weight w_i^{msn} corresponding to the i^{th} of m mission priorities. Example primary missions might represent some combination of the following:

- waypoint traversal with or without time of arrival constraints
- queuing or sensing of another vehicle (e.g., trailing or shadowing a submerged contact or object while maintaining a certain range, angle, and/or speed offset)
- loitering in a pre-determined geographical area to collect data until a particular state triggers a follow on action

The existence of multiple concurrent missions may quickly result in simultaneously competing objectives that must be weighed by the solver to determine the best combination of priorities when selecting a single velocity vector. For example, the

⁴A typical iteration frequency for marine autonomy is $\approx 4Hz$

⁵Backing down with astern propulsion is possible for slowing. Making way in an aft direction after slowing to a stop is not considered to occur at sufficient speeds to require altering the decision space. A vessel is therefore only considered to reason about speeds between 0 and v_{max} .

desired course to steer a sensor toward a trailed contact could place the vessel on a heading that forces the vessel to exit its allowed loiter area within a short period of time. When adding navigation and collision avoidance constraints, the available course-speed decision space may be significantly reduced.

Navigation Objective Functions

Safe navigation must remain a high priority to any reasonable vessel. Navigation objective functions must also allow for multiple competing behaviors. The utility function of each navigation behavior takes the form of Equation (3.2) where $f_i = nav_i(\theta, v)$ with some priority weight w_i^{nav} corresponding to the i^{th} of n navigational considerations. A buoy chain (or other static obstacles available from a navigation chart) might receive some variable scale of undesirability as range closes. Similarly, a confining region might represent a Notice to Mariners for a closed area as published by local maritime authorities. While not necessarily directly known when planning the primary mission, the navigation objective functions must adapt to allow appropriate consideration *in situ*. Within the scope of this research, all dynamic obstacles including other vessels are included in the collision avoidance decision area. All static obstacles fall in the realm of navigational constraints.

Collision Avoidance Objective Functions

Autonomous vessels must practice good seamanship to determine the appropriate maneuvers that comply with the laws of the sea while avoiding collision with other vessels. The concepts developed as part of this thesis apply generally to multi-contact collision avoidance in protocol-constrained, complex multi-mission scenarios. As a specific instantiation for testing and discussion, the international COLREGS for power-driven collision avoidance are invoked as the primary collision avoidance protocol requirement within this thesis. The concepts of this thesis generally apply to other collision avoidance protocols including those of other physical domains, though adaptation for other appropriate decision variables such as depth or altitude could be necessary.

As described in Section 2.5, the velocity obstacle prevails as the current underlying

means of quantifying safety of a candidate maneuver within state of the art marine autonomy collision avoidance literature [26, 27, 45, 46, 66, 70, 71, 90, 92]. While some collision avoidance algorithms allow consideration of a cost function for the selection of feasible velocity vectors outside the excluded region, they rely on knowing the *a priori* preferred velocity vector to achieve a given goal; this *a priori* preferred velocity vector of the velocity obstacle algorithm is often based exclusively on primary missions rather than including the collision avoidance input as another consideration for optimization. By considering that a vehicle might have more than one competing goal at any one time, a natural method for determining the desired velocity vector is to use multi-objective optimization. By further considering that each collision avoidance vehicle pair can be mapped to its own objective function, multi-objective optimization empowers designers to shape mission-specific collision avoidance algorithms while guaranteeing globally optimal velocity vector selection. This notion decouples the velocity obstacle’s biasing of a course-speed decision toward the contact-free mission-preferred choice of velocity vectors; instead, it allows a decision based without undue bias for the mission. To achieve this in a meaningful way, the developments of this research are necessary to give non-stepwise utility functions to find advantageous compromise when selecting the globally optimal course-speed vector.

The utility function of each collision avoidance behavior takes the form of Equation (3.2) where $f = avd_i(\theta, v)$ with some priority weight w_i^{avd} . Equation (3.3) demonstrates three examples of arbitrary utility functions for collision avoidance behaviors. The collision avoidance utility functions listed include range at CPA, time at CPA, and pose at CPA as parameters for returning a corresponding utility value. In protocol constrained collision avoidance, the governing protocol restrictions (\mathfrak{R}) must also be applied as shown in Section 3.3.5⁶. Further, time-based derivatives of these values may prove worthwhile of inclusion in future work.

⁶The governing protocol restrictions assumed in this thesis are the COLREGS. The notation \mathfrak{R} references protocol restrictions generally as well as the application of the COLREGS rule set for maritime surface vessels (here, Rules 13-17). Appendix A references details of the protocol rule set used in this work while Appendix B lists additional notation used for specific rules within the rule set.

$$\begin{aligned}
avd_1 &= avd(r_{cpa}) \\
avd_2 &= avd(r_{cpa}, t_{cpa}) \\
avd_3 &= avd(r_{cpa}, t_{cpa}, \Theta_{cpa})
\end{aligned} \tag{3.3}$$

Priority Weight Design

Priority weight w_i mathematically describes the relative importance of an objective function with respect to the overall multi-objective optimization problem. Some objective functions might receive a constant priority weight giving a static importance to the decision space. Other objective functions might have a varying priority weight whose value depends on state and environmental variables according to some policy. Priority weight can take many forms including step, linear, quadratic, and other arbitrary function shapes.

Equation (3.4) demonstrates three example priority weight functions that a designer might choose for a collision avoidance behavior depending on the overall mission profile. Collision avoidance priority weight often appears as some combination of instantaneous⁷ range (r), instantaneous range rate (\dot{r}), and range and/or time at CPA ($r_{cpa}^{\lambda_0}, t_{cpa}^{\lambda_0}$) on current trajectory λ_0 .

$$\begin{aligned}
w_1 &= w_1(r) \\
w_2 &= w_2(t_{cpa}^{\lambda_0}) \\
w_3 &= w_3(r, \dot{r}, r_{cpa}^{\lambda_0}, t_{cpa}^{\lambda_0})
\end{aligned} \tag{3.4}$$

⁷Instantaneous or current values of variables appear without subscript. Variables appearing with subscripts of “cpa” represent values at the time of CPA (Section 3.2). Variables appearing with “0” subscripts represent values at the time of detection ($t = 0$). Detailed explanation of notation can be found in Appendix B.

The priority weight for collision avoidance scenarios expresses the designer’s intentions on when and to what degree each collision avoidance behavior influences the overall velocity vector selection. Priority weight must be designed sufficiently high for any collision avoidance scenario to ensure safety and compliance with law and customs while not unnecessarily taking action prematurely to the detriment of mission performance.

Back-Seat Computing

Recent trends in marine autonomy allow for a division of processing consisting of front-seat and back-seat computers. This division allows for decoupling of the platform from the autonomy using a common interface. Actuators are controlled by the front-seat based on course-speed decisions passed from the back-seat⁸. The back-seat computer receives sensor and navigation information from payloads (e.g., GPS receiver, RADAR, etc.) either directly from a payload computer or through an interface with the front-seat computer. The back-seat determines the optimal course-speed pair from solving the multi-objective optimization problem of Equation (3.2) and sends driving orders in the form of a course-speed vector to the front-seat. This concept allows a modular back-seat computer to be quickly deployed in vehicles with different maneuvering characteristics. This naturally supports an autonomy structure based on all behaviors reasoning about a common set (or subset) of decision variables – in this case, course and speed. The designer of each underlying objective function must account for the appropriate state variables, environmental variables, and configuration parameters to achieve the desired actions by the vehicle. Within the framework of this research, an objective function results from each behavior that has a positive priority weight.

Nominally one or more behaviors exists for each of three major decision areas: mis-

⁸Back-seat autonomy was first proposed by Dr. David Battle at MIT and first run on a Bluefin-21® in Monterey Bay in August 2006. Previously, third party autonomy software was typically run on the vehicle manufacturer’s main vehicle computer. Payload computers primarily existed to process sensor data of 3rd party sensors.

sion, navigation, and collision avoidance. Each active behavior produces a piecewise linear objective function. A multi-objective solver determines the optimal solution of Equation (3.2) on each iteration. During each iteration of the solver, a single optimal course-speed output vector results. This single course-speed output is guaranteed to be globally optimal⁹ regardless of the underlying function form *vis-à-vis* any error in representing the underlying objective functions with piecewise linear approximations [3].

The interchangeability of the back-seat computer leads to the assumption of limited kinematic prediction for objective function design and creates a logical opening for future work incorporating kinematic prediction in the collision avoidance algorithms discussed throughout this chapter¹⁰. For autonomous marine collision avoidance, the selection of course-speed decision variables independent of controller input or actuator states is appropriate given the number of decision iterations achieved relative to the development and resolution of the collision avoidance encounter.

For the purpose of this thesis, a primitive Dubins-like turn radius limit is imposed on the design space. A Dubins-like turn radius appropriately models a human-like decision space where a watch officer might decide on a course and speed within the turn radius limitations of a full rudder. A human ship driver does not typically consider small differences in actuator position such as whether to order a 14° rudder rather than a 15° rudder. Rather, unless a situation occurs resulting in particular urgency, a standard rudder order is typically issued to achieve the desired course commensurate with current speed. The turn radius maneuvering limitation value is quickly configurable in the back-seat to properly match the vehicle’s physical limitations.

3.2 Closest Point of Approach

Closest point of approach (CPA) is defined as the point on ownship’s track where the range to the contact reaches its minimum value of the encounter. While many factors

⁹Global optimality refers to the instantaneous solution of Equation (3.2) rather than the time horizon of the entire mission.

¹⁰Future work is collectively addressed in Section 7.2.

are important to the CPA vernacular, the two most important values are the range between vessels at CPA (“range at CPA”, r_{cpa}) and the time until or at which CPA occurs (“time of CPA”, t_{cpa}).

Range at CPA is often colloquially referred to simply as “CPA.” CPA-based algorithms project vehicle trajectories in spatial coordinates rather than velocity space to compute the closest point of approach range as shown in Equation (3.5). While CPA as a general concept has been used as an intuitive component of human driving of both ships and airplanes, the concept has been largely avoided in the autonomous collision avoidance literature because of the velocity obstacle’s ease of implementation and relatively low computation load. Equation (3.5) was first introduced in [8] and more thoroughly described in [93] using Equations (3.6) through (3.12). In Equation (3.5), ownship and contact position $((x, y), (x_c, y_c))$, course (θ and θ_c), and speed (v and v_c) determine range at CPA within a specified time horizon $t_{horizon}$.

$$\begin{aligned}
 r_{cpa} &= r_{cpa}(x_c, y_c, \theta_c, v_c, x, y, \theta, v) & (3.5) \\
 &= \left\{ \sqrt{(x_c - x)^2 + (y_c - y)^2} \right\}_{cpa} \\
 &= \underset{time}{\operatorname{argmin}} \left\{ \sqrt{k_2 \cdot t^2 + k_1 \cdot t + k_0} \right\} \\
 &\quad \text{for } 0 \leq t \leq t_{horizon}
 \end{aligned}$$

$$k_2 = v^2 + v_c^2 - 2 \cdot \sin(\theta) \cdot \sin(\theta_c) \cdot v \cdot v_c - 2 \cdot \cos(\theta) \cdot \cos(\theta_c) \cdot v \cdot v_c \quad (3.6)$$

$$\begin{aligned} k_1 = & 2 \cdot \sin(\theta) \cdot v \cdot y - 2 \cdot \sin(\theta) \cdot v \cdot y_c & (3.7) \\ & - 2 \cdot \sin(\theta_c) \cdot v_c \cdot y + 2 \cdot \sin(\theta_c) \cdot v_c \cdot y_c \\ & + 2 \cdot \cos(\theta) \cdot v \cdot x - 2 \cdot \cos(\theta) \cdot v \cdot x_c \\ & - 2 \cdot \cos(\theta_c) \cdot v_c \cdot x + 2 \cdot \cos(\theta_c) \cdot v_c \cdot x_c \end{aligned}$$

$$k_0 = (y - y_c)^2 + (x - x_c)^2 \quad (3.8)$$

Equation (3.9) results from substituting Equations (3.6), (3.7), and (3.8) into Equation (3.5). By taking the partial derivative of Equation (3.5) with respect to time, and equating to zero (Equation (3.10)), the critical point for minimized range is determined. Time of CPA is found according to Equation (3.11) which can then be substituted into Equation (3.5) to give Equation (3.12). This value of CPA range found at the critical point in time is computed for all sampled heading and speed combinations at a nominal frequency of several times per second. In the case of $k_2 = 0$, Equation (3.11) has a denominator of zero and Equation (3.6) reduces to Equation (3.13). In the special case of $v = v_c$ and $\theta = \theta_c$, t_{cpa} is set to 0 for practical purposes since the vessels are effectively at a current and persistent CPA [8]. For the case of $t_{cpa} < 0$, CPA has already occurred, t_{cpa} is set to 0, and range will continue to open. For the case of $t_{cpa} > t_{horizon}$, t_{cpa} assumes the value of $t_{horizon}$ as a conservative approximation. To avoid brute force techniques while appropriately and sufficiently sampling the decision space, an intelligent sampling technique must be used (Section 2.7.1).

$$r_{cpa}^2(\theta, v, t) = k_2 \cdot t^2 + k_1 \cdot t + k_0 \quad (3.9)$$

$$\frac{\partial}{\partial t}(r_{cpa}^2) = 0|_{t=t_{cpa}} \quad (3.10)$$

$$t_{cpa} = \frac{-k_1}{2 \cdot k_2} \quad (3.11)$$

$$r_{cpa}(\theta, v, t_{cpa}) = \sqrt{k_2 \cdot t_{cpa}^2 + k_1 \cdot t_{cpa} + k_0} \quad \text{for } t_{cpa} \in [0, t_{horizon}] \quad (3.12)$$

$$\frac{v_c}{v} = \sin(\theta) \cdot \sin(\theta_c) + \cos(\theta) \cdot \cos(\theta_c) \quad (3.13)$$

$$\begin{aligned} & \pm \sqrt{2 \sin(\theta) \sin(\theta_c) \cos(\theta) \cos(\theta_c) + 2 \cos^2(\theta) \cos^2(\theta_c) - \cos^2(\theta) - \cos^2(\theta_c)} \\ & = 1 \pm \sqrt{\cos^2(\theta) \cdot (2 \cdot \sin^2(\theta) + 2 \cdot \cos^2(\theta) - 1 - 1)}, \quad \forall \theta = \theta_c, k_2 = 0 \\ & = 1 \pm \sqrt{0} = 1, \quad \forall \theta = \theta_c, k_2 = 0 \end{aligned} \quad (3.14)$$

$$\therefore \theta = \theta_c \ \& \ v = v_c \implies k_2 \equiv 0 \implies t_{cpa} = \infty$$

In addition to r_{cpa} and t_{cpa} , a third important value of CPA calculations is pose (“pose at CPA”, Θ_{cpa}). Pose in this context refers to the combination of relative bearing (β) and contact angle¹¹ (α) as shown in Equation (3.15). Pose at CPA is therefore not a single quantity, but rather a term to collectively consider relative bearing and contact angle in the context of each other. The pose at time of sighting or detection (Θ_0) often dictates which rules of a protocol apply. The pose at CPA (Θ_{cpa}) when combined with r_{cpa} yields considerable insight into the degree of risk at t_{cpa} . Equation (3.16) shows absolute bearing of a contact relative to ownship

¹¹Contact angle refers to the relative bearing of ownship as seen from the perspective of the contact in question. The term originated in World War II submarine operations under the names of “angle on the bow” and “target angle.” Contact angle serves as a clear means to distinguish between the two relative bearings: one from the perspective of ownship, the other from the perspective of the contact. Relative bearing (β) henceforth refers to ownship’s relative perspective of the contact; contact angle (α) refers to the contact’s relative perspective of ownship, or in other terms, relative bearing as viewed from the contact. See [25, 87]

(bng_{cn}^{os}) . Equation (3.16) accounts for the special cases that would otherwise make the denominator of the inverse tangent function zero and ensures a north-up, degree based system. Equation (3.17) relates the bearing of ownship from the perspective of the contact (bng_{os}^{cn}); this is defined equal to the absolute bearing of the contact from ownship plus 180° . Equation (3.18) shows relative bearing β of a contact relative to ownship using ownship's bow as 0° . Contact angle α takes the form of Equation (3.19). Because α represents a ship driving term for the number of degrees difference from the contact's bow pointing ownship as seen from ownship's bridge, the domain is conventionally $\alpha \in [-180^\circ, 180^\circ)$.

$$\Theta \equiv \begin{bmatrix} \alpha \\ \beta \end{bmatrix} \quad (3.15)$$

$$bng_{cn}^{os} = \begin{cases} 0^\circ & (x = x_c) \text{ and } (y \leq y_c) \\ 180^\circ & (x = x_c) \text{ and } (y > y_c) \\ \tan^{-1} \left(\frac{|y - y_c|}{|x - x_c|} \right) \cdot \left(\frac{180^\circ}{\pi} \right) + 90^\circ & (x < x_c) \text{ and } (y \leq y_c) \\ 90^\circ - \tan^{-1} \left(\frac{|y - y_c|}{|x - x_c|} \right) \cdot \left(\frac{180^\circ}{\pi} \right) & (x < x_c) \text{ and } (y > y_c) \\ \tan^{-1} \left(\frac{|y - y_c|}{|x - x_c|} \right) \cdot \left(\frac{180^\circ}{\pi} \right) + 270^\circ & (x > x_c) \text{ and } (y \leq y_c) \\ 270^\circ - \tan^{-1} \left(\frac{|y - y_c|}{|x - x_c|} \right) \cdot \left(\frac{180^\circ}{\pi} \right) & (x > x_c) \text{ and } (y > y_c) \end{cases} \quad (3.16)$$

$$bng_{os}^{cn} \equiv bng_{cn}^{os} + 180^\circ \quad (3.17)$$

$$relbng_{cn}^{os} = \beta = \begin{cases} bng_{cn}^{os} - \theta & (bng_{cn}^{os} - \theta) \geq 0^\circ \\ 360^\circ + bng_{cn}^{os} - \theta & \text{otherwise} \end{cases} \quad (3.18)$$

$$\beta \in [0^\circ, 360^\circ)$$

$$relbng_{os}^{cn} = \alpha = \begin{cases} bng_{os}^{cn} - \theta_c & (bng_{os}^{cn} - \theta_c) \geq 0^\circ \\ 360^\circ + bng_{os}^{cn} - \theta_c & \text{otherwise} \end{cases} \quad (3.19)$$

$$\alpha \in [-180^\circ, 180^\circ)$$

By substituting Equation (3.17) into Equation (3.19) and subtracting Equation (3.18), Equation (3.20) results. Equation (3.20) allows for efficient determination of contact angle when courses and relative bearing are known without performing the calculations of Equation (3.19). The temporal derivative of Equation (3.20) yields Equation (3.21) for α and β as parametric functions of time. For the special case of constant course (including linear track projections), Equation (3.21) reduces to Equation (3.22). That is, when under a constant course or assumed linear track for both contacts, the relative bearing rate and relative contact angle rate are numerically equivalent.

$$\beta - \alpha = \theta_c - \theta - 180^\circ \quad (3.20)$$

$$\dot{\beta} - \dot{\alpha} = \dot{\theta}_c - \dot{\theta} \quad (3.21)$$

$$\dot{\beta} = \dot{\alpha}, \text{ for } \dot{\theta}_c = \dot{\theta} = 0 \quad (3.22)$$

3.3 Full CPA Quantification Algorithm

Direct computation of CPA quantities results in explicit knowledge of r_{cpa} , t_{cpa} , and Θ_{cpa} for all candidate (θ, v) pairs. Detailed analysis can then be performed on range at CPA, pose, and times from several candidate course-speed pairs representing the entirety of the decision space to make an objective function fully defined for each point in the function domain (i.e., decision space) using a continuous utility mapping. Algorithms such as velocity obstacles effectively return a point along a step function that defines the candidate as either allowed or excluded without amplification; CPA-based techniques allow for creation of a continuous, non-stepwise function to map these CPA range, time, and pose values to utility values.

Typical approaches using velocity obstacles classify each candidate maneuver as either safe or unsafe [45, 66]. This single range threshold technique eliminates large swaths of feasible decision space that conflict with the chosen safety range threshold. For algorithms invoking a collision avoidance protocol, these restrictions further reduce the feasible decision space often in another stepwise manner. If a candidate maneuver evaluates to a range less than the designated “safe” range or if the candidate maneuver would violate a protocol constraint, it is eliminated from the feasible solution space. VO implementations commonly employ a heuristic to choose the least cost deviation from the primary mission’s desired velocity vector [45]. If the primary mission’s desired velocity vector is not contained in the feasible solution set, then most literature heuristically chooses the least cost deviation from the desired velocity vector in velocity space to a neighboring feasible solution according to the designer’s policies. This least cost feasible solution becomes the chosen course-speed pair.

The full CPA quantification algorithm evaluates all possible course-speed decisions either directly or interpolated between two nearby directly evaluated decisions. Velocity obstacles by definition operate in velocity-based coordinates as shown in Section 3.3.1 [27]; velocity obstacles therefore have no direct knowledge of (x, y) or pose as a function of time, including time of CPA. CPA algorithms by definition operate in spatial coordinates and have full access to all desired quantities including at time

of CPA. Therefore, any velocity obstacle algorithm desiring information (i.e., time, range, or pose at CPA) beyond whether a maneuver is safe require additional direct calculations for each desired candidate maneuver. The advances of computational power and improvements in intelligent sampling algorithms since the introduction of the velocity obstacle allow for sufficient decision space sampling within the required iteration frequency (typically 4Hz) using an onboard payload-size¹² computer. A key advantage of full CPA evaluation includes interpolation of unsampled points in the decision space as discussed in Sections 2.7.1–3.4. By using a full CPA sampling technique, information about time, range, relative bearing, and contact angle at CPA for each candidate maneuver may be incorporated into the decision making process. This enables a feasible yet penalized (lower utility) region of decision space that would otherwise be infeasible using velocity obstacle techniques. The full CPA sampling becomes especially beneficial in cases of dense contact situations or when mission rules compete or conflict with each other.

3.3.1 Velocity Obstacle

By considering a pre-defined standoff range from other vessels whose solution (position, course, and speed) is known, the transformation of the problem into velocity space allows for an exclusion wedge (velocity obstacle) to be drawn for each vehicle pair. By using any of the preferred types of velocity obstacle algorithms of Section 2.5 (e.g., velocity obstacles, generalized velocity obstacles, reciprocal velocity obstacles, generalized reciprocal velocity obstacles, etc.), any given ownship velocity (course and speed) that falls into the exclusion region is assumed to result in a collision. A velocity obstacle combination outside the exclusion region results in the solution being deemed safe. When a velocity obstacle-based approach considering multiple collision agents returns a null solution space, a heuristic algorithm to relax the excluded regions is required to obtain a non-excluded solution; this is often accomplished not

¹²Current on-board payload computer specifications include a 900MHz quad-core ARM Cortex-A7 CPU, 1GB RAM, 1200mA load at 5VDC, 85.60mm x 56mm x 21mm space requirement, mass \approx 45g, and cost \approx \$35USD. Appendix C discusses CPU loading details.

by direct assessment of a candidate maneuver’s CPA solution but rather on a factor based on the time to collision and deviation from an obstacle-free mission-desired velocity vector.

While selection of this nearest neighbor guarantees optimality of the given problem statement, it does not necessarily ensure selection of the most human-realistic choice in the context of non-mission specific considerations. In situations such as multiple near-term collision encounters, prioritization must often disregard the mission-preferred solution to allow the contact picture to resolve before proceeding. For collision avoidance scenarios that are heavily constrained by a dense contact picture and competing protocol requirements, evaluation techniques using a single fixed collision range can become over-constrained. Time to CPA (t_{cpa}), pose at CPA (Θ_{cpa}), COLREGS rule compliance (\mathfrak{R}), spatial track efficiency (η_{dist}), temporal efficiency (η_{time}), Safety (S), and exact range at CPA (r_{cpa}) all importantly contribute to the risk decision of a human operator. In contact-dense scenarios, these considerations are arguably more important than the amount of deviation required from the previously desired course and speed.

Designers often incorporate additional margins into an algorithm’s collision range including a buffer from actual physical contact at “collision,” uncertainties in contact maneuvers, uncertainties in contact shapes, and other model uncertainties. The velocity obstacle algorithm evaluates candidate maneuvers against a single threshold collision range (R_{col}^{vo}) in the velocity space resulting in a binary response: a candidate course-speed pair is either deemed allowed or excluded based on whether its resulting range at CPA (r_{cpa}) falls outside or inside the fixed collision range threshold within a given time horizon.

In effect, a velocity obstacle objective function avd_i^{vo} using the literature-standard techniques yields a step function in utility values: allowed candidate maneuvers receive a utility of 1 while excluded candidate maneuvers receive a utility of 0 as shown in Equation (3.23). When adding the protocol constraints, the step properties remain with further constraint as shown in Equation (3.24) for maneuvers violating the applicable rule set \mathfrak{R} .

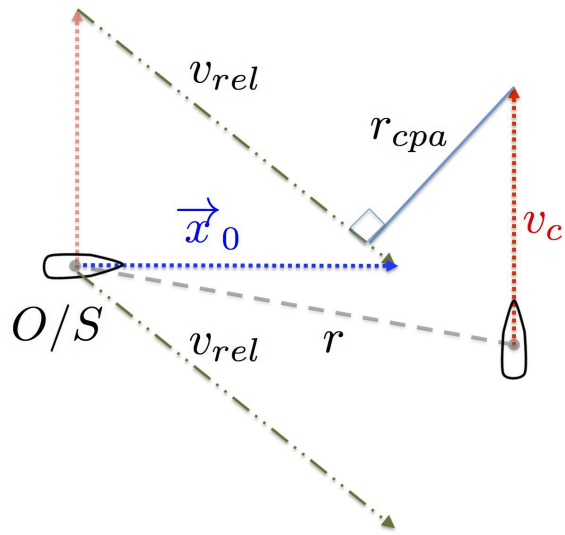
$$avd(\theta, v)_i^{vo} = \begin{cases} 0, & \text{if } r_{cpa} < R_{col}^{vo} \\ 1, & \text{if } r_{cpa} \geq R_{col}^{vo} \end{cases} \quad (3.23)$$

$$avd(\theta, v)_i^{vo} = \begin{cases} 0, & \text{if } r_{cpa} < R_{col}^{vo} \text{ or } \vec{x} \notin \mathfrak{R}_{allowed} \\ 1, & \text{if } r_{cpa} \geq R_{col}^{vo} \text{ and } \vec{x} \in \mathfrak{R}_{allowed} \end{cases} \quad (3.24)$$

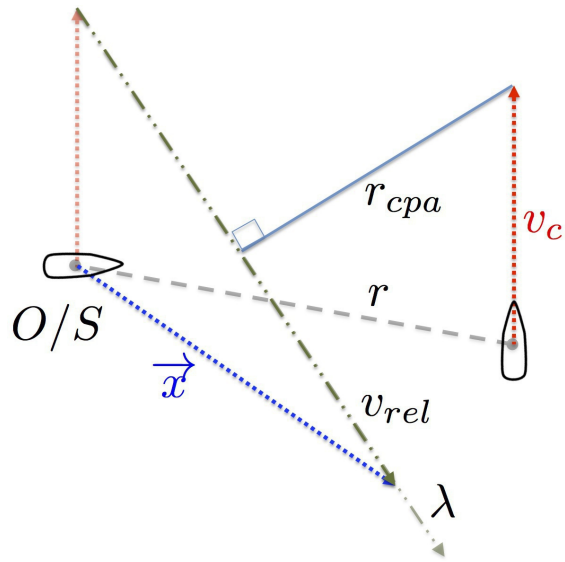
Designers then typically assign a cost value to each still-admissible candidate velocity vector using already known or derived information. Transforming the problem to velocity space inherently limits the velocity obstacle's available information, most importantly the exact value of candidate range at CPA. Techniques to relax over-constrained velocity obstacles or determine least cost neighbors to the mission-preferred velocity vector remain only aware of the threshold collision range at CPA (R_{col}^{vo}), range and time of CPA on current trajectory ($r_{cpa}^{\lambda_0}, t_{cpa}^{\lambda_0}$), current range to contact (r), and collision avoidance binary utility avd_i^{vo} . The velocity obstacle techniques lack explicit knowledge of r_{cpa}, t_{cpa} , and Θ_{cpa} unless deliberately calculated for specific candidate maneuvers. Any costing information based on other information requires full sampling beyond the computations already performed.

For the arbitrary collision geometry of Figure 3-1, if the current relative trajectory λ_0 results in a violation of the $r_{cpa} < R_{col}^{vo}$ threshold, an alternative maneuver must be found. Candidate maneuvers \vec{x} seek to find a relative trajectory λ that increases r_{cpa} to an acceptable level. The velocity obstacle algorithm uses velocity space calculations to map the results of the single CPA range for candidate maneuvers according to Equation (3.23) without directly computing values of r_{cpa} . Equation (3.23) is depicted graphically in Figure 3-2. The shaded region of Figure 3-3 demonstrates excluded (utility = 0) resulting candidate maneuvers using a velocity obstacle algorithm.

Human mariners, however, intuitively rely on knowing more detailed effects of a collision avoidance maneuver. In many cases, human operators in dense contact



(a) Initial Geometry



(b) Candidate Maneuver Geometry

Figure 3-1 Ownship (labeled “O/S”) is the give-way vessel in this canonical crossing geometry (COLREGS Rules 15/16) with current trajectory shown in (a). The stand-on contact (right; COLREGS Rules 15/17) is at a current range of r . With a risk of collision existing, a candidate maneuver (\vec{x}) is considered that results in a candidate relative velocity v_{rel} along the candidate relative trajectory λ as shown in (b). Each \vec{x} and its associated v_{rel} along λ changes the projected value of r_{cpa} .

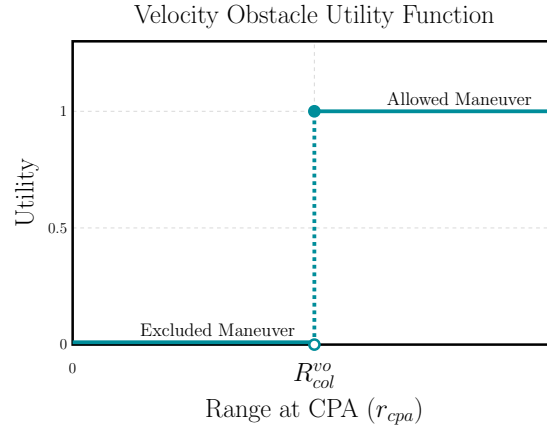


Figure 3-2 The velocity obstacle function of Equation (3.23) is shown as a step function at the velocity obstacle’s collision range (R_{col}^{vo}).

situations choose course-speed pairs based more on the contact picture and less on the mission’s priorities. In these cases of heavy contact density and conflicting rules, anchoring the course-speed pair selection to that of a weighted heuristic deviation from the mission’s preferred velocity vector can result in a poor collision avoidance decision. That is not to say that the mission should be wholly disregarded; however, priority commensurate with the severity of the collision avoidance picture should be granted to selection of the vehicle’s course-speed pair. Further, any relaxation of the collision range should involve explicit metrics such as resulting CPA range.

3.3.2 Collision Avoidance Utility Mapping

Using explicit values of range, time, and pose at CPA, a continuous utility mapping function can be created to replace the binary allowed/excluded velocity obstacle paradigm. Rather than the single collision range of Equation (3.23) to delineate the stepwise change of utility, the utility function can be a function of one or more CPA-related quantities. A non-stepwise function with a zero-utility left tail and a unity-utility right tail requires a minimum of two points of demarcation on the independent axis: one point corresponding to the transition from constant zero utility to a non-zero interior utility function, and one point corresponding to the transition from an interior utility function to constant unity. For the example of a linearly increas-

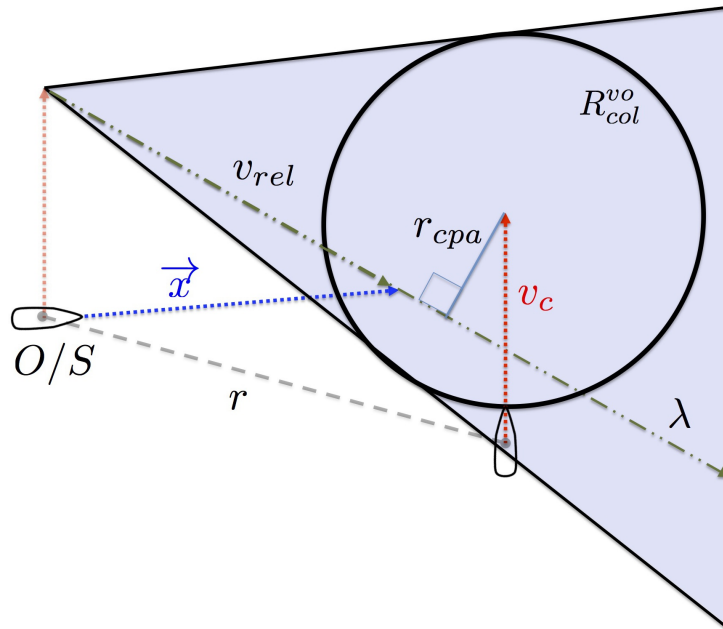


Figure 3-3 A velocity obstacle for ownship (O/S) traveling $\theta \approx 080^\circ$ for a near-canonical crossing geometry with a contact traveling north at speed v_c and range r shows the excluded (shaded) region of collision range violations. Any \vec{x} must produce a relative velocity v_{rel} such that the resulting range at CPA (r_{cpa}) along candidate trajectory λ falls outside the collision cone resulting from a single threshold fixed range of concern R_{col}^{vo} . The resulting maneuvers are known to be allowed (utility=1) or excluded (utility=0) without directly calculating r_{cpa} . This velocity obstacle does not reflect the added constraints of COLREGS rules which in this situation prevent ownship from turning to its left, thus further eliminating otherwise feasible candidate maneuvers. Costing is often performed based only on the information available or derivable from this graphic, less the actual value of r_{cpa} .

ing function connecting a zero utility to a full utility, the values of the independent variable where utility changes from constant zero to linearly increasing and where the linearly increasing changes to constant maximum utility must be identified. The three components functions (zero utility, linearly increasing, and full utility) fully define the objective function. Utility functions can take as parameters a single variable (range-only, time-only, etc.) or can be a function of multiple variables.

Objective functions can therefore be defined as being comprised of one or more component functions f_i . A single f_i will represent the utility function when its corresponding conditions are met such that one and only one f_i represents utility for any given combination of input parameters. The conditions used to select the function f_i to represent the utility function avd_i are called discriminators. Discriminators (\mathfrak{D}) allow the utility function avd to be mapped to the correct component function (f_i) for any given \vec{x} and system state as defined by the designer (Figure 3-4). For the example of a range-only discriminator, a utility function might have two threshold range values R_{min} and R_{pref} . Any CPA range r_{cpa} between these threshold values would receive a continuous utility value commensurate with the assigned interior utility mapping function. Equation (3.25) and Figure 3-4b represent a linear example where a single variable (r_{cpa}) is used to select the interior function. The discriminator concept described for utility functions also applies to non-stepwise priority weight functions (Figure 3-5) to select which component function (e.g., constant zero, linear, quadratic, constant unity, etc.) represents the priority weight for a given state.

$$avd(\theta, v)_i = \begin{cases} 0, & \text{if } r_{cpa} \in \mathfrak{D}_0 \\ f_1, & \text{if } r_{cpa} \in \mathfrak{D}_1 \\ 1, & \text{if } r_{cpa} \in \mathfrak{D}_2 \end{cases} \quad (3.25)$$

$$\text{where, } f_1 = f_1(r_{cpa}) = \frac{r_{cpa} - R_{min}}{R_{pref} - R_{min}}$$

With either an explicitly known or well-estimated full representation of the entire course-speed decision space with respect to collision avoidance quantities, the velocity obstacle threshold safety range can be expanded to other discriminators, threshold levels, and metrics based on the collision avoidance quantities of explicit CPA range, pose, and time, the governing protocol rule set, relative bearing, and target angle among others. The addition of multiple collision avoidance component functions improves the richness of the collision avoidance decisions over the velocity obstacle methods and more accurately depicts human ship driving by allowing threshold-specific objective function design. By allowing multiple threshold levels, a simple step function can be expanded to shape the decision space using piecewise continuous functions. As a real-world example of how a human-operated vessel would use multiple range thresholds, consider Example 3-1.

The notion of multiple threshold ranges for distinct actions in Example 3-1 can be expanded into a series of component functions (f_i) that collectively define the utility function. Consider that in addition to discrete actions being required at particular range thresholds, the watch officer of Example 3-1 would likely prefer larger CPA ranges where possible. There is not only some increasing risk with decreasing CPA range, but there is also an increasing workload and increasing inconvenience of the Captain's time with each additional measure. These would cumulatively result in a closer CPA range being less desirable than a more distant CPA range. Accordingly,

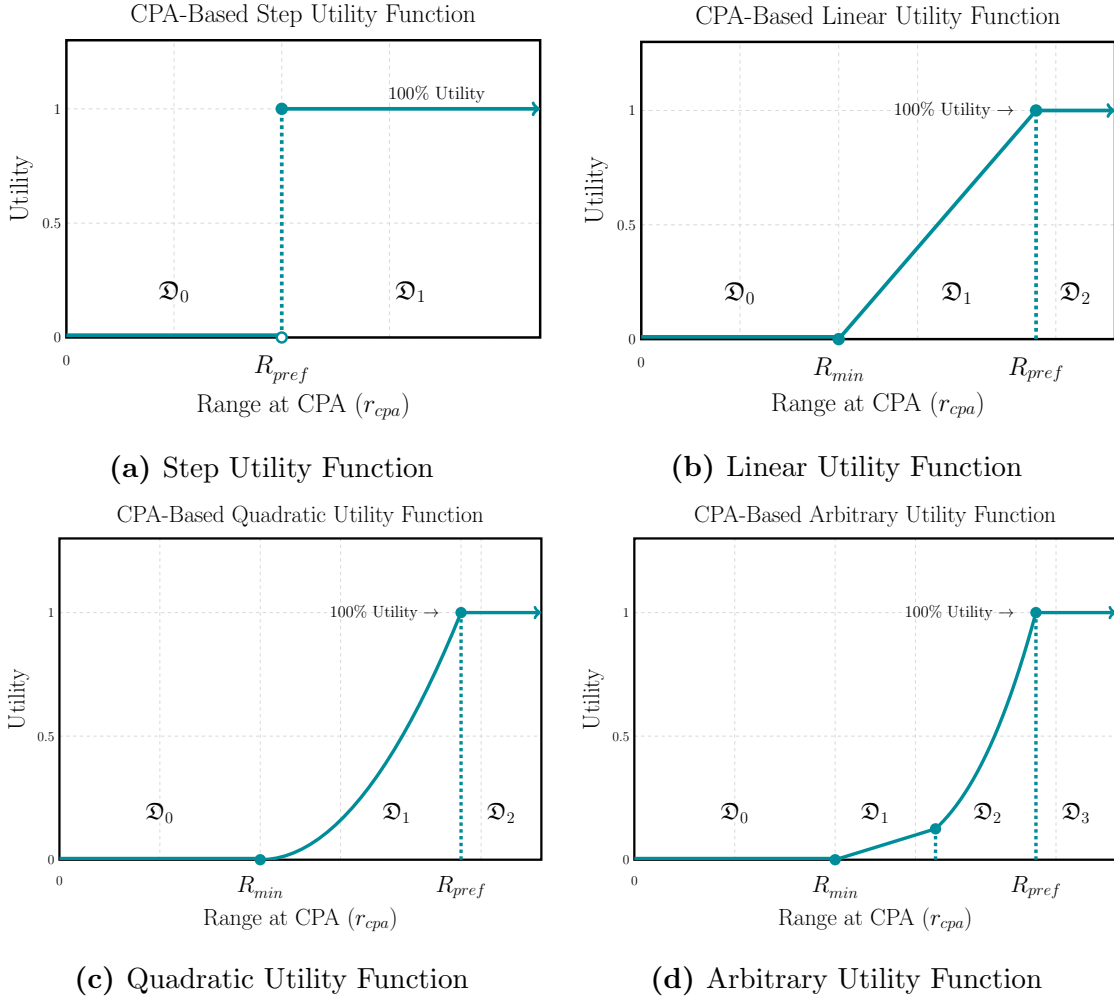


Figure 3-4 In (a), a nominal CPA utility function shows the utility for a single threshold mapping. In the case of a range-based function, the resulting maneuver’s range crosses the *a priori* determined “safe” range for a single range threshold and the velocity obstacle is recovered. In (b-c), a two-threshold, three-component utility function represents the collision avoidance objective function. Arbitrary interior functions can be used for a more advanced utility mapping than possible by velocity obstacles. The three-component linear function of (c) represents Equation (3.25) with an independent variable of range at CPA. In (d), an arbitrary non-uniform utility function is shown. The discriminators \mathcal{D} allow selection of the appropriate component function f_l based on one or more conditions usually involving range, time, pose, and collision avoidance rule. Expansion to more generalized collision avoidance utility functions allows for greater reasoning within the larger autonomous vessel mission scheme. Independent variables other than range can be designed, and multiple discriminators can be used. An example second discriminator would be to map all $t_{cpa} > t_{horizon}$ to the $f_l = 1$ component function without further evaluation of range.

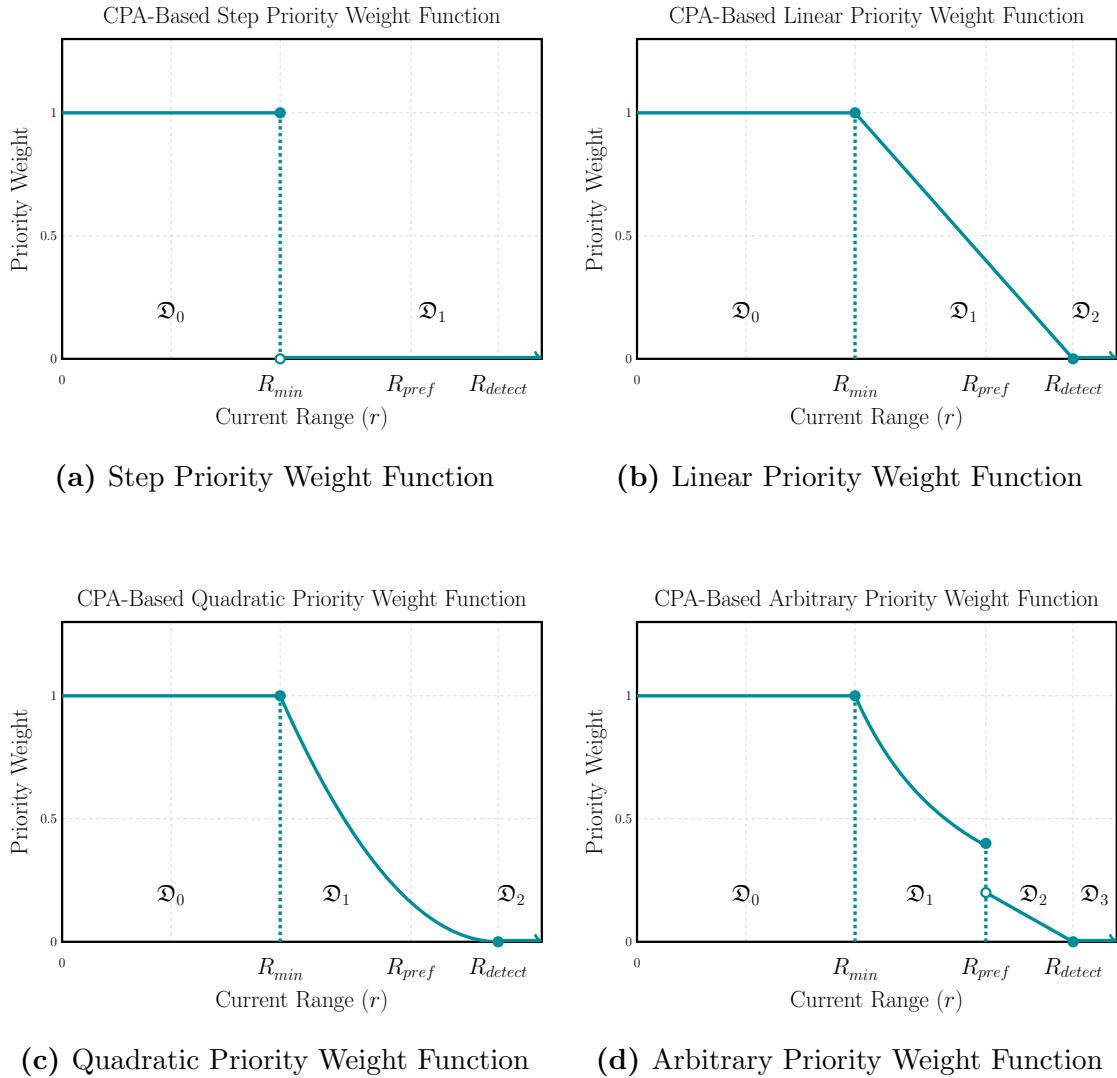


Figure 3-5 The selection of priority weight allows multiple objective functions to be added in accordance with their relative importance to select the globally optimal solution. Shown here are four priority weight functions. Each priority weight function is piecewise defined over some domain of its independent variable (e.g., instantaneous range, current time to CPA, etc.). The conditions that select the appropriate piece of the function to be used as the priority weight function are its discriminators (\mathcal{D}). In (a), a nominal priority weight function shows the priority for a single threshold mapping. The resulting maneuver's independent variable (range) crosses the *a priori* determined range at which collision avoidance maneuvers become important for a single range threshold. In (b-c), a dual-range threshold is used and a linear or quadratic function can be used for a more dynamic priority weight mapping. In (d), an arbitrary function is used to determine priority weight.

Example 3-1

Human Ship Driving Example

A vessel is operating in a congested traffic area. Depending on the mission sensitivity (e.g., payload value or fragility, security posture, etc.), the shape of the interior collision avoidance utility function can be tailored to fit the circumstances or general policies of the Captain. Accordingly, the vessel's Captain has ordered that all contacts should ideally be kept at a range greater than or equal to some preferred range, though deviations to closer ranges are allowed as necessary under the following provisos:

1. The Captain must be notified of any contact's expected CPA range less than some preferred range if CPA time is less than some time horizon of concern:

$$\begin{aligned}r_{cpa} &< R_{pref} \\t_{cpa} &< t_{horizon}\end{aligned}$$

2. The Captain's permission is required to bring any contact closer than some permission range within some time horizon of concern:

$$\begin{aligned}r_{cpa} &< R_{permission} < R_{pref} \\t_{cpa} &< t_{horizon}\end{aligned}$$

3. The Captain is stationed on the bridge for any contact whose expected CPA range is closer than some minimum range of concern and CPA time less than some time horizon of concern:

$$\begin{aligned}r_{cpa} &< R_{min} < R_{permission} < R_{pref} \\t_{cpa} &< t_{horizon}\end{aligned}$$

closer CPA ranges should map to lower utility values. To account for the additional burden of each discrete threshold (e.g., summoning the Captain to the bridge), an increasingly more drastic (e.g., linear then quadratic) utility mapping might occur upon crossing a subsequent threshold demarcation to avoid the next discrete action. This methodology reflects practical open ocean experience of vessel masters that realize some amount of consideration must be given to closer-than-desired ranges at CPA in multiple contact scenarios to allow for a globally optimal course-speed decision pair without neglecting the safety of the vessel.

Full CPA calculations allow for exact assessment of the resulting maneuver with respect to the preferred range. This quantifiable knowledge of CPA data for candidate maneuvers where $r_{cpa} < R_{pref}$ allows for direct calculation of risk (and therefore utility) rather than heuristic relaxation of the velocity obstacle. By choosing some set of CPA ranges to avoid a collision with decreasing utility to the watch officer, the Captain has empowered the crew to robustly manage collision avoidance encounters with reasonable flexibility while mitigating increased risk of closer CPA ranges.

Any unsafe CPA range ($r_{cpa} < R_{min}$) could be assigned zero utility. Likewise, the higher CPA range threshold (R_{pref}) could be considered as the range at which any greater CPA range provides no additional benefit to ownship. For the range-only utility discriminator, the CPA ranges of each sampled candidate maneuver are compared to the prescribed threshold ranges then mapped to a utility value. One can then define arbitrary component functions mapping CPA range values between R_{min} and R_{pref} . The overall collision avoidance utility function therefore can be broken into multiple piecewise continuous functions using the discriminator concept based on the designer's choice of discriminator variables to choose the appropriate component function.

In Example 3-1, the discriminators are range at CPA and time at CPA. Example 3-1 demonstrates why the discriminator concept is useful: here any $t_{cpa} \geq t_{horizon}$ immediately results in $avd_i = 1$ and eliminates further computation of utility. In the case of collision avoidance more generally, discriminators may include CPA quantities (r_{cpa} , t_{cpa} , Θ_{cpa}), environmental characteristics, instantaneous range r and relative angles

(α, β) , and any protocol-specific properties or rules (\mathfrak{R}). A discriminator \mathfrak{D} allows an objective function avd_i or priority weight function w_i to be split among two or more condition statements for the i^{th} contact allowing ease of graphical display of an algorithm. In Example 3-1, $\mathfrak{D} = \mathfrak{D}(r_{cpa}, t_{cpa})$. Discriminators may take more general forms such as $\mathfrak{D} = \mathfrak{D}(r, r_{cpa}, t_{cpa}, \Theta_{cpa}, \mathfrak{R})$.

3.3.3 Formal Description of Algorithm

To better adapt autonomous collision avoidance algorithms to the real-life decisions of mariners in complex scenarios, the full CPA quantification algorithm allows multiple threshold levels of CPA quantities to be considered when creating collision avoidance utility functions. Intermediate discriminator criteria (\mathfrak{D}_l) allow a candidate maneuver's CPA quantities to be mapped using a continuous utility mapping function f_l . The resulting collision avoidance objective function becomes information rich, non-stepwise across the decision space (unless necessary for protocol constraints), and more tailorable to human-like decision making. Equation (3.26) shows a multi-CPA range threshold design's collision avoidance objective function using the full CPA quantification algorithm representing the scenario of Example 3-1 for $t_{cpa} < t_{horizon}$. Equation (3.27) shows a more general multi-discriminator collision avoidance objective function using the full CPA quantification algorithm. Figures 3-6 and 3-7 graphically depict Equation (3.27). Equation (3.28) shows an example range-only linear utility function of r_{cpa} with two range-only discriminator values corresponding to the minimum (R_{min}) and preferred (R_{pref}) ranges at CPA.

$$avd(\theta, v)_i = \begin{cases} 0, & \text{if } r_{cpa} < R_{min} \\ \dots & \\ f_l, & \text{if } R_{l-1} \leq r_{cpa} \leq R_l \\ \dots & \\ 1, & \text{if } R_{pref} \leq r_{cpa} \end{cases} \quad (3.26)$$

where, $0 \leq f_l(\lambda, r, \dot{r}, r_{cpa}, t_{cpa}, \Theta_{cpa}, \mathfrak{A}) \leq 1$

$$avd(\theta, v)_i = \begin{cases} 0, & \text{if } \mathfrak{D} \in \mathfrak{D}_{min} \\ \dots & \\ f_l, & \text{if } \mathfrak{D} \in \mathfrak{D}_l \\ \dots & \\ 1, & \text{if } \mathfrak{D} \in \mathfrak{D}_{max} \end{cases} \quad (3.27)$$

where, $0 \leq f_l(\lambda, r, \dot{r}, r_{cpa}, t_{cpa}, \Theta_{cpa}, \mathfrak{A}) \leq 1$

$$f_l(r_{cpa}) = \frac{r_{cpa} - R_{min}}{R_{pref} - R_{min}} \quad (3.28)$$

The full CPA quantification method samples and evaluates the numeric CPA quantities $(r_{cpa}, t_{cpa}, \Theta_{cpa})$ throughout the decision space to create an underlying objective function. This technique shifts the collision avoidance decision to one of continuous context rather than boolean. The formal full CPA quantification algorithm takes the form of Algorithm 1 for arbitrary discriminators. Equation (3.26), Equation (3.28), and Algorithm 2 demonstrate a nominal full CPA collision avoidance algorithm whose r_{cpa} is determined for each sampled \vec{x} for a two-range threshold configuration using a linear interior function. Rather than act as a post-decision collision filter, the addi-

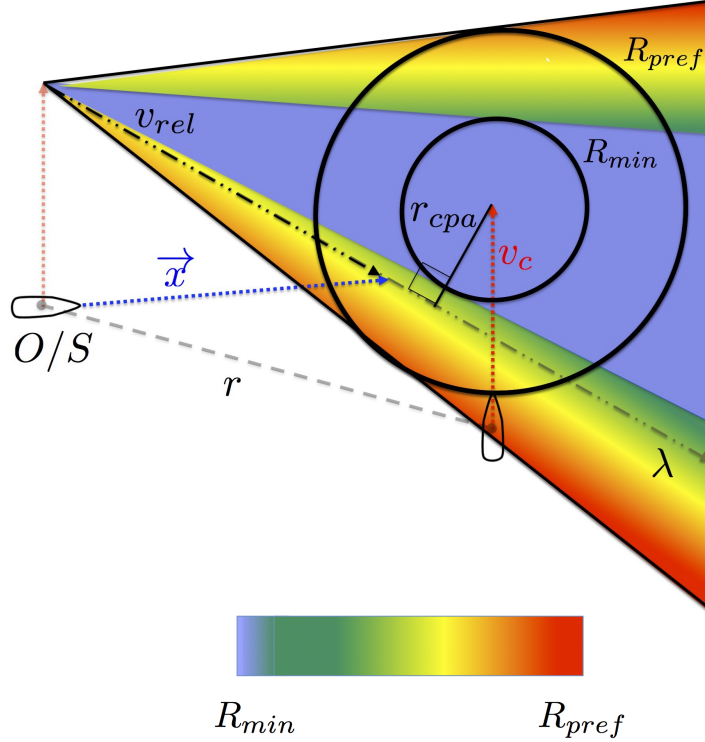


Figure 3-6 In the full CPA quantification algorithm with a range-only discriminator, candidate maneuvers \vec{x} are sampled (non-brute force) throughout the decision space while directly computing each sampled range at CPA (r_{cpa}). Explicit knowledge of r_{cpa} allows direct mapping of candidate maneuvers to non-integer utilities whose r_{cpa} falls between preferred CPA range R_{pref} (utility = 1) and the minimum acceptable range at CPA R_{min} (utility = 0) for all feasible \vec{x} where $R_{min} < r_{cpa} < R_{pref}$.

tional CPA information for each candidate maneuver informs the choice of \vec{x}^* with a more human-realistic continuous-utility decision process that appropriately considers resulting range, time, and pose at CPA of each maneuver in the context of mission and navigational objectives. Using intelligent sampling techniques such as interval programming (Section 2.7.1), direct CPA quantity calculations can be made with sufficient sampling resolution to appropriately characterize the decision space without approaching the inefficiencies of brute force techniques.

3.3.4 Generalization of the Velocity Obstacle

A fixed single collision range of R_{col}^{vo} creates a disc-shaped obstacle OBS_i in velocity space (Section 2.5). Fiorini described this velocity obstacle as a relative trajectory λ

Algorithm 1 Full CPA quantification algorithm for determining CPA range, time, and pose for sampled candidate maneuvers under COLREGS constraints.

```

1: procedure PSEUDOCODE FOR FULLCPAQUANTIFICATION()
2:   for  $i^{th}$  contact do
3:      $r_i \leftarrow$  current contact range
4:      $\theta_i \leftarrow$  current contact course
5:      $v_i \leftarrow$  current contact speed
6:     Calculate:  $r_{cpa}^{\lambda_0}, t_{cpa}^{\lambda_0}, \Theta_{cpa}^{\lambda_0}$ 
7:     Calculate: risk of collision (per COLREGS) w.r.t.  $i^{th}$  contact
8:     if (collision risk  $\geq$  collision risk threshold) then
9:        $\Theta_0 \leftarrow \Theta_0(x, y, x_c, y_c, \theta, \theta_c)$ 
10:       $\mathfrak{R}_i \leftarrow \mathfrak{R}(\Theta_0)$  ▷ determine governing protocol rule
11:       $w_i^{avd} \leftarrow w_l(r, \dot{r}, r_{cpa}^{\lambda_0}, t_{cpa}^{\lambda_0}, \Theta^{\lambda_0})$ 
12:       $f_l \leftarrow \mathfrak{D}(r, \dot{r}, t, \Theta, \mathfrak{R})$  ▷ inputs variables per designer
13:      for  $j = courses.min$  to  $courses.max$  do
14:        for  $k = speeds.min$  to  $speeds.max$  do
▷ sample appropriate subset, i.e., not brute force
15:           $avd_i[j, k] \leftarrow f_l(r_{cpa}(j, k), t_{cpa}(j, k), \Theta_{cpa}(j, k))$ 
16:           $avd_i[j, k] \leftarrow avd_i[j, k] - \mathfrak{R}_i(j, k)$ 
17:        end for
18:      end for
19:    end if
20:  end for
21: end procedure

```

such that $\lambda \cap OBS_i$. Using Figure 3-3, $\lambda \in R_{col}^{vo}$ implies a CPA range less than R_{col}^{vo} , or $r_{cpa} = \sqrt{r^2 - (v_{rel} \cdot t_{cpa})^2} < R_{col}^{vo}$.

In the special case of full CPA quantification in which only one fixed discrimination threshold range exists (i.e., $R = R_{min} = R_{pref}$ in Equation (3.26)), an arbitrary \vec{x} results in a relative trajectory λ , a collision for any $r_{cpa} < R$, and $f \equiv 1$ for all $r_{cpa} \geq R$, therefore recovering the velocity obstacle utility of Equation (3.23) where $R \equiv R_{col}^{vo}$.

3.3.5 Application to Protocol Collision Avoidance Constraints

Collision avoidance perhaps encompasses the largest growth area in marine autonomous design. The nuances of the rules including common practice and case law create non-trivial limitations on vessel maneuvers in given encounter geometries. Human mariners largely follow these nuances and likewise expect the same of other vessels,

Algorithm 2 Full CPA algorithm for determining collision avoidance utility for sampled candidate maneuvers under COLREGS constraints using range-only discrimination of Equation (3.26).

```

1: procedure PSEUDOCODE FOR FULLCPAQUANTIFICATION()
2:   for  $i^{th}$  contact do
3:      $r_i \leftarrow$  current contact range
4:      $\theta_i \leftarrow$  current contact course
5:      $v_i \leftarrow$  current contact speed
6:     Calculate:  $r_{cpa}^{\lambda_0}, t_{cpa}^{\lambda_0}, \Theta_{cpa}^{\lambda_0}$ 
7:     Calculate: risk of collision (per COLREGS) w.r.t.  $i^{th}$  contact
8:     if (collision risk  $\geq$  collision risk threshold) then
9:        $\Theta_0 \leftarrow \Theta_0(x, y, x_c, y_c, \theta, \theta_c)$ 
10:       $\mathfrak{R}_i \leftarrow \mathfrak{R}(\Theta_0)$  ▷ determine governing protocol rule
11:       $w_i^{avd} \leftarrow w_l(r, \dot{r}, r_{cpa}^{\lambda_0}, t_{cpa}^{\lambda_0}, \Theta^{\lambda_0})$ 
12:       $f_l \leftarrow \mathfrak{D}(r_{cpa}, \mathfrak{R})$  ▷ Per Equation (3.28)
13:      for  $j = courses.min$  to  $courses.max$  do
14:        for  $k = speeds.min$  to  $speeds.max$  do
▷ sample appropriate subset, i.e., not brute force
15:           $avd_i[j, k] \leftarrow \left\{ 0, \frac{r_{cpa} - R_{min}}{R_{pref} - R_{min}}, 1 \right\}$ 
16:           $avd_i[j, k] \leftarrow avd_i[j, k] - \mathfrak{R}_i(j, k)$ 
17:        end for
18:      end for
19:    end if
20:  end for
21: end procedure

```

regardless of whether the contact is human operated, autonomous, or some combination thereof.

To see the benefits of considering additional calculations to garner explicit collision avoidance information, consider the geometry scenario of Figure 3-1 with a range at CPA on current relative trajectory r_{cpa} requiring a maneuver to avoid collision. Raw CPA ranges for candidate course-speed maneuvers are displayed in Figure 3-8 as a polar plot with blue representing closer ranges and red representing farther ranges. Using the velocity obstacle algorithm, a polar collision avoidance objective function can be generated to show allowed (red) and excluded (blue) ownship candidate maneuvers (Figure 3-9a) subject to selection of a fixed collision range threshold R_{col}^{vo} of Equation (3.23). Under the limiting COLREGS protocol constraints for a give-way vessel, turns to the left are excluded to avoid crossing ahead of the stand-on vessel if

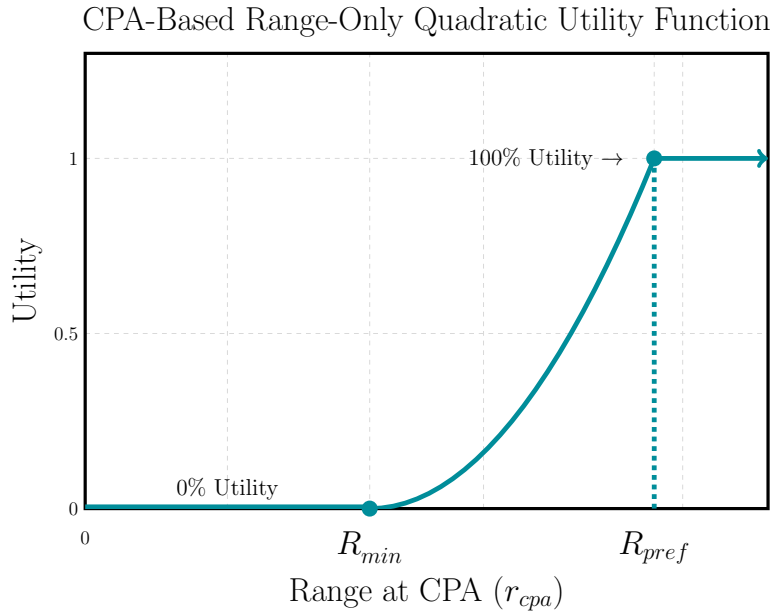


Figure 3-7 The full CPA quantification algorithm of Equation (3.27) is shown as an arbitrary continuous function for a two-threshold range configuration.

the circumstances of the case admit. This limitation significantly reduces the decision space, as shown in Figure 3-9b, especially when considering ownship’s desire to drive east.

Using the full CPA quantification algorithm, direct knowledge of r_{cpa} for candidate maneuvers allows for additional threshold values of CPA ranges of interest. Specifically in this demonstrative case, R_{col}^{vo} maps to R_{pref} of Equation (3.26); a closer range value of R_{min} represents ownship’s minimum acceptable CPA range. Samples of the decision space then allow mapping intermediate r_{cpa} values to continuous utility values between 0 and 1 for candidate maneuvers as shown in Figure 3-10. An exact value of r_{cpa} , and therefore some inference of goodness, and therefore risk, becomes known for any choice of maneuver considered between R_{min} and R_{pref} . The non-integer utility values present a quantified metric of risk to the multi-objective optimization solver using the same encounter geometry as Figure 3-9. After applying the COLREGS collision avoidance protocol constraints¹³, the full CPA quantification algorithm demon-

¹³COLREGS-specific considerations are presented for power-driven vessel encounters within rules 13-17 in Chapter 4. Portions of the COLREGS are presented for reference in Appendix A.

strates highly relevant collision avoidance information for higher speeds along the mission-desired path (East) that were otherwise excluded by the velocity obstacle algorithm (Figure 3-10b). If faced with a heavily constrained or over-constrained collection of objective functions, the solver may now reason about a previously excluded subset of decision space with a means of inferring the risk involved.

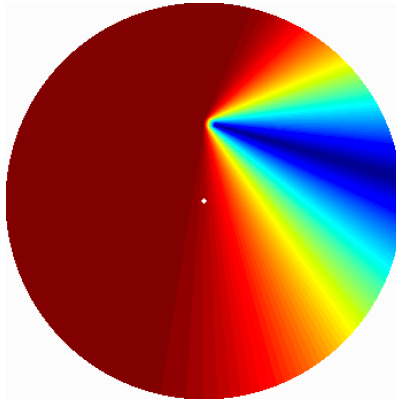
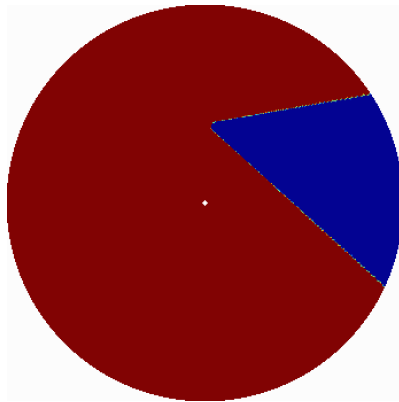
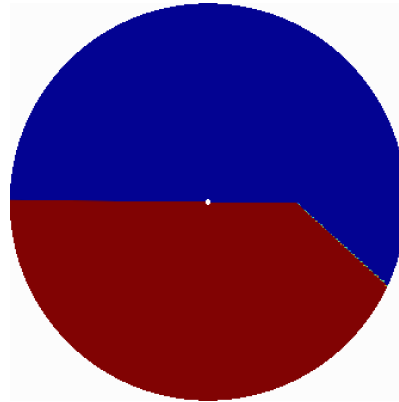


Figure 3-8 This polar objective function with radius = speed (v), polar angle (north up) = course (θ , North-up) depicts raw CPA ranges varying from smallest (dark blue) to largest (dark red). The red plateau depicts maneuvers where an opening aspect would occur, i.e., CPA is in the past.



(a) Velocity Obstacle



(b) Velocity Obstacle with COLREGS

Figure 3-9 These polar objective functions with radius = speed (v), polar angle (north up) = course (θ , North-up) represent the $\vec{x}(\theta, v)$ decision space for the single vehicle-pair collision avoidance scenario of Figure 3-1 using a velocity obstacle algorithm of Figure 3-3. The velocity obstacle algorithm shows both allowed (red, utility = 1) and eliminated (blue, utility = 0) candidate maneuvers without (Figure 3-9a) and with (Figure 3-9b) COLREGS protocol constraints (give-way vessel crossing astern of the stand-on vessel). The stepwise cliff in utility occurs along the lines corresponding to \vec{x} crossing into the excluded region of the velocity obstacle or violating a COLREGS protocol constraint. The amount of allowed (red) candidate maneuvers can be significantly reduced when protocol constraints are applied.

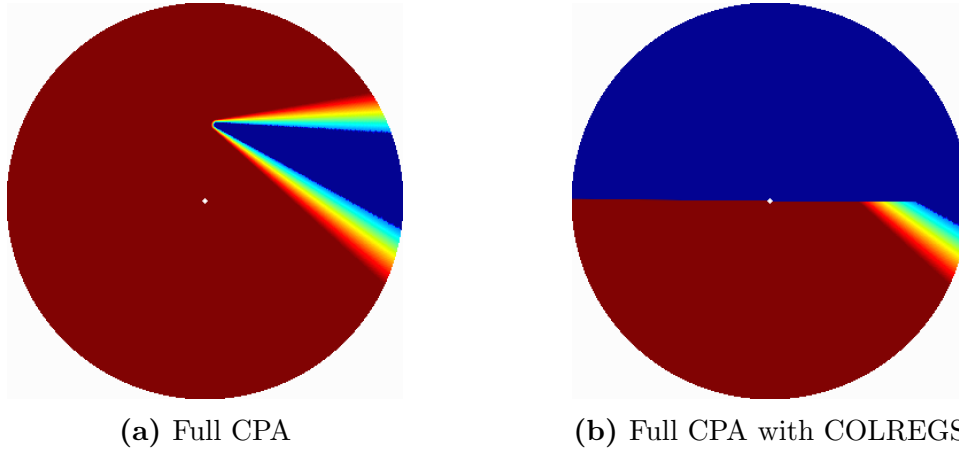


Figure 3-10 These polar objective functions showing the same collision avoidance scenario of Figure 3-1 demonstrate the continuous utility values available when using the full CPA quantification demonstrated in Figure 3-6 and Algorithm 1. Both allowed (red, utility = 1) and eliminated (blue, utility = 0) candidate maneuvers of this figure are consistent with the velocity obstacle. Intermediate continuous utilities (other colors) are allowed based on direct computation of range at CPA both without (Figure 3-10a) and with (Figure 3-10b) the added COLREGS protocol constraints for a give-way vessel crossing astern of the stand-on vessel (Rules 15/16). With the significant reduction in feasible candidate maneuvers after applying the COLREGS rules, the full CPA quantification algorithm allows direct sampling of otherwise excluded candidate maneuvers. Those sampled candidate maneuvers determined to have a resulting range at CPA (r_{cpa}) between the minimum allowed (R_{min}) and preferred (R_{pref}) ranges at CPA are considered for selection with a utility value commensurate with their corresponding value of r_{cpa} .

3.4 Techniques to Improve Computational Efficiency

3.4.1 Sampling Size

The number of pieces sampled to create an IvP function from an underlying objective function largely drives the tradespace between speed and accuracy *vis-à-vis* errors of imprecision. To avoid the speed scalability pitfalls of full brute force methods while being more accurate than simplified brute force methods, an appropriate selection of IvP function sample size is prudent. A piecewise linear approximation to the underlying objective function that is sufficiently accurate without being prohibitively slow becomes the goal of the designer. The selection of the appropriate sample size is a design choice, though it can be seen that a relatively few number of pieces generate a very representative model of the true underlying function. Figure 3-11 depicts the ability of IvP functions to represent an underlying objective function for a simple bimodal distribution with a large plateau of low utility. These example IvP functions enforce uniform spacing and uniform sampling size of varying values of precision in the IvP decision space domain; improvements to accuracy by allowing non-uniform spacing and sizes of IvP pieces is incorporated through smart refinement.

3.4.2 Smart Refinement

The smart refinement feature of IvP allows for greater resolution in areas of interest especially those areas where the underlying objective function experiences non-linear changes of shape within the sample subspace. As an IvP function initially creates its IvP pieces, the algorithm can grade its work to determine how accurate the linear fit matches the underlying objective function over the IvP piece's decision variable sub-domain [6]. IvP maintains a priority queue based on these grades that prioritizes poorly fitting pieces. The poorly fitting pieces are then refined up to the maximum piece limit selected by the behavior's designer.

Smart refinement demonstrates the power of IvP by allowing a rather course sampling of the underlying objective function for those areas lacking interesting features

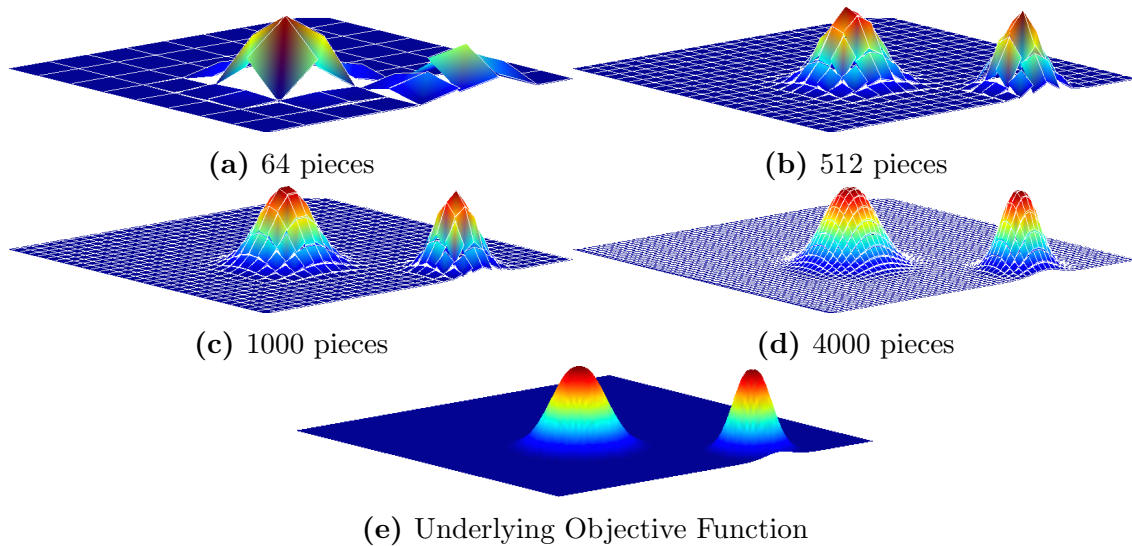


Figure 3-11 Selection of an appropriate number of pieces to sample the IvP function allows for very fast computation while retaining sufficient accuracy (red represents a high utility while blue represents an undesirable utility). Figure 3-11e shows the underlying objective function from which the four piecewise linear approximations were created. For these four IvP approximations, the same underlying bimodal objective function (e) is sampled using four different values of uniformly spaced and uniformly sized pieces. While IvP piece size and spacing is not required to be uniform, these examples illustrate the power of only changing the number of pieces on the area of interest. Figure (3-11a) shows 64 uniformly spaced and sized IvP pieces; note the degraded accuracy of the peak on the right with the degraded precision. The 512 piece approximation (b) demonstrates uniformly spaced and sized IvP pieces and shows a significantly improved representation of the second peak. The same underlying objective function sampled with 1000 and 4000 uniformly spaced and sized IvP pieces show considerable improvement in refinement ((c) and (d), respectively).

(e.g., low utility plateaus). For the underlying bimodal objective function shown in Figure 3-11e, the large areas of low utility plateau can be modeled with a course grid. After the initial modeling of the function, smart refinement adds several more samples that greatly improve the fitting in more dynamic areas such as the build up to the two peaks. Using the same bimodal distribution, consider its most course sampling (Figure 3-11a) with an 8x8 grid totalling 64 IvP pieces. Without any alteration to the sparsely sampled plateau regions, the addition of pieces in the regions of the two peaks quickly create a very precise and accurate model of the underlying objective function. The same 64-piece IvP function of Figure 3-11 undergoes smart refinement as shown in Figure 3-12 with 100, 200, 500, and 750 pieces. Note that even the 100 piece smart refinement model very reasonably fits the underlying bimodal objective function. By having a method of accurate modeling requiring few enough samples to be scalable, IvP introduces a data-rich region of desirable course-speed pairs rather than simply identifying poor (blue) plateau regions for exclusion.

While IvP allows the balance of accuracy, speed, and flexibility, improvements such as smart refinement allow a greater number of simultaneous contacts to be reasoned about for some given onboard processing capability without saturating the back-seat computer. Experimentation with 5 vehicles did not over stress back seat computational loading, therefore smart refinement was not required for the testing within this thesis. Expansion to greater numbers of simultaneous contacts may require the sampling efficiencies of this section and are reserved for future work. Results of this experimentation are presented in Chapter 6.

3.5 Sampling Algorithms Applied to Collision Avoidance

IvP creates a 3 dimensional (radius = speed, polar angle (North up) = course, z = utility) polar piecewise linear approximation of the underlying collision avoidance objective function by sampling a sub-space over appropriate intervals using meth-

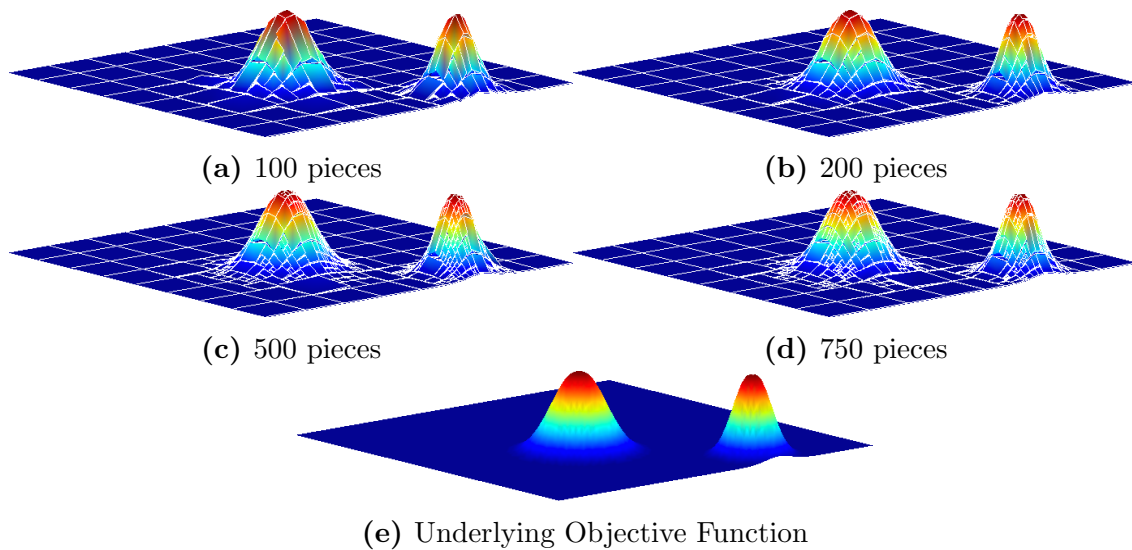


Figure 3-12 Smart refinement allows for increased sampling of the underlying objective function in areas where the IvP function would benefit from further refinement. The 64-piece IvP function of Figure 3-11a acts as a baseline for four successive smart refinements using 100, 200, 500, and 750 pieces. Note how few additional pieces are required to construct a representative IvP function based on the course 64-piece grid approximation of the underlying objective function (e). The smart refinement technique allows for a course underlying grid with sufficient sampling in high interest areas promoting a balance of accuracy and efficiency.

ods described in [3] and Section 3.1. In an extreme configuration, sampling could be forced over the entire decision space, though this is inefficient and unnecessary. By using the smart refinement algorithm of Section 3.4.2, large plateau regions of the course-speed decision space can be assigned large IvP pieces without further refinement. Therefore, the approximation of the underlying objective function using efficient sampling techniques enables identification of a globally optimal solution to multi-contact collision scenarios while operating under multiple and often competing mission objectives.

An example of an arbitrary collision avoidance objective function for a multi-contact complex geometry encounter with clear advantage of certain velocity vectors over others is shown in Figure 3-13. Several uniformly spaced and sized IvP pieces without invoking smart refinement, caching, or other efficiency enhancing techniques show the varying levels of accuracy while changing precision (Figures 3-13 (a)-(d)). This objective function uses a utility mapping with two threshold ranges at CPA and a linear interior mapping similar to that shown in Figure 3-4b. Figure 3-13e shows the underlying objective function while Figures 3-13a through 3-13d show the resulting approximation of various uniform sampling frequencies. The underlying objective function begins to take shape with relatively few samples while the higher sample sizes are nearly indistinguishable from the underlying objective function.

Smart refinement of the same arbitrary collision avoidance objective function is shown in Figure 3-14. Note that with the intelligent addition of a limited number of additional samples, the underlying objective function quickly begins to take shape using the techniques of Section 3.4.2. The complexities of this underlying objective function illustrate the importance of additional IvP pieces to more fully define nuances of the underlying function.

For a velocity obstacle-based algorithm, the data available to the autonomous decision maker is the area that is considered a protocol violation or unsafe. Techniques shown in Chapter 4 can be used to assign varying metrics of “goodness” in the final selection of a velocity vector, but the cost functions only know the excluded velocity space and the *a priori* determined preferred velocity vector. Maintaining consistency

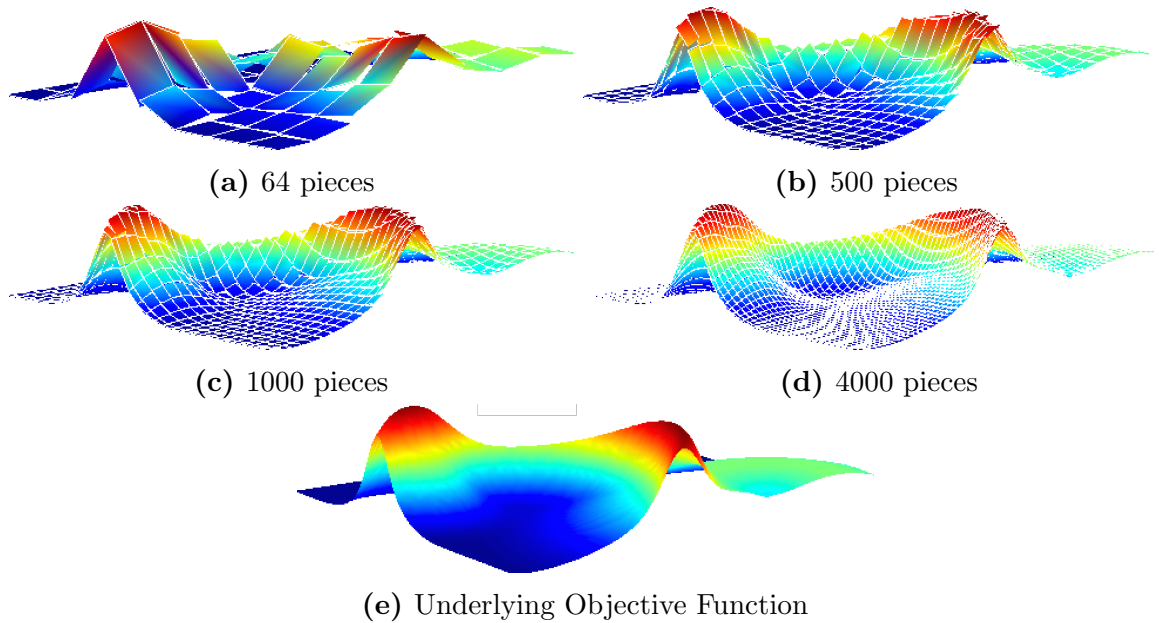


Figure 3-13 An arbitrary collision avoidance objective function is shown with IvP functions sampling at uniform sampling size and shape without refinement of any kind; here, red represents a high utility while blue represents an undesirable utility. This worst case sampling for the given number of pieces shows that a reasonably small sample size provides an accurate representation of the underlying objective function. By using IvP rather than a simple exclusionary technique such as the velocity obstacles family of algorithms, allowed regions of course-speed candidates can be incorporated into the selection of the globally optimal velocity vector. IvP approximations of the underlying objective function (e) are shown using 64, 500, 1000, and 4000 uniformly spaced and sized IvP pieces.

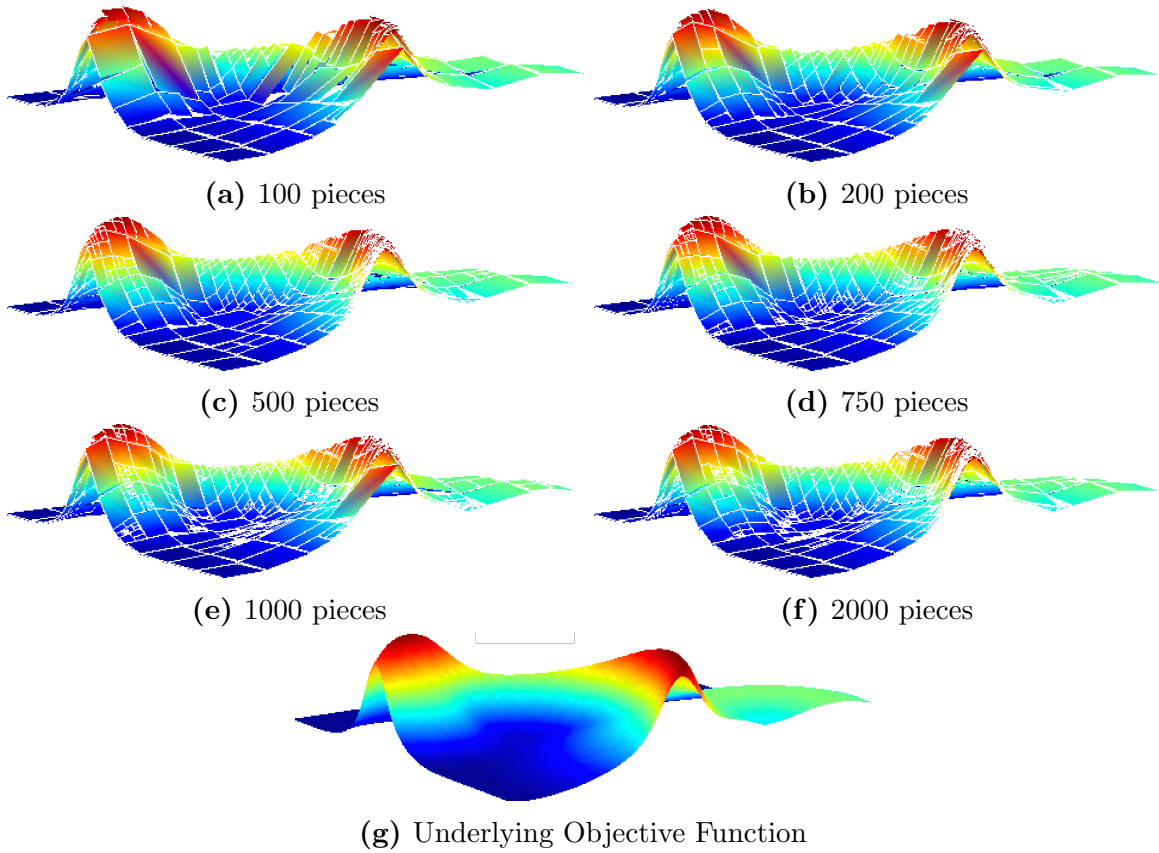


Figure 3-14 A representative collision avoidance objective function shown in Figure 3-13e is again approximated with IvP functions using the same 64-piece sample frequency of Figure 3-13a. The smart sampling techniques of IvP are applied to increase the sample frequency of the underlying objective function in local regions whose linear fit could be improved. The smart sampling algorithm results for 100, 200, 500, 750, 1000, and 2000 total pieces ((a)-(f) respectively) to further refine the underlying 64-piece IvP function show that few additional pieces are required before the underlying objective function takes shape in the IvP function approximation.

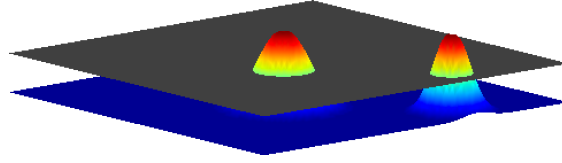
with these algorithms, one could consider the excluded velocity space as any velocity vector that results in a collision as defined by the designer’s collision range while accounting for safe stand off ranges.

A CPA-based objective function can be used for common demonstration between the two algorithms by using a plane of height $z = R_{col}^{vo}$ to bisect the underlying objective function. In velocity obstacle algorithms, any course-speed pair below the plane $z = R_{col}^{vo}$ is considered a collision and excluded from consideration. All points above the plane $z = R_{col}^{vo}$ are considered collision-free and are included without preference. For the same collision avoidance scenario, the CPA-based algorithm also excludes the region below the plane $z = R_{min}$ insofar as such a low utility is highly unlikely to receive selection as the final velocity vector assuming that the collision avoidance behavior’s objective function has a reasonable significant priority weight in the solver.

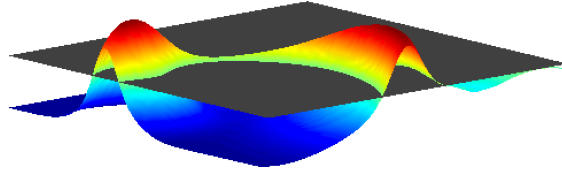
Depending on the velocity obstacle designer’s selection of R_{col}^{vo} , one of two important information losses occur when compared to the full CPA quantification algorithm:

- a low R_{col}^{vo} value neglects all important information above the plane that could be used to find a better-than-default solution
- a high R_{col}^{vo} value neglects all important information below the plane that could be used in lieu of heuristic relaxation

Considering the objective functions shown in Figures 3-11 and 3-13, the value of R_{col}^{vo} is shown graphically as the transition between blue and green. By adding the horizontal plane at $z = R_{min}$, the region excluded from consideration in both velocity obstacle and CPA-based algorithms is shown by the black plane in Figures 3-15 and 3-16. All values of color above the black plane indicate a candidate course-speed pair that is considered collision-free and therefore admissible as a feasible solution for the cost function of each designer’s choice. While velocity obstacles consider all points in color above this plane to be of equal “goodness,” the full CPA quantification algorithms consider the rich green, yellow, and red regions as different degrees of “goodness” when solving for the yet-to-be-determined optimal velocity vector that balances all active behaviors (mission, navigation, and collision avoidance) according



(a) Bisected Objective Function of Figure 3-11e



(b) Bisecting Objective Function of Figure 3-13e

Figure 3-15 A plane at $z = R_{min}$ bisects the underlying objective functions of Figures 3-11 and 3-13 represented here by the transition from blue to green. All blue values (below the black plane) result in a violation of the collision range and are considered inadmissible for velocity obstacles. Identically, all values below the black plane result in a violation of R_{min} and are highly discouraged from selection when appropriate priority weight is applied to the behavior's objective function in full CPA quantification algorithm based collision avoidance. Information rich decisions can be made for points above the plane of discrimination.

to their respective priority weights.

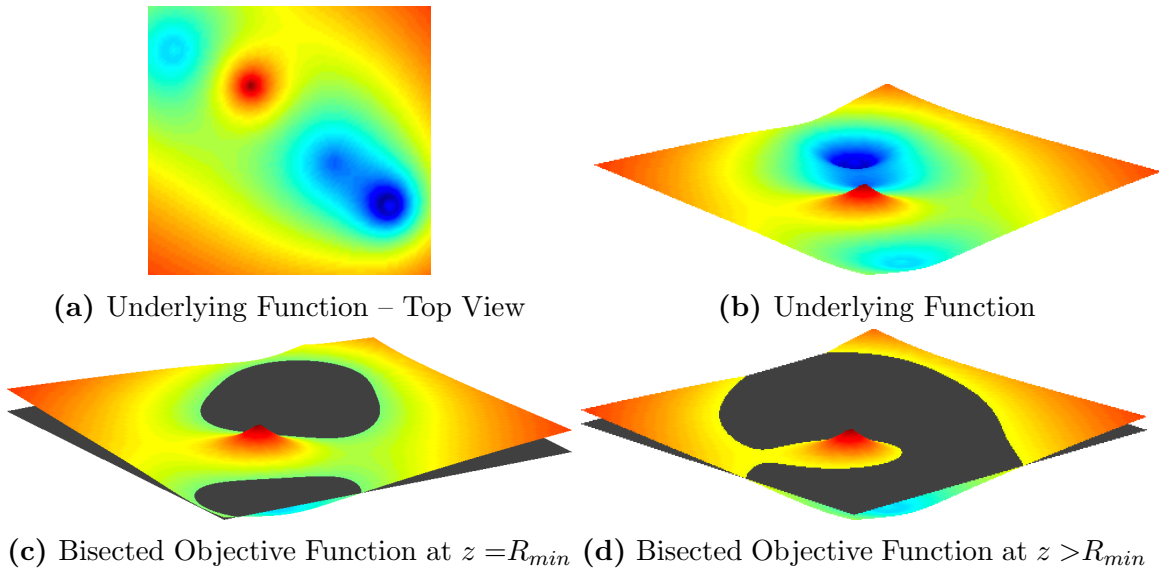


Figure 3-16 An arbitrary complex collision avoidance objective function without approximation (a) demonstrates the complexities of multi-contact collision avoidance. Red colors again represent desirable conditions while blues represent unfavorable collision conditions (ranges less than R_{min} , or equivalently, excluded regions from multi-contact velocity obstacle solutions). The topographic view (b) demonstrates the existence of three highly desired red peaks. By again bisecting the true objective function with a plane at $z = R_{min}$, the black plane represents the exclusion zone of velocity obstacles (c). By choosing some $z > R_{min}$, the more highly desirable solutions with ranges at CPA approaching R_{pref} become evident to present a more decision-rich input to the velocity vector solution.

3.6 Designing for Patience

The patience parameter¹⁴ introduces an additional objective function design parameter allowing an active tradespace between constant course decisions (speed may vary) and constant speed decisions (course may vary). By using multi-objective optimization with a non-binary collision avoidance decision space based on the resulting closest point of approach, intelligent compromise can be achieved to choose a velocity vector consistent with considerations of a human operator. This parameter does not affect the primary mission objective function's peak value for the unconstrained case; rather, it gives the primary mission objective function a policy-consistent method for shaping alternative primary mission utilities when the preferred velocity vector is infeasible or highly undesirable to other weighted priorities. The patience parameter represents a weighted preference to alter either course or speed. This patience parameter gives the mission objective function designer wide latitude in tuning routines to behave as desired with respect to performance metrics. Specific performance metrics are presented in Chapter 4.

Effects on primary mission and collision avoidance performance when deviations are required has been little studied in the literature. The literature is especially bare when comparing a tendency to prefer a course or speed dominated maneuver over the other. Rather, users of the velocity obstacle have little choice but to deviate from the mission prioritized velocity vector using a heuristic lowest cost maneuver. In the case of recent collision avoidance literature using a velocity obstacle, the heuristic least cost deviation is usually determined using a 2-norm over the two-dimensional course-speed decision space such as in [45].

When designing a mission objective function, consideration must be given for deviations from the mission preferred course and speed. In situations with multiple conflicting protocol requirements, more complex consideration must be given for how to best deviate if all else were equal. The three maneuvering deviations within the two-dimensional course-speed decision framework include:

¹⁴Section 3.6 first appeared in part in [94].

- maintain current course with change of speed as necessary (usually slowing)
- maintain current speed with change of course as necessary (under protocol, usually a turn to starboard)
- change both course and speed according to some policy.

A tradespace between the possibilities of a course-only or a speed-only maneuver presents a new region of autonomous design for collision avoidance routines as shown in Figure 3-17. Thoroughly exploring this deviation tradespace requires performance metrics to be identified, incorporated into design, and used for evaluation (Chapter 4). Primary mission objective functions must incorporate the ability to gracefully deviate within this tradespace when under non-mission constraints such as collision avoidance. In the context of protocol-constrained collision avoidance, evaluating vessel performance using spatial efficiency (Section 4.2.1), temporal efficiency (Section 4.2.2), and safety (Section 4.4) provides insight into future performance in similar scenarios. Under various decision points within the course-speed tradespace, some designer-selected combination of metrics can be maximized yielding a preference toward either a course or speed maneuver. The exploration of these maneuvering decisions and their consequences allows for both design changes and online autonomous tuning of objective functions when collision avoidance routines are active (i.e., their priority weight is greater than zero).

3.6.1 Course-Speed Design Ratio

The concept of a maneuvering tradespace when deviating from a contact-free decision can be formalized according to Equation (3.29). In the two extreme cases of maneuvering considerations, either course or speed is held constant while the other is varied appropriately. For the combination of some amount of both course and speed change, one can identify a preference toward a course-dominated or speed-dominated deviation by assigning a weight to each. A tendency to prefer course deviations are represented with a course weight (π_θ) while speed deviations are represented using a

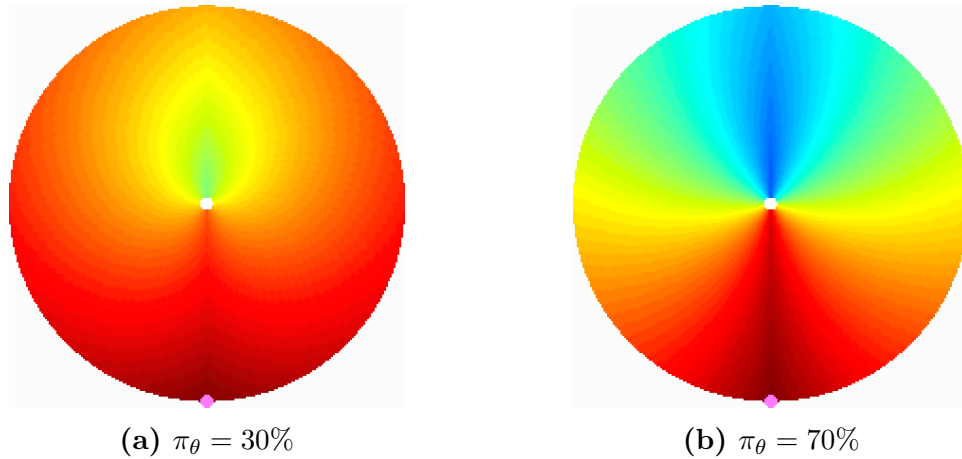


Figure 3-17 These polar heat maps show course (angle) and speed (radius) for patience parameters with values of $\pi_\theta = 30$ (a) and $\pi_\theta = 70$ (b). Desirable velocities are dark red while less desirable velocities are blue. Both examples are trying to achieve a course of 180° . The fuchsia point represents the peak value of each objective.

speed weight (π_v). To identify the preference of a course change over a speed change, or *vice versa*, the course-speed design ratio of Equation (3.29) is introduced. Course weight and speed weight are defined on a domain of $[0, 1]$ and are required to sum to 1 (Equation (3.30)). The introduction of these relative course and speed weights on a $[0, 1]$ domain allow for greater ease of configuration. Figure 3-17 demonstrates two mission objective functions: one preferring course-dominated deviations and one preferring speed-dominated deviations.

$$\pi = \frac{\pi_\theta}{\pi_v} \quad (3.29)$$

$$\pi_\theta \in [0, 1]$$

$$\pi_v \in [0, 1]$$

$$\pi_\theta + \pi_v = 1 \quad (3.30)$$

3.6.2 Patience Parameter

In the case of a pure course change (speed constant), the course-speed design ratio reaches a value of $\pi = \infty$. Similarly, a pure speed change results in a course-speed design ratio of $\pi = 0$. To allow a more computationally attractive form, the patience parameter of Equation (3.31) is introduced. The patience parameter expresses the normalized general maneuver preference for a two-dimensional collision avoidance decision space.

$$\bar{\pi} = \frac{\pi_{\theta}}{\pi_v + 1} \quad (3.31)$$

$$\pi_{\theta} \in [0, 1]$$

$$\pi_v \in [0, 1]$$

$$\bar{\pi} \in [0, 1]$$

$$\pi_{\theta} + \pi_v = 1$$

A designer may choose a static or dynamic patience parameter. A static patience parameter implies the designer pre-tuning a patience configuration for some constant preference of a vessel's deviation characteristics. While a tendency might be to prefer a course change over a speed change (or *vice versa*), having robustly designed mission objective functions capable of deviating from a preferred velocity vector opens a new spectrum of collision avoidance decisions and therefore optimization.

The patience parameter of Equation (3.31), when dynamic, allows variation based on online autonomous determination of its “best” value. This tuning must account for several possibilities of variation including some combination of the following:

- recognition of a geometric configuration (Section 5.4)
- designer preference
- configuration parameters

- environmental conditions (e.g., limited visibility, etc.)
- explicit protocol restrictions or requirements

Once proper metrics for evaluation are identified, a dynamic patience parameter value can be found for the collision avoidance situation and current mission to achieve the most desirable performance characteristics. If the collision avoidance scenario changes such as by the detection of a new contact in a conflicting rule, the dynamic patience parameter would be re-evaluated to determine the new “best” deviation policy.

Additional discussion of metrics and evaluation techniques can be found in Chapter 4. On-water results using these metrics and evaluation techniques can be found in Chapter 6.

3.7 Conclusions

In conclusion, this chapter presented the range-, time-, and pose-informed closest point of approach-based method of calculating risk of collision. This “full” CPA-based approach was used to construct collision avoidance objective functions using a more human-like utility function than the literature-standard velocity obstacle. The CPA-based approach was shown to be a mathematical generalization of the velocity obstacle for the range-only case where two range thresholds were set equal to each other and to the “collision” range of a velocity obstacle. The notion of patience for autonomous vessels was introduced to allow a spectrum of primary mission modification to prefer a speed dominated, course dominated, or speed-course weighted preference when deviating from the mission’s contact free choice of course and speed. Chapter 4 expands this chapter’s concept of pose-informed collision risk to introduce metrics for evaluation of safety and protocol compliance. Mission performance metrics and evaluation techniques are introduced to inform a holistic (i.e., mission, safety, and collision avoidance protocol compliance) testing framework for simulation (Chapter 5) and on-water (Chapter 6) testing.

THIS PAGE INTENTIONALLY LEFT BLANK

Chapter 4

Collision Avoidance Metrics and Evaluation

The ability to deliberately, consistently, and rigorously quantify autonomous collision avoidance enables society to assess compliance and performance with confidence. Insurance companies can use these performance scores when giving policies to autonomous vessels. Regulatory bodies can use these metrics for an autonomous or remotely operated vehicle’s “road test” before certification. Humans can train with real-time feedback with measurable performance values. Autonomous collision avoidance systems can use machine learning to improve behavior using aggregated data. The methods discussed in this thesis are intended to be a first step toward a more robust and standardized autonomous collision avoidance evaluation process. These methods can further serve to standardize literature regarding collision avoidance compliance, especially under protocol constraints.

This chapter¹ describes the metrics, scope, and evaluation techniques for quantifying compliance and performance of autonomous collision avoidance under protocol constraints. With the methods of this thesis, conversations in future literature can be more exact in their meaning of compliance in protocol-constrained collision avoidance research. Using the foundation of the continuous collision avoidance utility functions of Chapter 3, Section 4.1 introduces metrics for evaluating autonomous collision avoid-

¹parts of this Chapter first appeared in [93–95]

ance performance in the context of the overall vessel’s mission. Section 4.2 introduces evaluation of mission performance including spatial and temporal efficiencies. Evaluation techniques for collision avoidance protocols are introduced in Section 4.3 with examples given specific to COLREGS. Techniques for evaluating safety with the incorporation of pose are presented in Section 4.4. Introduction of evaluation techniques for both human operators and autonomous collision avoidance algorithms based on admiralty case law and on-water experience is presented in Sections 4.5 through 4.6.

Chapter 6 presents experimental results using the algorithm advancements of Chapter 3, the evaluation techniques of this chapter, and the testing considerations and techniques of Chapter 5.

4.1 The Tradespace of Safety, Efficiency, and Protocol Compliance

Current autonomous collision avoidance designs are based on least cost heuristic deviation from the *a priori* determined preferred mission velocity vector. These algorithms are, by design, intended to achieve the primary mission at all reasonable costs. A more human-realistic approach, however, is to consider the primary motivations of a normal operator. The five main considerations that a human operator intuitively balances when choosing how best to maneuver include a weighted combination of the following:

- spatial efficiency (Section 4.2.1)
- temporal efficiency (Section 4.2.2)
- protocol compliance (Section 4.3)
- safety (Section 4.4)
- other mission considerations

The requirement to obey a prescribed set of rules such as COLREGS often further restricts a collision avoidance decision space; deciding on how best to deviate requires an appropriate balance of safety, efficiency, and compliance. While rule compliance has often been considered largely binary throughout the literature (compliant or non-compliant), Chapter 4 presents algorithms that describe a continuous domain of protocol compliance scores. These continuous metrics of performance and protocol compliance allow more precise conversation in the literature and more robust design in practice.

Each of these performance characteristics necessitates a quantifiable metric for inclusion in autonomous collision avoidance and consideration for mission design tradeoffs. In partnership with the patience parameter of Section 3.6 and testing techniques such as the iterative geometric testing of Section 5.4, a designer’s preferences on the balance of these metrics allows appropriate selection of a maneuver.

By using these metrics rather than simple binary characteristics, comparison and tradeoffs can be made as the objective space of a true multi-objective optimization problem. Examples of tradeoffs are shown in Section 5.1.

4.2 Efficiency and Mission Performance

For the standard transiting vessel, “mission” simply refers to the desire to reach the next waypoint within reasonable parameters of time and deviation from track² (energy consumption). More complex scenarios might include using a sensor that requires a particular orientation with respect to an Earth-fixed location or a moving object. In most mission cases, track deviation distance and transit time are likely contributing factors to a measurement of success. The ideas of track deviation and transit time may be quantified using spatial efficiency and temporal efficiency as described below. Missions that value non-standard metrics of performance (e.g., maintaining contact with an underwater entity) may use alternative measures of performance that those presented below. A collision avoidance encounter begins from the point of first de-

²Track refers to the ideal path a vessel would follow to achieve its primary mission [10].

tection and ends when the contact is well clear, opening range, and approaching its initial detection range.

4.2.1 Spatial Efficiency

Spatial efficiency as an output metric represents the additional distance travelled from an intended track between any two points of reference. The nominal track need not be linear, nor do the points of reference necessarily need to correlate with mission waypoints. More formally, Equation (4.1) describes the notion of spatial efficiency as the ratio of nominal track distance to actual track distance between any two specified points.

In the case of a collision avoidance maneuver, spatial efficiency can be considered nominally in two ways. Spatial efficiency could be measured from the waypoint preceding a collision avoidance encounter to the waypoint following the collision avoidance encounter. Alternatively, spatial efficiency could be measured from the point in space at which a contact is first detected to the point in space where a vessel returns to her intended track. Figure 4-1 graphically demonstrates spatial efficiency between a starting point A and ending point B along ownship's track in the context of Equation (4.1). Spatial efficiency measures by ratio of intended track distance $\hat{\rho}$ and the actual distance traversed (ρ) between any two points A and B . While depicted linearly, a general non-linear ship's track may be considered in appropriate circumstances where a vessel's mission would not necessarily dictate a constant course transit.

$$\eta_{\rho} = \frac{\hat{\rho}}{\rho} \quad (4.1)$$
$$\eta_{\rho} \in [0, 1]$$

The notion of spatial efficiency transcends missions more broadly than simply trying to minimize resources such as fuel. A desire for high spatial efficiency may

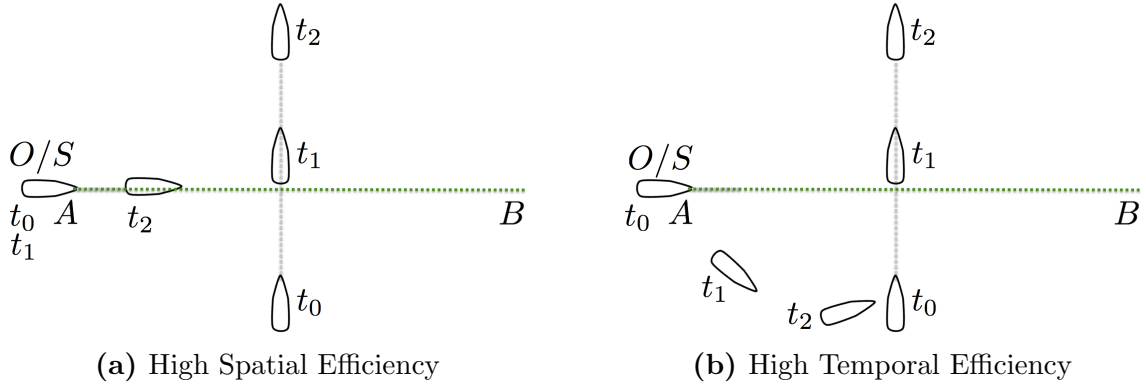


Figure 4-1 Two example canonical crossing encounters are shown. In (a), ownship (“O/S”) chooses to slow and allow the contact to pass. Positions at times t_0 and t_1 are nearly identical resulting in near zero deviation from track. When the contact passes at time t_1 , O/S proceeds down track (green line). In (b), O/S chooses to deviate from track to maintain speed and proceed in general direction of track.

accompany certain primary mission characteristics. For example, a vessel may be towing a sensor that would cause poor data quality if altering course; however, a speed reduction may provide little to no loss of data quality.

4.2.2 Temporal Efficiency

Temporal efficiency provides a metric of the additional time required to complete a collision avoidance maneuver. Similar to the spatial efficiency metric of Section 4.2.1, temporal efficiency may take place between waypoints or during specific parts of a voyage that are affected by collision avoidance encounters. Temporal efficiency measures the ratio of nominal and actual times to transit a specified track as shown in Equation (4.2). Actual time to traverse A to B is given by τ while $\hat{\tau}$ denotes time to traverse the intended track assuming constant initial speed.

$$\eta_{\tau} = \frac{\hat{\tau}}{\tau} \quad (4.2)$$

$$\eta_{\tau} \in [0, 1]$$

4.3 Evaluating Protocol Compliance: Quantifying the Rules

Several authors have studied collision avoidance with claims of “compliance” with the Collision Regulations (also referred to as COLREGS or Rules). Compliance, however, lacks objectivity partly due to the inherent vagueness of the COLREGS and partly due to the varying scope of many collision avoidance algorithm solutions. This intentional vagueness allows the human operator liberty to interpret the vast array of complex collision avoidance scenarios without being overly restricted from a common sense yet safe approach.

A further complicating factor results from the disconnect between experienced mariners and autonomous designers. Few designers of marine autonomous collision avoidance algorithms have demonstrated significant experience using COLREGS in open ocean navigation for non-academic purposes. The varying scope of what authors claim as compliant largely depends on the scope of interest of a particular researcher. For example, a perception and sensing author might claim COLREGS compliance if day shapes or vessel types are correctly identified. An acoustician might claim compliance for properly identified sound signals. The notion of compliance, however, should be amplified with the applicable scope of the COLREGS.

This section proposes several categories of scope as a first pass means of grouping similar research and subsequent evaluation. With the development of metrics and evaluation techniques within each category of scope, performance can be reliably demonstrated to a certifying body to a required degree of satisfaction within each given category. A means would then exist to properly combine work of differing categories to produce more fully compliant solutions. The techniques of this section permit the admission of a road test (Section 5.6) to offer a means for regulatory bodies to consider certification of autonomous collision avoidance algorithms operating under the protocol restrictions of COLREGS.

Protocol compliance is often asserted by authors in the collision avoidance realm with no metric of verification or validation. The term compliance is often used in

the general context of COLREGS protocols to ambiguously describe only the power-driven vessel rules in nominal operating conditions (COLREGS Rules 13-17). Little discussion exists in the literature as to how protocols such as COLREGS should be examined for compliance for either human-controlled or autonomous vessels for the complete set of protocol requirements. The Rules are intentionally vague to allow a reasonably experienced human operator the flexibility to take the most appropriate action within the context of the Rules. There are no well-defined universally recognized rubrics to measure or grade any vessel on how best to be “compliant” with the protocol nor what protocol compliance means. There are, however, extensive cases in admiralty law and practical experience of seasoned mariners that offer insight into means of shaping a framework for protocol evaluation. Literature pre-dating autonomous collision avoidance has consolidated many scenarios, lessons, and court rulings regarding collision avoidance on the seas [17]; however, many of these lessons are violated in recent academic literature on the subject due to the unintentional disregard of human-established customs and case law.

Proper testing of compliance requires a thorough understanding of the protocol constraints. These constraints are more than what appears in the few sentences agreed to by international law. Rather, it is a combination of the written rules, years of case law, and accepted common customs and implementation of the rules in the sea-going world. Section 4.3 discusses the evaluation of protocol constraints within the context of COLREGS including an examination of particular failures or omissions in recent literature.

4.3.1 Categories for COLREGS Scope

Collision avoidance compliance in the most general sense involves maneuvering one’s vessel to properly interact with a contact for a given initial geometry. To counter the disparity between claims and actual performance, this thesis quantifies the scope and requirements of COLREGS compliance as part of an autonomous collision avoidance approach. Notional algorithms are presented to measure each applicable rule’s derived metrics and to assess a performance grade. Accordingly, the COLREGS rules

are separated into categories to allow a vehicle to demonstrate compliance of appropriate COLREGS subsets. International Maritime Organization guidance, US Coast Guard's local issuance of inland-specific requirements, and other local guidelines can be adopted as appropriate.

The categories proposed to define scope of work within the international COLREGS and compliance thereof are listed in Table 4.1 and include:

- general requirements of vessels including Rules 1-3
- conduct of vessels in any condition of visibility including Rules 4-8
- special cases for channels and separation schemes including Rules 9-10
- conduct of two sailing vessels in sight of one another and operating under Rule 12
- general vessel encounters including conduct of vessels in sight of one another and operating under Rules 13-17
- responsibilities of vessels in sight of one another as exhibited in Rules 11 and 18
- conduct of vessels in restricted visibility under Rule 19
- lights and shapes required of vessels under Rules 20-31
- sound and light signals required of vessels under Rules 32-37
- inter-vehicle communications to include sending, receiving, interpreting, and appropriately acting on messages to/from other vessels or third parties (e.g., USCG district)
- cumulative performance of the above categories to ensure a satisfactory holistic approach to safe navigation and collision avoidance

Rule categorization allows one designer to claim compliance within one or more categories (for example, maneuvering requirements of power driven vessels) while deferring evaluation of rules related to other areas (for example, sound identification

Table 4.1 *Categories of Scope for Evaluation of COLREGS Compliance*

Category	Description
I	General Rules (Rules 1-3)
II	General Conduct of Vessels (Rules 4-8)
III	Special Traffic Schemes (Rules 9-10)
IV	Sailing in Sight of Another Sailing Vessel (Rule 12)
V	Vessel Encounters in Sight of One Another (Rules 13-17)
VI	Responsibilities in Sight of One Another (Rules 11, 18)
VII	Restricted Visibility (Rule 19)
VIII	Lights and Shapes (Rules 20-31)
IX	Sound and Light Signals (Rules 32-37)
X	Inter-Vehicle Communications
XI	Cumulative Performance Including Local Customs

and response) to other authors. By defining the scope of applicable rules and demonstrating quantifiable levels of compliance within each category of rules, autonomous collision avoidance algorithm designers can sufficiently articulate their contributions to the literature. It should be noted that evaluation within the scope of one category may rely on compliance of another category to some degree. For example, because Category II includes maintaining a lookout, determining safe speed, determining risk of collision, and taking action to avoid a collision, it heavily influences evaluation of Categories III-VII.

4.3.2 Approach

A means to quantify the power driven rules is presented to include a numeric scale of compliance (0-100) for each applicable rule and its subsequent contribution to the applicable categories of rules. Qualitatively mapping grades of pass, marginal, and fail with configurable threshold levels allow ease of initial viewing of performance by the certification authority. Detailed numeric evaluation of scenarios may accompany the top level grade to provide additional feedback and amplification of score penalties.

COLREGS collision avoidance evaluation within this thesis consists of two primary metrics: safety and protocol compliance. Safety is based on a combination of range and pose of the vessels at CPA. Protocol compliance is based on collision avoidance

rule-specific requirements. Pose at CPA, specific values of range at CPA, complexity of simultaneous contact geometries, and total contact picture are complicating factors that are not directly quantified in the COLREGS except in limited circumstances or as a consideration without specific definition. Each of these factors are, however, important to collision avoidance decision making.

Examination of past encounters can be used to help train algorithms to understand safe values of these quantities. These are related yet can provide additional value when in context of the other. For example, a sufficiently compliant maneuver with respect to the written rules might have varying degrees of safety depending on certain configuration parameters. By examining the components of safety and compliance to include range, speed, pose, and similar quantities, much insight into true performance can be inferred. Section 4.4 discusses the safety metrics of evaluation. Section 4.5 discusses protocol compliance metrics and considerations.

4.4 Evaluating Safety Using CPA Range and Pose

The safety metric gives a quantifiable means to evaluate the danger associated with a particular maneuver. Gains in temporal and spatial efficiency possibly compromise the range or pose at closest point of approach. Safety must therefore be quantified in order to understand the risk associated with efficiency gains. By introducing the protocol compliance metrics of Section 4.3, safety and protocol compliance can be largely decoupled³ to determine when a rule provides an otherwise safe closest point of approach regardless of its adherence to the Rules. This decoupling allows exploration of degrees of protocol compliance and resulting risk to the vessel.

While range is the predominant metric of traditional methods such as the velocity obstacle, some account must be given to pose at CPA. This is especially important when considering relaxation of range at CPA. Figure 4-2 demonstrates two collision avoidance encounters of equal CPA range. Note, however, the intuitive inclination to prefer the parallel CPA of Figure 4-2b over Figure 4-2a. Near-parallel CPA geometries

³Compliance of some rules incorporates safety as a component based on specific requirements.

have several advantages over near-orthogonal CPA geometries. First, near-parallel collision avoidance solutions require less dependence on ship geometry parameters (inherently slender bodies with high aspect ratios have less target area when in a narrow aspect). These solutions are also less sensitive to maneuvering casualties such as engine failure (stopping of one vessel requires no additional action by the other vessel to avoid collision). Finally, the near-parallel aspect allows greater predictability despite a more quickly closing range.

Using contact angle, relative bearing, range, and speed, a complete contact geometry can be realized. Contact angle assumes positive increasing values clockwise from the starboard bow and negative values counterclockwise from the port bow, such that $\alpha = 0^\circ$ represents the contact's bow and $\alpha = \pm 180^\circ$ represents the contact's stern. Pose at CPA is therefore not a single quantity, but rather a combination of values that give great insight into the collision avoidance problem. The pose at time of sighting or detection (Θ_0) often dictates which rule(s) of a protocol applies. The pose at CPA when combined with r_{cpa} and relative speed gives considerable insight into the degree of risk at t_{cpa} . Figure 4-3 shows relative bearing and contact angle for an arbitrary initial geometry and geometry at CPA. Figure 4-4 shows the importance of considering pose for two different encounters of the same range at CPA.

Maneuvers that are otherwise compliant with required turn direction and speed but maneuver in a way that results in unnecessarily close range at CPA are penalized in the safety score. The resulting range and pose at closest point of approach are considered when penalizing unsafe maneuvers. An autonomous collision avoidance routine is configured to know four primary configurable range values of importance, including in descending order:

- preferred range at CPA (R_{pref})
- minimum acceptable range at CPA (R_{min})
- range value considered to be a “near miss” encounter (R_{nm})
- range value considered to be a true collision (R_{col})

A tiered range approach allows for maneuverability considerations between the minimum acceptable CPA range and preferred CPA range. This technique gives a more informed score for values closer than the minimum preferred CPA range compared to binary safe/unsafe algorithms such as the traditional velocity obstacle. While any range closer than R_{min} is undesirable, quantifying each encounter allows more thorough insight into the overall effectiveness of a collision avoidance algorithm, collision avoidance configuration parameters, performance under certain rule constraints, and other similar variables. Continuous or stepwise penalty functions can be assigned between the configuration parameter values. In a basic example, a linear function maps values between each of the configuration ranges with a collision ($r_{cpa} < R_{col}$) having zero value (maximum penalty) and any range greater than R_{pref} having maximum value (zero penalty). Penalty values at each transition range can be tailored by the evaluator. Pose of the two vessels accounts for the notion that two identical ranges are not necessarily equally dangerous at CPA as seen in Figure 4-4. For example, a ship crossing in front of another (ownship's bow pointing a contact's beam at CPA) is considerably more dangerous than two vessels passing at the same range in a port-to-port or stern-to-beam arrangement.

An arbitrary safety function at CPA (S) primarily depends on CPA values of pose ($\Theta_{cpa} = \langle \alpha_{cpa}, \beta_{cpa} \rangle$) and range (r_{cpa}) as shown in Equation (4.3). Equation (4.4) defines an example range-based discontinuous piecewise-linear safety function S_r with stepwise penalties corresponding to each range threshold (Figure 4-5). Safety functions might take alternative forms such as quadratic, logarithmic, or stepwise designs. Equation (4.5) defines a pose-based safety function to reward an encounter where the contacts are not pointing each other at CPA. By combining a reward for target angle with Equation (4.6) and relative bearing with Equation (4.7), a reward may be granted for beam or stern aspects at CPA up to a maximum value of S_{Θ}^{max} . Contact angles at CPA aft of a configurable cutoff value α_{cut} may be given a uniform reward value. Similarly, relative bearings at CPA aft of a configurable cutoff value β_{cut} may be given a uniform reward value.

Combining Θ and r to form a collective safety metric may take many forms in-

cluding weighted summation or multiplication as shown in Equations (4.8) and (4.9), respectively. The appropriate weights for pose (s_Θ) and range at CPA (s_r) are left configurable to the evaluator. Pose can act to reward a vessel for passing astern, for example, by some reasonable percentage defined by S_Θ^{max} using a combination of Equations (4.4), (4.5), and (4.10). An example discontinuous piecewise linear mapping of safety scores based on pose-adjusted range at CPA is shown in Figure 4-5. Equation (4.4) would give the general discontinuous piecewise linear shape while an additional reward percentage would be computed based on pose using Equations (4.5) and (4.10). Figure 4-6 uses Equation (4.6) to construct a reward for non-bow contact angles at CPA using $\alpha_{cut} = 90^\circ$. An example algorithm for assessing safety as a function of both range and pose is shown in Algorithm 3.

$$S = S(r_{cpa}, \Theta_{cpa}) \quad (4.3)$$

$$S_r = S_r(\Delta S^{R_{min}}, \Delta S^{R_{nm}}, R_{col}, R_{nm}, R_{min}, R_{pref}) \quad (4.4)$$

$$S_\Theta = S_\Theta^{max} \cdot S_\Theta^\alpha \cdot S_\Theta^\beta \quad (4.5)$$

$$S_\Theta^\alpha = \begin{cases} 1 - \cos(\alpha_{cpa}), & \text{if } |\alpha_{cpa}| < \alpha_{cut} \\ 1 - \cos(\alpha_{cut}), & \text{if } |\alpha_{cpa}| \geq \alpha_{cut} \end{cases} \quad (4.6)$$

$$S_\Theta^\beta = \begin{cases} 1 - \cos(\beta_{cpa}), & \text{if } |\beta_{cpa}| < \beta_{cut} \\ 1 - \cos(\beta_{cut}), & \text{if } |\beta_{cpa}| \geq \beta_{cut} \end{cases} \quad (4.7)$$

Algorithm 3 General Approach of Safety Evaluation

```
1: procedure PSEUDOCODE FOR ANALYZESAFETY()  
2:   Input: range thresholds and associated penalty values  
3:   Input: safety functions (linear, quadratic, etc.)  
4:   Input: pose/range combination type (sum, product, etc.)  
5:   for each encounter do  
6:      $\Theta_{cpa} \leftarrow$  pose at CPA  
7:      $r_{cpa} \leftarrow$  range at CPA  
8:      $S_r \leftarrow S(r_{cpa})$  ▷ penalize close range  
9:      $S_\Theta \leftarrow S(\Theta_{cpa})$  ▷ reward safe pose  
10:     $S \leftarrow S(r_{cpa}, \Theta_{cpa})$  ▷ combine  
11:   end for  
12: end procedure
```

$$S = s_r \cdot S_r + s_\Theta \cdot S_\Theta \quad (4.8)$$

$$s_r + s_\Theta = 1$$

$$S = S_r \cdot S_\Theta \quad (4.9)$$

$$S = S_r \cdot (1 + S_\Theta) \quad (4.10)$$

4.5 Rule-Specific Algorithms and Considerations

Standardized measures of performance and effectiveness allow consistent evaluation of COLREGS for both human-operated and autonomous vessels. Creating rule categories, assigning each rule to a category, and defining metrics for each applicable rule enables consistent evaluation and allows for more clear scientific conversation regarding the advancement of autonomous collision avoidance. Incorporation of the appropriate case law and knowledge of the evolution of the COLREGS are vital to ensuring appropriate behavior in nuanced situations. While the Rules give general guidance, actions generally consistent with human behavior and expectations must

Algorithm 4 General Approach of Evaluation Technique

```
1: procedure PSEUDOCODE FOR EVALUATEENCOUNTER()  
2:   Input: vehicle positions (x,y), courses ( $\theta$ ), and speeds ( $v$ )  
3:   Input: configurable threshold ranges and angles  
4:   Input: configurable penalty values and functions  
5:   for each encounter do  
6:     Calculate: initial pose ( $\Theta_0$ )  
7:     Calculate: pose at CPA ( $\Theta_{cpa}$ )  
8:     Calculate: final CPA range ( $r_{cpa}$ )  
9:     Calculate: changes in speed ( $\Delta v, v_{min}, v_{max}$ )  
10:    Calculate: changes in course ( $\Delta\theta$ )  
11:    Determine  $\mathfrak{R}$  using Algorithm 5       $\triangleright$  applicable protocol rule for each vehicle  
12:     $\mathfrak{R} \leftarrow \mathfrak{R}(\Theta_0, \Theta_{cpa}, r_{cpa}, \Delta v, \Delta\theta)$   
         $\triangleright$  evaluate for each contact with respect to its rule set  $\mathfrak{R}$   
13:     $S \leftarrow S(r_{cpa}, \Theta_{cpa})$   
         $\triangleright$  evaluate safety for each contact using AnalyzeSafety() routine  
14:  end for  
15: end procedure
```

be the objective when integrating autonomous systems into human-present environments. Appropriately modeling and accounting for human intuition, common practice, and human expectations are among the many factors not found on any page of written rules. For example, the colloquial Law of Gross Tonnage states that a small craft generally stays out of the way of a large vessel such as an intercontinental merchant even when, strictly by the protocol requirements, the small vessel might have right of way. Adherence to custom and human expectation must be considered and honored in order to integrate autonomous platforms into a human-dominated environment.

Algorithm 4 demonstrates the general approach of evaluating COLREGS compliance. Protocol compliance functions take the symbol \mathfrak{R} with a superscript denoting the applicable COLREGS rule(s) (e.g., \mathfrak{R}^{14} denotes evaluation of head-on compliance). Each subsection below presents an algorithm and brief discussion of evaluation technique and nuance regarding a category of COLREGS scope.

4.5.1 Vessel Encounters in Sight of One Another

Each collision avoidance rule except Rule 14 (COLREGS Rules 12-13, 15-18) allows for entry criteria that assign one vessel to be stand-on (maintain course and speed⁴) and the other give-way (keep out of the way of the other) based on geometry, ship type or maneuverability restrictions, and environmental (wind) conditions for the specific case of two sailing vessels. Rules 13-17 are presented with considerations below. Rule 18 is discussed in Section 4.5.2. Algorithm 4 demonstrates the general approach of the evaluation of a collision avoidance encounter including calculation of the safety score using Algorithm 3. Algorithm 5 demonstrates entry criteria for Rules 13-17 assuming no overriding Rule 18 precedence. Figure 4-7 demonstrates example poses for rule entry criteria and the critical contact angles used throughout this section.

⁴Maintaining course and speed gives appropriate latitude to normal actions required per case law [1, 17, 100].

Algorithm 5 COLREGS Entry Criteria: Determining the Appropriate Rule Set

```

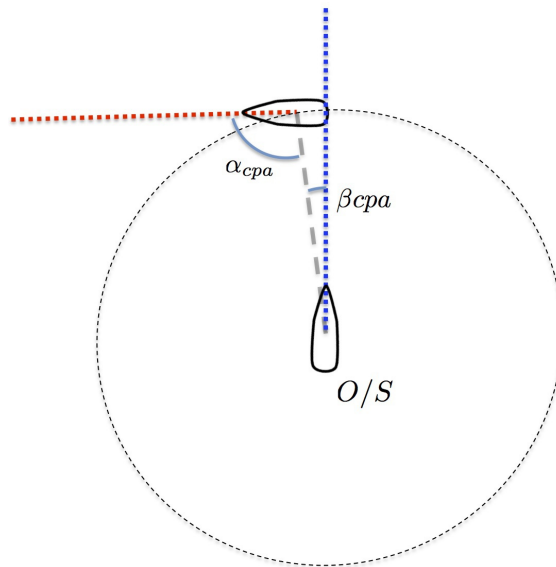
1: procedure PSEUDOCODE FOR COLREGS ENTRY CRITERIA
2:    $\alpha_{crit}^{13} \leftarrow$  overtaking tolerance     $\triangleright$  default  $45^\circ$ ; tolerance for “coming up with” pose
                                                 $\triangleright$  also require closing range and risk of collision
3:    $\alpha_{crit}^{14} \leftarrow$  head-on tolerance       $\triangleright$  default  $13^\circ$ 
                                                 $\triangleright$  tolerance for “reciprocal or nearly reciprocal courses”
                                                 $\triangleright$  “When...in any doubt...assume...[head-on].”
4:    $\alpha_{crit}^{15} \leftarrow$  crossing aspect limit  $\triangleright$  default  $10^\circ$ 
                                                 $\triangleright$  all  $\alpha_{crit}$  values are configurable by evaluator

5:    $\alpha_0 \leftarrow$  initial contact angle ( $\alpha \in [-180, 180)$ )
                                                 $\triangleright \alpha_0^{360^\circ}$  maps  $\alpha_0$  from  $[-180, 180) \rightarrow [0, 360)$ 
6:    $\beta_0 \leftarrow$  initial relative bearing ( $\beta \in [0, 360)$ )
                                                 $\triangleright \beta_0^{180^\circ}$  maps  $\beta_0$  from  $[0, 360) \rightarrow [-180, 180)$ 

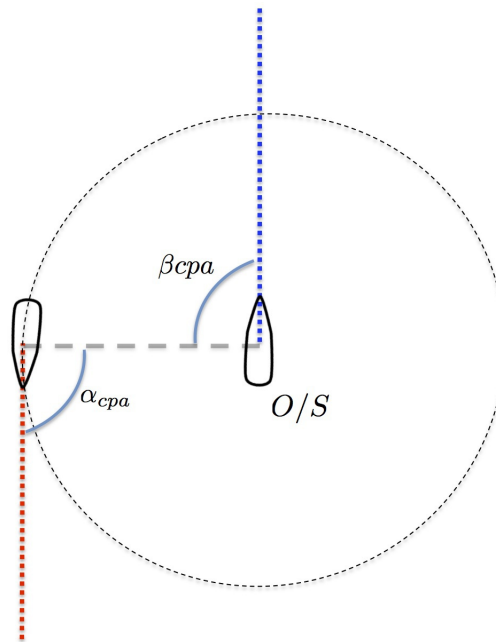
7:   if ( $\beta_0 > 112.5$ ) && ( $\beta_0 < 247.5$ ) && ( $|\alpha_0| < \alpha_{crit}^{13}$ ) then
8:      $\mathfrak{R} \leftarrow \mathfrak{R}^{13/17}$   $\triangleright$  vessel is overtaken (stand-on)

9:   else if ( $\alpha_0^{360^\circ} > 112.5$ ) && ( $\alpha_0^{360^\circ} < 247.5$ ) &&
10:  ( $|\beta_0|^{180^\circ} < \alpha_{crit}^{13}$ ) then
11:      $\mathfrak{R} \leftarrow \mathfrak{R}^{13/16}$   $\triangleright$  vessel is overtaking (give-way)
12:   else if  $|\beta_0^{180^\circ}| < \alpha_{crit}^{14}$  &&  $|\alpha_0| < \alpha_{crit}^{14}$  then
13:      $\mathfrak{R} \leftarrow \mathfrak{R}^{14}$   $\triangleright$  vessel is head-on; tolerance is configurable
14:   else if ( $\beta_0 > 0$ ) && ( $\beta_0 < 112.5$ ) && ( $\alpha > -112.5$ ) &&  $\alpha < \alpha_{crit}^{15}$  then
15:      $\mathfrak{R} \leftarrow \mathfrak{R}^{15/16}$   $\triangleright$  vessel is crossing give-way; crossing aspect limit is configurable
16:   else if ( $\alpha_0^{360^\circ} > 0$ ) && ( $\alpha_0^{360^\circ} < 112.5$ ) &&
17:  ( $\beta_0^{180^\circ} - 112.5$  && ( $\beta_0^{180^\circ} < \alpha_{crit}^{15}$ ) then
                                                 $\triangleright$  crossing aspect limit is configurable
18:      $\mathfrak{R} \leftarrow \mathfrak{R}^{15/17}$   $\triangleright$  vessel is crossing stand-on
19:   else
20:      $\mathfrak{R} \leftarrow \mathfrak{R}^{cpa}$   $\triangleright$  vessel likely has no risk of collision but remains detectable
                                                 $\triangleright$  verify and continue tracking with  $r_{cpa}$ , range-rate, and bearing-rate
21:   end if
22: end procedure

```



(a) Perpendicular CPA



(b) Parallel CPA

Figure 4-2 Safety of an encounter with two equivalent values of r_{cpa} can be shown to require a pose component. In (a), a contact reaches CPA ahead of ownship, while in (b) the vessel is safely abeam at the same range and quickly opening range. Human drivers intuitively prefer encounters whose CPA where one vessel is not pointing or nearly pointing another while still making way.

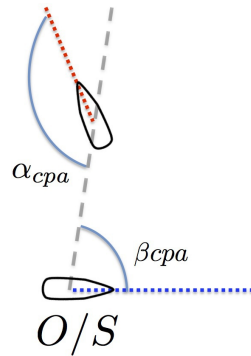
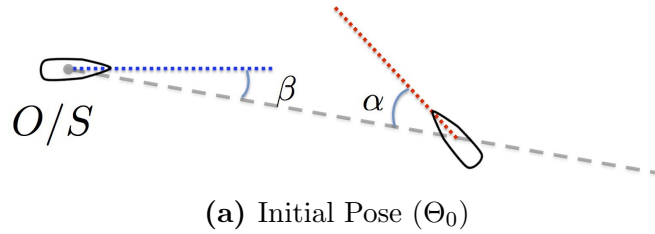


Figure 4-3 Ownship (labeled “O/S”) is traveling east and first sites a contact at relative bearing β with contact angle α in (a). Speed is represented by the length of the colored lines from each vessel (red for contact, blue for ownship). From the perspective of the contact looking at ownship, α and β are simply interchanged. These two angles give great insight into the collision avoidance picture and quickly aid in determining the applicable protocol constraints. Combined with CPA range and time (r_{cpa}, t_{cpa}), pose at CPA ($\Theta_{cpa} = \langle \alpha_{cpa}, \beta_{cpa} \rangle$) gives important information as to risk of collision, collision avoidance protocol compliance, and overall safety of a maneuver. Relative bearing and contact angle at CPA are shown in (b). CPA (b) occurs when the range between contacts reaches its minimum value of the encounter.

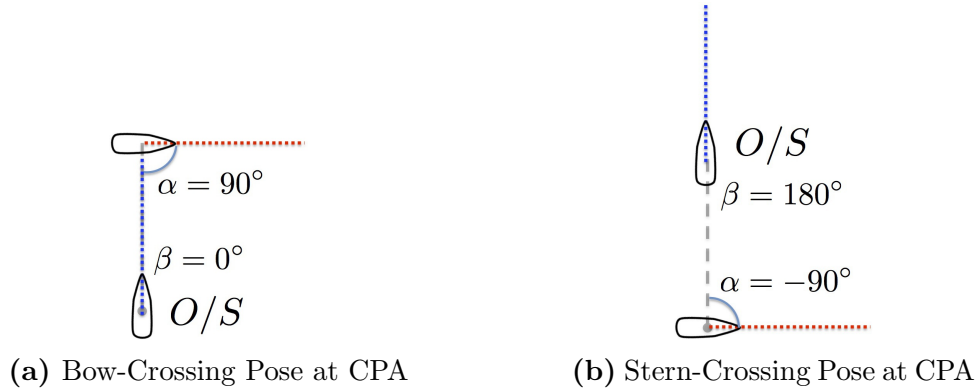


Figure 4-4 Ownship (labeled “O/S” and traveling north) encounters two scenarios of a canonical track crossing with identical ranges at CPA. The bow crossing scenario of (a) demonstrates a much more dangerous encounter than the stern crossing of (b). While many techniques treat all ranges equally, this canonical example of equivalent ranges demonstrates the necessity of incorporating pose into calculations of risk and performance. A decision to more appropriately cross astern of the stand-on vessel at the same range gives an equivalent range with a safer pose at CPA. The stand-on vessel (O/S) is given higher confidence in the give-way vessel’s intentions to respect right-of-way while also allowing for engineering casualties to have less likelihood of a resulting collision.

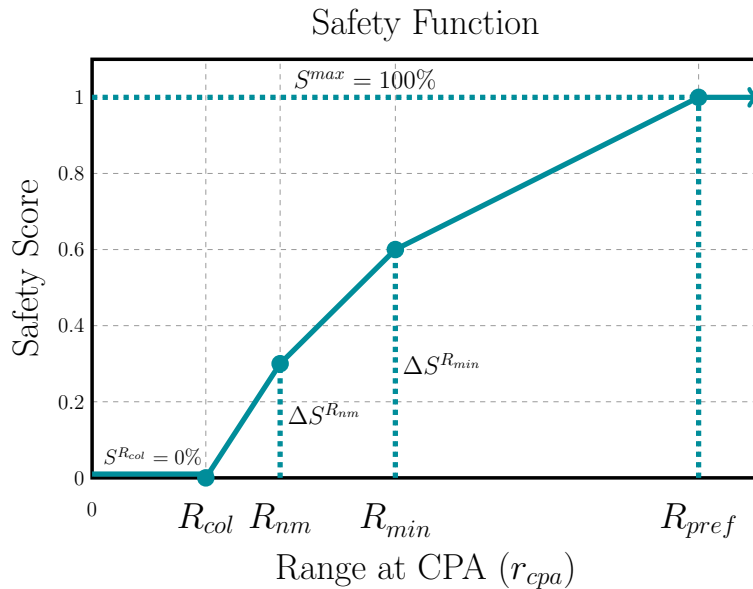


Figure 4-5 Safety scores consider range and pose at CPA. This figure demonstrates a linear mapping of range at CPA (r_{cpa}) to safety scores using the configuration parameters of Equation (4.4). Additional penalty or reward may be assigned for pose considerations according to the evaluator’s preference of a safety function. Safety functions of the general form of Equation (4.3) may take the form of Equations (4.8), (4.9), and (4.10).

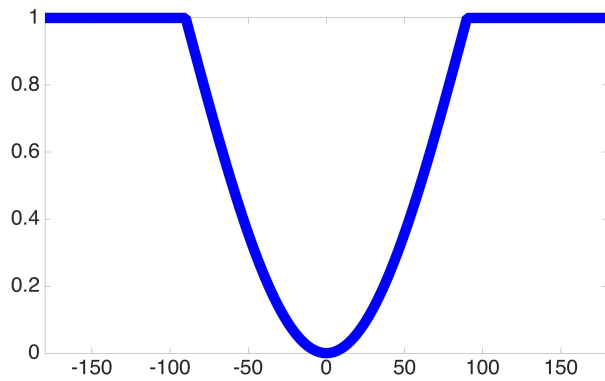


Figure 4-6 COLREGS pose reward functions can be used to give preference to passing contacts with relative bearing and contact angle that are least likely to increase risk of collision. This function rewards beam and stern contact angles at CPA using Equation (4.6). This example shows the cutoff angle set to $\alpha_{cut} = 90^\circ$ to give equal preference to beam and stern aspects. No reward is given for beam aspects.

Entry Criteria

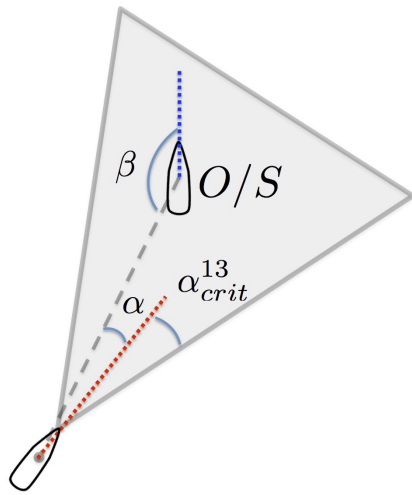
Entry criteria for Rules 13-17 largely depend on a combination of relative geometry, relative speeds, and an assessed risk of collision. While relative bearing is specified explicitly in the COLREGS for Rule 13, ambiguity exists for Rule 14. Contact angle offers significant insight into the appropriate rule and helps discriminate risk of collision before making more costly calculations. Configurable critical contact angles (α_{crit}) shown in Figure 4-7 help specify whether a vessel should take action per the COLREGS. The ability to configure α_{crit} gives flexibility to the evaluator.

Rule 13 – Overtaking

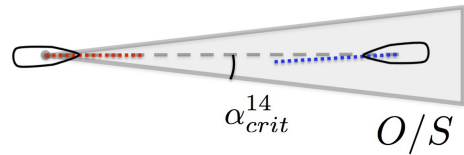
Overtaking vessels are defined in Rule 13 and assigned responsibilities under Rules 16 and 17. The overtaking rule allows a faster vessel to safely pass a slower vessel.

Collision avoidance routines for overtaking vessels (Figure 4-7a) may rely on explicit entry criteria specified in the COLREGS with respect to initial pose: a contact must be more than 22.5° abaft the other vessel's beam. Different countries have interpreted the “coming up with” phrase to take different meanings including a notable admiralty case in England involving *Nowy Sacz* and the *Olympian* [1, pp. 402-411]. Most courts contend, however, that the overtaking rule applies when the appropriate encounter geometry exists, the astern vessel has a higher speed than the overtaken vessel, the vessels are closing range, and an expected range at CPA would reasonably require prudence.

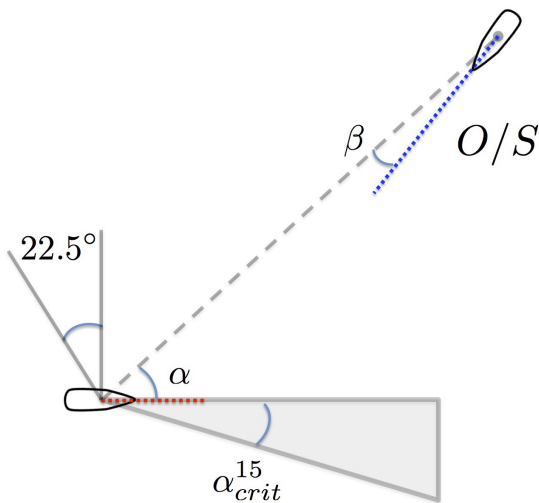
The overtaking (higher speed) vessel is defined as a give-way vessel by Rule 16 [1, 17]. Pose becomes an important aspect of measuring performance for the overtaking vessel due to both common practice and specific requirements in the Rules including her “duty of keeping clear ... until past and clear.” Overtaking on near-parallel tracks (such as in a merchant transit lane) allows for safe pose at CPA and accounts for a significant and mostly trivial case in the absence of other collision avoidance, environmental, or navigational constraints. A reasonable set of entry criteria for Rule 13 generally include a contact angle (α) within the exclusive sternlight region,



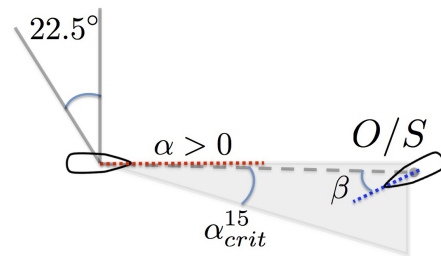
(a) Overtaking



(b) Head-on



(c) Crossing



(d) Crossing (edge case)

Figure 4-7 Entry criteria for Rules 13-17. All critical angles are relative to ownship's heading. Critical angles of Rules 13 and 14 represent half-angles of the shaded region. All critical contact angles are configurable to the evaluator as they have no prescribed value in the COLREGS.



(a) Initial overtaking geometry

(b) Overtaking astern of contact

Figure 4-8 Ownship's (O/S) initial encounter geometry, closing range, and proximity at CPA require action under an overtaking scenario of Rule 13. Dotted lines indicate the blue (O/S) and red (contact) speeds and demonstrate a closing range given the initial contact pose $\langle \alpha, \beta \rangle$ in (a). By appropriately altering course to starboard early in the collision avoidance encounter (b), O/S will pass to the contact's stern without causing the stand-on vessel to maneuver for a risk of collision.

a sufficient speed and relative bearing (β) for closing range, and a CPA range and CPA pose consistent with a risk of collision.

When the contact situation or initial geometry requires overtaking on non-parallel tracks such as in Figure 4-8, preference should be given to overtaking astern of the overtaken vessel when possible. Passing track in front of the overtaken vessel creates an encounter with higher risk and less evasive maneuverability for the overtaken vessel. Passing in front of the overtaken vessel within a range considered a risk of collision further degrades the overtaken vessel's ability to maintain its course and speed. Therefore, a penalty is assessed for overtaking vessels who cross ahead of track of an overtaken vessel within a certain range.

The vessel being overtaken is, by the definition of Rule 17, a stand-on vessel and must keep her course and speed [1, 17]. This nuance is often unknowingly neglected by autonomous collision avoidance authors and emphasizes the need for incorporation of practical at-sea experience of those involved in designing and evaluating collision avoidance algorithms for autonomous vessels [45, 46]. Vessels deemed to be overtaken must therefore demonstrate their obligation to maintain course and speed within the context of their contact-free intentions [1].

Algorithm 6 Rule 13/16: Overtaking Vessels

1: **procedure** PSEUDOCODE FOR OVERTAKING VESSELS
2: $\mathfrak{R}^{13} \leftarrow \mathfrak{R}^{16}$ \triangleright overtaking vessels are give-way vessels (Rules 13 & 16)
3: **end procedure**

Overtaking algorithms must be validated for correct contact angle, relative bearing, and speed considerations to verify mode entry criteria and algorithm robustness. A final necessary check in evaluation of overtaking collision avoidance algorithms is to ensure that modes do not shift from overtaking to crossing. Any mode changes from overtaking to crossing should be deemed a failure of the overtaking collision avoidance algorithm, as it violates an explicit clause of Rule 13.

A general approach for evaluating overtaking vessels under Rules 13 and 16 is shown in Algorithm 6 *viz* Algorithm 10 give-way requirements and includes the following attributes:

- penalize for unnecessary crossing of contact's bow at close ranges
- penalize for unnecessary hindrance of overtaken vessel's desired maneuvers
- penalize for delayed action (range of maneuver relative to detection range and CPA range if a maneuver is required) (Algorithm 12)
- penalize for safety violations including sufficient range and early action (Rules 7 - 8)

A general approach for evaluating overtaken vessels under Rules 13 and 17 is shown in Algorithm 7 *viz* Algorithm 11 stand-on requirements and includes the following attributes:

- penalize the overtaken vessel in accordance with requirements of a stand-on vessel (Rule 17)
- penalize for safety violations resulting from neglecting to invoke Rule 17.a.ii
- compensate for changes in course or speed required as a result of being *in extremis*

Algorithm 7 Rule 13/17: Overtaken Vessels

1: **procedure** PSEUDOCODE FOR OVERTAKEN VESSELS
2: $\mathfrak{R}^{13} \leftarrow \mathfrak{R}^{17}$ \triangleright overtaken vessels are stand-on vessels (Rules 13 & 17)
3: **end procedure**

Rule 14 – Head-on

The head-on policy of Rule 14 prevents two vessels on nearly reciprocal courses from colliding by requiring a port-to-port passage. A nuance often over-looked by novice approaches though specifically required by combining Rules 8 and 14 occurs when a vessel must cross the track of an on-coming vessel to achieve a port-to-port passage [17]. While a starboard-to-starboard passage might seem intuitive to the novice to avoid entering the head-on rule, any alteration for a contact on a nearly reciprocal course – including a slight alteration to port for an otherwise starboard-to-starboard passage – is acknowledgment of a risk of collision and must therefore result in a maneuver to starboard for a port-to-port passage.

Head-on situations (Figure 4-7b) provide arguably the most ambiguous entry criteria of the rules for power-driven vessels. The definition of “reciprocal or nearly reciprocal courses” is vague and left to interpretation. The compass course is required to be used when assessing course difference due to the ship-fixed masthead light and sidelight definition of ship’s course in Rule 14. Confusion arises when environmental parameters greatly affect the course-over-ground; non-visual means (e.g., radar, lidar, etc.) measure course-over-ground, so care must be taken in evaluating contact geometry for proper entry criteria and resolution of ambiguity. Similarly, a consistent entry criterion for “nearly reciprocal course” should be configurable and set in accordance with local customs or certifying agency requirements. Environmental conditions such as sea-state, current, or fluctuating wind might also warrant a change to the entry criteria angle (α_{crit}^{14}) tolerance or use of a filter.

Evaluation scenarios should incorporate sufficient set and drift to realize an appreciable distance between course-over-ground and compass heading before certification as compliant with Rule 14. Small sequential maneuvers should also be penalized, as a single, readily apparent maneuver is required (Rule 8). The size of a readily apparent

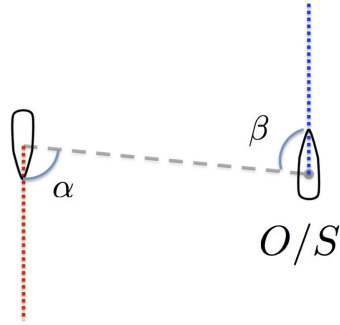
maneuver is not explicitly defined in the COLREGS, though turns of 30° have been determined by custom to be sufficient [85]. Some texts suggest a minimum of 35° for a sufficient turn [1]. The intention of the rule is to ensure that turns are apparent by both radar and visual observation; the single large turn clearly communicates to the other vessel that a risk of collision has been assumed and the vessel is taking appropriate early action in accordance with the COLREGS.

When evaluating maneuvers for a head-on scenario, both vessels must maneuver to starboard in an appreciable and timely way. Maintaining course or turning to port should be viewed as a failure to maneuver in accordance with Rule 14. Rule 14 further specifies that passing pose must be port-to-port. Pose should therefore enter into the protocol compliance metric for head-on encounters. Equation (4.11) demonstrates an arbitrary Rule 14 pose function ($\mathfrak{R}_{\Theta_{cpa}}^{14}$) accounting for both relative bearing and contact angle at CPA. Equation (4.12) uses specific pose functions to give large preference to near-canonical port aspects.

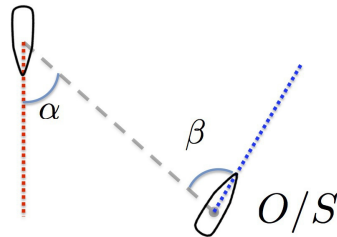
$$\mathfrak{R}_{\Theta_{cpa}}^{14} = \mathfrak{R}_{\alpha_{cpa}}^{14} \cdot \mathfrak{R}_{\beta_{cpa}}^{14} \cdot \mathfrak{R}^{max} \quad (4.11)$$

$$\mathfrak{R}_{\Theta_{cpa}}^{14} = \left(\frac{\sin(\alpha_{cpa}) - 1}{2} \right)^2 \left(\frac{\sin(\beta_{cpa}) - 1}{2} \right)^2 \mathfrak{R}^{max} \quad (4.12)$$

This example pose reward uses combinations of sinusoidal functions of relative bearing (β) and contact angle (α) at CPA. A true port-to-port passage will be a relative bearing of $\beta = 270^\circ$ and a contact angle of $\alpha = -90^\circ$ as seen in Figure 4-9. Within an allowable tolerance, large deviations from port-to-port passage in open-ocean scenarios likely indicate insufficient or delayed maneuvers by one or both vessels. In Figure 4-9a, a nearly canonical head-on CPA geometry gives a high pose reward score. In Figure 4-9b, a likely late maneuver by ownship and a subsequent narrow contact angle at CPA results in a smaller pose reward. Algorithm 8 demonstrates an approach to evaluate head-on encounters. Alternative functions are available in the



(a) Near-canonical head-on geometry at CPA.



(b) Head-on geometry at CPA resulting from delayed action of ownship (O/S).

Figure 4-9 Rule 14 requires head-on contacts to maneuver to starboard and pass port-to-port. The geometry of a nearly canonical case (a) shows the preferred CPA geometry including relative bearing β and contact angle α . Using Equation (4.12), a nearly maximum pose score would result. In (b), a delayed maneuver from ownship (“O/S”) results in a port relative bearing at CPA; contact angle α_{cpa} , however, accounts for the less than ideal CPA geometry. Equation (4.11) would reduce the overall performance score for the situation in (b).

evaluation library discussed in Section 4.6.

Figure 4-10 shows an example port-to-port pose function. Figure 4-11 shows a more severe preference to port angles. Possible scores range from 0 to the maximum possible protocol compliance score ($\mathfrak{R}^{max} = 100\%$).

Algorithm 8 Rule 14: Head-on Vessels

1: **procedure** PSEUDOCODE FOR HEAD-ON VESSELS

2: Input: α_{cpa}

3: Input: β_{cpa}

4: $\mathfrak{R}^{14} \leftarrow \mathfrak{R}^{max}$

5: $\mathfrak{R}^{14} \leftarrow$ assess non-starboard turn penalty

▷ “each shall alter her course to starboard”

6: $\mathfrak{R}^{14} \leftarrow$ assess delayed action penalty ▷ “made in ample time” (Algorithm 12)

7: $\mathfrak{R}^{14} \leftarrow$ assess non-apparent turn penalty

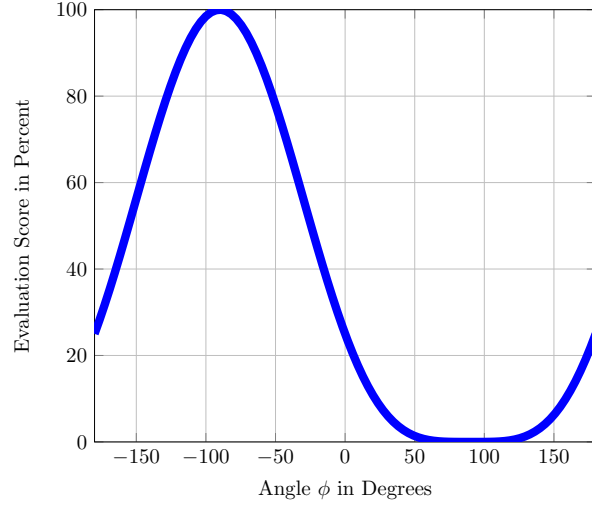
▷ “be large enough to be readily apparent” (Algorithm 14)

8: $\mathfrak{R}^{14} \leftarrow$ assess $\mathfrak{R}_{\Theta_{cpa}}^{14}$ penalty if not port-to-port ▷ Equation (4.11)

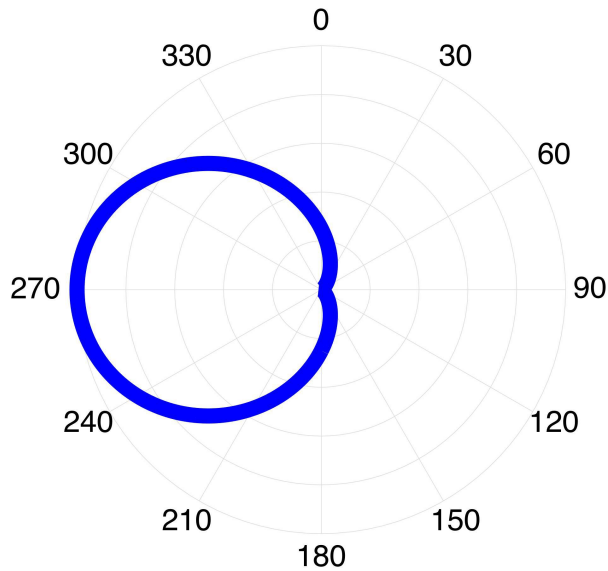
▷ “each shall pass on the port side of the other”

▷ configurable per library of Section 4.6.1

9: **end procedure**

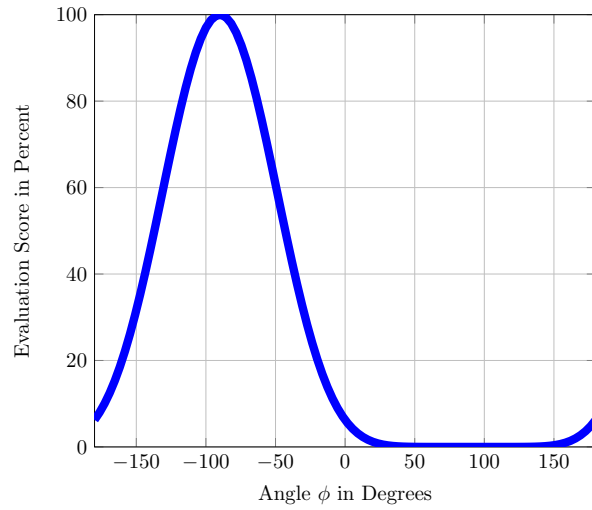


(a) Plot of $\left(\frac{\sin(\phi) - 1}{2}\right)^2$

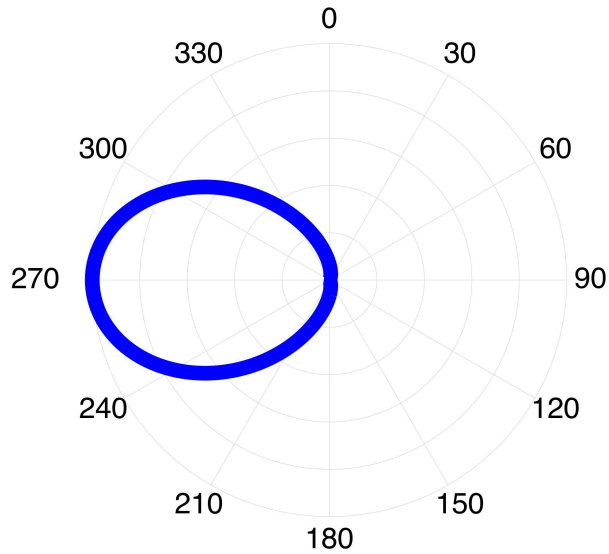


(b) Polar plot of $\left(\frac{\sin(\phi) - 1}{2}\right)^2$

Figure 4-10 The example protocol evaluation function $\left(\frac{\sin(\phi) - 1}{2}\right)^2$ allows strong reinforcement of port-to-port passage when substituting both relative bearing and contact angle for ϕ as shown in Equation (4.12). The plot of the Rule 14 cost function (a) demonstrates high reward for near-port angles. The polar plot representation (b) demonstrates the same reward function in a top-down view more natural to a collision avoidance encounter. The radius of the polar plot indicates the percentage of \mathfrak{R}^{max} ; the origin corresponds to zero while the outer ring corresponds to $\mathfrak{R}^{max} = 100\%$.



(a) Plot of $\left(\frac{\sin(\phi) - 1}{2}\right)^4$



(b) Polar plot of $\left(\frac{\sin(\phi) - 1}{2}\right)^4$

Figure 4-11 A function such as this fourth-order sinusoidal function imposes a more strict requirement for beam passing than those of Figure 4-10.

Rule 15 – Power-Driven Crossing

Rule 15 assigns give-way and stand-on responsibilities to each of two crossing power-driven vessels with a risk of collision (Figure 4-7c). The geometric entry criteria are derived from eliminating head-on and overtaking geometries while retaining a risk of collision. Relative bearing therefore spans $\{\beta : (\beta < 112.5^\circ) \text{ or } (\beta > 247.5^\circ)\}$ with an appropriate contact angle (α) such that a risk of collision exists without inducing head-on or overtaking obligations.

Crossing give-way vessels are specifically required to not cross ahead of the stand-on vessel; this notion has been reinforced in admiralty courts [1]. Note that a risk of collision must exist for Rule 15 to apply. Therefore a risk of collision invoking crossing give-way actions requires a stern crossing. Verification that a vessel crossed astern of the stand-on vessel is possible using pose at CPA. For example, a stern crossing or near-stern crossing will result in a narrow or negative contact angle if the stand-on vessel does not maneuver (Figure 4-4). If the stand-on vessel determines that an *in extremis* situation exists and maneuvers to starboard, the give-way vessel should similarly be penalized for failure to act in accordance with the COLREGS.

A general approach to evaluating a crossing give-way power-driven vessel under Rule 15 can be seen in Algorithms 9 and 10 and includes the following attributes:

- penalize crossing ahead (e.g., $-25^\circ < \alpha_{cpa} < 165^\circ$ (configurable) where α_{cpa} is the stand-on vessel's contact angle if no action is taken under Rule 17.a.ii)
- penalize forcing an *in extremis* maneuver by the stand-on vessel in accordance with Rule 17.a.ii
- penalize give-way requirements of Rule 16 (Section 4.5.1)
- include safety penalty for early and substantial action clause of Rule 16

Requirements of the stand-on vessel in a power-driven crossing situation are discussed in Section 4.5.1 and Algorithm 11.

Algorithm 9 Rule 15: Power-Driven Crossing

```
1: procedure PSEUDOCODE FOR POWER-DRIVEN CROSSING VESSELS
2:   if crossing give-way vessel then
3:      $\mathfrak{R}^{15/16} \leftarrow \mathfrak{R}^{16}$     $\triangleright$  crossing give-way vessel must obey Rule 16 (Algorithm 10)
4:      $\mathfrak{R}^{15/16} \leftarrow$  assess pass-ahead penalty
5:      $\triangleright$  “avoid crossing ahead of the other vessel” (case law [1, 17, 82])
6:   else if crossing stand-on vessel then
7:      $\mathfrak{R}^{15/17} \leftarrow \mathfrak{R}^{17}$     $\triangleright$  crossing stand-on vessel must obey Rule 17 (Algorithm 11)
8:   end if
9: end procedure
```

Rule 16 – Give-way

Give-way vessels are to take early action, to take substantial action, and to keep well clear. This yields three measurable criteria for all give-way vessels:

- time of maneuver relative to the times of detection, determination of collision risk, and CPA
- determination of substantial action as measured by the size and direction of the maneuver (turn and/or speed change consistent with Rule 8)
- range and pose at CPA

It should be noted that Rule 16 does not apply exclusively to power-driven vessels nor does it apply exclusively to crossing situations [1, 17]. Rather, Rule 16 may be invoked as a result of Rules 12, 13, 15, or 18. Claims of “compliance” with Rule 16 have been implicitly made in autonomous collision avoidance literature with a scope limited to crossing give-way situations (Rule 15) without discussion of its wider implications. Full Rule 16 compliance claims must, however, specify that they include the scope of Rule 12 (sailing vessels), Rule 13 (overtaking), Rule 15 (power-driven crossing), and Rule 18 (precedence) to be complete and truly compliant. Algorithm 10 demonstrates Rule 16 evaluation.

Rule 17 – Stand-on

Stand-on vessels are by definition the vessel not assigned give-way responsibilities for an encounter requiring one vessel to keep clear (i.e., Rule 16 give-way). Stand-

Algorithm 11 Rule 17: Stand-on Vessels

```
1: procedure PSEUDOCODE FOR STAND-ON VESSELS
2:    $\mathfrak{R}^{17} \leftarrow \mathfrak{R}^{max}$ 
3:    $\mathfrak{R}^{17} \leftarrow \text{AnalyzeSafety}()$  (Rules 8,17,18)
       $\triangleright$  “she shall take such action as will best aid to avoid collision”
4:    $\mathfrak{R}^{17} \leftarrow \text{penalizeCourseChange}()$   $\triangleright$  Algorithm 16
5:    $\mathfrak{R}^{17} \leftarrow \text{penalizeSpeedChange}()$   $\triangleright$  Algorithm 17
       $\triangleright$  “shall keep her course and speed”
6:    $\mathfrak{R}^{17} \leftarrow \text{compensate for maneuvers required of normal navigation}$ 
       $\triangleright$  case law [1, 17, 82]
7:   if in extremis then
8:      $\mathfrak{R}^{17} \leftarrow \text{compensate for maneuvers required in extremis}$ 
       $\triangleright$  “take action to avoid collision by her maneuver alone”
9:     if power-driven crossing then
10:       $\mathfrak{R}^{17} \leftarrow \text{penalize port maneuvers for port contacts}$ 
       $\triangleright$  “...not alter course to port for a vessel on her own port side”
11:    end if
12:  end if
13: end procedure
```

to be *in extremis* should focus on safely avoiding a collision subject to the power-driven restriction of Rule 17.c. With the exception of Rule 17.c, evaluation of evasive action should use the safety score as a primary metric for rule compliance of the stand-on vessel.

For stand-on vessels, a change in speed is a violation of Rule 17 within the aforementioned caveats. To quantify speed change, the speed at the declaration of entry into the stand-on obligation must be identified. A penalty can then be assigned for any subsequent speed up or slow down relative to this initial speed value. A speed change that is likely undetectable by the contact or insignificant to the collision avoidance scenario should be disregarded. Speeding up or slowing down by appreciable amounts without navigational necessity, however, violates Rule 17 and can result in unnecessary complication of the collision avoidance scenario.

Similarly, course changes greater than some threshold noise level (say, 2°) must be penalized for stand-on vessels not otherwise invoking Rule 17.a.ii. Some small heading change up to the generally accepted substantial value of 30° must be increasingly penalized. An example metric uses a linear or quadratic mapping between minimum detectable and substantial course changes (2° - 30°) with a plateau of penalty outside

Algorithm 12 Penalize for Delayed Action

```
1: procedure PSEUDOCODE FOR PENALIZEDelayedAction()  
2:    $r_{detect} \leftarrow$  range to contact at time of detection ▷ default  $1.8 \cdot R_{pref}$   
3:    $r_{maneuver} \leftarrow$  range to contact at time of ownship's maneuver  
4:    $r_{cpa} \leftarrow$  range to contact at CPA  
5:    $\mathfrak{R}^{delay} \leftarrow$  maximum score deduction (percent)  
6:    $\mathfrak{R}^{delay} \leftarrow \mathfrak{R}^{delay} \cdot \left( \frac{r_{detect} - r_{maneuver}}{r_{detect} - r_{cpa}} \right)$   
7:    $\mathfrak{R}^{rule} \leftarrow \mathfrak{R}^{rule} \cdot (1 - \mathfrak{R}^{delay})$   
8: end procedure
```

Algorithm 13 Penalize for Non-Readily Apparent Maneuver

```
1: procedure PSEUDOCODE FOR PENALIZENon-ApparentManeuver()  
2:    $\mathfrak{R}^{\Delta\theta_{app}} \leftarrow$  Non-ApparentCourseChange()  
3:    $\mathfrak{R}^{\Delta v_{app}} \leftarrow$  Non-ApparentSpeedChange()  
4:    $thresh \leftarrow$  threshold penalty before non-apparent maneuver deducts from score  
5: ▷ default 30%  
6:   if ( $\mathfrak{R}^{\Delta\theta_{app}} < thresh$ ) || ( $\mathfrak{R}^{\Delta v_{app}} < thresh$ ) then  
7:     return;  
8:   else if ( $\mathfrak{R}^{\Delta v_{app}} < thresh$ ) then  
9:      $\mathfrak{R}^{rule} \leftarrow \mathfrak{R}^{rule} \cdot (1 - \mathfrak{R}^{\Delta\theta_{app}})$   
10:  else  
11:     $\mathfrak{R}^{rule} \leftarrow \mathfrak{R}^{rule} \cdot (1 - \mathfrak{R}^{\Delta v_{app}})$   
12:     $\mathfrak{R}^{rule} \leftarrow \mathfrak{R}^{rule} \cdot (1 - \mathfrak{R}^{\Delta\theta_{app}})$   
13:  end if  
14: end procedure
```

Algorithm 14 Check for Non-Readily Apparent Course Change

```
1: procedure PSEUDOCODE FOR Non-ApparentCourseChange()  
2:    $\mathfrak{R}^{\Delta\theta_{app}} \leftarrow$  max penalty for non-apparent course maneuver  
3: ▷  $\mathfrak{R}^{\Delta\theta_{app}} \in [0, 1]$ , default 50%  
4:    $|\Delta\theta| \leftarrow$  absolute course deviation  
5:    $\Delta\theta_{app} \leftarrow$  apparent course deviation threshold ▷ default  $30^\circ$   
6:    $\Delta\theta_{md} \leftarrow$  minimum detectable course deviation ▷ default  $0^\circ$   
7:   if  $|\Delta\theta| > \Delta\theta_{app}$  then  
8:     return ( $\mathfrak{R}^{\Delta\theta_{app}} \leftarrow 0$ )  
9:   end if  
10:   $\mathfrak{R}^{\Delta\theta_{app}} \leftarrow \mathfrak{R}^{\Delta\theta_{app}} \cdot \left( \frac{\Delta\theta_{app} - |\Delta\theta|}{\Delta\theta_{app} - \Delta\theta_{md}} \right)$   
11: end procedure
```

the linear region. Several small turns resulting in a larger effective turn should also be penalized accordingly.

Algorithm 15 Check for Non-Readily Apparent Speed Change

```
1: procedure PSEUDOCODE FOR NON-APPARENTSPEEDCHANGE()
2:    $\mathfrak{R}^{\Delta v_{app}} \leftarrow$  max penalty for non-apparent speed maneuver
3:    $\triangleright \mathfrak{R}^{\Delta v_{app}} \in [0, 1]$ , default 50%
4:    $\delta_v \leftarrow$  apparent speed reduction threshold  $\triangleright \delta_v \in [0, 1]$ , default 50%
5:    $v_0 \leftarrow$  initial ownship speed at time of detection
6:    $v_{min} \leftarrow$  speed after slowing
7:    $\Delta v \leftarrow \left( \frac{v_0 - v_{min}}{v_0} \right)$ 
8:   if ( $\Delta v \geq \delta_v$ ) then
9:     return ( $\mathfrak{R}^{\Delta v_{app}} \leftarrow 0$ )  $\triangleright$  sufficiently apparent speed change
10:  end if
11:   $\mathfrak{R}^{\Delta v_{app}} \leftarrow \mathfrak{R}^{\Delta v_{app}} \cdot \left( \frac{\delta_v - \Delta v}{\delta_v} \right)$ 
12: end procedure
```

Algorithm 16 Penalize Course Change

```
1: procedure PSEUDOCODE FOR PENALIZECOURSECHANGE()
2:   if  $t_{maneuver} > t_{cpa}$  then
3:     return;
4:   end if
5:    $\mathfrak{R}^{max} \leftarrow$  maximum penalty for changing course  $\triangleright$  default 50%
6:    $|\Delta\theta| \leftarrow$  maximum heading deviation
7:    $\Delta\theta_{app} \leftarrow$  apparent turn threshold  $\triangleright$  default 30°
8:    $\Delta\theta_{md} \leftarrow$  minimum detectable heading deviation  $\triangleright$  default 2°
9:   if ( $|\Delta\theta| < \Delta\theta_{md}$ ) then
10:    return;
11:   else if ( $|\Delta\theta| > \Delta\theta_{app}$ ) then
12:     return ( $\mathfrak{R}^{rule} \leftarrow \mathfrak{R}^{rule} - \mathfrak{R}^{max}$ )
13:   end if
14:    $\mathfrak{R}^{rule} \leftarrow \mathfrak{R}^{rule} - \mathfrak{R}^{max} \cdot \left( \frac{|\Delta\theta| - \Delta\theta_{md}}{\Delta\theta_{max} - \Delta\theta_{md}} \right)$ 
15: end procedure
```

4.5.2 Responsibilities of Vessels within Sight: Rules 11, 18

Identification of the contact's type (e.g., power-driven, sailing, etc.) gives necessary knowledge for determining precedence under Rule 18. Certain vessels yield right-of-way to others by the nature of their vessel type; similarly, other vessels expect and are afforded right-of-way. To be compliant with Rule 18, autonomous vessels must be able to correctly classify vessel types and properly assign give-way hierarchy.

Detection of another vessel being under sail is insufficient for some scenarios in-

Algorithm 17 Penalize Speed Change

```
1: procedure PSEUDOCODE FOR PENALIZESPEEDCHANGE()  
2:   if  $t_{maneuver} > t_{cpa}$  then  
3:     return;  
4:   end if  
5:    $\mathfrak{R}^{max} \leftarrow$  maximum penalty for slowing ▷ default 50%  
6:    $\Delta v_{fast} \leftarrow v_{max} - v_0$   
7:    $\Delta v_{slow} \leftarrow v_0 - v_{min}$   
8:    $\Delta v_{max} \leftarrow \max(\Delta v_{fast}, \Delta v_{slow})$   
9:    $\Delta v_{md} \leftarrow$  minimum detectable speed change ▷ default 0.2m/s  
10:  if  $\Delta v_{max} < \Delta v_{md}$  then  
11:    return;  
12:  end if  
13:   $\mathfrak{R}^{rule} \leftarrow \mathfrak{R}^{rule} \cdot \left( \frac{v_0}{v_{max}} \right)^2$  ▷ penalize speeding up  
14:   $\mathfrak{R}^{rule} \leftarrow \mathfrak{R}^{rule} - \mathfrak{R}^{max} \cdot \left( \frac{\Delta v_{slow}}{v_0} \right)$   
15:  end procedure ▷ penalize slowing down (not mutually exclusive)
```

volving multiple sailing craft in the vicinity of a power-driven autonomous vessel. In order to anticipate the likely movements of a sailing give-way to avoid a sailing stand-on, each autonomous vessel should be able to identify which sailing vessel is stand-on and which is give-way to the other. By determining environmental conditions such as wind, a power-driven autonomous vessel can anticipate a likely maneuver of a sailing give-way vessel that might interfere with ownship’s intentions to give-way to both sailing vessels.

4.5.3 General Rules (Rules 1-3)

Much debate exists as to whether an autonomous vessel without a human physically present constitutes a “vessel” under international law. This thesis assumes that the definition accorded in Rules 1-3 apply equally to any floating structure (or “watercraft”) as if a human were physically present and operating it. Rule 3 defines the scope of COLREGS to include any “vessel” without specification of control, be it human, machine, or some combination thereof. The only distinctions drawn by the COLREGS are related to propulsion (e.g., sail, power-driven, etc.) and maneuver-

ability (e.g., fishing, not under command, etc.) constraints. This is consistent with case law dating back to the 19th century [33, 89, 93]. As recently as 2013, the U.S. Supreme Court rejected a permanently moored house boat meeting the definition of a vessel. In doing so, the court affirmed that the definition of a vessel is met if a reasonable observer would consider it designed to a practical degree for carrying people or things over water citing the house boat’s absence of a rudder or steering mechanism as well as a lack of capacity to generate or store electricity [88].

Accordingly, COLREGS must apply to autonomous vessels as though they were human controlled and performing the same tasks. Rule 3 further stipulates that “Vessels shall be deemed to be in sight of one another only when one can be observed visually from the other.” Various work to emulate a human lookout by use of on-board sensors and sensor processing enables “sight,” including cameras, infra-red sensors, and other similar technologies. The COLREGS deliberately address a visual requirement when two vessels are in “sight” of each other, though this does not exclude non-sight sensors (e.g., radar, lidar, sonar) from assisting with initial detection, classification, or queuing of sight sensors. Similarly, the “restricted visibility” definition of Rule 3 must consider the limitations of human-operated vessels especially as it relates to the human-visible spectrum of light; the inherent safety implications of entering a restricted visibility constraint even if an autonomous vessel’s sensors allow greater detection range than that of a human operator must be considered.

The intention of the restricted visibility sections of COLREGS are two-fold:

1. increase detectability to other contacts to maximize detection range
2. reduce allowable speed while further limiting maneuver directions to account for and partially mitigate limited detection distances

Autonomous designers require clarification from the international governing bodies as to what officially constitutes “sight” of a non-human controlled vessel.

4.5.4 General Conduct of Vessels and Special Traffic Schemes (Rules 4-10)

Rules 4-10 address the requirements of all vessels including the stationing of a look-out, use of safe speed, determining risk of collision, the action required to avoid collision, behavior in narrow channels, and behavior in traffic separation schemes [84]. One point of contention is the requirements of Rule 5 to maintain a look-out. Several boards have been formed in the international community to address the perceived discrepancy in what, if any, non-human means may constitute a look-out in accordance with the COLREGS. This thesis assumes that any means of “sight and hearing” whether human or machine may constitute a look-out so long as it sufficiently functions within the spirit of the COLREGS and to the standards of a qualified human lookout.

Rule 5 – Lookout

Rule 5 requires a look-out to be stationed “by sight and hearing as well as by all available means appropriate in the prevailing circumstances.” Evaluation should prefer coordination between sight and hearing algorithms consistent with a reasonably trained human look-out. Metrics for Rule 5 under the assumption of machine-based lookout include:

- listening with on-board auditory sensors at all times while underway. Above-waterline sensors must always be functional. Sonar may supplement if installed but must never replace a surface vessel’s above-waterline auditory sensor requirement
- observing with a sufficient combination of on-board non-auditory (visual, radar, lidar, infrared, etc.) sensors at all times when underway
- conditionally supplementing with additional on-board sensors (e.g., radar), off-board sensors (e.g., accompanying aerial vehicle), and externally provided data (e.g., AIS) as necessary

Rule 6 – Safe Speed

Environmental factors and ship dynamics predominantly enter with Rule 6. Rule 6 specifically identifies 12 areas – assuming that the autonomous vessel has radar – requiring evaluation when determining a safe speed. The state of visibility, contact density, stopping distance, turning ability, sea state, and draft are just some of the parameters identified when determining a safe speed. Autonomous vessels must be able to independently determine their effective time-distance capabilities, turning kinematics and dynamics, and effects of contact density when selecting a maximum allowable speed to be fully compliant with Rule 6.

Rule 7 – Risk of Collision

As in human-operated ship driving, autonomous marine vehicles enjoy widely varying interpretation of what a “risk of collision” means based on operating style and design. Several factors allow mariners to make assumptions about the other vessel’s level of tolerance when assessing a risk of collision including vessel type, cargo, primary mission, maneuverability, and pose. For example, merchant vessels often have similar desired ranges at CPA based on common training, similar ship maneuverability characteristics, and maritime customs. A liquid Nitrogen gas tanker might have a tendency for larger, more conservative ranges at CPA than say a transiting fishing trawler who is more accustomed to high contact density environments with greater maneuverability. Pose becomes a highly relevant consideration for determination of collision risk. Both pose at CPA and initial pose must be considered in conjunction with speed and range when assessing risk of collision.

Another consideration is the underlying flexibility of the collision avoidance algorithms. Human operators often use multiple CPA range thresholds to determine risk of collision and necessary actions. To determine risk of collision, one must know the conditions present in the decision space of the vessel as well as the vessel’s current capabilities. For example, certain crew members offer greater levels of experience, while certain machinery conditions or watch-stander configurations allow for greater

maneuverability or performance. Requiring the vessel's Captain or additional watch officers on the bridge for certain encounter scenarios is one example of a modified watch-stander configuration. These factors directly contribute to the level of conservativeness of the subsequent maneuver.

A vessel master's policy often dictates that certain precautionary measures must be in place before taking contacts closer than certain ranges [85, 86]. This might include certain qualified watch-standers present on the bridge, certain machinery configurations, or certain environmental conditions. Similarly, restricted visibility and other detectability considerations must be considered in the determination of risk of collision.

Two considerations are specifically required as components of determination of collision risk, namely, 1) contacts with constant compass bearing with corresponding decreasing range, and 2) approaching large vessels, tows, or close range contacts. If either of these two areas are not explicitly considered in risk determination, an immediate failure score is warranted for Rule 7. Additional metrics should include the appropriate configuration of range thresholds, the tolerance for determining a constant bearing/decreasing range scenario, early warning capabilities, and analysis of "scanty information". Such scanty information [84] might be considered with appropriate weight based on radar return strength, fusion of other sensor data, and sensor filter settings.

4.5.5 Sailing in Sight of Another Sailing Vessel (Rule 12)

Sailing vessels must be properly identified in order to discriminate precedence per Rule 18 and, in the case of ownship also being a sailing vessel, determine stand-on and give-way status per Rule 12. In the case of both vessels being under sail, proper identification of the windward side of both vessels is required (both wind direction as well as the location of the mainsail or the largest fore-and-aft sail). Failure to properly identify other sailing vessels must result in a failure of Rule 12. Further evaluation using the requirements of Rules 16 and 17 applies as appropriate.

4.5.6 Restricted Visibility (Rule 19)

In addition to the discussion of Section 4.5.3, Rule 19 addresses situations of reduced visibility, i.e., when vessels cannot see the other due to the environmental reasons prescribed in Rule 3. Specific checks should be made during algorithm testing to ensure restrictions are in place to limit speed consistent with Rules 6 and 19. The two specific cases addressed in Rule 19.d should be explicitly tested in conditions emulating restricted visibility, including:

- ensuring a vessel does not alter course to port for a vessel forward of the beam, except in cases of overtaking
- ensuring a vessel does not alter course toward a vessel abeam or abaft the beam

Testing should also consider the cases of auditory detection of fog signals ahead of the beam to ensure invocation of the bare-steerage clause of Rule 19.e.

4.5.7 Lights and Shapes (Rules 20-31)

There are two main areas of scope in the lights and shapes section of the COLREGS. First, designers must properly display the required lights and shapes on ownship according to certain ship characteristics. This requires self-awareness of whether a particular section of the COLREGS which requires special lights and shapes applies. In addition, the ability to actually transmit the appropriate signal for the correct duration of time is required. Second, a vehicle must be able to properly identify lights and shapes of other vessels including assignment of proper meaning. This recognition and application to the contact directly complements Rule 18 requirements of precedence with respect to ownship's collision avoidance role *viz* stand-on or give-way. Special lights and shapes may be necessary for autonomously operated vessels to display. The community would be well served by international governing bodies issuing guidance stating whether a special day shape or light signal is required to identify autonomously operated vehicles, and if so, making such display or signal

standard across the world⁵.

4.5.8 Sound and Light Signals (Rules 32-37)

Quite similarly to the lights and shapes requirements of Section 4.5.7, vessels must be able to properly communicate using sound and light signals in accordance with the COLREGS. Autonomous vessels are in need of clarification of any special sound and/or light signals required for autonomous vessels. To avoid *ad hoc* signals intended to indicate an autonomous vessel encountering a human vessel, international governing bodies should provide articulated guidance. Advances in the field within the scope of this section would focus on multiple areas including:

- receiving a contact’s light and sound signals
- interpreting these light and sound signals then influencing ownship’s autonomous collision avoidance behaviors appropriately
- transmitting light and sound signals to a contact when ownship autonomously determines necessity in accordance with the COLREGS

4.6 COLREGS Testing and Evaluation

A COLREGS testing and evaluation software program was designed to be used from a third party neutral “shoreside” observer with assumed perfect sensing data of the vessels under observation. The purpose of the testing and evaluation program is to act as a neutral grader of a ship’s performance in complying with the COLREGS, especially in the absence of human intervention. Third party perfect sensing represents a reasonable assumption for a road test or other evaluator entity, as the vessel autonomy could be evaluated in a well-sensored testing range with verified GPS-based location data recorded for all vessels. A position reporting protocol such as AIS may

⁵Submarines operating on the surface are currently the only special signal not contained as a requirement within the numbered international rules.

prove satisfactory if reports can be deemed trustworthy. Future work could incorporate sensor fusion and imperfect sensing scenarios that would enable this concept to be used outside the realm of certification-focused testing and evaluation.

Scope of the testing and evaluation program was limited to power-driven vessel rules, specifically Rules 13-18. A library was developed to allow for both real-time (Section 4.6.2) and post-mission analysis (Section 4.6.3). Complex multi-contact encounters such as the one shown in Figure 4-12 are capable of real-time or post-mission analysis. A graphical example of a cumulative post-voyage report is shown in Figure 4-13 using the categories of scope from Table 4.1. In this example, performance was limited to Categories I-V while omitting evaluation in Categories VI-IX.

The testing and evaluation program for a multi-contact power-driven scenario includes the ability to:

- identify that the geometry of two vehicles requires action per the COLREGS
- identify the specific rules assigned to each vessel
- quantify the actions of each vessel with respect to the identified rules
- generate a report of each vessel's actions at the conclusion of the encounter
- populate a scoring system for each vehicle and a cumulative performance assessment based on various scenarios and interactions over a specified duration
- provide quantified data to support determination of a vessel's scope of COLREGS compliance after performing specified encounters
- conduct sufficient encounters in various multi-vessel, multi-rule scenarios to achieve the "road test" described in Section 5.6

4.6.1 Evaluation Library

The protocol-constrained collision avoidance evaluation library allows a common repository for evaluation algorithms. The library enables expansion of functionality

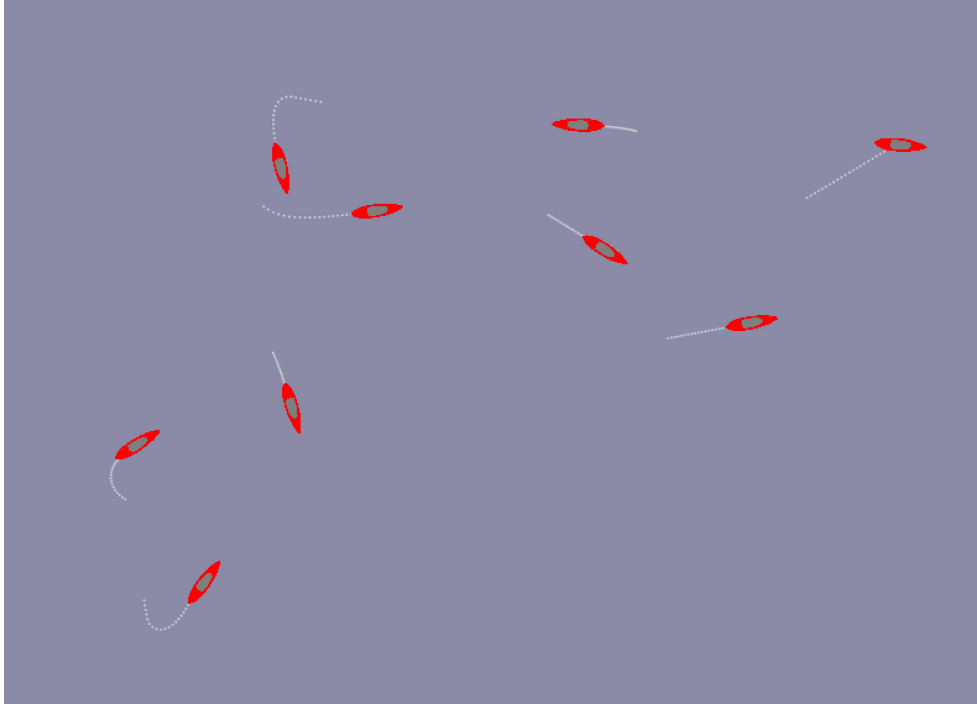


Figure 4-12 COLREGS evaluation allows consideration of complex scenarios such as this non-canonical geometry, multi-rule encounter. Note that multiple collision avoidance rules exist simultaneously between these power-driven vessels.

to multiple programs using a common set of algorithms while maintaining standardized configuration of collision avoidance parameters and adaptability to other protocol rule sets. This allows real-time and post-mission analysis programs to use equivalent means of evaluation; however, it also allows post-mission evaluation using different penalty functions or configuration settings according to the evaluator's preference. The library of algorithms allows configuration parameters to properly tune weights and metrics to local customs or requirements of certification authorities.

Users may use Equations (4.13)-(4.16) as an initial library to construct relevant evaluation functions based on pose angles. The input angle ϕ may be configured to use the contact angle α or relative bearing β . A steering angle ϕ_0 allows tailorable directionality for alternative use of the same functions. An alternative use might represent a passing arrangement agreed via bridge-to-bridge radio, such as a rare starboard-to-starboard passage. Linear and quadratic functions of range and speed are also available within the initial evaluation library release. Incorporation of other

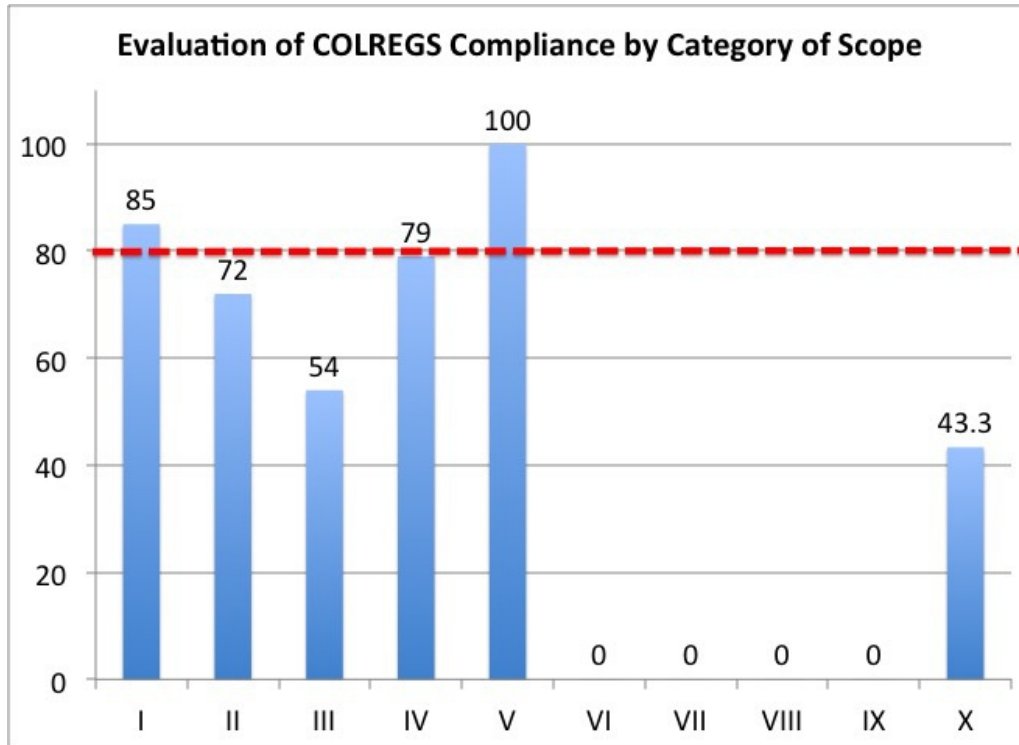


Figure 4-13 After separating rules into categories, graphical displays such as this can demonstrate the scope of work as well as the level of compliance within the scope. Here a report shows work in autonomous collision avoidance for Categories I-V with performance below the configurable threshold for “compliance” visually indicated by the red dashed line at a score value of 80%. The evaluation of this example certification authority uses an unweighted average across Categories I-IX to compute a Category X score. This thesis primarily considers evaluation of Categories II,V, and VI.

functions and input parameters is reserved for future work.

$$\sin^2(\phi + \phi_0) \tag{4.13}$$

$$step(\phi) - step(\phi_0) \tag{4.14}$$

$$\left(\frac{\sin(\phi + \phi_0) - 1}{2} \right)^2 \tag{4.15}$$

$$\left(\frac{\sin(\phi + \phi_0) - 1}{2} \right)^4 \tag{4.16}$$

Configuration is possible for several parameters of interest to a designer or evaluator including:

- preferred range at CPA
- minimum acceptable range at CPA
- range at which a near-miss occurs
- range at which a collision is assumed
- threshold COLREGS rule compliance score below which instantaneous reports should be made
- threshold safety score below which instantaneous reports should be made
- vessel types to consider (allows knowledge of aerial, ground, and undersea vehicles without interference of collision avoidance evaluation)
- range at which contact detection likely occurs
- maximum time threshold allowed for comparison of a contact's position report and ownship's position report
- display of visual indicators when configuration ranges or minimum rule compliance scores are violated
- sounding of audible alerts when configuration ranges or minimum rule compliance scores are violated

4.6.2 Real-Time Analysis

Using the protocol library for COLREGS developed in this thesis, a real-time collision avoidance evaluation program gives instantaneous feedback to vessel designers and a means of real-time evaluation to any certification entity. This can be used to assign penalties or warnings to vessels violating the COLREGS, especially but not limited to training and design verification scenarios. Notifications can be sent to vessels in the

vicinity of non-compliant actors to allow increased caution while operating. Reports of egregious actions can be passed to designers, insurance agencies, or enforcement entities as appropriate or required by statute.

Within the scope of the current work, the real-time protocol evaluation tool was used to display important information at the shoreside observation center including:

- COLREGS compliance scores for power-driven rules
- safety scores after an encounter
- rules required as determined by the observer
- range at CPA
- time of CPA
- vessel names and types

A real-time text report is posted to the mission console including summaries of overall performance (e.g., safety, protocol compliance, type of interaction) as shown in Figure 4-14. To assist a shoreside observer with several vehicles underway, a series of visual and audible indicators were incorporated to provide real-time warning of dangerous or inappropriate action. Colored range rings (Figure 4-15) appeared whenever violations occurred including:

- $r_{cpa} < R_{min}$ (green)
- $r_{cpa} < R_{nm}$ (yellow)
- $r_{cpa} < R_{col}$ (red)
- COLREGS score less than the threshold value (blue)

```

=====
uFldProtocolEval shoreside                                0/0 (554)
=====

Delay to Clear Messages [sec]: 500
Checking for Compliance: ON
Vehicle Types Checked: kayak,sailboat
Pulse on Violations: true

Collision Range: 3
Near-Miss Range: 5
CPA Violation Range: 15
Preferred CPA Range: 25
Nominal Detection Range: 30

COLREGS Violations: 2 (Threshold = 80)
Safety Violations: 2 (Threshold = 80)
Collisions: 0
Near-Misses: 0
CPA Violations: 2
Tolerable CPAs: 0
Greater than Preferred CPAs: 0

UID  Ownship  Contact  Rule#  Safety  COLREGs  CPA  Type  Tcpa
----  -
0    abe      ben     15/17  60.70  0.00    13.2  min_cpa_violation  7.8
0    ben     abe     15/16  60.70  76.30   13.2  min_cpa_violation  7.8

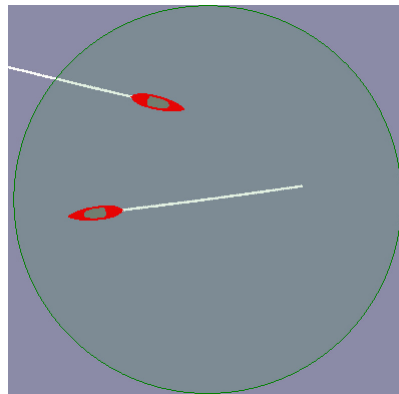
```

Figure 4-14 Scoring of COLREGS collision avoidance rules allow for real-time evaluation of vehicle performance at the shoreside observation center. Configurable range parameters include nominal detection range, preferred range at CPA, minimum acceptable range at CPA, threshold range at which a near-miss occurs, and the range at which a collision is assumed. An aggregate tally of COLREGS violations (scores below a configurable threshold value) and of each configuration range are displayed. Vehicle types as specified by each vessel are used as a filter to allow consideration of only certain entities within the “visibility” of the shoreside observation center. This allows underwater, ground, and aerial vehicles to share the shoreside observation display without unnecessarily being considered as COLREGS compliance candidates.

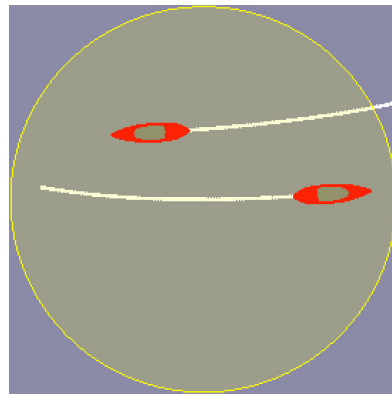
4.6.3 Post-Mission Analysis

A post-mission analysis tool was constructed to provide detailed insight into collision avoidance performance of vessels. The post-mission analysis requires only vehicle position logs; the real-time assessment program was not required to be running to conduct post-mission analysis.

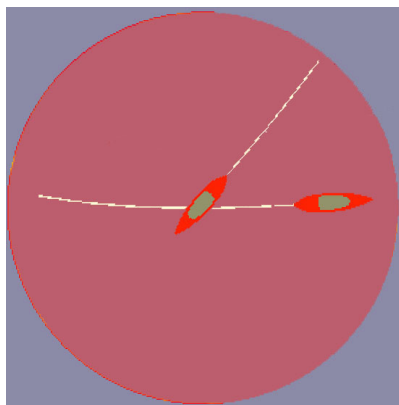
A report is generated for each run of the post-mission analysis tool with a configurable scale of verbosity. In more verbose modes, detailed explanations of cause for score deduction allows designers and operators to understand the rationale for evaluation scores. This can be used to provide feedback and tune future actions. In addition to the verbosity option, all configuration parameters of Section 4.6.1 are available in



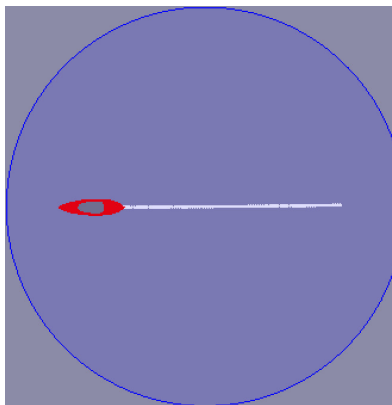
(a) Minimum desired range violation



(b) Near-miss range violation



(c) Collision range violation



(d) COLREGS violation

Figure 4-15 Violations of range below configurable threshold values ((a) minimum desired, (b) near-miss , and (c) collision) result in display of green, yellow, then red rings, respectively, around the vehicle and sounding of an optional audible indicator. This allows real-time warning to an evaluator of a dangerous collision situation. Violations of COLREGS collision avoidance rules below a configurable threshold value result in display of a blue ring (d) around the vehicle and sounding of an optional audible indicator.

the post-mission analysis tool. Evaluation data are exported to a comma-separated value report for ease of meta analysis in a user's favorite data analysis program. This data can then be used for performance analysis by vehicle, by rule combination, or by other parameters of interest to the evaluator.

4.7 Validation of Protocol Evaluation Algorithms

Once evaluation algorithms were developed, a means of validation was required to ensure that appropriate rules were detected, protocol agnostic behavior was identifiable, and collision agnostic behavior was identifiable. A test scenario was designed allowing four vehicles to encounter each other under random geometry. The scenario consisted of two vehicles traversing in a North-South lane while two other vehicles were placed at large distances away: one to the East and one to the West. The North-South vehicles transited along an oval in either an overtaking fashion or a head-on fashion. Each of the East-West vehicles drove within a small polygon until such a time that a random polygon was generated on the opposite side of the North-South lane. That is, each of the two East-West vehicles would switch sides while driving to a new and randomly generated polygon. The polygons were sufficiently far away such that the vehicles in the polygon could only detect the other vehicles during a switching of sides.

The pattern forced random geometries of encounter while leaving a known mixture of overtaking, head-on, and crossing scenarios with up to four vehicles simultaneously. An example configuration of this validation scenario is shown in Figure 4-16. Three primary modes were run for the validation scenario: all vehicles running COLREGS, one vehicle agnostic to COLREGS, and one vehicle agnostic to collisions. Long duration simulations of the latter two modes demonstrated that the evaluation algorithms could accurately detect and classify the non-compliant vehicle.

4.7.1 Validation of Protocol Agnostic Vehicle

A long duration simulation using the construct of Figure 4-16 tested the ability of three vessels operating under the protocol constraints of COLREGS and one vessel using a generic collision avoidance algorithm. The generic collision avoidance algorithm mapped r_{cpa} to utility based on a linear function similar to Equation (3.28) without any preference to maneuver in accordance with the rules. Results of 3,840 encounters demonstrated a clear decline in protocol compliance scores for the proto-

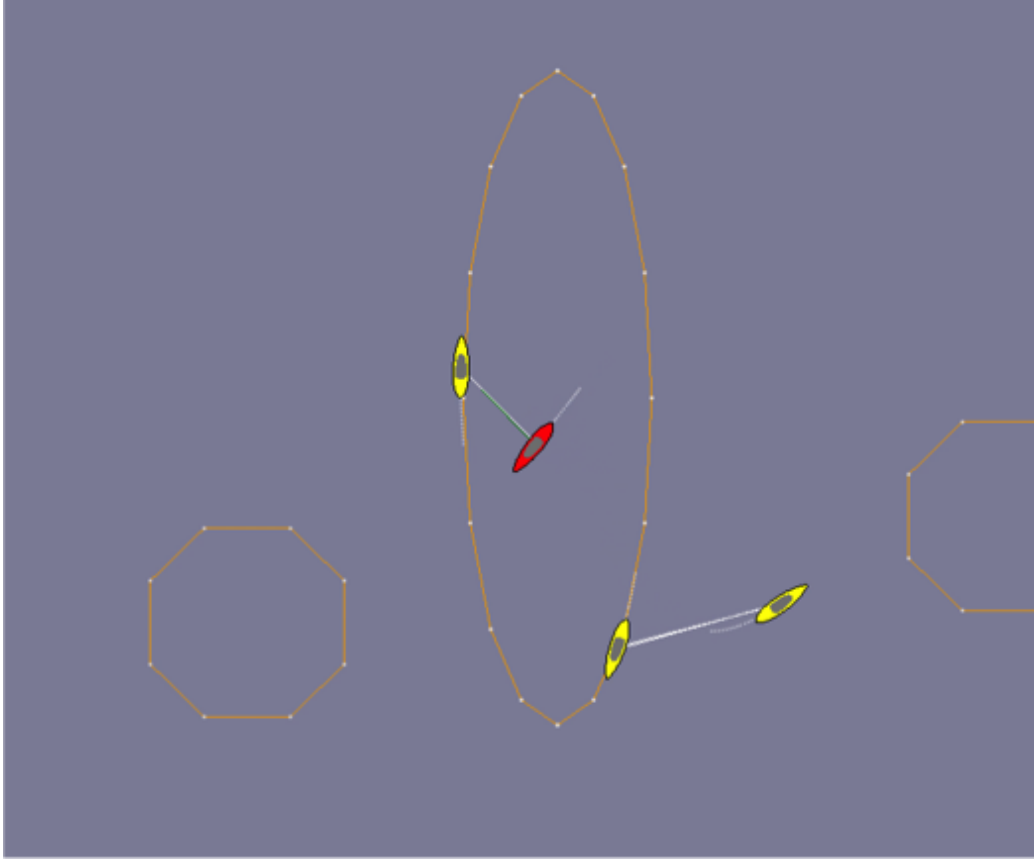


Figure 4-16 A validation scenario allowed for testing of the evaluation algorithms. Four vehicles traversed in a sequence such that two vehicles traded sides to randomly generated polygons while two other vehicles continuously transited in North-South lanes.

col agnostic vehicle with the exception of the stand-on overtaking rule as shown in Figure 4-17. A clear drop in the head-on protocol compliance score of approximately 50% confirms the intuitive expectation that a vehicle equally likely to turn left or right would correctly choose right approximately half the time. The crossing give-way score was approximately equal for the protocol constrained and protocol agnostic vehicles. This is consistent with knowing a vehicle's desire to avoid a contact is generally consistent with giving way. When controlling for the tendencies of the generic algorithm to mimic a COLREGS-compliant give-way maneuver, a clear distinction in protocol compliance scores exists as shown in Figure 4-18.

Mean Protocol Compliance
for Protocol-Agnostic Vehicle
4 Vehicles; $N = 3,840$; msn:m2_detect

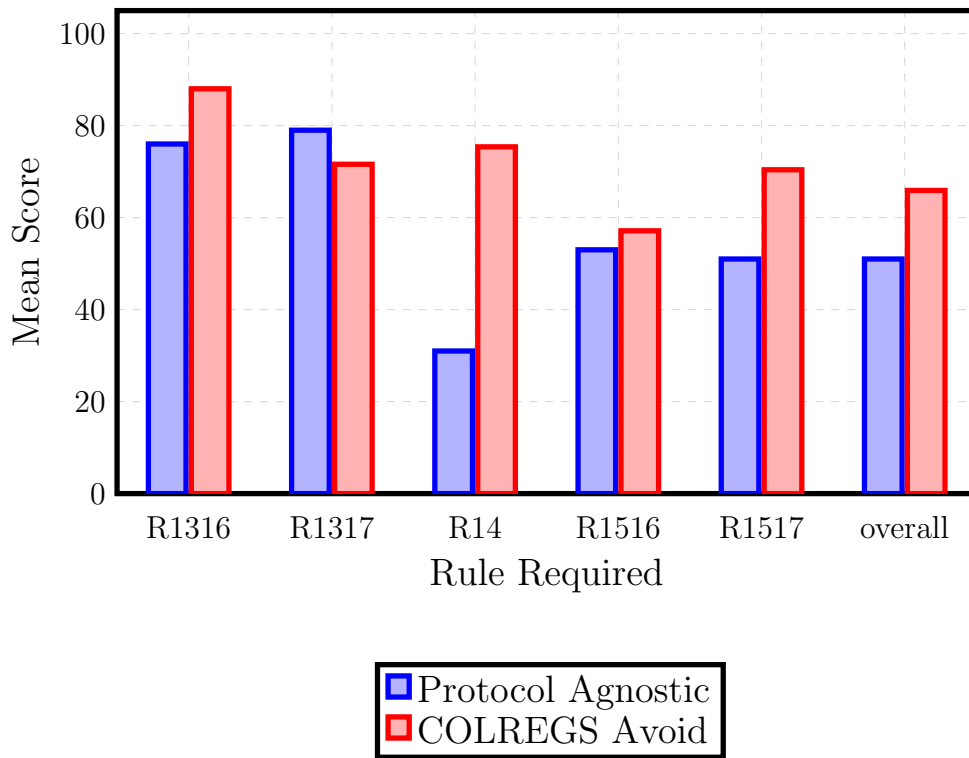


Figure 4-17 Mean protocol compliance for three protocol constrained vehicles and one protocol agnostic vehicle demonstrated the ability to identify the offending vehicle. A total of 3,840 encounters demonstrated that the most clear reduction in compliance score occurred for the head-on case (\mathfrak{R}^{14}).

Mean Protocol Compliance
for Protocol-Agnostic Vehicle
4 Vehicles; $N = 3,840$; msn:m2_detect

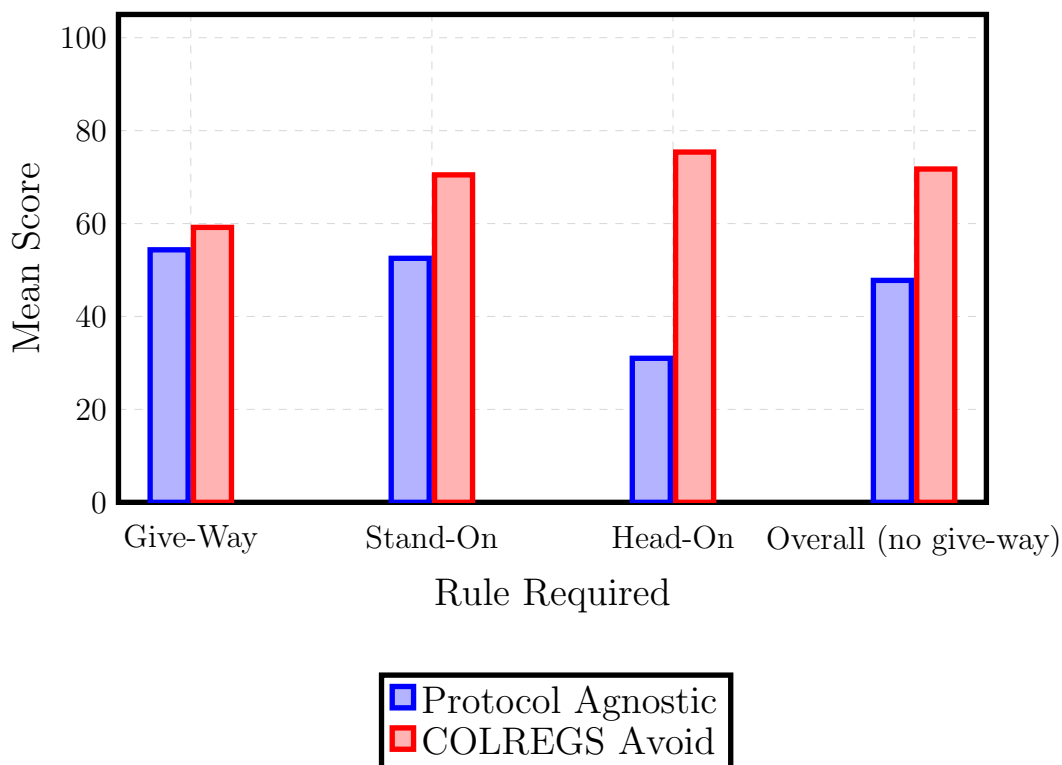


Figure 4-18 Mean protocol compliance for three protocol constrained vehicles and one protocol agnostic vehicle demonstrated the ability to identify the offending vehicle. A total of 3,840 encounters demonstrated that the most clear reduction in compliance score occurred for the head-on case (\mathfrak{R}^{14}). By controlling for the give-way case, a clear distinction can be made between performance of COLREGS-compliant vessels operating in the vicinity of protocol agnostic vehicles and the protocol agnostic vehicles themselves.

4.7.2 Validation of Collision Agnostic Vehicle

A long duration simulation using the construct of Figure 4-16 tested the ability of three vessels operating under the protocol constraints of COLREGS and one vessel using no collision avoidance algorithms. The collision agnostic vehicle had zero preference to avoid collisions and maneuvered exclusively for its primary mission. Results of 1,788 encounters demonstrated a clear ability to identify a collision agnostic vehicle as being in violation of the COLREGS as shown in Figure 4-19. The head-on scenarios showed the most clear reduction of score (0% average for the collision agnostic vehicle). Stand-on rules benefited the collision agnostic vessel with the exception of the times that the vessel failed to maneuver when being *in extremis*. When controlling for the stand-on encounters, a comparison of COLREGS-compliant vessels operating in the vicinity of a collision agnostic vehicle and the collision agnostic vehicle yielded a reduction in score of approximately 50% as shown in Figure 4-20.

4.7.3 Significance Testing for Compliance Detection

To ensure the protocol compliance algorithms sufficiently detected non-compliant behavior, an additional series of experiments were developed using up to four vehicles to test for statistical significance. The scenarios again allowed for testing one of three compliance settings:

- COLREGS cognizant
- protocol agnostic
- collision agnostic

COLREGS cognizant vehicles made decisions based on protocol compliance and safety. In the protocol agnostic case, a generic collision avoidance algorithm mapped r_{cpa} to utility (see Equation (3.28 where $avd(r_{cpa} = R_{min}) = 0$ and $avd(r_{cpa} = R_{pref}) = 1$) without bias or penalty for protocol compliance, i.e., only using safety. In this protocol agnostic case, for example, a contact in a head-on encounter (reciprocal course with risk of collision) would be approximately 50% likely to turn

Mean Protocol Compliance
for Collision-Agnostic Vehicle
4 Vehicles; $N = 1,788$; msn:m2_detect

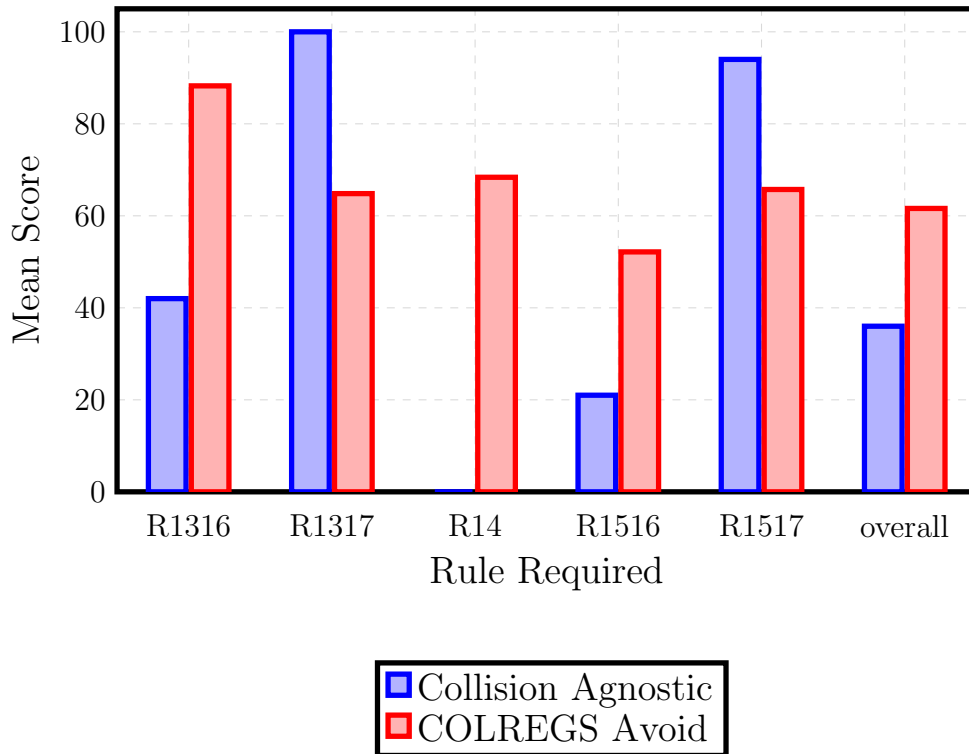


Figure 4-19 Mean protocol compliance for three protocol constrained vehicles and one collision agnostic vehicle demonstrated the ability to identify the offending vehicle. A total of 1,788 encounters demonstrated that the most clear reduction in compliance score occurred for the head-on case (\mathfrak{R}^{14}). The stand-on rules were largely compliant as maintaining course and speed was natural for the collision agnostic vehicle. A lower than perfect score for $\mathfrak{R}^{15/17}$ resulted from the few cases where the collision agnostic vehicle failed to take evasive action when *in extremis*.

Mean Protocol Compliance
for Collision-Agnostic Vehicle
4 Vehicles; $N = 1,788$; msn:m2_detect

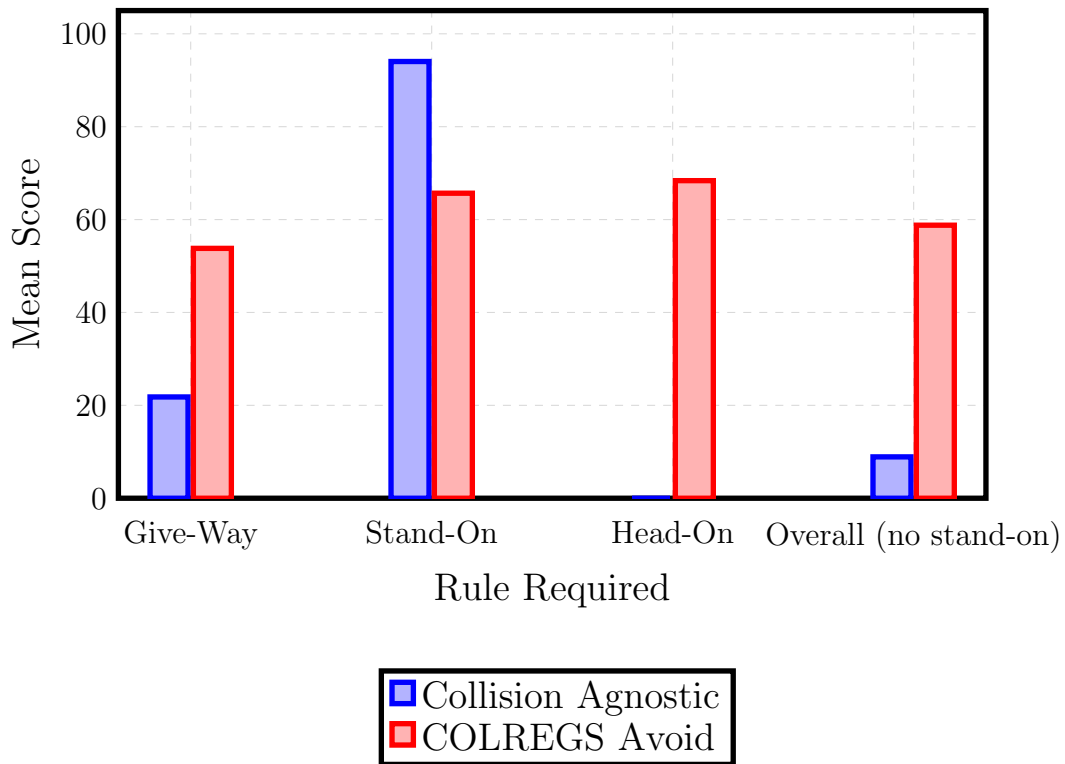


Figure 4-20 Mean protocol compliance for three protocol constrained vehicles and one collision agnostic vehicle demonstrated the ability to identify the offending vehicle. A total of 1,788 encounters demonstrated that the most clear reduction in compliance score occurred for the head-on case (\mathfrak{R}^{14}). By controlling for the stand-on case, a clear distinction can be made between performance of COLREGS-compliant vessels operating in the vicinity of collision agnostic vehicles and the collision agnostic vehicles themselves.

the protocol-compliant direction (starboard). For the collision agnostic vehicle, all collision avoidance was removed from the decision making process.

Validation was performed by placing one vessel in a field of 3 or more protocol compliant vessels under long duration simulation. Table 4.2 shows p -values for statistical significance, while t -test values and degrees of freedom are shown in Table 4.3 and Table 4.4, respectively. These validation tests showed that a protocol agnostic vehicle was detectable in a field of COLREGS cognizant vehicles under all power-driven rules to a significance value of $p < 0.01$.

A vehicle operating without regard to COLREGS cognizant vessels (i.e., collision agnostic) was detectable ($p < 0.01$) by the evaluation algorithms in all cases except when the collision agnostic vehicle was being overtaken. In the specific case of a collision agnostic vehicle being overtaken by a COLREGS cognizant vehicle, significance was shown to $p = 0.017$. This case confirms intuition where an overtaken (slow) vessel would normally maintain course and speed unless placed *in extremis*; in this case, the overtaking vessel is COLREGS cognizant and unlikely to place the overtaken vessel *in extremis* given the long t_{cpa} associated with an overtaking geometry. Vehicles operating in a protocol agnostic mode were detectable in a field of COLREGS cognizant vehicles by the evaluation algorithms to significance values of $p < 0.01$.

Table 4.2 *Significance Testing for Compliance Detection*

Inference for Two Independent Samples			
	p-values for 1-sided test, significance assumed at $p < 0.01$		
	COLREGS & Generic	COLREGS & No Avoid	Generic & No Avoid
Rule 13/16	< 0.001	< 0.001	0.001
Rule 13/17	< 0.001	0.017	0.002
Rule 14	< 0.001	< 0.001	< 0.001
Rule 15/16	0.006	< 0.001	< 0.001
Rule 15/17	< 0.001	< 0.001	< 0.001

4.7.4 Human Agreement with Evaluation Results

Nine collision avoidance scenarios were analyzed by the evaluation tools presented in Chapter 4 including assignment of a required protocol rule and assessment of blame

Table 4.3 *Significance Testing: t-Test Values*

Inference for Two Independent Samples			
	t-test values		
	COLREGS & Generic	COLREGS & No Avoid	Generic & No Avoid
Rule 13/16	6.70912	4.05034	-3.26807
Rule 13/17	-4.67568	-2.12754	2.91374
Rule 14	19.36010	72.03438	-10.00225
Rule 15/16	2.52264	14.06200	-11.77708
Rule 15/17	13.11400	-8.46315	14.52719

Table 4.4 *Significance Testing: Degrees of Freedom*

Inference for Two Independent Samples			
	Degrees of Freedom		
	COLREGS & Generic	COLREGS & No Avoid	Generic & No Avoid
Rule 13/16	178	111	33
Rule 13/17	232	329	349
Rule 14	372	472	310
Rule 15/16	2232	1917	613
Rule 15/17	2151	1917	550

when a collision or near miss occurred. These nine scenarios were then presented to self-identified ship drivers claiming significant on-water experience driving under the protocol requirements. Respondents first identified the rule required in each scenario, then identified the vessel or vessels to which they would assign primary blame. One of the scenarios had two blame questions for a total of nine rule identification questions and ten blame questions. Responses by the self-identified experienced protocol experts overwhelmingly supported the conclusions of the evaluation algorithms. A total of 98.15% of rule questions agreed with the decisions of the evaluation algorithms. A total of 90.83% of blame assignments agreed with the decisions of the evaluation algorithms as shown in Figure 4-21.

These rates of agreement are far higher than the assessed rates of correct rule identification by students testing in COLREGS (see Appendix D). Blame assignments in the evaluation algorithm were consistent with case law, and may be cause for some of the less than 10% discrepancy with respondents. For example, a stand-on vessel

Evaluation Validation by Self-Assessed Ship Drivers and Rules Experts

($N_{respondents} = 12$; $N_{rule} = 9$; $N_{blame} = 10$)

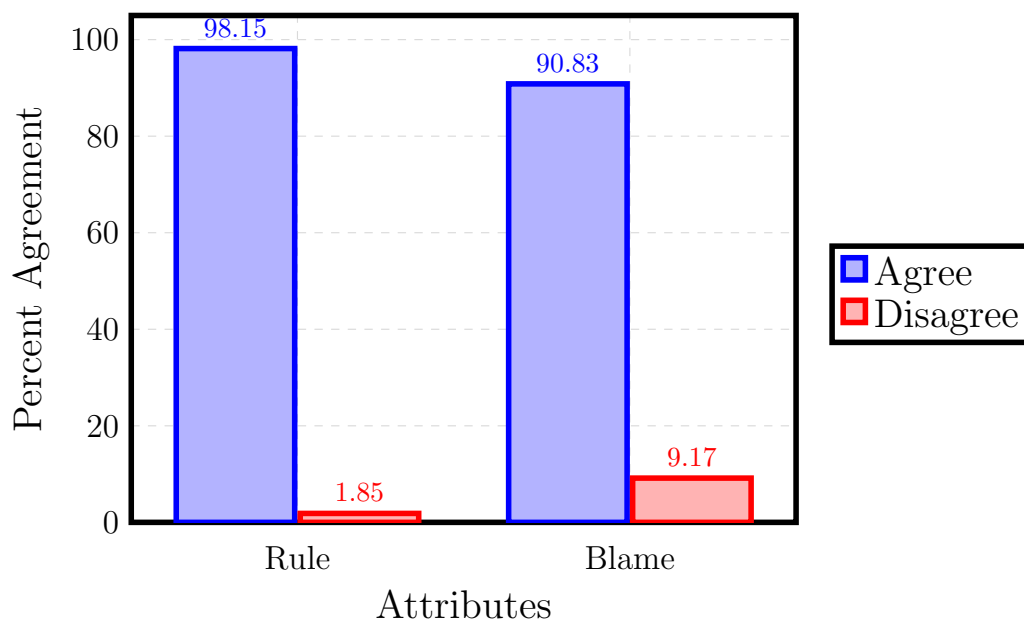


Figure 4-21 A human survey validated the evaluation results of the evaluation algorithm with self-identified experienced protocol experts agreeing with over 98% of rule assignments and over 90% of blame assignments.

rarely receives more than 25% blame in a collision though often receives some blame for not taking action . In the majority of the 9.2% of disagreement between the evaluation algorithm and the respondents, the respondents assigned blame to both parties, however in a reversely proportionate fashion. Further surveys with conditioning the respondent to know the likely percentage of blame assigned for particular rule violations would likely yield higher correlation between responses and evaluation algorithm blame. This conditioned survey is reserved for future work.

4.8 Conclusions

In summary, this chapter defined metrics and algorithms to quantify protocol compliance, safety, and mission performance *viz* spatial and temporal efficiency. Algorithms were validated using long term statistics and human sampling from self-described rules experts. A library of functions was proposed to allow configuration of the protocol evaluation tools in both real-time and post-mission analysis. Specific instantiation of protocol quantification and evaluation was demonstrated for the rules of the road for sea-going vessels, i.e., COLREGS. Chapter 5 presents simulation testing techniques and an example case study framework using the methods of this chapter. Chapter 6 presents on-water testing techniques and results using the methods of this chapter.

Chapter 5

Performance Testing and Simulation Methods

Chapters 3 and 4 developed methods to quantify and evaluate safety and protocol compliance of individual collision avoidance encounters. This chapter uses the individual encounter tools to test, analyze, and assess autonomous vehicle performance in the larger context of balancing mission performance, safety, and collision avoidance protocol compliance. This chapter then develops methods for simulation testing to exercise the collision avoidance algorithms in simultaneous multi-contact encounters under complex geometries. More specifically, this chapter:

- develops methods for understanding trades between safety, efficiency, and protocol compliance
- introduces algorithms to perform edge case searches using a systematic framework that incorporates non-canonical encounter geometries
- introduces the concept of egregiousness to prioritize edge cases for evaluator or designer consideration based on combined safety and protocol compliance scores
- enables a design of experiments to use multi-contact initial detection geometry as a testing parameter

Rigorous testing allows the use of specific metrics and population of decision data structures for analyzing various configurations of collision avoidance parameters, mission requirements, and available platforms. Specific tuning of collision avoidance algorithms changes performance characteristics. Placing a well-tuned collision avoidance algorithm on a vehicle with different operating characteristics such as a high-speed vessel requires examination of affects on performance metrics prior to fielding. By using these testing and evaluation techniques in high volume simulation, an extensive edge case search and sensitivity analysis may be performed prior to subjecting an algorithm to on-water testing. By using a systematic approach to testing in a simulation environment, some understanding can be made as to the performance of autonomy algorithms under edge cases that might be hard to create – at least in sufficient quantity – with on-water testing. By varying algorithm configuration parameters and inserting random noise into initial conditions, sensitivity analysis may be performed to determine the likelihood of unwanted behavior under certain conditions prior to experimenting in an on-water scenario that is likely costly, time consuming, and exposes human testers to possible danger if an algorithm responds unexpectedly.

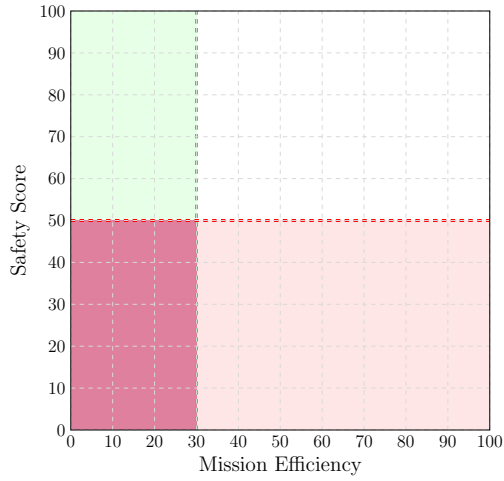
Section 5.1 discusses a means for the designer or evaluator to visualize the performance metrics of Chapter 4 in the larger context of mission performance. Section 5.2 discusses the necessity of safe default maneuvers and what those maneuvers might mimic to be recognizable to humans and consistent with human behavior. Section 5.3 presents a method to prioritize edge cases for evaluator or designer consideration based on combined safety and protocol compliance scores. Section 5.4 presents the iterative geometric testing framework for edge case search and sensitivity analysis prior to on-water fielding. Section 5.5 demonstrates results of a case study of the iterative geometric testing framework applied to a high-speed vessel with two slow speed contacts using the patience parameter of Section 3.6 as a design variable of consideration. Section 5.6 presents considerations for autonomously operating in the vicinity of and teaming with human operated vehicles.

5.1 Performance Curves of the Objective Tradespace

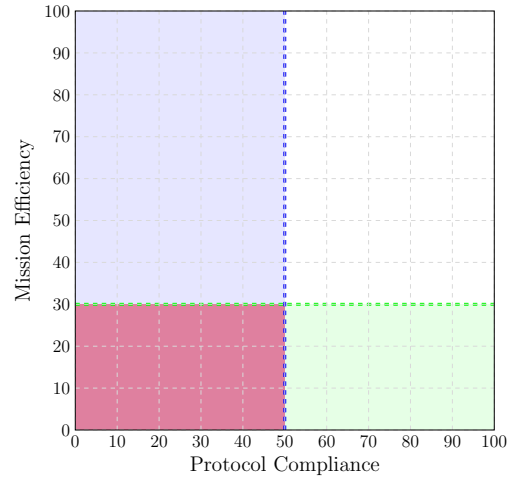
Each designer or operator must choose a policy that appropriately balances the performance metrics to best achieve the goals of the autonomous system. Using the surrogate mission performance metrics of spatial and temporal efficiency (Section 4.2), a collision avoidance algorithm may be examined under numerous scenarios to determine its sensitivity and performance with respect to protocol compliance and safety. In the absence of a clearly defined metric for mission performance, either temporal or spatial efficiency may represent the preferred mission performance metric. Three two-dimensional tradespace comparisons are shown in Figure 5-1.

Three primary functions of a populated performance curve may provide human designers with greater understanding of the autonomous system including:

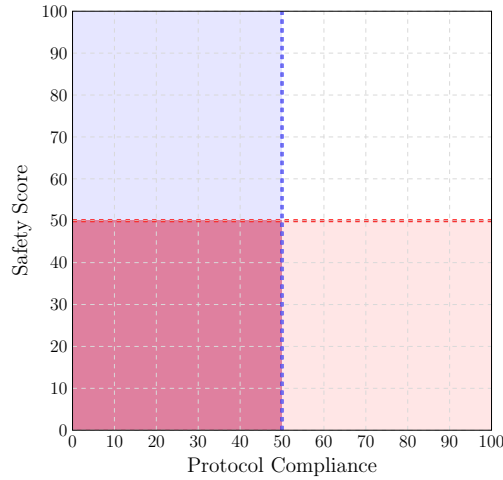
1. For an algorithm whose curve has yet to reach the well-populated state, outliers in performance may be identified in real time to signal possible edge case detection for designer review. For example, a particular experimental configuration might result in exceptionally low efficiency or safety scores below some design threshold identifying a possible flaw in the algorithm or an undesirable configuration state.
2. Once well populated, a performance curve may give great insight as to what configuration combinations yield the most preferred results for given initial conditions. One such initial condition set might be the multi-contact encounter geometry at the time of detection. If a vehicle detects a known or nearly known geometry with a well-populated data set of performance outcomes, then the collision avoidance and mission configuration parameters that best achieved the desired performance metrics may be tuned in real time by the autonomous vehicle. An example of this would be to pick the dynamic patience parameter (Section 3.6) that achieves the desired efficiency performance while not reducing safety or protocol compliance below configurable threshold values.
3. For a system that is well populated, deviation outside of an expected tolerance



(a) Mission vs. Safety



(b) Protocol Compliance vs. Mission



(c) Protocol Compliance vs. Safety

Figure 5-1 Two-dimensional performance curves allow mapping of autonomous collision avoidance results to easily visualized graphs. This allows for edge case detection, discovery of optimization characteristics such as Pareto optimal solutions, and selection of the desired performance ratio within a given tradespace. In this case, a simplifying assumption that mission performance is represented by a single efficiency (either spatial or temporal) yields three two-dimensional performance curves for analysis: (a) mission and safety, (b) protocol compliance and mission, and (c) protocol compliance and safety. Here the safety threshold violations are shown by red, mission performance (efficiency) by green, and protocol compliance by blue. With a configurable setup such as this, performance points falling below threshold values may quickly be examined to determine edge case discovery or undesirable affects of configuration variables.

can give insight into algorithm degradation, lack of either precision or accuracy in determining the assumed initial conditions, non-compliance by the other vehicle, or detection that a change to the plant (i.e., the vehicle) has occurred requiring recalibration of the decision space.

As an autonomous collision avoidance algorithm becomes used by more vehicles, data may be aggregated across various vehicles to determine higher fidelity performance characteristics, and when appropriate, further populate the performance space to allow distributed autonomous learning. Consideration may be granted to having more specialized performance curves to best represent specifically identified scenarios by reasoning about attributes such as:

- the number of vehicles involved in a collision avoidance situation
- the combination of collision avoidance protocol rules simultaneously required
- tonnage of ownship and contacts
- environmental parameters including but not limited to sea-state, visibility, and wind
- degradation of detection and classification equipment such as visual or auditory sensors, radar, or AIS
- alternatively required protocols such as Inland COLREGS or alternative direction of buoyage¹
- recognized encounter geometries² using combinations of the above attributes

Once a more specific performance curve is referenced when available, the designer's performance preferences (e.g., maximize temporal efficiency without violating given threshold of safety and protocol compliance) may reduce the problem to a subset of

¹The International Association of Lighthouse Authorities has different regions throughout the world for determining the color of buoys one should expect to see on a particular side of the vessel when entering port. This has led to numerous groundings and collisions.

²Geometry refers to a specific combination of range, pose, and speed for a given contact relative to ownship.

course-speed pairs from the Pareto optimal frontier. The decisions of the designer may be imposed by policy on the autonomous system [58].

5.2 Default Safety Maneuvers

When humans operate in human-only environments, an implicit assumption is that each vehicle will act in due regard to other vehicles in the event of an emergency that causes maneuverability restrictions or when a dangerous collision avoidance encounter inadvertently arises. Not only must autonomous vehicles assess plant health in real-time, but they must possess a means of confidently knowing that actions taken in collision avoidance scenarios achieve sufficient safety for all involved. Autonomous designers must incorporate a means of identifying when a collision avoidance scenario falls outside the scope of the vehicle's reasoning or maneuvering abilities. Ideally, these edge cases would be discovered and mitigated prior to fielding. Sufficiently identifying over-constrained or unrecognizable scenarios are necessary to build trust with human operators and society more generally.

In the event that an autonomous vehicle cannot with confidence take action to avoid collision, a default safety maneuver should be activated. In some scenarios this might be simply taking all way off the ship, backing down, and communicating its distress to neighboring vehicles and the designer. This communication can be both in protocol-formal means such as sounding a danger signal as well as relaying information via communication protocols such as AIS. In the event of losing confidence in its own ability to determine safe actions, an autonomous vessel under protocol constraints of COLREGS should consider presenting itself to other vessels as being not under command (Rules 3, 27, 35).

Autonomous designers must understand the human aspect of safe maneuvers in different scenarios. For example, taking way off the ship may indeed be a very attractive default maneuver, though create an extremely dangerous outcome if done with no warning and without additional action. In the case of a heavily congested traffic separation scheme or narrow strait, an autonomous vessel with high drag might

stop too quickly to prevent a vessel astern from taking necessary action to prevent a collision, allision, or grounding. In more open ocean scenarios, turning to starboard may be prudent. Several default safety maneuvers must be considered and the appropriate cases identified for when to enact each. Autonomous designers would be well served by having consensus in the international community as to what human ship driving expectations would be in the event of a need to execute a safety maneuver under various initial conditions or causes. By giving more predictability and standardization in both maneuvers and means to communicate the necessity of emergency action, human trust can be gained knowing that a well communicated and properly executed safety maneuver that emulates human driving is pre-programmed into autonomous vehicles. Exercise of autonomous vehicles in situations that would create over-constrained decision spaces or otherwise require use of a default safety maneuver should be conducted prior to fielding.

5.3 Egregiousness

While Sections 4.3 and 4.4 establish methods to quantify protocol compliance and safety, respectively, coupling of the two metrics provides a measurement of egregiousness of encounters. A measure of egregiousness provides a means to determine when a maneuver is both non-compliant and unsafe as shown in Equation (5.1) and Figure 5-2.

$$E(S, \mathfrak{R}) = \frac{(S^{max} - S) \cdot (\mathfrak{R}^{max} - \mathfrak{R})}{S^{max} \cdot \mathfrak{R}^{max}} \quad (5.1)$$

$$E \in [0, 1]$$

A vessel may maneuver in such a way to be non-compliant due to a series of small, non-apparent maneuvers that ultimately results in a safe distance and pose at CPA. While this is not compliant with the protocol constraints, its safety is sufficiently high to not necessarily warrant prioritization over a case with equally bad protocol

Egregiousness (E) as a Function of Safety (S) and Protocol Compliance (\mathfrak{R})

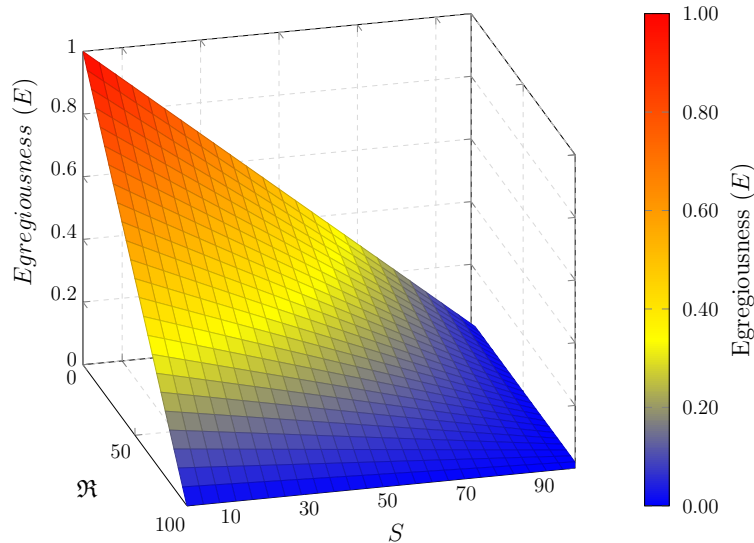


Figure 5-2 A vessel may maneuver in such a way as to be readily apparent but also result in a dangerous and unsafe CPA. The apparent maneuver is necessary but not sufficient to warrant a high compliance score. The egregiousness score assists designers and evaluators in prioritizing collision avoidance encounters for analysis and corrective action

compliance and a more severe safety violation. A vessel may maneuver in such a way to be readily apparent but also result in a dangerous and unsafe CPA. The apparent maneuver is necessary but not sufficient to warrant a high compliance score. The resulting egregiousness score would be high and thus the decision would be identified as a prioritized edge case. Figure 5-3 demonstrates both non-compliant but safe maneuvers as well as non-apparent and unsafe maneuvers. Egregiousness allows easy identification of values that are both unsafe and non-compliant. Encounters having a high egregiousness score represent edge cases for immediate evaluator attention and designer rectification. By having a means of finding and ranking dangerous and non-compliant maneuvers, a means of prioritization of edge cases is possible.

5.3.1 Blame

When a dangerous encounter occurs, a natural tendency exists to assign blame to one or both parties. Case law gives guidance in how blame might be assigned in certain scenarios. Often case law assigns blame in a way that consistent with the give-way vessel not giving way early or sufficiently to avoid a dangerous encounter. The exact manner of the blame determination remains dependent on case law; however, an initial blame may be assigned by one of two methods:

1. consistent with case law, assign majority (at least 75%) blame to the give-way vessel, if one exists
2. assign blame proportionally to each vessel according to the proportion of egregious factors

In scenarios of evaluation using proportional blame assignment, blame may be

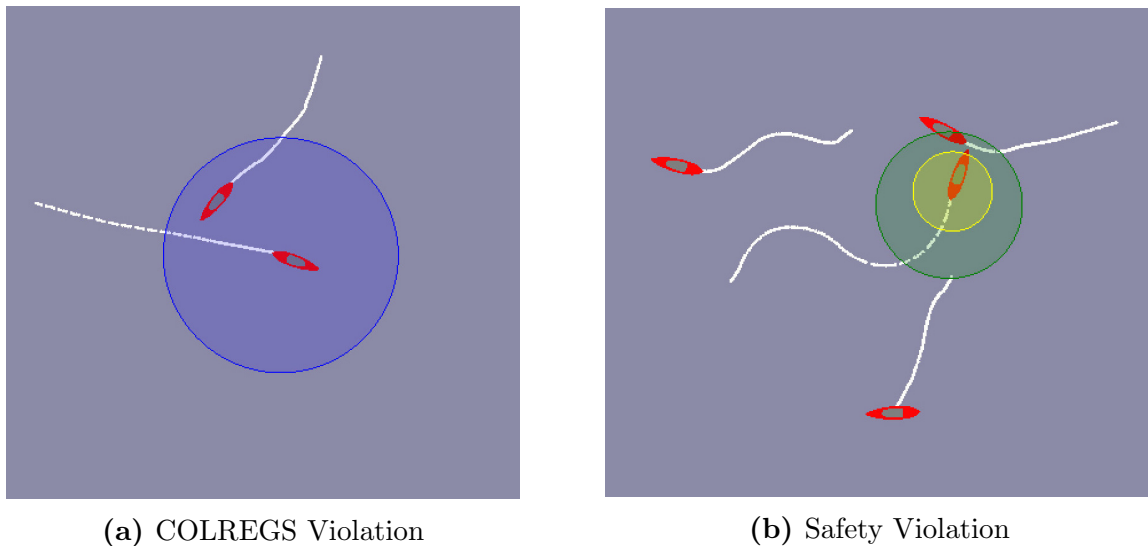


Figure 5-3 These on-water experimental results demonstrate the necessity of evaluating both safety and protocol compliance in conjunction with each other. The first encounter demonstrates that vessels with acceptable CPA ranges can still violate the requirements of the COLREGS. In (a), a crossing give-way vessel maneuvers to starboard to cross astern of the crossing stand-on vessel. While an acceptable CPA is achieved, the maneuver of the crossing give-way vessel was neither substantial nor early, thus violating COLREGS. In (b), a maneuver that was both early and substantial still resulted in an unsafe collision range. In addition, the crossing stand-on vessel of (b) began *in extremis* action under Rule 17.a.ii.

used to quickly identify a vessel who under performs other vessels in conjunction with scores of egregiousness.

5.4 Iterative Geometric Testing

To advance the canonical nature and relatively small variation of geometries found throughout the literature, a geometry generation and testing scheme was developed. This section introduces a testing framework to:

- perform edge case searches using non-canonical, multi-contact encounter geometries
- determine aggregate performance characteristics using large variations of initial detection geometry
- conduct a design of experiments using initial detection geometry as a variable of the design

A collision avoidance algorithm may be subjected to large variations of initial geometry while holding constant collision avoidance and primary mission algorithm configurations. These geometries and experiments could then be repeated using variations of collision avoidance and primary mission algorithm configurations to further perturb the system while holding initial detection geometry configurations in known states for future analysis. These iterative geometries produce varying combinations of required protocol rules and interaction scenarios. After successive testing of a particular algorithm configuration over the desired geometries, analysis can determine the influence of initial geometry and protocol rule requirements on the metrics of concern with the given settings. Additionally, the other design variables may be analyzed for sensitivity in resulting performance to initial detection geometry. Iterative geometric testing forces edge cases and non-trivial multi-contact encounters to the surface.

To create a design of experiments, the number of desired geometries, contacts, and variations on collision avoidance parameters is first determined. Initial speeds

and headings of the primary testing vehicle are then selected for each experiment. These parameters are used to seed a geometry generation algorithm (Algorithm 18) for the vehicles. A baseline geometry configuration \mathcal{G} for the contacts is assumed and uniformly (or normally) distributed noise perturbs the initial headings and speeds of the contacts. By inserting these variations for each of the contacts, sufficient deviation from canonical cases is achievable while testing the general effects of the iterative vehicle's encounter geometries. By maintaining a baseline geometry of the contacts *vis-à-vis* heading and speed noise, initial relative contact geometry can be used as a variable for a design of experiments. Each perturbation of the design may have a different initial nominal geometry of the contacts from which ownship geometry perturbations are seeded. Once initial vehicle headings and speeds are determined, all contacts in the encounter are placed such that they arrive at a shared collision point simultaneously in the absence of any maneuvers.

An example iterative geometric testing experiment is shown in Figure 5-4. Ownship (C) is iteratively tested at various initial positions and speeds as shown in Figure 5-4b while the contacts (A & B) are given perturbations of initial heading and speed.

The placement of vehicles such that they share a simultaneous collision point creates encounters that require consideration of multiple simultaneous rules that often conflict with each other. Operational compromises³ must be made between safety, efficiency, protocol compliance, and perhaps other performance considerations. A common tie-breaking scheme in the literature is to use time to CPA [45] or collision probability [67] to choose which constraint to relax; in this testing geometry configuration, time to CPA and collision probability are equivalent by design for all vehicles; therefore, a more elegant tie-breaking scheme and decision is required within the collision avoidance algorithm being tested.

By repeating this experiment for several geometries of protocol-constrained initial

³With the admission of these evaluation metrics, a set of Pareto optimal solutions can be found and preference information incorporated when choosing course-speed solution vectors. Additional information regarding use of the objective space more generally and related formal multi-objective optimization can be found in [58].

Algorithm 18 Iterative Geometry Generation

```

1: procedure GENERATEGEOMETRY
2:    $[\theta_c] \leftarrow$  nominal contact heading matrix ( $\#$  experiments  $\times$   $\#$  contacts)
3:    $[v_c] \leftarrow$  nominal contact speed matrix ( $\#$  experiments  $\times$   $\#$  contacts)
4:    $[\tilde{\theta}_c] \leftarrow$  angle variation matrix ( $\#$  experiments  $\times$   $\#$  contacts)
5:    $[\tilde{v}_c] \leftarrow$  speed variation matrix ( $\#$  experiments  $\times$   $\#$  contacts)
6:    $[v] \leftarrow$  nominal ownship speed vector ( $\#$  experiments  $\times$  1)
7:    $[\tilde{v}] \leftarrow$  ownship speed variation allowed ( $\#$  experiments  $\times$  1)
8:    $\sigma_\theta \leftarrow$  heading noise standard deviation
9:    $\sigma_v \leftarrow$  velocity noise standard deviation
10:   $t_{col} \leftarrow$  time to simultaneous collision
11:   $P = (P_x, P_y) \leftarrow$  simultaneous collision point
12:  for experiment  $i$  do
13:    for contact  $j$  do
14:      % adjust contact's initial heading and speed for random noise %
15:      if uniform noise then ▷ default
16:         $[\theta_c]_{(i,j)} \leftarrow [\theta_c]_{(i,j)} + [\tilde{\theta}_c]_{(i,j)} \cdot U(-0.5, 0.5)$ 
17:         $[v_c]_{(i,j)} \leftarrow [v_c]_{i,j} + [\tilde{v}_c]_{(i,j)} \cdot U(-0.5, 0.5)$ 
18:      else if normally distributed noise then
19:         $[\theta_c]_{(i,j)} \leftarrow [\theta_c]_{(i,j)} + [\tilde{\theta}_c]_{(i,j)} \cdot N(0, \sigma_\theta)$ 
20:         $[v_c]_{(i,j)} \leftarrow [v_c]_{i,j} + [\tilde{v}_c]_{(i,j)} \cdot N(0, \sigma_v)$ 
21:      end if
22:       $(x, y)_{(i,j)} \leftarrow P - [v_c]_{(i,j)} \cdot t_{col} \cdot \begin{bmatrix} \cos([\theta_c]_{(i,j)}) \\ \sin([\theta_c]_{(i,j)}) \end{bmatrix}$ 
23:    end for
24:     $[\theta]_i \leftarrow U(0, 360)$  ▷ determine initial conditions for ownship (o/s)
25:     $[v]_i \leftarrow [v]_i + \tilde{v} \cdot U(-0.5, 0.5)$ 
26:     $(x, y)_i \leftarrow P - [v]_i \cdot t_{col} \cdot \begin{bmatrix} \cos([\theta]_i) \\ \sin([\theta]_i) \end{bmatrix}$ 
27:  end for
28: end procedure

```

conditions, the nature of the autonomy's scheme for resolving conflicting priorities is forced to the surface. The true ability of the underlying collision avoidance algorithms to successfully reason about more complex scenarios of each rule set is tested in concert with mission performance and navigational restrictions.

Discovery of edge cases for particular rule pairs in one-on-one collision avoidance scenarios is not trivial; however, the edge case search for advanced autonomous collision avoidance algorithms requires advanced techniques. When properly designed with large numbers of iterations, this iterative geometric testing scheme allows testing of the full geometry spectrum using multi-rule, multi-contact scenarios in protocol-

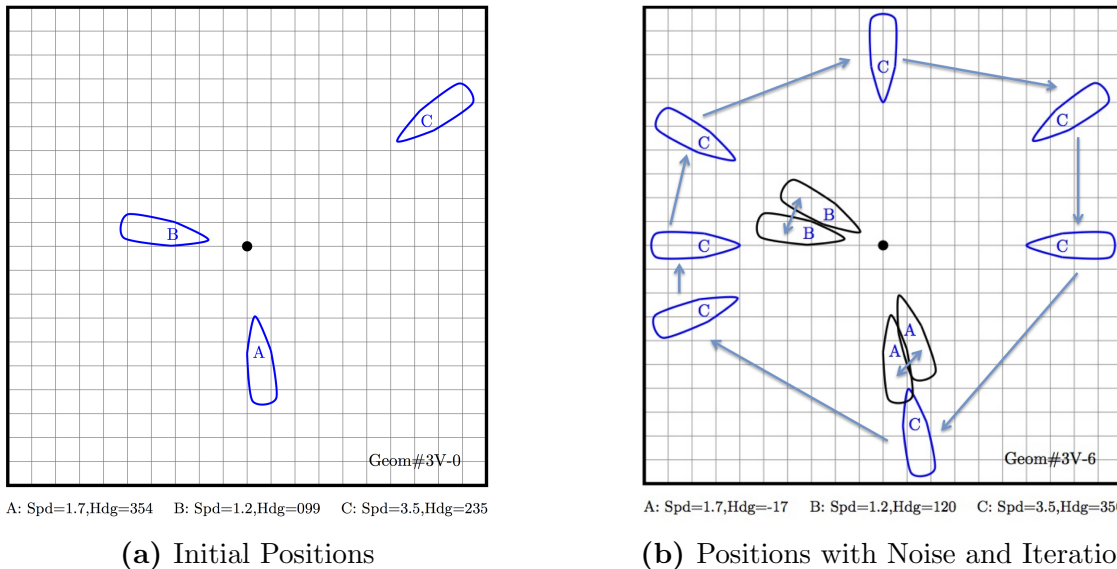


Figure 5-4 An example three-vehicle encounter (a) shows the initial positions of a random experiment. The dot in the center represents the simultaneous collision point. Distance from the collision point represents the initial speed of the vehicle where farther distance implies faster initial speed. Slow speed vessels *A* and *B* are in nominal crossing patterns with initial heading noise to preclude canonical geometries (b) while high-speed vessel *C* assumes initial headings throughout the range of 0° to 360° . Each geometry configuration \mathcal{G} is iterated over the variations of the design of experiments.

constrained environments.

Beyond the testing advantages of iterative geometric testing, this technique provides a means to improve performance while underway. By aggregating performance data in complex collision avoidance scenarios, a mapping of algorithm configuration and its associated performance to the contact geometry at initial detection is possible by using the methods of Section 5.1 with initial detection geometry as a filterable attribute. When a vehicle finds itself in a complex collision avoidance encounter, estimations of performance in similar cached encounters may enable selection and self-tuning of collision avoidance and mission algorithms to achieve the most desirable performance attributes. This allows, for example, selection of various dynamic patience parameter configurations (Section 3.6) to achieve the desired mission, spatial, and temporal efficiencies for a given minimum required score of protocol compliance and safety. Table 5.1 lists a summary of iterative geometric testing attributes. Sec-

tion 5.5 presents a case study of iterative geometric testing for a high-speed vessel encountering two slower speed vessels.

Table 5.1 *Iterative Geometric Testing Attributes*

Number	Attribute
I	Systematically test non-canonical collision avoidance encounters for multiple simultaneous contacts
II	Inject noise into otherwise standard testing geometries
III	Perform an extensive edge case search
IV	Perform sensitivity analysis of performance metrics such as mission performance, efficiencies, safety, and protocol compliance
V	Populate a cache of known encounters for auto-tuning of collision avoidance algorithm configurations

5.5 Case Study on High-Speed Vessels

The iterative geometric testing framework was applied to a high-speed vessel encountering two vehicles already in a crossing scenario. This case study demonstrated how these techniques would be applied by a developer or an evaluator interested in the effects of the patience parameter of Section 3.6 for a high-speed vessel encountering two slower speed vessels at various initial detection geometries. The testing in this case study was performed as a demonstration of the framework of Section 5.4. Testing was demonstrated under complex, multi-contact, multi-rule encounters within the constraints of protocol-based rules using international COLREGS for power-driven vessels. For statistically significant results, additional testing runs using the methodology of this framework should be performed for each of the configurations.

The case study shows how iterative geometric testing would explore whether the collision avoidance algorithms of normal speed vessels could be more broadly applied to high-speed vessels without more specific tuning of algorithm parameters. More generally, if a designer were to trust his or her algorithms sufficiently to propagate them to vehicles outside the original scope of testing, this framework would enable determination of whether adverse performance would result. If the performance were

indeed degraded or if the designer was conservatively reluctant to blindly extend the work to high-speed vehicles, then determination of an appropriate design envelope or bounds on vehicle specifications could be identified. Any operation outside of these bounds must be done with an assumed risk or deferred until sufficient information became available through additional testing – either simulated or on-water as appropriate.

5.5.1 Experimental Setup

The framework for a design of experiments was developed to test the effects of initial geometry and the patience parameter on the performance metrics of high-speed vessels. A three vehicle experiment was conducted using simulated vehicles: 1 fast, 2 normal (slow). Eight geometries were considered with eleven patience parameter settings each as shown in Figure 5-5. All vehicles within each experiment operated with the same patience parameter setting for the entirety of the experiment.

Three vehicles existed on the course with no other vehicles or navigational constraints present; this scenario simulated an open-ocean interaction of three transiting vehicles with extreme collision risk if no action were taken. Two of the vehicles were given speeds similar to transiting merchants that might be found on the open seas (12 and 17 knots). The third vehicle, a high-speed transiting vessel, was assigned a speed of 35 knots. The two slower craft were positioned such that they would nominally start in a crossing situation (Rules 15, 16, and 17 of COLREGS); however, their initial courses were each chosen using random noise of up to 20 degrees (10 degrees either port or starboard) to create non-canonical initial detection geometries. The high-speed vessel started at headings chosen by the experiment designer encompassing all 360 degrees. With the unique initial headings and vehicle speeds assigned for each experiment, the vessels were positioned at (x, y) coordinates such that without autonomous collision avoidance action, all three vehicles would collide simultaneously at the origin.

Each vessel's primary mission was to achieve the next navigational waypoint. The waypoint's location was a point on the initial track line of each vessel such that

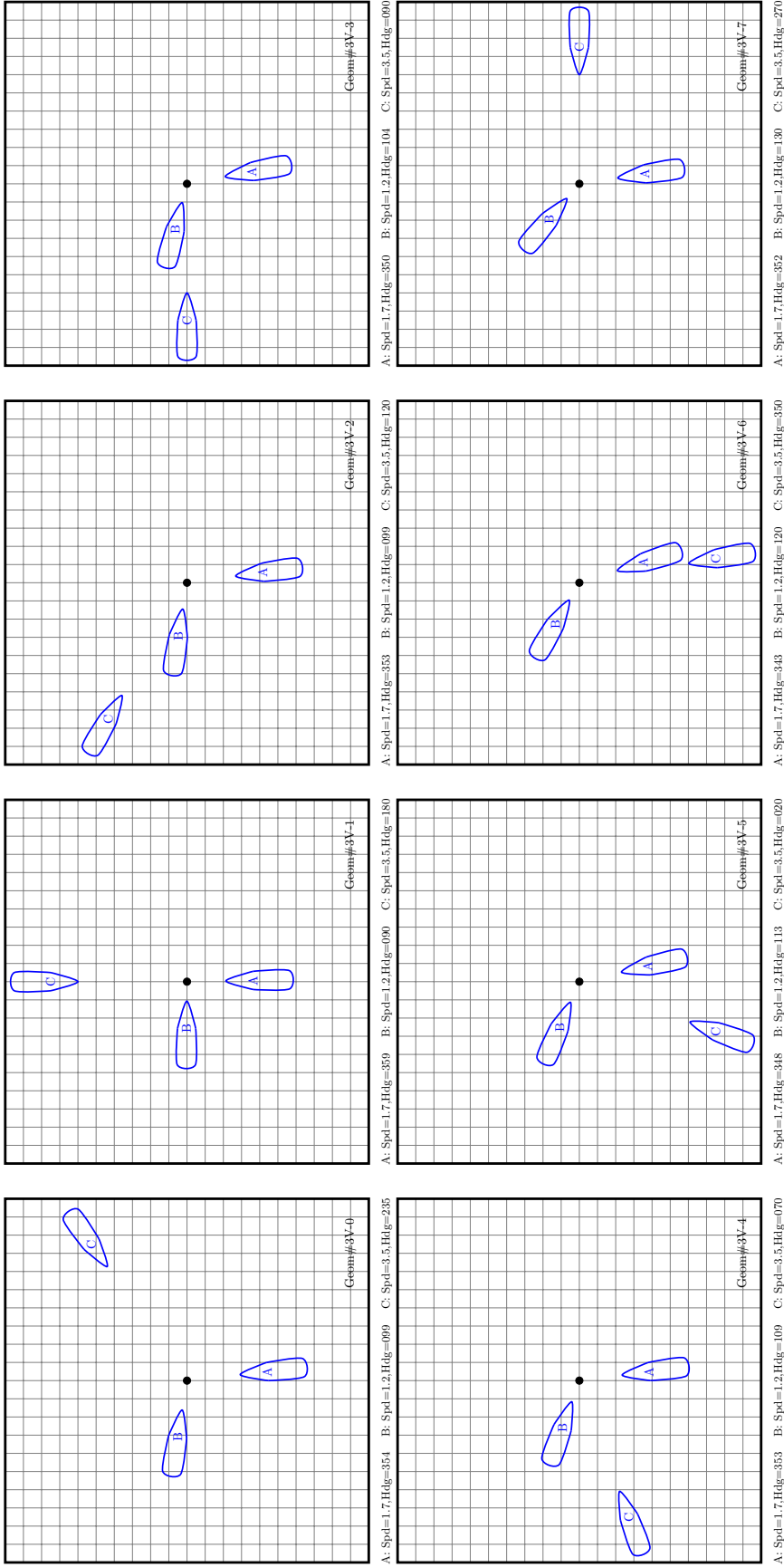


Figure 5-5 The case study of the high-speed autonomous vessel included the 8 geometries shown here. Each geometry was repeated over all 11 experimental patience parameter values for a total of 88 experiments. Each vessel's initial speed and starting position resulted in all three vessels reaching the collision point simultaneously unless action was taken.

Table 5.2 *Iterative Geometry Experimentation Configuration*

$100 \cdot \pi_\theta$	$100 \cdot \pi_v$	π	$\bar{\pi}$	$100 \cdot \bar{\pi}$
1	99	0.01	0.01	1
10	90	0.11	0.05	5
20	80	0.25	0.11	11
30	70	0.43	0.18	18
40	60	0.67	0.25	25
50	50	1.00	0.33	33
60	40	1.50	0.43	43
70	30	2.33	0.54	54
80	20	4.00	0.67	67
90	10	9.00	0.82	82
99	1	99.00	0.98	98

the simultaneous collision point existed at one-third of initial track distance. The experiment was iterated over varying levels of patience parameters with $\pi_\theta = 0.01$ to $\pi_\theta = 0.99$ (11 steps total) as shown in Table 5.2. This forced all three vehicles to be in stressing situations while allowing analysis of the underlying algorithm performance. All other collision avoidance tuning parameters were held constant.

The experimental parameters included initial geometry, initial velocity, protocol rule combinations, and the vessel’s emphasis on prioritizing course over speed (or *vice versa*). By forcing a multi-contact simultaneous encounter with sufficient bearing spread to prevent contact lumping, the autonomous solver was forced to choose velocity vectors that might ultimately conflict with the desires of the mission (here, achieving the next waypoint down track) and other collision avoidance rules required. As an example, a vessel might be in a stand-on situation with one contact and simultaneously be in a give-way situation with another contact.

Robust testing scenarios such as this case study exercise the autonomous collision avoidance algorithms in ways that current literature does not discuss thus allowing a more thorough understanding of full spectrum response. Specific maneuvering characteristics of the vessels were considered and values were chosen to be consistent with open ocean going vessels including turn radius, limiting accelerations, and similar parameters. These maneuvering characteristics were not varied as experimental

parameters, and thus were not examined as part of the post-mission analysis. Future work should consider the influence of individual vessel constraints on collision avoidance algorithm design in conjunction with the parameters studied here.

5.5.2 Example Encounter Analysis

Two such experiments of the same initial detection geometry and nearly identical instantaneous geometries illustrate the variation possible in the decision space. The geometry configuration for this example experiment at a critical decision point for the high-speed vessel is shown in Figure 5-6. A snapshot of the high-speed vessel's objective functions for patience parameters of $\pi_\theta = 0.30$ (left column) and $\pi_\theta = 0.70$ (right column) is shown in Figure 5-7. The combination of collision avoidance objective functions (rows 1-2 of Figure 5-7) and primary mission objective function (row 3) correspond to a collective objective function (row 4) according to priority weights. For this same initial geometric configuration, the snap shot of objective functions taken at nearly identical⁴ points in the experiment gives insight into the high-speed vessel's decision space.

The first row of objective functions represents collision avoidance for the high-speed vessel encountering slow speed vessel *A*. The second row of objective functions represents collision avoidance for the high-speed vessel encountering slow speed vessel *B*. Based on the time that this experiment was frozen, the objective functions are nearly identical for collision avoidance in the two variations of patience parameter.

The third row of objective functions represents the primary mission objective: transiting along track to the next waypoint. Note that the variation in patience parameter values was the most prominent difference in the two experiments and was the primary variable of interest to each iterative geometric test. The $\pi_\theta = 0.30$ (left column) experiment shows high desire to maintain speed at the cost of altering course. Likewise, the $\pi_\theta = 0.70$ (right column) experiment shows a high desire to maintain

⁴The areas of slight variation seen in the angle of excluded (blue) decision space in objective functions for the high-speed vessel encountering slow speed vessel *B* (row 2) were not in regions of peak values (darkest red) for the collective objective function, and are therefore valid for comparison.

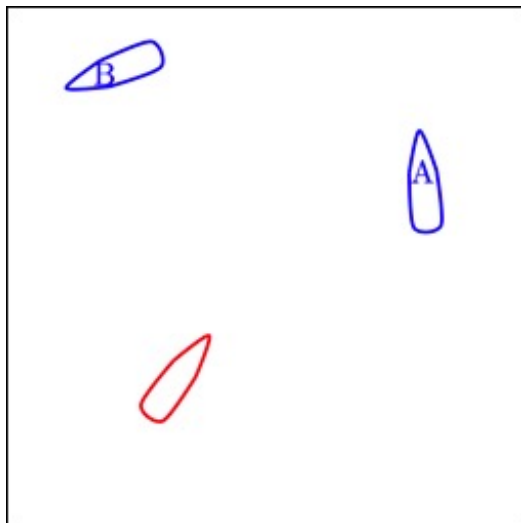


Figure 5-6 Instantaneous relative geometries are shown for comparison of the objective functions of Figure 5-7 (vessel size not to scale). The high-speed vessel is shown in red at a critical decision point of whether to speed around vessel A or slow and allow vessel A to proceed down its track.

course while allowing the vessel to slow as necessary.

The final pair of objective functions represent the collective objective function based on the weighted summation of rows 1-3. This experiment demonstrates the variation of the chosen course-speed pairs as shown by a fuchsia dot on the cumulative objective function polar plot. The $\pi_\theta = 0.30$ vessel chose maximum speed at course $\approx 90^\circ$; the $\pi_\theta = 0.70$ vessel chose near-zero speed while maintaining course. The resulting maneuvers caused significant reduction in temporal efficiency (90% vs. 68%) while maintaining relatively high spatial efficiency (Figure 5-8). Examining this in the context of the overall mean for the same geometry exemplifies the need for tuning based on mission priorities.

Testing within this case study was limited to power driven vessels in sight of each other. Assumptions for vessels operating in degraded sensing environments, non-power driven or special exemption status, and other advanced considerations should be incorporated into similarly challenging testing regimes that incorporate similar metrics for effectiveness.

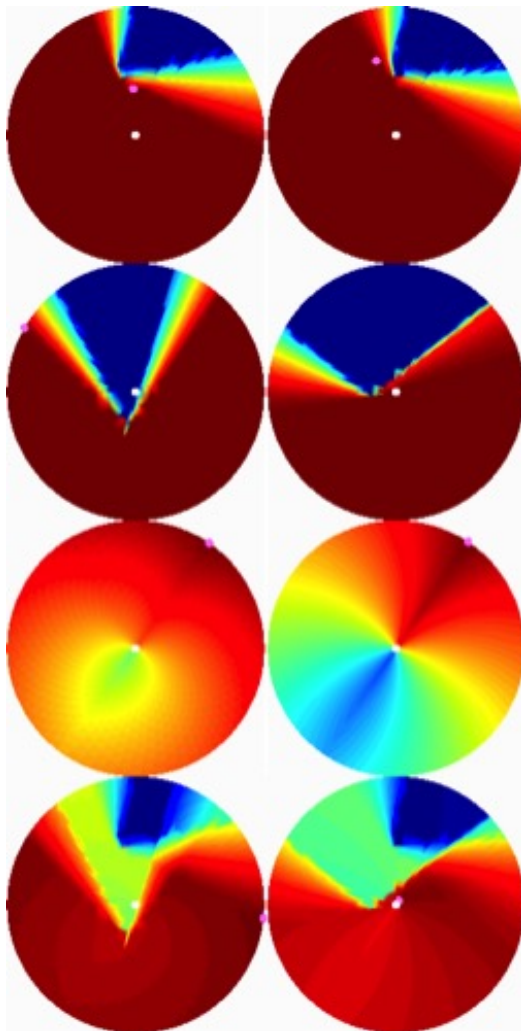
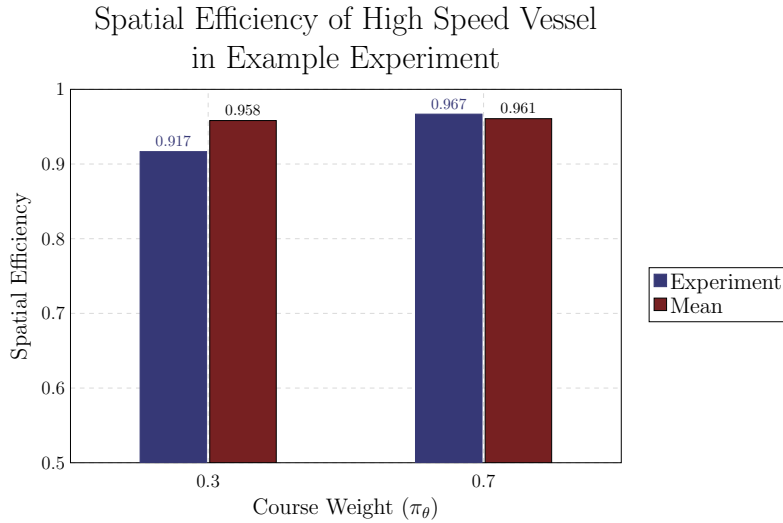


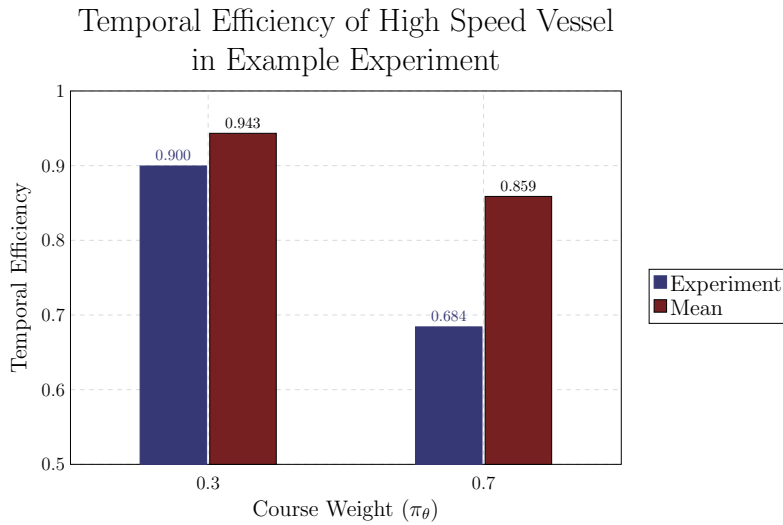
Figure 5-7 The high-speed vessel’s objective functions for patience parameters of $\pi_\theta = 0.30$ (left column) and $\pi_\theta = 0.70$ (right column). These polar objective functions represent the high-speed vessel’s decision space. In this heat map of candidate velocity vectors, red is most desired while blue is least desired. Radius corresponds to desired velocity; maximum speed is represented by the outer edge of each circle. The polar angle corresponds to heading with North being vertical.

5.5.3 Case Study Analysis

The example encounter of Section 5.5.2 demonstrates the need to examine performance characteristics more closely prior to fielding collision avoidance algorithms outside their initially intended scope. Trends for geometries and algorithm configurations (here, patience parameter settings) may be identified from aggregate data and a regression analysis performed [93]. Results are shown for the 8 tested geometries and



(a) Spatial Efficiency



(b) Temporal Efficiency

Figure 5-8 The efficiencies varied for the high-speed vessel depending on the patience parameter chosen. The spatial and temporal efficiencies for the experiment of Figures 5-6 and 5-7 demonstrates that a significant fluctuation in efficiencies is possible when changing the patience parameter. Careful study of the affects of configuration settings on performance parameters are necessary extending a known configuration to a new type of vessel. Here the experiment performance values are shown in blue. The mean performance over all geometries for the same value of patience parameter is shown in blue.

11 patience parameter combinations of this framework demonstration for all three vessels using the methods of Section 5 in Figure 5-9.

An aggregate examination of performance data shows several interesting trends worth closer examination and further experimentation from this example case study framework:

- protocol scores range from 0% - 100% necessitating edge case searches and examination for any underlying variable
- safety scores remained high with respect to protocol compliance with the exception of a notable dip for some protocol scores approximately between scores of 45 and 80 necessitating edge case searches and examination for any underlying variable
- temporal efficiency varied more for the high-speed vessel than it did for the slow speed vessels
- spatial and temporal efficiencies deviate from an otherwise linear mapping for some high-speed tracks warranting examination for any underlying variable

5.5.4 Limiting Range and Safety Analysis

In scenarios where multiple contacts are present, statistics of all vehicles encountered may obscure the most important collision avoidance information. For example, in a scenario where two contacts are simultaneously avoided, the mean range may seem reasonable; however the closer of the two r_{cpa} values might give more meaningful insight to algorithm performance. For this reason, examination of the limiting (i.e., minimum over all contacts) range of CPA in a simultaneous encounter should be examined. While this aggregate data seems to show reasonably consistent results, the safety scores examined as a function of the minimum r_{cpa} of each encounter (Figure 5-10) may demonstrate an underlying variable (here, either geometry or patience setting).

Within this section, a linear mapping of the minimum r_{cpa} of each encounter to S allows for ease of discussion of either safety score or range at CPA though the concepts would hold for a more complicated safety scoring such as that in Section 4.4.

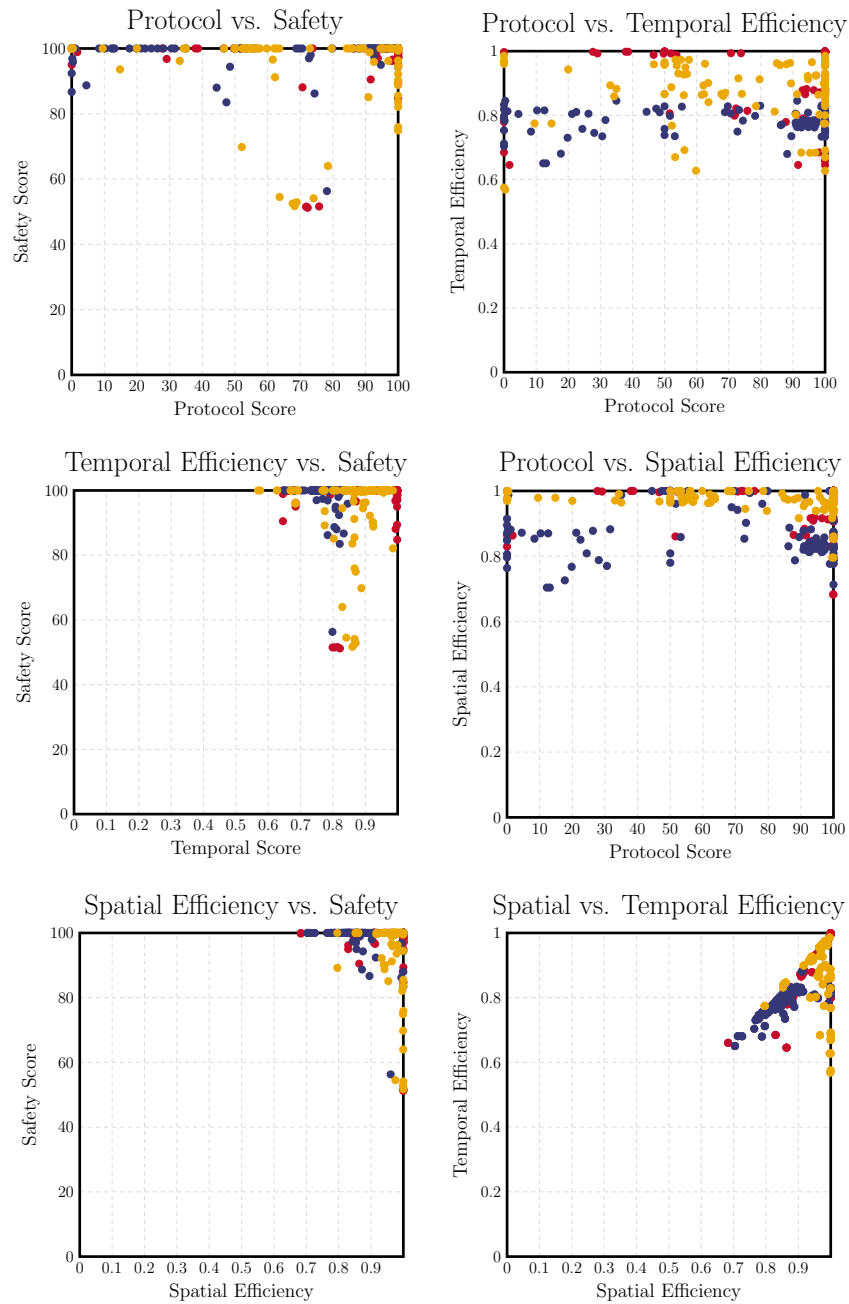


Figure 5-9 The high-speed vehicle performance was compared across the four performance metrics of spatial efficiency, temporal efficiency, safety, and protocol compliance. By evaluating performance using different metrics, trades can be made based on metrics that are given preference. Note the wide variation of protocol compliance. The high-speed vessel is shown in yellow while slow speed vessels *A* and *B* are shown in red and blue, respectively.

The value of S therefore is convenient to map as $S = \min(r_{cpa})$ of each multi-contact encounter to $[0, 100]$ as a percentage of preferred range at CPA (R_{pref}) for the purposes of discussion of the case study. This minimum of all safety scores in each configuration may demonstrate wide variation of performance in some configurations and across some geometries. A need to further study collision avoidance tuning in specific scenarios before attempting to propagate standard settings to other vehicle types such as a high-speed vessel could therefore be warranted.

For a study of aggregate data, there is insight to be gained from examining the overall limiting range from all vehicles in a multi-contact encounter. Statistics on this minimum encounter range (and by extension, safety score S) of all vehicles in a single encounter may be examined by fixing several parameters. The two parameters most easily fixed in this example case study are initial geometry configuration \mathcal{G} and patience parameter π . The geometry that results in the minimum r_{cpa} for a given patience parameter is given by Equation (5.2) while the patience parameter that results in the minimum r_{cpa} for a given geometry configuration is given by Equation (5.3).

Equation (5.4) defines the minimum contact range over all encounter geometries for a given patience parameter as $r_{min}^{\mathcal{G}|\pi}$. Equations (5.5)-(5.6) define the mean $\overline{r_{min}^{\mathcal{G}|\pi}}$ and standard deviation $\sigma(r_{min}^{\mathcal{G}|\pi})$, respectively. Equation (5.7) defines the minimum contact range over all patience parameters for a given geometry configuration as $r_{min}^{\pi|\mathcal{G}}$. Equations (5.8)-(5.9) show the mean $\overline{r_{min}^{\pi|\mathcal{G}}}$ and standard deviation $\sigma(r_{min}^{\pi|\mathcal{G}})$.

Examination of aggregate statistics allows analysis of overall performance. The standard deviation may reveal wide variation within each parameter further justifying the need to actively explore any underlying variable. If sufficient data existed once fielded, use of these aggregate performance statistic for the variables of the design of experiment might allow selection of configuration parameters if real-time tuning were not possible. In the case of this example case study, a patience parameter could be selected to an appropriate aggregate performance standard.

If a vehicle had sufficient data and capability to identify its initial detection geometries in real-time, an active configuration tuning scheme could be used. If sufficient and significant data were available in this example case study, a vehicle that values

only safety might recognize its initial detection geometry and select the range of patience parameter values that maintain a safety score above a desired threshold value. For example, a vehicle desiring to maintain safety above 85 and determining itself to be in Geometry 0 might use cached performance data such as Figure 5-10 to choose a course weight between 50 and 70. The mission objective function would therefore be tuned in real-time with a preference toward maximizing safety when deviations for collision avoidance were necessary. While this case study examined variations of geometries and patience parameters, additional testing would be necessary before having sufficiently and significantly populated data to make a tuning decision such as this.

$$\mathcal{G}_{min}^{r_{cpa}|\pi} = \underset{\mathcal{G}|\pi}{\operatorname{argmin}} \{r_{cpa}\} \quad (5.2)$$

$$\pi_{min}^{r_{cpa}|\mathcal{G}} = \underset{\pi|\mathcal{G}}{\operatorname{argmin}} \{r_{cpa}\} \quad (5.3)$$

$$r_{min}^{\mathcal{G}|\pi} = \min_{\mathcal{G}|\pi} \{r_{cpa}\} \quad (5.4)$$

$$\overline{r_{min}^{\mathcal{G}|\pi}} = \operatorname{mean}(r_{min}^{\mathcal{G}|\pi}) \quad (5.5)$$

$$\sigma(r_{min}^{\mathcal{G}|\pi}) = \operatorname{std}(r_{min}^{\mathcal{G}|\pi}) \quad (5.6)$$

$$r_{min}^{\pi|\mathcal{G}} = \min_{\pi|\mathcal{G}} \{r_{cpa}\} \quad (5.7)$$

$$\overline{r_{min}^{\pi|\mathcal{G}}} = \operatorname{mean}(r_{min}^{\pi|\mathcal{G}}) \quad (5.8)$$

$$\sigma(r_{min}^{\pi|\mathcal{G}}) = \operatorname{std}(r_{min}^{\pi|\mathcal{G}}) \quad (5.9)$$

Minimum High Speed Vessel Safety Score
of Each Geometry for Given Patience Values

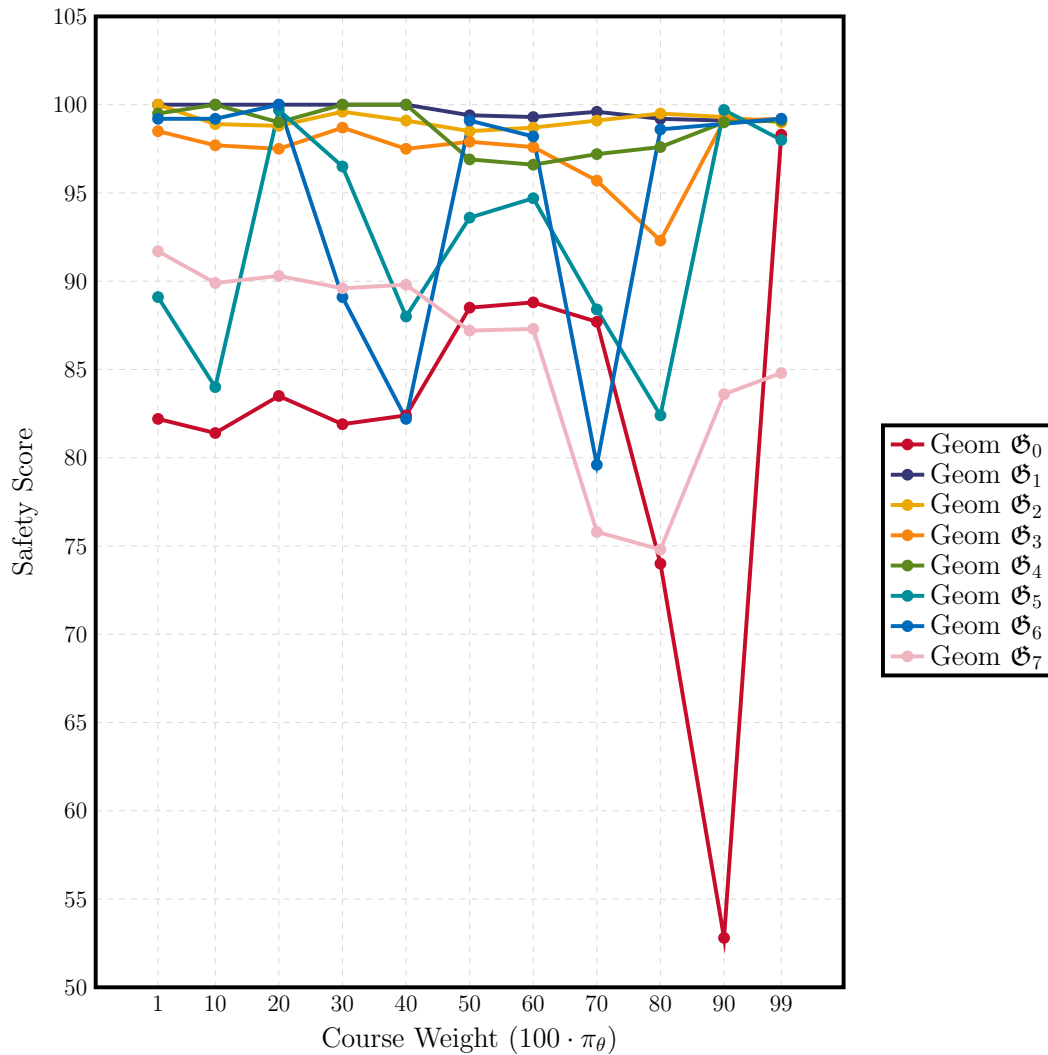


Figure 5-10 The minimum safety score of each encounter allowed the limiting case in a multi-contact collision avoidance scenario to be identified. Statistics based on this data give insight to performance for either fixed geometry or fixed patience parameter. Course weights shown on the horizontal axis represent $100 \cdot \pi_\theta$. For a well-populated and statistically significant data set, an analysis using a method such as this chart could give insight into tuning preferences to maximize performance metrics (safety, efficiency, protocol compliance, etc.). This example data indicate that most geometry and patience combinations yield a minimum safety greater than 80; additional testing in areas below 80 may provide interesting edge cases for particular combinations of geometry and patience values. Additional testing would be necessary to draw conclusions worthy of tuning. If an initial contact geometry could be determined and the data populating a chart such as this were sufficient and significant, tuning of experimental variables would be possible to operate according to a designer's policy.

5.6 Integrating Autonomous Systems with Humans

Clare *et al.* examined human-robot trust by priming operators and measuring system performance in a decentralized network of heterogeneous unmanned vehicles [15]. Several aspects of Clare’s work reinforces the need to establish, sustain, and monitor human trust in autonomous systems using metrics and techniques of this thesis. Extensive use of human-understandable metrics such as those in Chapter 4 and the systematically thorough techniques of this chapter further build trust with evaluators and ultimately the human operator who would interact with the autonomous vehicles.

Clare found that participants with significant (as self-reported) experience playing computer and video games over trusted the automation of their experiment. Previous work had found that operators that had an appreciably low amount of trust in the system spent excessive amounts of time in either replanning or adjusting the mission when working under a Rules of Engagement protocol scenario, especially when final plans did not seem “logical” [16]. These two concepts reinforce the need for measurable and unbiased means to quantify performance in human-understandable ways. Trusting an operator who might in fact over trust his or her algorithms could lead to disaster. Similarly, an under trusting evaluator might spend unnecessary time and money to attempt to test all possible scenarios if there is no quantifiable means to establish a baseline passing performance.

The concept of human trust inertia [35] may be extended to the field of autonomous collision avoidance. Having just one accident using autonomous collision avoidance algorithms could likely set back society’s trust in not only specific algorithms but autonomous collision avoidance more generally. Great cost and time would be required to simply regain lost trust. Rigorous and methodical testing regimes are therefore prudent to more fully understand not only the capabilities but perhaps more importantly the limitations of collision avoidance algorithm performance.

In situations where robot-robot interactions are expected, human concerns remain abundant. Human crew members may be onboard to perform maintenance or cargo-tending roles while the vessel is autonomously underway. Cargo or mission may be

of high value causing excessive shoreside human involvement or increased insurance costs if trust cannot be raised to an acceptable level. Groundings, allisions, and collisions would likely result in significant environmental damage raising the likelihood of government restrictions and requirements until a sufficient and consistent level of trust existed.

Establishing a rigorous, consistent, deliberate, and transparent testing and evaluation scheme allows designers and society alike to know and agree to the standards to which autonomous collision avoidance algorithms must be held. These standards also therefore define the limitations of trust and performance of these systems. Section 5.5 demonstrated the dangers possible in assuming a high-speed vessel using sufficient computational power could simply default to similar collision avoidance configuration parameters of slower vessels operating under the exact same protocol algorithms. Similar cases could be found where innocent extensions of otherwise working collision avoidance algorithms may prove disastrous if not subjected to a methodical testing regime.

5.7 Conclusions

In summary, this chapter presented methods to use the tools of Chapters 3 and 4 to test and evaluate large scale performance characteristics by:

- developing methods to understand trades between mission performance, safety, and protocol compliance
- introducing algorithms to perform edge case searches using a systematic framework that incorporates non-canonical encounter geometries
- introducing the concept of egregiousness to prioritize edge cases for evaluator or designer consideration
- enabling a design of experiments to use multi-contact initial detection geometry (*viz* range, pose, and speed) as a testing parameter

An example case study of using the iterative geometric testing framework was presented for a high-speed vessel encountering two slower speed vessels in simulation. Methods to reason about a fully populated data set were introduced to determine underlying variables affecting collision avoidance performance. A limiting range safety analysis was developed for multi-contact encounters. A method to autonomously self-tune collision avoidance configuration settings in real-time to achieve a desired level of performance metric(s) was proposed.

Using the techniques of this chapter, an evaluator or designer would be empowered to view and reason about performance characteristics in the context of the vehicle's mission, have large simulation data sets to discover edge cases, determine the effects of initial detection geometry through simulation testing, set preliminary configuration values to maximize desired performance characteristics, and identify a prioritized list of edge cases for algorithm improvement. After sufficient iteration using the methods of this chapter to improve collision avoidance performance to an acceptable level, on-water testing is prudent to certifying algorithms before fielding in a non-testing environment. Chapter 6 demonstrates scenarios, techniques, and results of on-water experimentation for testing collision avoidance algorithms.

THIS PAGE INTENTIONALLY LEFT BLANK

Chapter 6

On-Water Experimentation and Results

Chapter 6 presents the scenarios, techniques, and results of on-water experimentation using the algorithms and methods of Chapters 3, 4, and 5. Section 6.1 presents the scenarios for experimentation. Section 6.2 describes the vehicles, laboratory setup, and testing environment used in conjunction with these on-water experiments. Section 6.3 presents the results from each scenario.

6.1 Extended Scenarios and Evaluation Techniques

Testing was performed such that all vehicles on the course operated under identical vehicle software configurations including collision avoidance algorithms and parameters at any one time. Results were then aggregated for each algorithm for comparison. All autonomy computations including collision avoidance were performed on a payload computer that was connected to the vehicle's front seat control computer via on-board ports. On-board payload computer specifications included a 900MHz quad-core ARM Cortex-A7 CPU, 1GB RAM, 1200mA load at 5VDC, 85.60mm x 56mm x 21mm space requirement, mass \approx 45g, and cost \approx \$35USD. Each payload computer was interchangeable to the other vehicles.

Five autonomous marine vehicle encounter scenarios were constructed. One to

three emulated vehicles completed the five vehicle field in times of maintenance and were running the same mission parameters as the fielded autonomous marine vehicles. Fielding emulated vehicles allowed for long duration testing by performing routine maintenance such as battery changes without stopping the experiments. Vehicles consisted of those described in Section 6.2. All vehicles assumed perfect contact sensing within their limited range of awareness; detection range was limited to approximately $2 \cdot R_{pref}$ which represents a reasonable approximation for visual detection range of a human-operated vessel relative to its conservatively desired range at CPA.

Maneuvers for collision avoidance were constrained by the protocol requirements of open-water international rules for power-driven vessels (COLREGS Rules 1-8, 11, 13-18). Scope of protocol evaluation was therefore limited to power-driven vessels acting under Category V of Table 4.1. Safety was evaluated using the cost function shown in Figure 4-5. That is, $\Delta S^{R_{nm}} = 30\%$, $\Delta S^{R_{min}} = 60\%$, $R_{min} = 0.5 \cdot R_{pref}$, $R_{nm} = \frac{5}{16} \cdot R_{pref}$, and $R_{col} = \frac{3}{16} \cdot R_{pref}$. Encounter scenarios are listed in Table 6.1 and focused on non-canonical geometries using the nominal tracks of Figure 6-1 and 6-2 unless otherwise specified. Perturbations off track occurred as necessary for collision avoidance. Multi-encounter scenarios with 4-5 autonomous vehicles simultaneously interacting were common.

Table 6.1 *Scenarios for On-Water Experimentation*

Scenario	Description of 5-Vessel Encounter Scenario
A	Open ocean star pattern using CPA-based algorithm
B	Open ocean star pattern using velocity obstacle-based algorithm
C	Traffic-constrained monitoring of underwater entity
D	Open ocean star pattern with human-driver encounters
E	Open ocean star pattern with one vehicle ignoring COLREGS
F	Open ocean star pattern with one vehicle dead-in-water
G	Open ocean star pattern with one vehicle ignoring all contacts
H	Navigationally-constrained using quadratic priority weight
I	Navigationally-constrained using linear priority weight
J	Navigationally-constrained using power function priority weight

6.1.1 Algorithm Comparison (Scenarios A & B)

On-water experimentation with protocol evaluation allows for comparison of different collision avoidance algorithms, certification of compliance, and tuning of designs. In Scenarios A and B, two COLREGS-based collision avoidance algorithms were tested. Scenario A represented a CPA-based method derived from work in [5] (see Chapter 3) and known as the full CPA quantification algorithm. Scenario B represented the popular velocity obstacle method modeled from [45]. Both scenarios used the same underlying COLREGS algorithms while the means of determining risk (CPA or velocity obstacles) was varied. All vehicles in Scenarios A and B used the same algorithm and configuration parameters at any one time. The course consisted of the five-vehicle simultaneous-collision star pattern shown in Figure 6-1 and 6-2.

A multi-contact collision avoidance scenario was constructed to deliberately stress the vehicles beyond the current literature standard. Five vehicles were placed on near-simultaneous collision paths involving combinations of multiple concurrent COLREGS rules: head-on, overtaking, and crossing. The primary mission objective for each vehicle was a simple waypoint traversal along a straight track while maintaining a minimum desired range at CPA without violation of the COLREGS. Upon reaching a desired waypoint outside the collision avoidance area, each vessel reversed course to follow its track to the previous waypoint. The tracks were constructed such that non-canonical geometries were represented in nominal track design; deviations of initial course and therefore encounter angles were realized from granting an allowance to achieving each waypoint.

Two complex collision avoidance experiments were developed using a starburst-type geometry of five vehicles. Scenario A used five vehicles traversing five nominal tracks at similar speeds as shown in Figure 6-1. Scenario B allowed five vehicles to traverse three tracks. Two vehicles were simultaneously assigned to each of two tracks and one vehicle assigned its own track as shown in Figure 6-2. One vehicle of each shared track in Scenario B was given a higher speed to induce overtaking as well as shorter times to CPA for cross-track contacts. Each scenario showed complicated

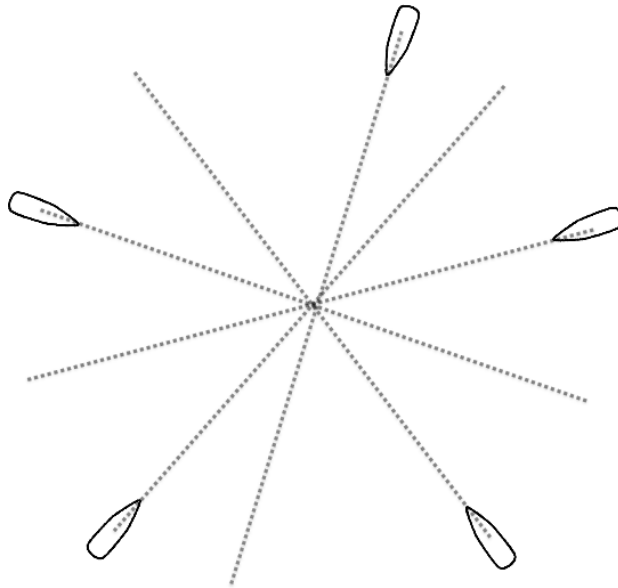


Figure 6-1 A 5-vehicle 5-track starburst pattern was used for on-water Monte Carlo testing with each vehicle on its own nominal track. Small perturbations in initial course allowed for non-canonical geometries of simultaneous encounter at the origin under multiple simultaneous COLREGS rules.

characteristics in its own right: five simultaneous collision tracks of different headings is indicative of a congested waterway, while five simultaneous collision tracks of three nominal headings is indicative of a vessel encountering two crossing merchant lanes. Results are presented in Section 6.3.2.

On-water Monte Carlo experimentation tested complicated collision avoidance geometries for both a traditional velocity obstacle algorithm and a full CPA quantification algorithm. The traditional velocity obstacle was modeled such that certain characteristics were consistent with recent marine autonomy literature and allowed a fair comparison to the methods of this thesis, including:

- This thesis assumes perfect sensing thus removing the need to model safety margin offsets such as the one found in [45]. Fair comparison of a traditional velocity obstacle method can then be made once accounting for a designer's costing function.

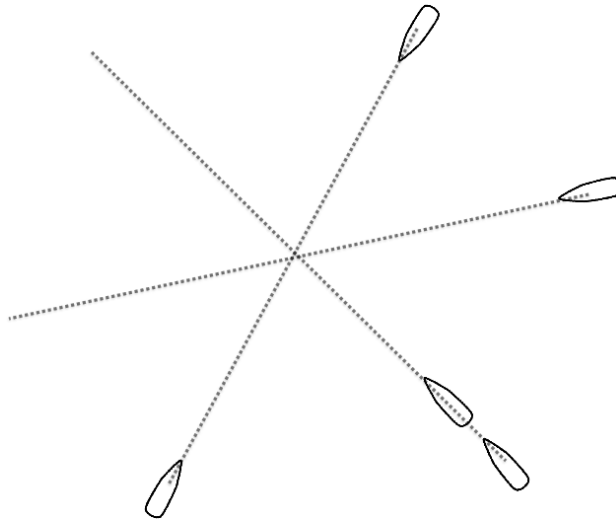


Figure 6-2 A 5-vehicle 3-track starburst pattern allowed for complicated interactions. Each of 2 vehicle pairs shared 2 tracks and 1 vehicle had its own track. On-water Monte Carlo testing allowed for non-canonical geometries of simultaneous encounter at the origin under multiple simultaneous COLREGS rules. The shared tracks each had a fast and normal speed vessel.

- Both collision avoidance algorithms used the same underlying COLREGS algorithms. Performance was therefore a function of the collision avoidance algorithm performance and not specific implementation of the rules of the road.
- Costing of admissible solutions that involve time to collision was accounted for using a priority weight w_i^{avd} based on current contact range on the collision course assuming a constant current speed. Distant times to collision are sometimes used as a cost penalty for velocity obstacle candidate solutions. This thesis modeled priority weight of a traditional velocity obstacle as a quadratic function of current range to the contact. This gives increasing priority to contacts as they become closer to ownship and is consistent with a common literature cost function of inverse time to collision.
- Deviation from the mission-preferred velocity vector received appropriate penalty by adding the two-plateau velocity obstacle model with the mission objective function. The mission objective function rewarded behavior that was consistent with its desired velocity vector.

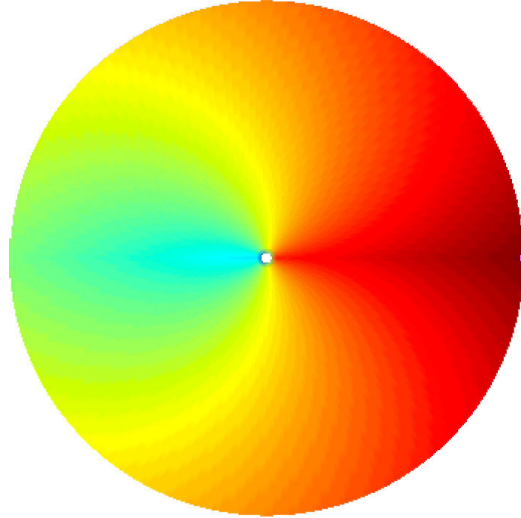


Figure 6-3 This polar objective function with radius = speed (v), angle = course (θ , North-up) depicts a nominal waypoint behavior that favors the best course and speed to achieve its desired waypoint (pink dot at maximum speed and $\theta = 90^\circ$). The color gradient from the optimal point indicates a costing function that increasingly penalizes velocities that deviate from the optimum waypoint solution.

A two-plateau method was used to map a velocity obstacle to an objective function consistent with Figure 3-9. A plateau of full utility value accounts for acceptable solutions while a plateau of zero utility value accounts for inadmissible solutions. Addition of the mission objective function and the velocity obstacle plateau regions according to Equations (3.2) and (3.23) accounts for a velocity obstacle designer's cost function that penalizes deviation from mission preference. An example mission objective function that imposes a cost for deviations from mission-desired course and speed is shown in Figure 6-3.

6.1.2 Traffic-Constrained Monitoring Missions (Scenario C)

To evaluate protocol compliance of more complex (non-waypoint following) missions, a simulated unmanned underwater vehicle (UUV) was monitored by one of the autonomous surface vessels with traffic in near-parallel tracks to emulate a merchant transit lane (Scenario C). The monitoring vessel was subject to any collision avoidance restrictions required of it due to surrounding surface vessel traffic. The simulated underwater vehicle was traversing in the vicinity of the transit lane in such a way that

required the monitoring vessel to choose between COLREGS compliance and losing desired position with respect to the UUV. Figure 6-4 shows the experimental geometry and on-water data of the traffic-constrained monitoring scenario.

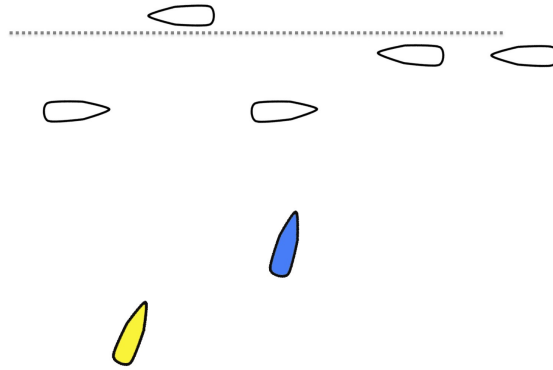
The autonomous vessel in a dynamic mission such Scenario C must be able to determine when breaking contact is necessary to honor collision avoidance protocol requirements and maintain safe encounters with other vessels in the area. Using the evaluation concepts of this thesis, autonomous designers can explore the tradespace of mission goals, safety, and protocol compliance as configuration parameters are changed (perhaps in real time) given the many variables of importance to each component.

6.1.3 Testing Human Integration (Scenario D)

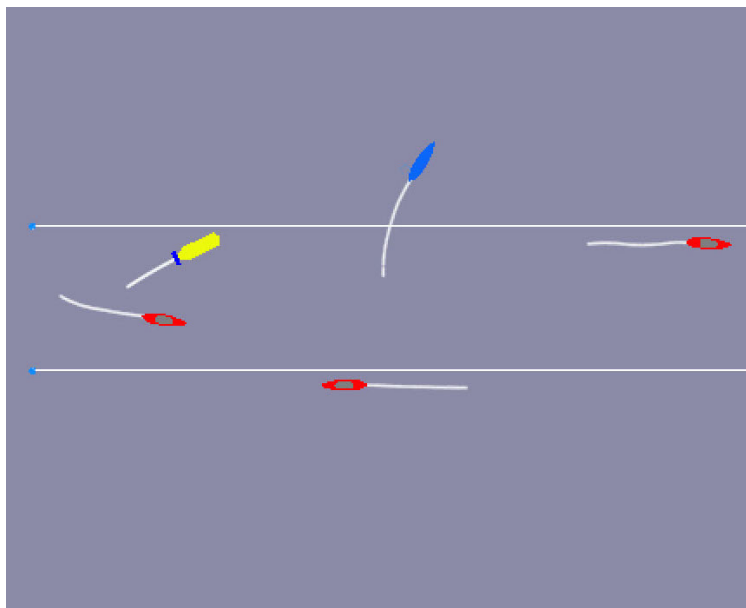
Using the open-water experimental setup of Figure 6-5, additional perturbations were inserted using a human-operated high-speed motorized kayak (Scenario D). Adding a human-operated vessel to the experiments increased the complexity of the testing and allowed for more fine-tuned experimental encounters. Human experimentation was focused on stressing the full CPA quantification algorithm with close encounters and unexpected deviations by the human operator.

The stresses that autonomous vessels faced as a result of the human operator included the human:

- maneuvering without regard of the autonomous vessels
- maneuvering for the autonomous vessels in violation of the collision avoidance rules
- approaching the autonomous vessel at unsafe speeds for the contact geometry or contact density
- approaching the autonomous vessel at unacceptably close ranges after a compliant maneuver (curious observer)



(a) Traffic-constrained monitoring experimental geometry



(b) Traffic-constrained monitoring on-water testing

Figure 6-4 The nominal on-water testing geometry of (a) allowed up to 4 autonomous vessels and several simulated surface vessels of varying speeds the ability to interact in successive, non-deterministic, non-canonical encounter geometries taking the form of an open ocean merchant lane. Maneuvers for other vessels caused deviation from both nominal track and encounter geometry of subsequent contacts. A simulated UUV (yellow) was being monitored by an M200 autonomous vessel (blue). On-water experiments (b) provided perturbations to stress the underlying collision avoidance algorithms outside of their normal testing scenarios. The monitoring vessel was required to autonomously determine when a maneuver for safety and protocol compliance was necessary while maximizing contact. Using the evaluation tools, an autonomous designer can determine what mission configuration parameters are appropriate given the importance of the mission, the nature of the surrounding contacts, and the degree of conservativeness desired with respect to rule and safety scores.

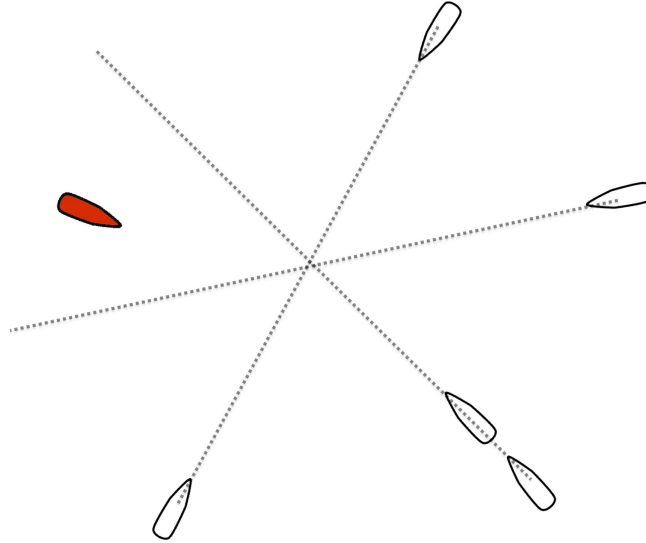


Figure 6-5 This nominal on-water testing geometry allowed up to 5 autonomous vessels of varying speeds the ability to interact in successive, non-deterministic, non-canonical encounter geometries. The human-operated high-speed motorized kayak (shown in red) operated without track restrictions which allowed for further perturbation during the on-water Monte Carlo experimentation of Scenario D. The human also inserted non-compliant behavior to further stress the autonomous vessels.

6.1.4 Non-Compliant and Unresponsive Vehicles (Scenarios E - G)

One of the five vessels was given one of three non-compliant behaviors. The other four vehicles were responsible for appropriately maintaining COLREGS compliance and completing their mission without *a priori* knowledge of the vehicle being non-compliant. Scenario E demonstrated one vehicle operating without knowledge of COLREGS. Scenario E's non-compliant vehicle maneuvered to maintain the same desired CPA values as the COLREGS-cognizant vessel, however, without a protocol bias for maneuvering in a particular way. Scenario F demonstrated one vehicle drifting dead in the water (not under command) without properly identifying itself as such. Scenario G demonstrated a vehicle driving with complete disregard of other vehicles. This vessel was willing to accept collisions to achieve its mission without compromise. Scenarios E, F, and G used the star pattern geometry of Figure 6-1.

6.1.5 Navigationally-Constrained Environment (Scenarios H - J)

A pattern with closer tracks and smaller allowable ranges than the open ocean scenario was constructed with navigational barriers along two sides to simulate a navigationally constrained environment. Figure 6-6 shows the notional geometry for the navigationally constrained environment test. Experimentation involved the same fleet of autonomous vessels using the full CPA quantification algorithm. Priority weight was varied from the default quadratic function (Scenario H) using linear (Scenario I) and power (Scenario J) functions. Scenario J used an exponent of 1.5 for the priority weight power function. All priority weight functions reasoned about instantaneous range to the contact in question. CPA range values used for calculating risk were reduced by 37.5% of the open ocean scenario to allow the vehicles to accept closer ranges given the increased constraints on their operating environment.

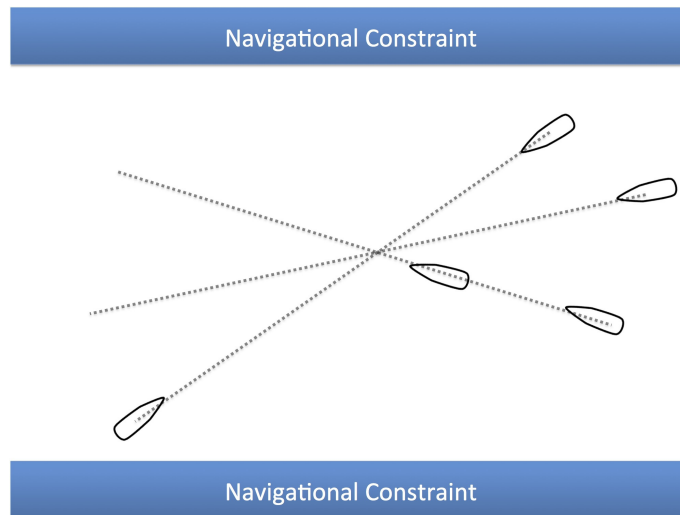


Figure 6-6 The nominal on-water testing geometry of the navigationally constrained encounters placed up to five autonomous vessels in close proximity with each other and bounded two sides with navigational constraints. The collision avoidance parameters were tightened to allow closer encounters.

6.2 On-Water Experimentation Setup

On-water testing was completed at the MIT Marine Autonomy Lab located on the Charles River in Cambridge, MA, USA. Vehicle communication was possible using a Bullet wifi antenna broadcasting across the river. A shoreside computer continuously operated to provide situational awareness and emergency control of vehicles to the laboratory personnel. Vehicles were unable to directly communicate with each other. To emulate an environment consistent with open ocean navigation, course-speed-heading tuples of each contact within visual detection range were given to the vehicles.

6.2.1 Vehicles

Three types of vessels were used directly in testing:

1. Clearpath[®] M100 trimaran autonomous vessels with propeller propulsion
2. Clearpath[®] M200 catamaran autonomous vessels with water jet propulsion
3. Mokai[®] human-driven gas-powered kayak

Support vessels were used for safety of other river traffic and performing routine maintenance such as battery changes. These support vessels were not detectable to the autonomous vessels which enabled long duration on-water testing without interference by lab staff during operations such as battery changes. The human-driven kayak served three functions: inducing human interaction with the autonomous vessels, acting as a high-speed contact in the testing environment, and allowing a highly maneuverable platform to cause otherwise undesirable encounter scenarios for edge case and robustness testing. Figure 6-7a shows the vessels used in on-water testing stored in the shoreside lab. Figures 6-7b and 6-7c show the vehicles that were used in on-water experimentation.

6.2.2 Experimentation Field

To establish a safe area clear of other vessels, a buoy field (Figure 6-8) was deployed during close encounter testing and congested harbor scenarios (Section 6.1.5). To



(a) Vehicles in Shoreside Lab



(b) Vehicles on Dock



(c) M200 Autonomous Catamarans

Figure 6-7 Testing was performed using the autonomous vessels displayed here. High-speed and human interactions were achieved using the motorized human-operated kayak by Mokai.

give larger maneuvering freedom to the vessels, an experimentation field was used as shown in Figure 6-9. To maximize the use of the field and avoid interactions with vessels outside the scope of the experiments, testing was performed between sunset and sunrise. Running lights and safety lights on the autonomous vessels were more readily visible than most common river traffic allowing for verification of vessel locations. Operating status queues such as battery levels and hardware malfunctions were visible by light signals as well as messages sent to the shoreside station. A closer view of vehicle testing within the buoy field is shown in Figure 6-10.

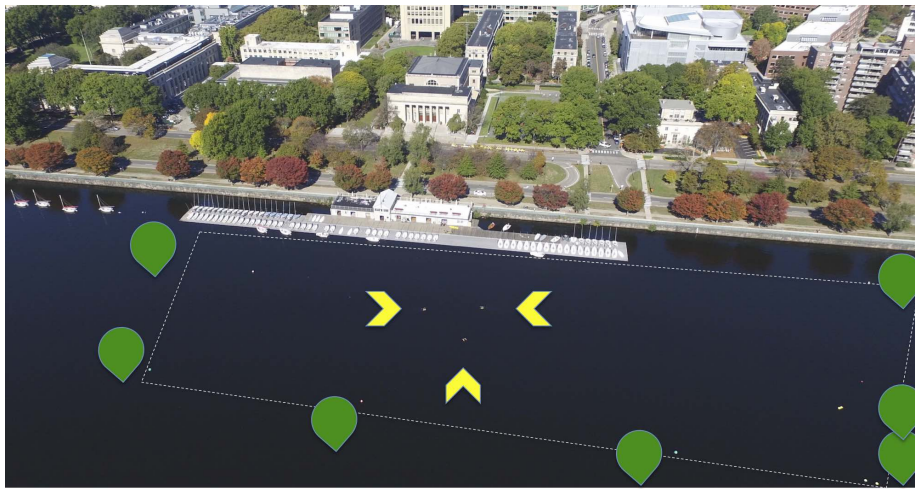


Figure 6-8 The daytime testing range was marked with a buoy field and allowed for constrained vehicle testing.

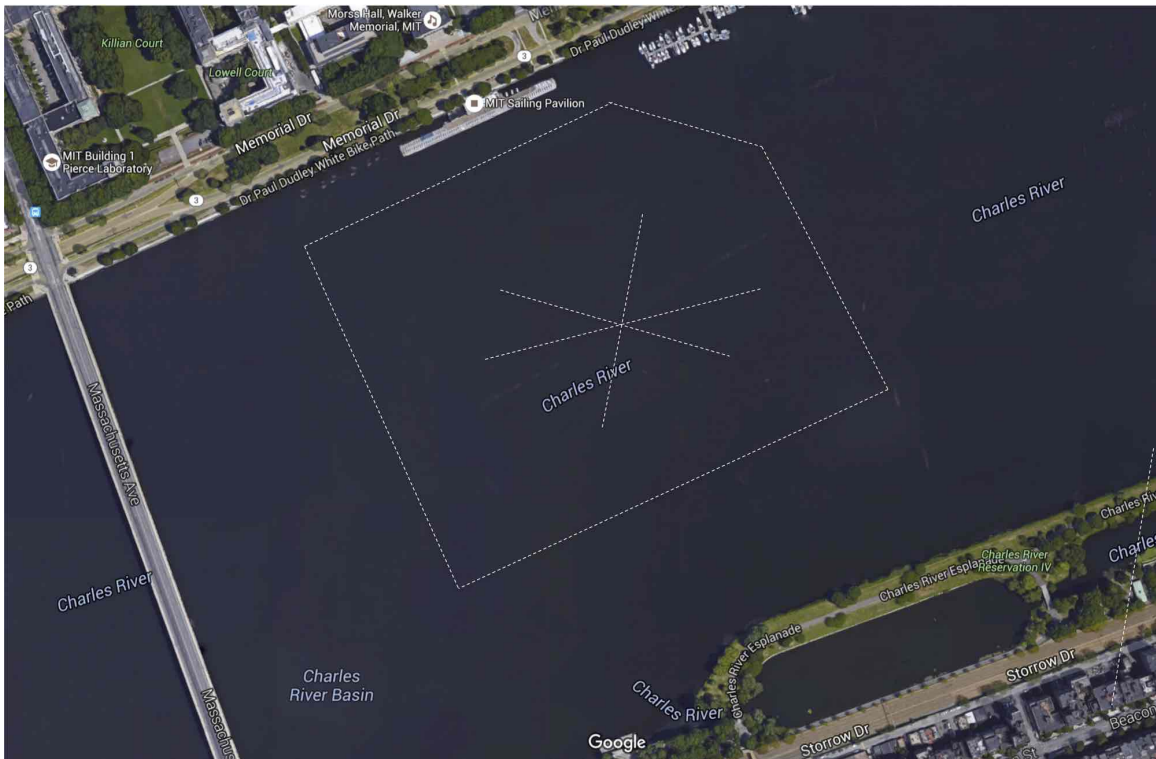


Figure 6-9 Night testing was the primary setup and allowed for extensive use of large scale experiments. The three track pattern of Figure 6-2 is shown with the safety region surrounding the testing area.



Figure 6-10 Vehicles were allowed to operate in close proximity to each other during Scenarios H-J as shown here. Prioritization of when to make collision avoidance decisions relative to the time of contact detection greatly influenced safety and protocol compliance results.

6.3 On-Water Experimentation Results

On-water experimentation using the 10 scenarios of Table 6.1 accounted for over 6,150 vehicle-pair encounters as shown in Table 6.2. Sixty-five experimental sessions totalling over 272 vehicle-hours provided the on-water experimental data presented in this chapter as shown in Table 6.3. The 65 experimental sessions totalled 6488 encounters, however 332 of these were isolated one-on-one human-robot testing that did not count toward the aggregate experiments shown in Table 6.2. Multi-rule combinations are denoted using their two-number identifier (e.g., R15/16 denotes crossing give-way). Encounters labeled “CPA-only” indicate vehicle pairs that were within detection distance but did not warrant entry into a particular rule at any time during the interaction. Tables 6.4 - 6.10 demonstrate performance of the algorithms of Sections 2.5 and 3.3. Aggregated results are shown in Tables 6.11 - 6.14 and discussed in Section 6.3.2. Scenario B uses the velocity obstacle collision avoidance algorithm. All other scenarios of Table 6.1 use the full CPA quantification algorithm of Section 3.3.

Table 6.2 *Number of On-Water Encounters Observed per Scenario*

Scenario	Rule Set					
	R13/16	R13/17	R14	R15/16	R15/17	CPA-only
A	224	224	232	997	997	318
B	255	255	264	1016	1016	276
C	76	76	140	211	211	222
D	102	102	96	297	297	170
E	37	37	22	123	123	48
F	9	9	10	17	17	8
G	52	52	48	142	142	58
H	158	158	206	791	791	170
I	41	41	68	239	239	54
J	28	28	32	104	104	32

Table 6.3 *Summary of On-Water Experiments*

Experimental Session	Scenario	Vehicle-Hours	Vehicle Encounters	Number of AMVs	Human Interaction
1	A	1.87	64	5	
2	B	0.56	16	5	
3	B	0.62	21	5	
4	B	9.57	339	5	
5	A	6.55	219	5	
6	A	3.14	109	5	
7	B	1.87	26	5	
8	B	2.42	88	5	
9	B	4.16	148	5	
10	A	5.85	221	5	
11	A	2.43	88	5	
12	A	1.14	17	5	
13	A	2.55	56	5	
14	B	6.62	189	5	
15	A	6.09	163	5	
16	B	4.63	119	5	
17	B	3.93	129	5	
18	B	8.54	291	5	
19	A	1.73	37	5	
20	A	7.24	211	5	
21	A	6.03	162	5	
22	D	4.92	208	5	Yes
23	B	4.75	175	5	
24	A	1.04	6	5	
25	A	6.21	143	5	
26	D	6.35	150	5	Yes
27	D	6.13	86	5	Yes
28	D	7.26	68	5	Yes
29	D	2.46	50	5	Yes
30	D	3.65	21	5	Yes
31	D	9.03	148	5	Yes
32	C	4.55	36	5	
33	C	1.26	14	5	
34	C	1.27	12	5	
35	C	3.52	35	5	
36	H	5.53	124	5	Yes
37	H	1.94	124	5	Yes
38	C	5.77	211	5	
39	C	1.03	13	5	
40	C	8.81	98	5	

Summary of On-Water Experiments

Experimental Session	Scenario	Vehicle-Hours	Vehicle Encounters	Number of AMVs	Human Interaction
41	C	5.83	49	5	
42	H	2.19	24	5	
43	H	10.16	242	5	
44	H	0.93	13	5	
45	H	1.26	16	5	
46	H	7.16	145	5	
47	H	7.28	115	5	
48	H	3.59	76	6	
49	H	7.38	58	6	
50	H	2.27	14	6	
51	H	7.57	203	6	
52	H	3.06	84	6	
53	H	4.53	32	6	
54	I	1.43	13	5	
55	I	1.64	21	5	
56	I	0.66	9	5	
57	I	1.22	12	5	
58	I	1.38	10	5	
59	I	4.51	127	5	
60	I	1.43	149	5	
61	J	6.37	121	5	
62	J	2.60	43	5	
63	G	6.06	247	5	
64	F	1.93	35	5	
65	E	6.84	195	5	
Total		272.2	6488		9

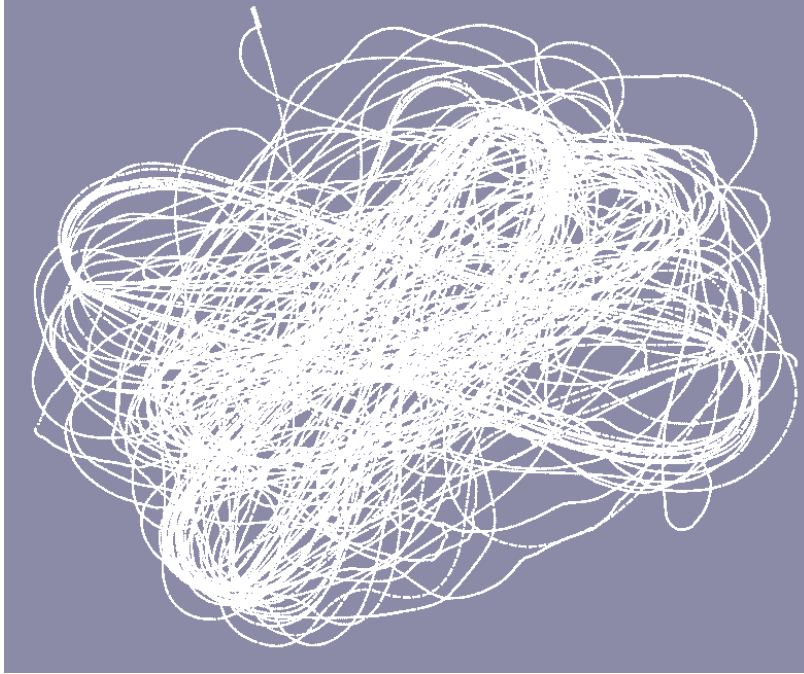


Figure 6-11 This track data shows the perturbations of geometry possible with a long duration experiment using the starburst pattern of Figure 6-2.

6.3.1 Scenario A & B Results

Compromises that used direct knowledge of the resulting r_{cpa} , t_{cpa} , and Θ_{cpa} for a candidate course-speed pair improved collision avoidance and mission performance as demonstrated by the reduced number of violations of the minimum acceptable CPA range and improved spatial and temporal efficiencies. On-water track data showing the non-canonical geometries possible using long duration experiments are shown in Figure 6-11. Figure 6-12 demonstrates an example on-water 5-vehicle collision encounter using Scenario B. The corresponding ownship decisions for contacts A, B, and C at the beginning of the track lines are shown with necessary compromises in Figure 6-13.

The full CPA quantification experiments considered r_{cpa} as well as Θ_{cpa} for COLREGS rule penalties. Extensive on-water tests of Scenarios A and B resulted in more than 3,050 vehicle-pair interactions requiring a collision avoidance maneuver. Performance of both algorithms was evaluated using the same metrics.

The nominal velocity obstacle collision range was used as the upper threshold

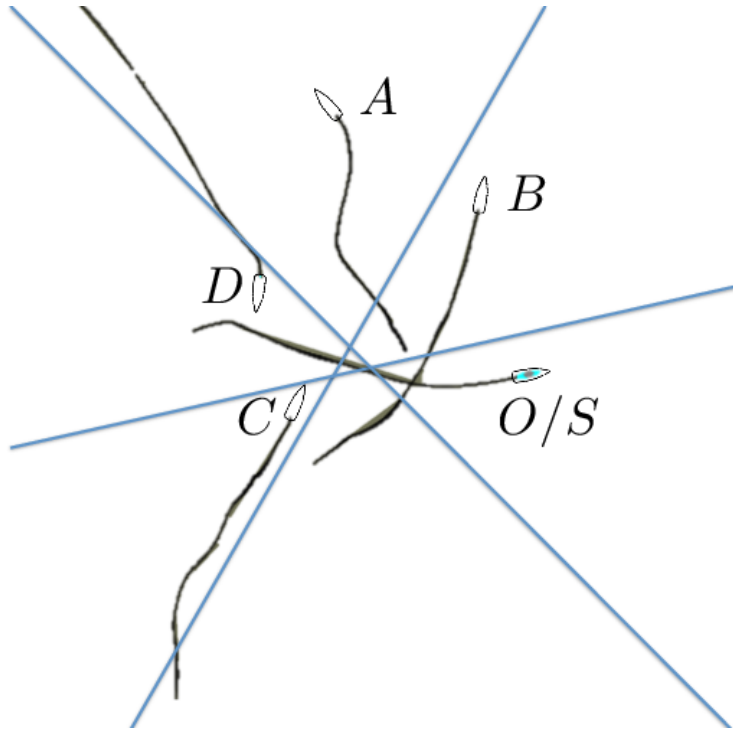


Figure 6-12 The geometry for the 5-vehicle, 3-track on-water experiment of Figure 6-2 shows concurrent maneuvers required for multiple simultaneous COLREGS rules. Ownship's (O/S) accompanying decisions based on the full CPA quantification algorithm are shown in Figure 6-13.

for the CPA-based method ($R_{col}^{vo} = R_{pref}$); a lower threshold of half the velocity obstacle collision range was set for the lower threshold of the CPA-based method ($R_{min} = 0.5 \cdot R_{col}^{vo}$) consistent with experienced ship driving practice as shown in Figure 6-14. Any range at CPA less than half the velocity obstacle collision range ($r_{cpa} < R_{min}$) was considered a violation of the minimum acceptable CPA range regardless of the underlying algorithm. Violations of R_{min} represent a significant and unsafe deviation from operator-desired range at CPA and therefore constituted the primary metric for comparison of algorithm performance under the five vehicle scenarios.

Algorithm comparison was baselined to mean collision avoidance CPA range ($\overline{r_{cpa}}$) normalized by preferred CPA range. The normalized mean CPA ranges for both algorithms were consistent to three significant digits indicating fair comparison of algorithms as shown in Table 6.4. The number of experiments in each configuration

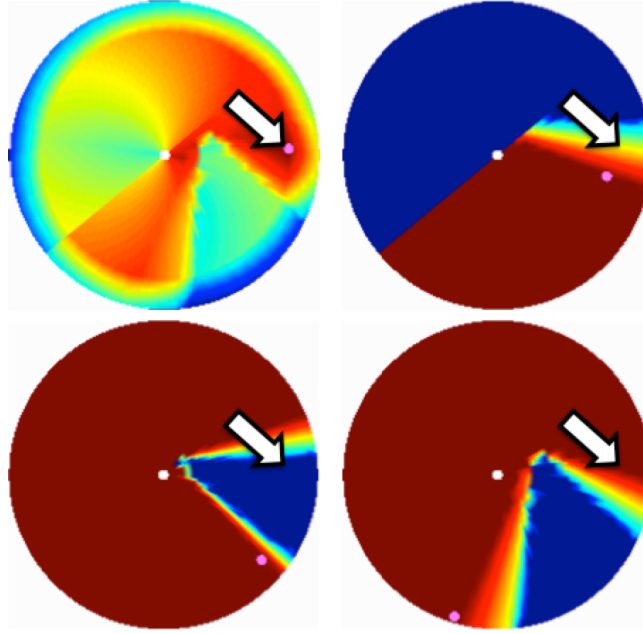


Figure 6-13 Example on-water objective functions with full CPA quantification. This snapshot of a point in time shows ownship’s objective functions corresponding to the beginning of the tracks displayed in Figure 6-12. The white dot at the center of each figure represents the center of the decision space. The pink dot represents the maximum value of each objective function. The top left figure shows the combined objective function for a desired transit to the east (mission objective function shown as Figure 6-3) with three simultaneous contacts of concern. Ownship’s optimal course-speed pair (\vec{x}^* of top left image) is depicted by the white arrow in each graphic. Ownship’s COLREGS collision avoidance objective functions (A - top right, B - bottom right, C - bottom left) at the same instant show compromised (non-red) values for A and B with an optimal value for C.

is shown in Table 6.5. When placed under the loading of the five-vehicle simultaneous collisions of Scenarios A and B, both algorithms resulted in mean CPA ranges approximately 10% closer than desired.

Under the loading of these simultaneous five vehicle encounters, the traditional velocity obstacle algorithm violated of the minimum acceptable CPA range ($r_{cpa} < R_{min}$) in 4.5% & 4.7% of encounters for Scenarios A & B, respectively. For the same nominal “collision range” ($R_{pref} = R_{col}^{vo}$), the full CPA quantification algorithm achieved an improvement over the traditional velocity obstacle in both geometry

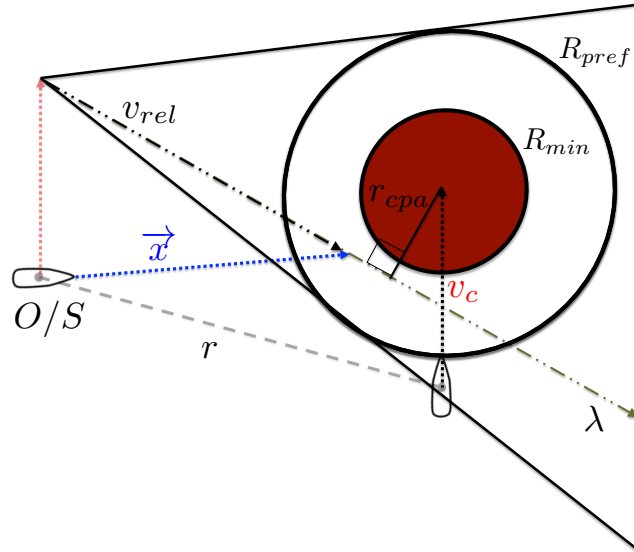


Figure 6-14 The velocity obstacle and CPA methods were compared in Scenario A using ($R_{col}^{vo} = R_{pref}$). The red circle indicates ranges that violated ($R_{min} = 0.5 \cdot R_{col}^{vo}$). Experimentation using on-water encounters demonstrated that the full CPA method reduced the number of occurrences where a contact entered the red circle as shown in Table 6.6.

Table 6.4 Mean CPA Range Normalized to Desired CPA[†] for 5-Vehicle Scenarios

Algorithm	3-Tracks	5-Tracks
Velocity Obstacles ($\bar{r}_{cpa}/R_{col}^{vo}$)	89.9%	90.9%
Full CPA (\bar{r}_{cpa}/R_{pref})	89.9%	90.9%

[†] $R_{pref} \equiv R_{col}^{vo}$ for Scenarios A & B

scenarios as shown in Table 6.6. The full CPA quantification algorithm resulted in violations of the minimum acceptable CPA range for 3.3% & 3.7% of encounters for Scenarios A & B, respectively. This represents a non-trivial reduction of range-violating encounters.

Spatial and temporal efficiencies were calculated for each traversed track when collision avoidance was required and averaged over the aggregate of all encounters. Similar improvements were achieved in long term means of both spatial and temporal efficiencies between the two algorithms as shown in Tables 6.7 and 6.8, respectively. Standard deviations are shown in Tables 6.9 and 6.10, respectively. This demonstrates

Table 6.5 *Number of On-Water Experiments Performed for 5-Vehicle Scenarios*

Algorithm	3-Tracks	5-Tracks
Velocity Obstacles	921	682
Full CPA	699	753

Table 6.6 *Percent of $r_{cpa} < R_{min}$ Events for Scenario A & B 5-Vehicle On-Water Collision Avoidance Encounters*

Algorithm	3-Tracks	5-Tracks
Velocity Obstacles	4.5%	4.7%
Full CPA	3.3%	3.7%

that the full CPA quantification algorithm resulted in fewer range collisions than the traditional velocity obstacle while reducing track deviations and time between waypoints for complex 5-vehicle encounters.

With more range violations using velocity obstacle techniques, one would assume velocity obstacles would achieve higher spatial efficiency (less track deviation) or higher temporal efficiency (shorter overall time). Rather, the full CPA quantification algorithm out performed the velocity obstacle-based technique in both efficiency metrics as well as the safety metric.

The standard deviations of unadjusted range at CPA between Scenarios A and B are lower for CPA-based algorithms indicating more predictability in maneuvers for the CPA-based method. The exception is overtaking vessels (R13/16 and R13/17) that are likely less willing to cross track given the less flexible velocity obstacle risk calculation.

Table 6.7 *Mean Spatial Efficiency for Scenario A & B 5-Vehicle On-Water Collision Avoidance Encounters*

Algorithm	3-Tracks	5-Tracks
Velocity Obstacles	0.843	0.774
Full CPA	0.853	0.821

Table 6.8 *Mean Temporal Efficiency for Scenario A & B 5-Vehicle On-Water Collision Avoidance Encounters*

Algorithm	3-Tracks	5-Tracks
Velocity Obstacles	0.564	0.514
Full CPA	0.581	0.556

Table 6.9 *Standard Deviation of Spatial Efficiency for Table 6.7*

Algorithm	3-Tracks	5-Tracks
Velocity Obstacles	0.072	0.090
Full CPA	0.074	0.119

Table 6.10 *Standard Deviation of Temporal Efficiency for Table 6.8*

Algorithm	3-Tracks	5-Tracks
Velocity Obstacles	0.215	0.210
Full CPA	0.190	0.206

6.3.2 Scenarios C - J Results

Scenarios C-J demonstrated that the primary mission of a vehicle largely affects the collision avoidance performance capabilities with respect to both safety and protocol compliance. A more complicated mission that relies on real-time reactive responses such as underwater vehicle monitoring showed variation in safety and protocol compliance compared to a waypoint following mission. If a waypoint following mission were used for validation of collision avoidance algorithms, it is possible that performance would be below thresholds in more complex primary missions.

Figure 6-15 and Table 6.11 show mean protocol compliance scores with standard deviations shown in Table 6.12. Safety was measured using the cost function of Figure 4-5 with a 30% pose reward based on Equations (4.5) and (4.10) ($S^{max} = 30\%$). Safety function values were consistent with other experiments: $\Delta S^{R_{nm}} = 30\%$, $\Delta S^{R_{min}} = 60\%$, $R_{min} = 0.5 \cdot R_{pref}$, $R_{nm} = \frac{5}{16} \cdot R_{pref}$, and $R_{col} = \frac{3}{16} \cdot R_{pref}$. A pose reward was assigned according to Figure 4-6 using Equations (4.6) and (4.7) with $\alpha_{cut} = 70^\circ$ and $\beta_{cut} = 110^\circ$. Figure 6-16 and Table 6.13 show mean safety scores with standard deviations shown in Table 6.14. Vehicles using the full CPA quantification algorithm were allowed to accept risk (with decreasing utility) as close as 50% of the preferred CPA range similar to Section 6.3.1.

Within the navigationally constrained environments (Scenarios H - J), both safety and collision avoidance scores were lower than the Scenario A baseline as expected. The safety evaluation scores were compensated commensurate with the 35% reduction in range thresholds discussed in Section 6.1.5. This indicates that despite the closer ranges allowed, range violations still occurred. This is expected when forcing vessels into a more contact dense environment with little room to maneuver. High standard deviations were also seen in both the non-compliant and navigationally constrained scenarios. This is consistent with having less room to maneuver as desired or encountering a contact that is not acting as expected.

Some amount of the lower safety score of Scenario D resulted from the intentionally forced maneuvers by the human operator. This included closer-than-desired encoun-

On-Water Mean Protocol Compliance Scores for Each Rule and Scenario

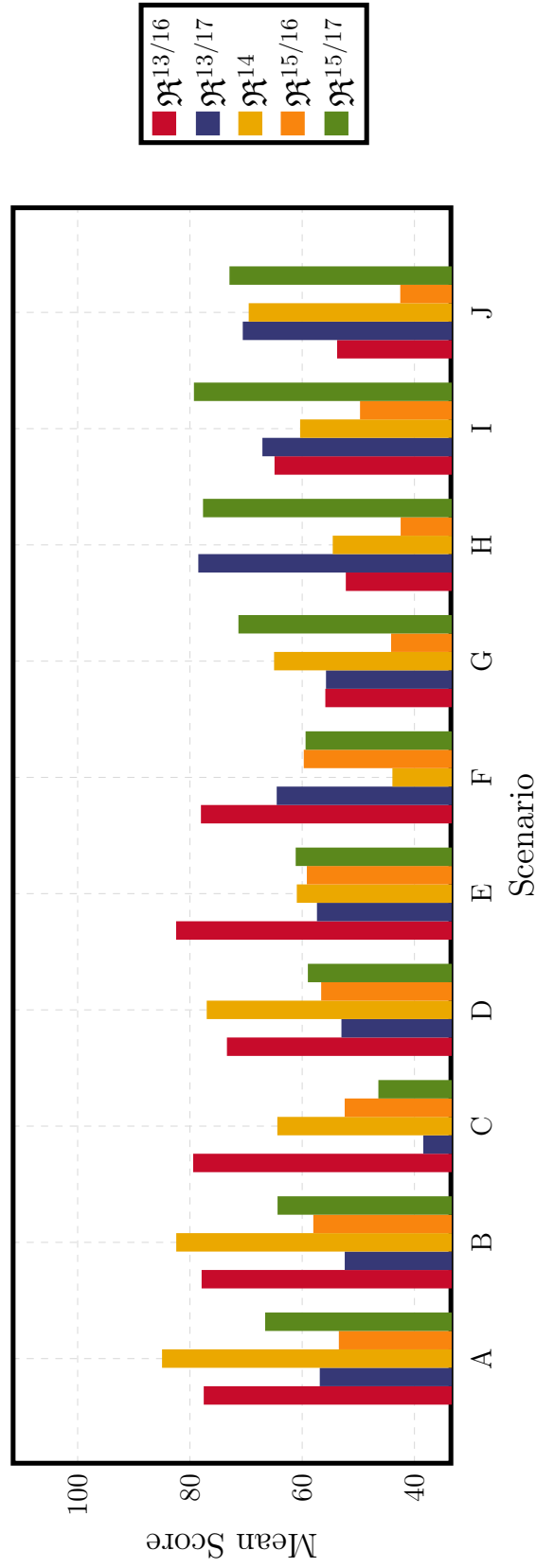


Figure 6-15 Protocol scores were computed using the concepts of Sections 4.3. Scores ranged from 0-100.

Table 6.11 *Mean Protocol Score*

Scenario	Rule Set				
	R13/16	R13/17	R14	R15/16	R15/17
A	77.11	56.44	84.54	53.04	66.17
B	77.49	51.99	82.01	57.59	63.96
C	79.00	38.00	64.00	52.00	46.00
D	72.98	52.58	76.58	56.19	58.56
E	82.03	56.94	60.53	58.74	60.73
F	77.61	64.11	43.50	59.29	58.97
G	55.45	55.33	64.58	43.73	70.93
H	51.80	78.08	54.13	42.03	77.24
I	64.50	66.66	59.94	49.27	78.86
J	53.35	70.16	69.10	42.10	72.53

Table 6.12 *Standard Deviation of Protocol Score*

Scenario	Rule Set				
	R13/16	R13/17	R14	R15/16	R15/17
A	25.03	41.73	27.45	31.95	40.28
B	21.90	42.79	29.52	31.18	40.89
C	22.79	43.71	26.72	32.97	41.11
D	27.16	43.46	29.80	32.42	41.17
E	23.64	46.16	40.04	35.03	42.12
F	24.30	44.72	33.51	40.23	41.62
G	39.10	43.33	33.77	35.50	38.57
H	29.64	38.46	37.35	30.55	37.08
I	26.40	43.48	36.17	29.08	38.08
J	28.13	44.41	32.87	30.55	43.08

On-Water Mean Safety Scores for Each Rule and Scenario

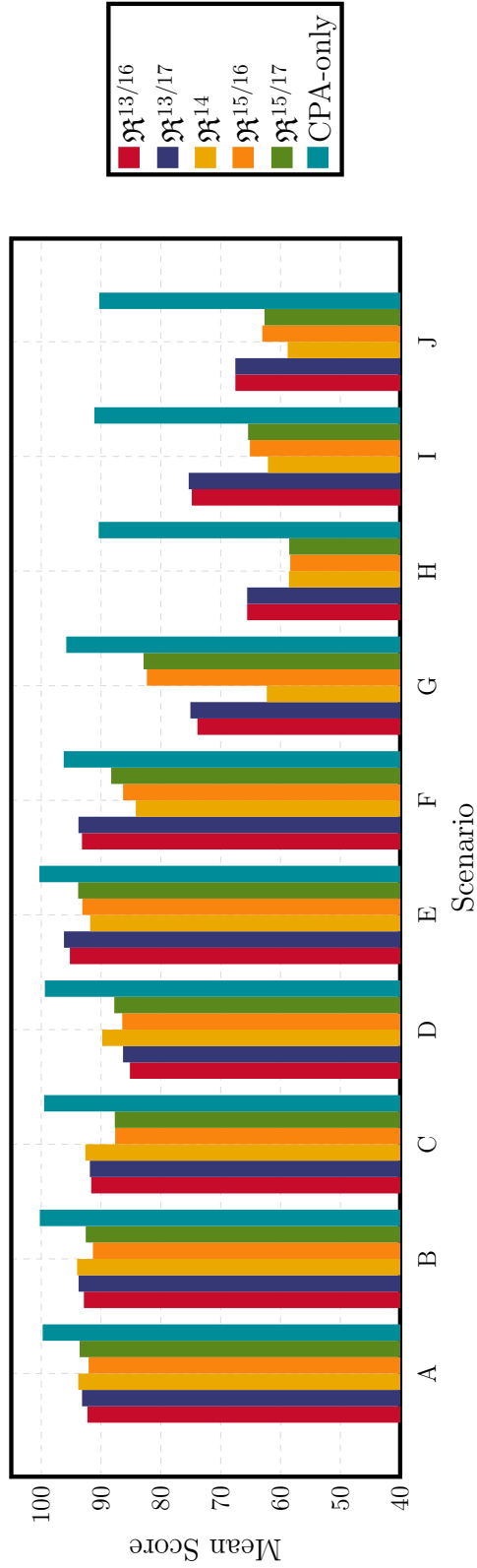


Figure 6-16 Safety scores were computed using the concepts of Sections 4.4. Scores ranged from 0-100.

Table 6.13 *Mean Safety Score*

Scenario	Rule Set					
	R13/16	R13/17	R14	R15/16	R15/17	CPA-only
A	91.92	92.82	93.45	91.72	93.23	99.40
B	92.51	93.40	93.64	91.00	92.20	99.88
C	91.28	83.6	87.8	85	83.8	99.16
D	84.81	85.97	89.45	86.10	87.43	99.03
E	94.85	95.84	91.46	92.78	93.47	99.95
F	92.83	93.42	83.83	85.96	87.95	95.88
G	73.53	74.71	61.94	81.98	82.54	95.45
H	65.22	65.22	58.24	58.02	58.19	90.04
I	74.47	74.99	61.75	64.76	65.07	90.75
J	67.19	67.20	58.45	62.68	62.32	89.94

Table 6.14 *Standard Deviation of Safety Score*

Scenario	Rule Set					
	R13/16	R13/17	R14	R15/16	R15/17	CPA-only
A	19.18	18.94	12.34	13.71	12.59	4.91
B	14.82	14.65	10.95	16.23	15.64	0.92
C	20.31	20.32	11.65	18.73	18.02	4.46
D	20.61	20.56	15.13	21.63	21.44	3.98
E	12.11	11.64	17.93	12.47	12.00	0.37
F	20.40	19.73	10.02	22.97	22.28	5.27
G	35.20	34.82	34.57	26.76	26.25	8.92
H	27.81	28.01	23.48	26.33	26.10	10.66
I	22.56	23.43	23.36	20.31	20.03	10.50
J	25.86	25.98	20.69	23.69	23.28	10.01

ters which were used to stress the collision avoidance algorithms. An examination of human-to-human interactions compared to human-to-robot interactions without the intentional stresses of Section 6.1.3 will be explored in future work.

Several cases of behavior deemed either 1) resulting in less-than-desirable ranges at CPA but otherwise COLREGS-compliant, or 2) safe but in violation of the COLREGS reinforced the concept of using both safety and protocol compliance scores to quantify performance. Two example cases from on-water experimentation are shown in Figure 5-3.

6.4 Conclusions

In summary, the experiments presented in this chapter demonstrated that:

- multi-contact encounter performance as measured by safety, efficiency, and protocol compliance varied depending on the scenario (e.g., waypoint following navigation, UUV following, etc.)
- complex (non-waypoint following) scenarios altered protocol compliance and safety scores in multi-contact encounters for collision avoidance configurations
- collision avoidance algorithm testing for compliance with protocol requirements must account for the expected operational scenario including the likely number of simultaneous contacts
- human-present interactions in on-water encounters may alter performance characteristics of an autonomous collision avoidance algorithm
- changing when and how a vehicle prioritizes collision avoidance over mission achievement (i.e., priority weight functions) greatly affected safety and protocol compliance performance
- the presence of a collision-agnostic vehicle greatly reduced the protocol compliance and safety performance of COLREGS-cognizant vehicles

- quantifying risk using a more full approach such as the algorithms presented in Section 3.3 rather than the velocity obstacle improved decision making in multi-contact encounters as demonstrated by the reduced number of minimum acceptable range violations

THIS PAGE INTENTIONALLY LEFT BLANK

Chapter 7

Conclusions and Future Work

7.1 Conclusions

With increasingly complex autonomous mission demands and congested contact environments, algorithms that can simultaneously reason about and appropriately balance collision avoidance and mission priorities must be explored and rigorously tested. The full CPA quantification algorithm allows collision avoidance utility function designs to reason about numeric values of r_{cpa} , t_{cpa} , and Θ_{cpa} for candidate maneuvers using a non-brute force sampling technique. This empowers autonomous algorithms to reason about risk of collision similar to humans throughout the entire decision space.

Real-time on-vehicle instantiations of the COLREGS evaluation program in this thesis are possible to detect non-compliance of other vessels and adjust collision avoidance parameters accordingly. Results validated the thesis assertions of Section 1.3 and demonstrated that the full CPA quantification algorithm allowed for reduced number of violations of the minimum acceptable CPA range and improved both spatial and temporal efficiencies compared to the traditional velocity obstacle algorithm under similar configuration. Traditional methods for calculating collision risk and validating a mission-preferred velocity vector have wide applicability to autonomous decision making. Processing improvements and intelligent sampling techniques such as interval programming make explicit calculations of range, time, and pose at CPA using non-brute force techniques feasible for small on-board computers.

Experimentation with high-speed vessels in protocol-constrained, multi-contact, multi-rule scenarios demonstrated that both geometry and patience parameters influenced key metrics of performance. Comparison of slow and high-speed vessels showed inconsistencies in performance that should be considered by high-speed collision avoidance algorithm designers especially when tuning for desired performance. If considering pose as a primary factor in the quantification of safety or protocol compliance, designers should also consider pose as a factor in the selection of velocity vectors in any collision avoidance scenario. The tuning of autonomous collision avoidance algorithms is a little-studied area. The effects of placing equivalent collision avoidance algorithms on both slow and high-speed vessels require further investigation before fielding. As demonstrated in the results of the high-speed vessel case study, several effects can be seen to cause pause when a designer arbitrarily assigns a collision avoidance or corresponding primary mission algorithm to a vessel for all initial speeds and encounter geometries. Rather, designers should use approaches to robustly test their algorithms to determine which variables require tuning specific to the real-time mission and collision avoidance scenario.

In summary, this thesis has made the following primary contributions in conjunction with the attributes of Section 1.2.2:

- demonstration that a range-, time-, and pose-informed CPA-based collision avoidance algorithm generalizes and outperforms the velocity obstacle
- development of protocol-based collision avoidance evaluation metrics, algorithms, and testing techniques
- performance of over 6,150 on-water experiments spanning 10 complex multi-contact scenarios

7.2 Future Work

Further generalization of the multi-threshold concept of Section 3.3 to incorporate more than two threshold levels of CPA range into multi-objective optimization al-

gorithm design are reserved for future work. The assumption of limited kinematic prediction leads to a simplified decision tradespace. Incorporation of more explicit vehicle dynamics is possible to further expand these techniques for highly maneuverable vehicles.

Research into the protocol evaluation techniques of this thesis would benefit from additional work in the following areas:

- incorporating vehicle kinematics to assist with determining safe speed, stopping speed and distance, and maneuverability
- incorporating environmental parameters such as daylight, fog and visibility, sea state (visibility and bearing errors), and radar sensitivity
- accounting for detection range (radar, mast head height, sea state)
- designing more thorough evaluation of other rules including Rules 6, 9, 10, 19, 20-38
- assessing when action warranting *in extremis* action per rule 17.a.ii is appropriate by standards using the above considerations
- allowing communication-based negotiations such as bridge-to-bridge radio agreements
- incorporating self-reporting schemes such as AIS including the perceived trustworthiness of the reports
- allowing a vessel to detect compliance scores less than a threshold value and choose to maneuver sooner than normal or seek a more conservative range or pose at CPA
- expansion of the evaluation libraries to include more complex and tailorable functions to be applied and tuned as appropriate

Other future work within the field of autonomous collision avoidance more broadly includes:

- examination of what circumstances may justify contact lumping to be both sufficient and appropriate
- incorporation of trajectory prediction literature
- incorporation of perception and sensor integration literature including reliance on probability of detection and false alarm as well as proper contact classification
- adjustment of decision space based on real-time identification of compliance
- incorporation of additional protocols and rules into the software produced by this thesis including:
 - sailing, sounds, and lights
 - inland rules
 - Rules of the Air
- investigation of human-to-human, human-to-robot, and robot-to-robot interactions and performance results under similar environments and decision policies
- investigation of human-robot teaming and negotiation
- incorporation of human behaviors and kinesics in close aboard scenarios to further amplify incorporation of human expectations into autonomous behavior

Future work will enable third-party evaluation of the full rule sets rather than limitation to power-driven vessels. Further work is required to more fully model contact-free intentions when maintaining course and speed of a stand-on vessel in complex scenarios such as slowing to pick up a pilot.

7.2.1 Collision Avoidance Road Test

In order to certify autonomous collision avoidance algorithms for use outside of a testing environment, this section proposes a framework for a road test comprised of a comprehensive scope of examination and quantifiable metrics of performance. To

be compliant with the appropriate protocol rule set being examined, a satisfactory level of performance must be met across each category of evaluation. The categories of Section 4.3.1 comprise the evaluation areas for this test when using the protocol requirements of COLREGS. Adaptations must be considered for other physical domains and protocols such as Rules of the Air as required.

This constitutes the first known road test framework for autonomous collision avoidance and would allow consistent testing and certification of algorithms with configurable metrics prior to fielding. Differing degrees of road tests may be possible for various levels of certification for operation. Table 7.1 lists performance areas important for a collision avoidance road test. Table 7.2 lists attributes of the road test.

A road test would provide the following functionality to the testing and evaluation community prior to certification of an autonomous vehicle and any associated algorithms for operation in human-present environments:

- identify protocol and safety requirements to be evaluated
- ensure sufficient testing of non-canonical geometries
- verify the ability to choose an appropriate combination of course, speed, or depth/altitude changes
- verify the ability to properly enter and exit each rule set as required
- quantify specific vehicle and more general algorithm performance with respect to protocol and safety compliance

7.2.2 Incorporating the Human Factor

A road test of autonomous collision avoidance algorithms also allows for examining human performance in controlled testing environments. By expanding the notion of this road test, humans would be able to certify aspiring or seasoned ship drivers to the same standards that their autonomous counterparts would be certified. Scoring

Table 7.1 *Road Test Performance Areas*

Number	Performance Area Description
I	Achieving passing scores for all applicable categories of scope as set by the appropriate certification authority†
II	Determination of obligations and governing rule(s) for both own-ship and the contact for various geometric configurations at time of visual or radar detection
III	Determination of role hierarchy when nested rules apply (e.g., own-ship overtaking a vessel that is already overtaking a third (slower) vessel)
IV	Identification of redundant contacts and sufficiently performing contact fusion
V	Releasing priority for contacts past CPA and opening
VI	Verification of unsaturated CPU loading‡ for up to N -simultaneous contacts, where N is set by the certification authority

† For autonomous surface vessels, scope is identified in Table 4.1.
‡ Verification of unsaturated CPU loading is presented in Appendix C.

metrics would allow comparison of performance of both humans and robots to ensure sufficient abilities throughout key areas (Table 7.1) while achieving particular testing attributes (Table 7.2).

Holding humans and robots to the same standards would allow experienced mariners the opportunity to train the evaluation algorithms to best represent customs and decisions of human operators. Holding all parties to human standards and requiring human-like behavior of autonomous vehicles allows for a natural incorporation into human-operated environments. Humans seeing predictable human-like behavior from all vehicles (whether human or robot operated) would reinforce the trust in autonomous collision avoidance. It is possible that a future observer of protocol-constrained collision avoidance track data and evaluation scores may not be able to pick the human from the robot, thus a form of a collision avoidance Turing test.

Care must be taken however to incorporate human factors research to assess the degree of bias (if any) that might be applied to human operators if and when a human (likely remote) operator must take control of an autonomous vehicle. Work in the aerial collision avoidance community has demonstrated that those with experi-

Table 7.2 *Road Test Attributes*

Number	Road Test Attribute Description
I	Non-canonical and reasonably exhaustive geometries†
II	Multi-contact, multi-rule scenarios
III	Conflicting simultaneous collision avoidance rules
IV	Conflicting mission, rule, and navigational priorities
V	Multi-speed encounters
VI	Non-compliant contacts (disregarding or delayed action)
VII	Over-constrained encounters
VIII	Robot-robot and robot-human interactions
IX	Exercise of a default safe mode
X	Statistical significance of testing encounters
XI	Broadcasting appropriate signals (including distress) to other vehicles or shoreside/ground entities as necessary

† Thorough geometric testing approaches such as the iterative geometric testing of Section 5.4 are encouraged.

ence with a system may be “prone to over trusting the automation” especially with positive priming [15]. In a situation where an autonomous vehicle requests human involvement in a collision avoidance decision – or likely worse with respect to bias if the autonomous vehicle were to propose a course of action for a human’s concurrence – work in the aerial community suggests the human may be prone to deferring to the autonomous system’s inclination without stepping back to fully appreciate the full collision avoidance scenario.

7.3 Final Thoughts

Before integrating human controlled and autonomous systems outside of laboratory environments, the common practices, customs, and interpretations of human operators must be fully understood. Autonomous designs that incorporate expectations and norms of human operators will achieve solutions that more naturally integrate autonomous and human-operated vessels. The categorization of scope and the incorporation of the nuance, applicable case law, and customs related to COLREGS allows appropriate and quantifiable assessment of autonomous collision avoidance per-

formance. The International Maritime Organization and other governing bodies may choose to include these metrics as a means to inform both regulation and policy in maritime collision avoidance protocols.

The techniques of this thesis may be applied more generally to other physical domains. Ground, air, or undersea vehicles might discover ways of improving performance characteristics by examining exact range, time, and pose of all sampled candidate maneuvers rather than generally preferring a particular range alone for discrimination. General obstacle avoidance may find value in populating these algorithms with sensed real time data and intelligently sampling the available decision space to achieve more informed collision avoidance decisions, evaluation metrics, and testing routines.

Autonomous vehicle trust in society requires that these last few percent of safety be realized, as demonstrated with the reduction of R_{min} violations in this thesis. Improvements such as the full CPA quantification algorithm are necessary to reduce the number of high contact density near miss and collision occurrences to as close to zero as possible. Quantifiable metrics and extensive, robust testing including a standardized framework for road tests present a means of establishing and articulating trustworthiness to the humans that will inevitably share the open seas with autonomously operated vessels.

Appendix A

COLREGS Reference

A.1 Collision Regulations for Power-Driven Vessels in Sight

The most relevant selection of International COLREGS collision avoidance rules are included within this appendix for ease of reference. They may be found in their entirety in [84].

Rule 13: Overtaking

- (a) Notwithstanding anything contained in the Rules 4-18, any vessel overtaking any other shall keep out of the way of the vessel being overtaken.
- (b) A vessel shall be deemed to be overtaking when coming up with a another vessel from a direction more than 22.5 degrees abaft her beam, that is, in such a position with reference to the vessel she is overtaking, that at night she would be able to see only the sternlight of that vessel but neither of her sidelights.
- (c) When a vessel is in any doubt as to whether she is overtaking another, she shall assume that this is the case and act accordingly.
- (d) Any subsequent alteration of the bearing between the two vessels shall not make the overtaking vessel a crossing vessel within the meaning of these Rules or relieve her of the duty of keeping clear of the overtaken vessel until she is finally past and clear.

Rule 14: Head-on Situation

(a) [Unless otherwise agreed] when two power-driven vessels are meeting on reciprocal or nearly reciprocal courses so as to involve risk of collision each shall alter her course to starboard so that each shall pass on the port side of the other.

(b) Such a situation shall be deemed to exist when a vessel sees the other ahead or nearly ahead and by night she could see the masthead lights of the other in a line or nearly in a line and/or both sidelights and by day she observes the corresponding aspect of the other vessel.

(c) When a vessel is in any doubt as to whether such a situation exists she shall assume that it does exist and act accordingly.

Rule 15: Crossing Situation

When two power-driven vessels are crossing so as to involve risk of collision, the vessel which has the other on her own starboard side shall keep out of the way and shall, if the circumstances of the case admit, avoid crossing ahead of the other vessel.

Rule 16: Action by Give-way Vessel

Every vessel which is directed to keep out of the way of another vessel shall, so far as possible, take early and substantial action to keep well clear.

Rule 17: Action by Stand-on Vessel

(a) (i) Where one of two vessels is to keep out of the way, the other shall keep her course and speed. (ii) The latter vessel may, however, take action to avoid collision by her maneuver alone, as soon as it becomes apparent to her that the vessel required to keep out of the way is not taking appropriate action in compliance with these Rules.

(b) When, from any cause, the vessel required to keep her course and speed finds herself so close that collision cannot be avoided by the action of the give-way vessel alone, she shall take such action as will best aid to avoid collision.

(c) A power-driven vessel which takes action in a crossing situation in accordance with Rule 17(a)(ii) to avoid collision with another power-driven vessel shall, if the circumstances of the case admit, not alter course to port for a vessel on her own port side.

(d) This Rule does not relieve the give-way vessel of her obligation to keep out of the way.

A.2 Example Collision Avoidance Geometries

Appendix B

Lexicon and Notation

B.1 Lexicon

Table B.1 *Table of Definitions*

collision avoidance	the avoidance of dynamic obstacles, specifically other vessel traffic. Collision avoidance can be protocol or non-protocol based. The primary protocol for ships is the COLREGS [84].
COLREGS	international rules as formalized at the Convention on the International Rules for Preventing Collisions at Sea, developed by the International Maritime Organization, and ratified as an international treaty by Congress. These rules were further formalized by the U.S. International Navigational Rules Act of 1977, and are sometimes referred to as the Collision Regulations outside the United States.
contact angle	“angle on the bow” or “target angle”
CPA	closest point of approach
designer	an author of a design (e.g., collision objective utility function) or by extension the operator entering configuration parameters as allowed by the author. The term designer in this thesis is extended to an evaluator who makes collision avoidance decisions for the purpose of testing.
encounter	a collision avoidance interaction is defined to start at the expected range of contact detection and ends when a contact is well clear, opening range, and approaching its initial detection range
full CPA	a CPA calculation that is informed by explicit values of range, time, and pose at CPA
geometry	specific combination of range, pose, and speed for a given contact relative to ownship

Table B.2 *Table of Definitions*

mission	a mission behavior represents the current primary purpose of a vessel's actions less any navigation or collision avoidance constraints. This encompasses the primary motivation(s) for a vessel not being tied to a pier in port.
navigation	the avoidance of static obstacles including but not limited to land, shoals, buoys, day markers, traffic separation schemes, etc.
ownership	the vessel of reference as though the operator were on-board.
track	the ideal positions that a vessel would travel to achieve its mission.
tradespace	the range of values of performance metrics resulting from configuration settings that are used to inform a decision policy. For example, an operator might be willing to trade a small out of safety to realize greater temporal efficiency.
vehicle	any means of transit through a physical domain; occasionally used in place of vessel, but by default more general to all physical domains
vessel	a vehicle specifically operating on the sea surface
waypoint	a navigational point sometimes associated with a particular time. A vessel's track is often defined by a list of waypoints.

B.2 Notation

Table B.3 *Table of Notation*

<u>Subscripts</u>	
\square_0	initial value; when used in context of a collision avoidance scenario, the value at the time of detection or rule determination
\square_c	variable associated with the contact rather than ownship
\square_{cpa}	value at the time of closest point of approach; can be used to describe both a future CPA prediction or a statement of fact for a posteriori encounters
$\square_{horizon}$	limiting value of interest, such as in the time horizon of interest
\square_{min}	global minimum of a value over all relevant time (usually duration of an encounter)
\square_{max}	global maximum of a value over all relevant time (usually duration of an encounter)
\square_{now}	value at the current time or geometry

<u>Superscripts</u>	
\square^*	optimal
\square^{180°	angle converted to $[-180, 180)$ as in β^{180°
\square^{360°	angle converted to $[0, 360)$ as in α^{360°
\square^{VO}	quantity associated with the traditional velocity obstacle; absence of VO implies the full CPA quantification algorithm of Chapter 3

<u>Special Symbols</u>	
$\bar{\square}$	mean
$\dot{\square}$	temporal derivative; $\dot{\square} = \frac{d}{dt}\square$

Table B.4 *Table of Notation*

<u>Decision Variables</u>	
α	contact angle
$\dot{\alpha}$	contact angle rate; temporal derivative of α
α_{cut}	cutoff contact angle to define reward functions
α_{crit}	critical angle to determine entry criteria
β	relative bearing
$\dot{\beta}$	relative bearing rate; temporal derivative of β
β_{cut}	cutoff relative bearing to define reward functions
ϕ	arbitrary angle for generic functions
avd_i	collision avoidance objective function
avd_i^{vo}	velocity obstacle collision avoidance objective function
CPA	closest point of approach; point of minimum encounter range
r	current range to obstacle
$f(\vec{x})$	generic objective function of msn_i, nav_i, avd_i
f_l	component objective function, where one or more components comprise a full objective function
\mathcal{G}	geometry configuration
ρ	intended track distance between the measured starting and ending points
$\hat{\rho}$	actual distance traveled between the measured starting and ending points
τ	time to traverse the intended track assuming constant initial speed
$\hat{\tau}$	actual time to traverse between the measured starting and ending points
η_ρ	spatial track efficiency between waypoints
η_τ	temporal efficiency between waypoints
λ	linear relative trajectory of \vec{x}
λ_0	linear relative trajectory of current course and speed
msn_i	objective function of primary mission(s)
nav_i	objective function of static navigational constraints
OBS	obstacle; contact where a risk of collision exists
π	course-speed design ratio
$\bar{\pi}$	patience parameter
π_θ	course weight
π_v	speed weight
r	range to a contact
r_{cpa}	predicted or actual CPA range
$r_{cpa}^{\lambda_0}$	predicted CPA range on current course/speed
\bar{r}_{cpa}	mean of CPA ranges for given algorithm
$\overline{\bar{r}_{cpa}}$	mean of CPA ranges for given algorithm

Table B.5 *Table of Notation*

<u>Decision Variables</u>	
R	configurable range to any contact; a threshold value rather than an actual range
R_{col}^{vo}	velocity obstacle “collision” range
R_{min}	min acceptable range at CPA in explicit algorithm
R_{nm}	range considered a near-miss encounter
R_{pref}	preferred range at CPA in explicit algorithm
$R_{50\%}$	range equal to 1/2 the desired range at CPA
R_l	l^{th} intermediate CPA range threshold
\mathfrak{D}	discriminator used to determine applicable <i>avd</i>
\mathfrak{R}	governing protocol rule set
\mathfrak{R}^{max}	maximum possible COLREGS compliance score
\mathfrak{R}_Θ	pose component of COLREGS compliance score
$\mathfrak{R}_{allowed}^{13}$	set of allowed maneuvers based on a particular rule, here rule 13
S	safety function for an encounter
S_r	range component of safety function
S_Θ	pose component of safety function
t_{cpa}	time of CPA on candidate course/speed
$t_{cpa}^{\lambda_0}$	time of CPA on current course/speed
θ	candidate or actual course ($\theta \in [0, 360)$)
Θ	pose consisting of $\langle \alpha, \beta \rangle$
Θ_0	initial relative pose (determines rule set)
Θ_{cpa}	relative pose at CPA (measure of safety)
v	speed, $ \vec{x} $
v_{max}	maximum possible speed in decision space
w_i	priority weight of i^{th} objective function
(x, y)	position of a vessel in North-up coordinate system
\vec{x}	candidate decision vector $\langle \theta, v \rangle$
\vec{x}^*	optimal, chosen decision vector $\langle \theta^*, v^* \rangle$

Appendix C

Computational Loading

C.1 Computational Loading

Figures C-1, C-2, and C-3 demonstrate CPU load for vehicles operating a small payload computer for two contacts including all mission and navigational processes. Sufficient computational reserve is available when using the full CPA quantification algorithm of Section 3.3. An additional payload computer would be advantageous for any sensor processing data necessary for feeding the collision avoidance algorithm real-time contact information.

Real-time CPU loading is shown by the blue line as a fraction of total CPU capacity per iteration. The red line gives the maximum CPU loading per iteration. There are nominally four iterations per second. In reality, if loading were too burdensome, relaxation to a lower iteration frequency (e.g., $2Hz$) would likely be sufficient for calculation of collision avoidance maneuvers given the pace at which most maritime collision avoidance scenarios develop. Computation in other domains would benefit from this type of chart, though higher computation frequency may be warranted.

The vertical dashed lines indicate when a collision avoidance rule set was started or changed. The integer numbers in the center indicate the total number of vehicles being avoided starting at that time. The statistics at the top offer valuable insight into performance. The percentage of time that i contacts are being simultaneously avoided within the scope of the displayed chart is given as χ_i . The mean μ_i and standard deviation σ_i of the CPU loading for i simultaneous contacts offer further insight into algorithm performance and CPU capability. The *max* values displays the maximum overall load experienced by the CPU during the experiment.

Normalized Helm Iteration Length for HIGHSPEED
 Multi-Objective CPA-Based COLREGS Algorithms using Interval Programming
 Helm Computation Frequency = 4 Hz

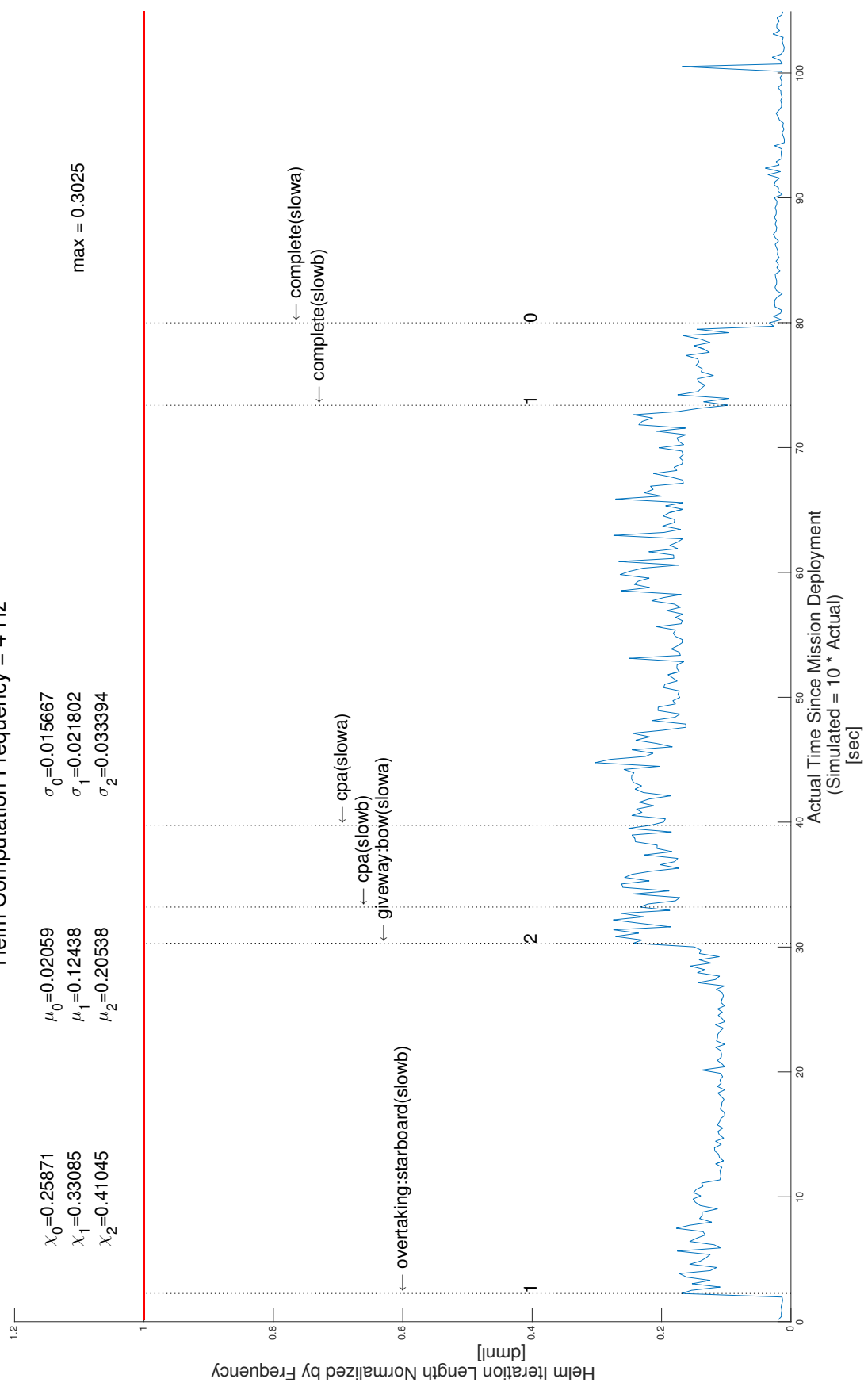


Figure C-1 High speed vehicle avoiding two slow vehicles A and B.

Normalized Helm Iteration Length for SLOWA
 Multi-Objective CPA-Based COLREGS Algorithms using Interval Programming
 Helm Computation Frequency = 4 Hz

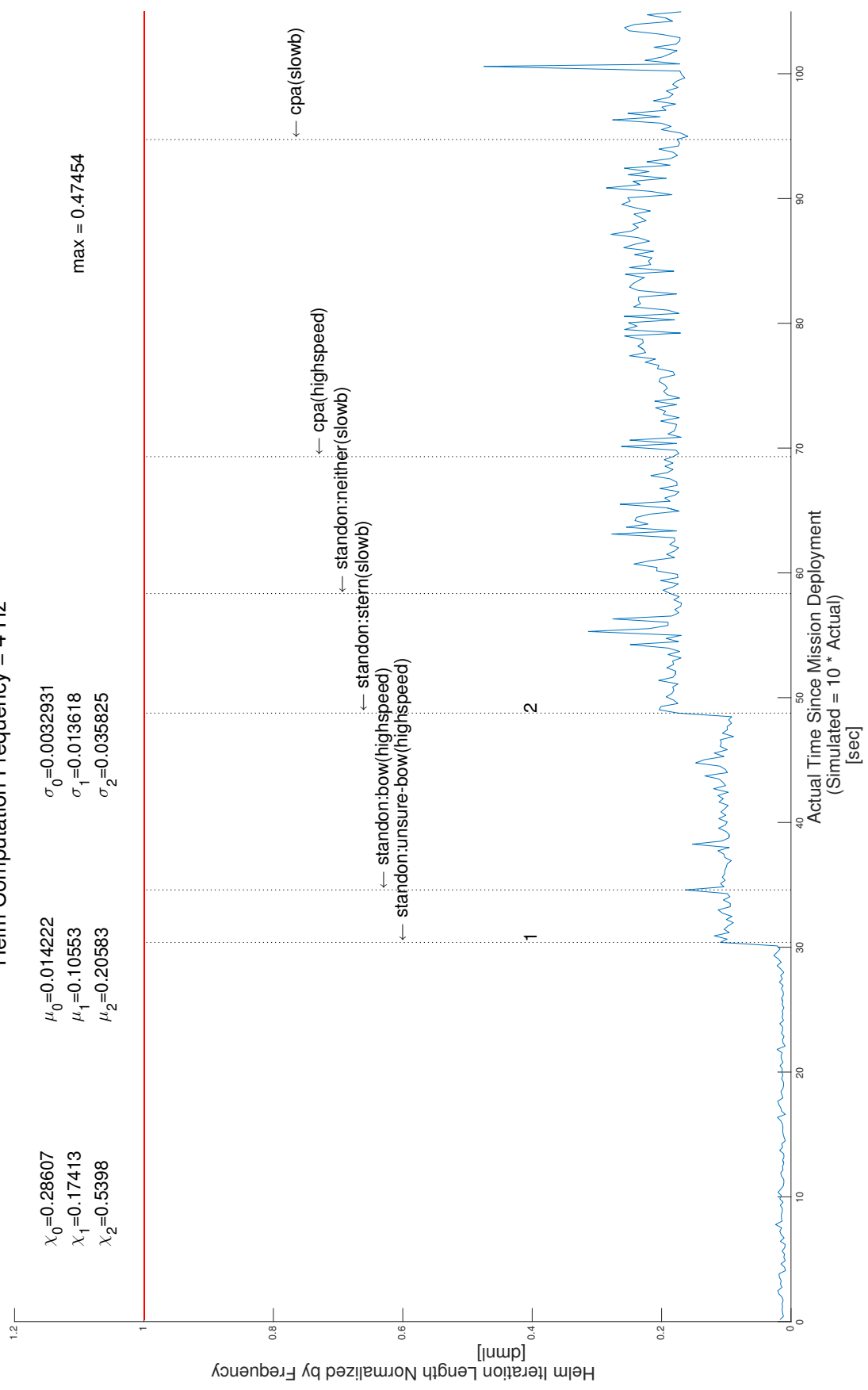


Figure C-2 Slow speed vehicle A avoiding a high speed vehicle and slow vehicle B.

Normalized Helm Iteration Length for SLOWB
 Multi-Objective CPA-Based COLREGS Algorithms using Interval Programming
 Helm Computation Frequency = 4 Hz

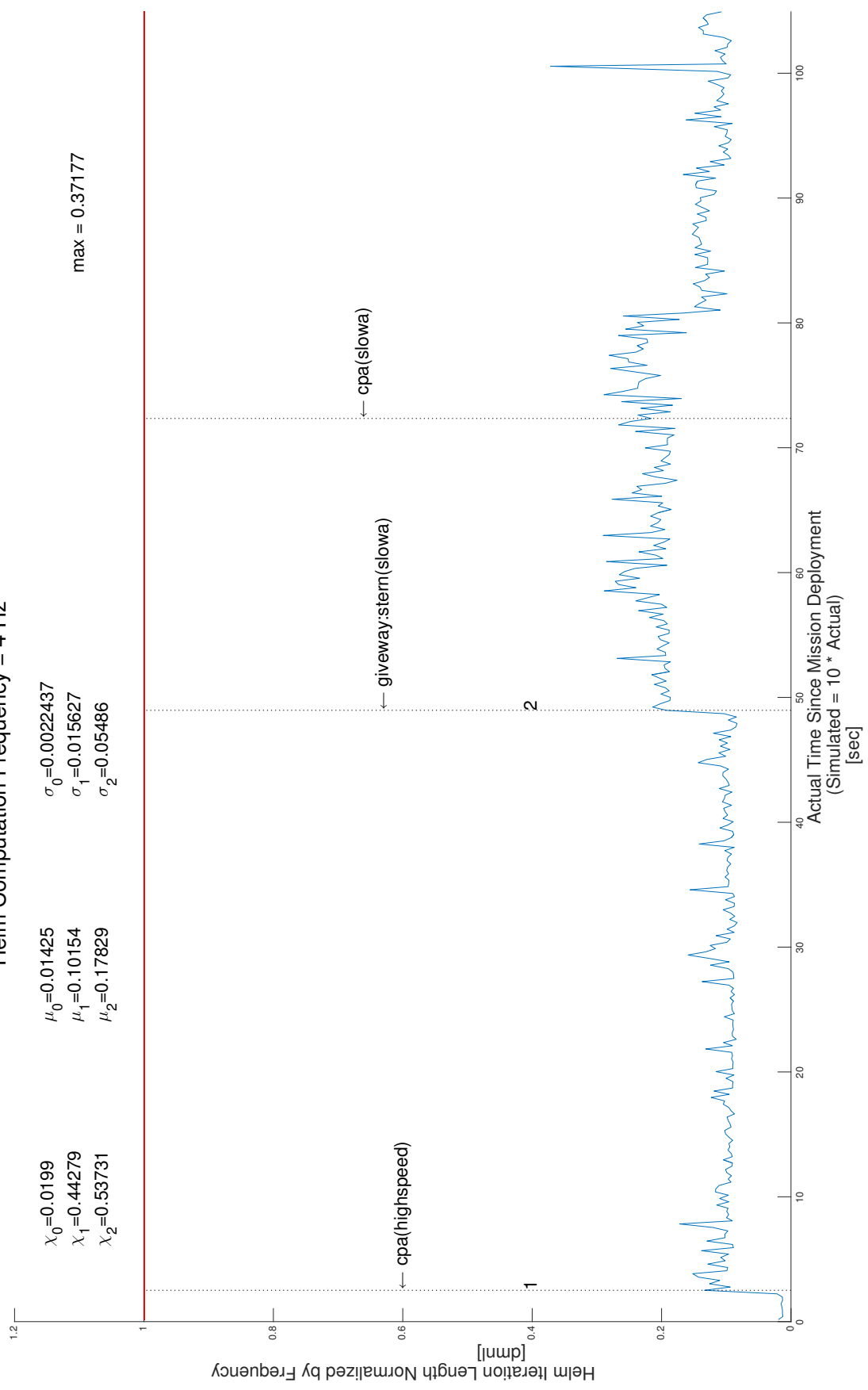


Figure C-3 Slow speed vehicle B avoiding a high speed vehicle and slow vehicle A.

THIS PAGE INTENTIONALLY LEFT BLANK

Appendix D

Validation of Evaluation Algorithms

A survey was presented to a number of experienced ship drivers to validate the evaluation algorithm results. Survey correlation to the evaluation algorithm is presented in Section 4.7.4. The questions posed to the respondents are presented throughout this Appendix. Raw response data is shown in Table D.1.

D.1 Experience Question

1. Which best describes your experience with COLREGS?
 - I have driven power-driven vessels in the open ocean under the obligations of international law (COLREGS).
 - I have COLREGS experience in collision avoidance coding or testing in academic environments.
 - I have COLREGS experience in collision avoidance coding or testing with industry.
 - I have no experience with COLREGS.

D.2 Scenario Questions

All scenario questions were prefaced with the following guidance:

Assume that all vessels are power-driven and operating under international COLREGS with full visibility. No other vessels are present and no restrictions in abilities to maneuver exist for any reason. Vessels are not drawn to scale – rely on the text for clarification. Assume a risk of collision sufficiently exists to require a rule.

D.2.1 Scenario 1

1. What rule is required of these vessels?
 - overtaking

- head-on
 - crossing
2. If a dangerous condition were to have resulted in this scenario, to which vessel would you assign blame?
- slower vessel (solid track line)
 - faster vessel (dashed track line)
 - both the slower and faster vessels

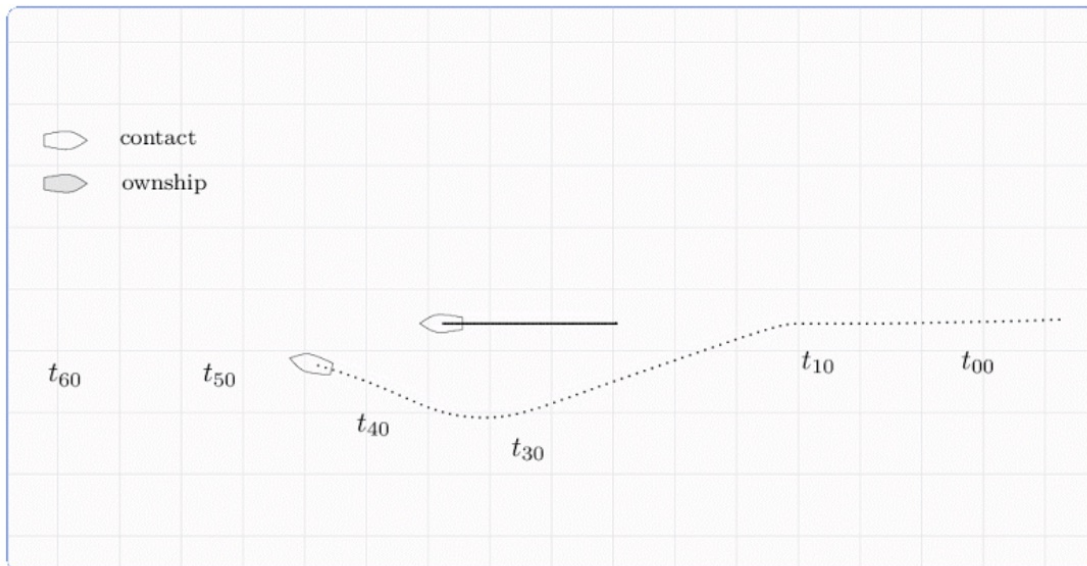


Figure D-1 This still image represents the most meaningful part of Scenario 1 as presented to the respondent. The actual survey included a moving image (Graphics Interchange Format) from time of detection to just pass time of CPA.

D.2.2 Scenario 2

1. Assume the vessels are on nearly reciprocal courses at the time of detection. What rule is required of these vessels?
 - overtaking
 - head-on

- crossing
2. The graphics are not to scale. Assume archie (green) maneuvered just after detecting evan on a nearly-reciprocal course. If a dangerous condition were to have resulted in this scenario, to which vessel would you assign blame? [Note: white never maneuvers]
- archie (green)
 - evan (white)
 - both vehicles equally

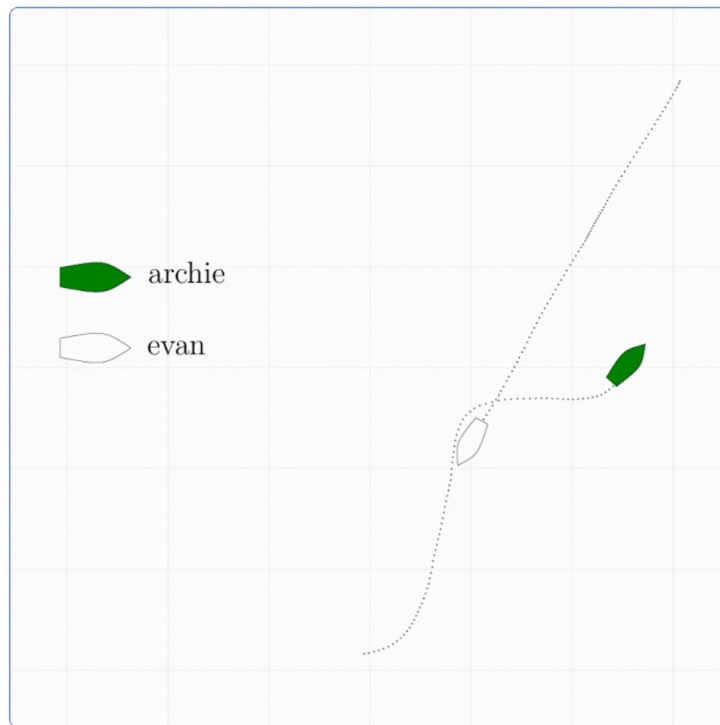


Figure D-2 This still image represents the most meaningful part of Scenario 2 as presented to the respondent. The actual survey included a moving image (Graphics Interchange Format) from time of detection to just pass time of CPA.

D.2.3 Scenario 3

1. Assume these vessels are on nearly reciprocal courses at the time of collision. What rule is required of these vessels?

- overtaking
- head-on
- crossing

2. Assume Mokai (blue) maneuvered 30 degrees to starboard. If a dangerous condition were to have resulted in this scenario, to which vessel would you assign blame?

- mokai (blue)
- felix (yellow)
- both vehicles equally

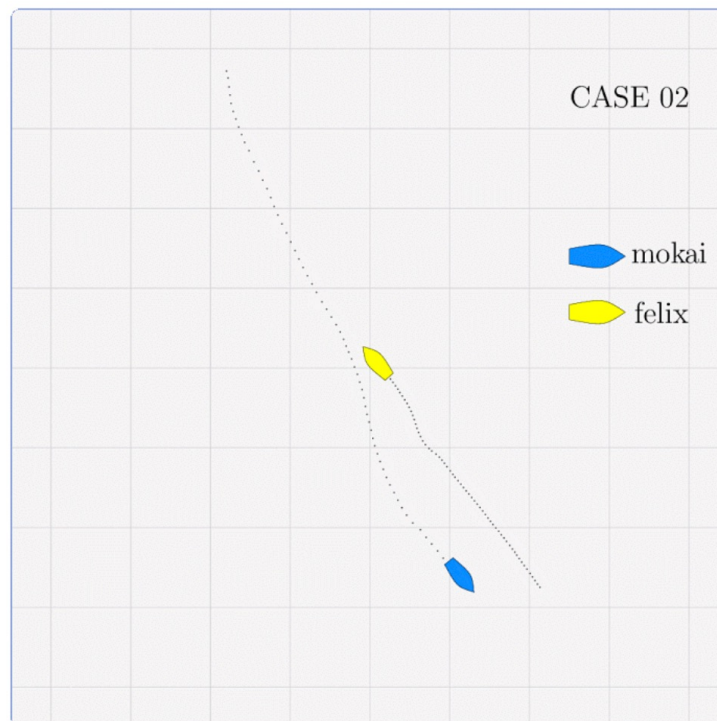


Figure D-3 This still image represents the most meaningful part of Scenario 3 as presented to the respondent. The actual survey included a moving image (Graphics Interchange Format) from time of detection to just pass time of CPA.

D.2.4 Scenario 4

1. At the time of first detection, these vessels are on nearly reciprocal courses.

What rule is required of these vessels?

- overtaking
- head-on
- crossing

2. Assume the vessels are not in sight of each other until on reciprocal courses.

If a dangerous condition were to have resulted in this scenario, to which vessel would you assign blame?

- betty (blue)
- felix (yellow)
- both vehicles equally

D.2.5 Scenario 5

1. Assume these vessels are detectable to each other from the beginning of the graphic. What rule is required of these vessels?

- overtaking
- head-on
- crossing

2. At the time of the collision, to which vessel would you assign blame?

- betty (blue)
- mokai (yellow)
- 75% to betty (blue), 25% to mokai (yellow)
- 25% to betty (blue), 75% to mokai (yellow)

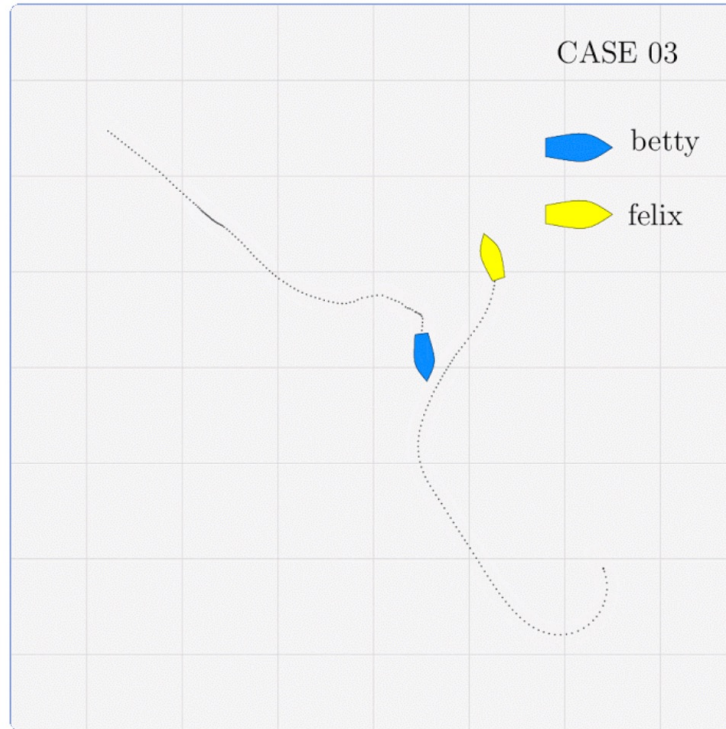


Figure D-4 This still image represents the most meaningful part of Scenario 4 as presented to the respondent. The actual survey included a moving image (Graphics Interchange Format) from time of detection to just pass time of CPA.

D.2.6 Scenario 6

1. Assume vessels are on constant courses from time of detection until yellow maneuvers. What rule is required of these vessels?
 - overtaking
 - head-on
 - crossing

2. Assume that the evan (yellow) was crossing the track in front of charlie (blue) at the time that both vehicles simultaneously maneuvered (evan to starboard; charlie to starboard – ignore the small fluctuation of charlie to port). Assuming this encounter resulted in a near miss, to which vessel would you assign blame? [Note: case law normally awards majority penalty to give-way vessels]
 - charlie (blue)

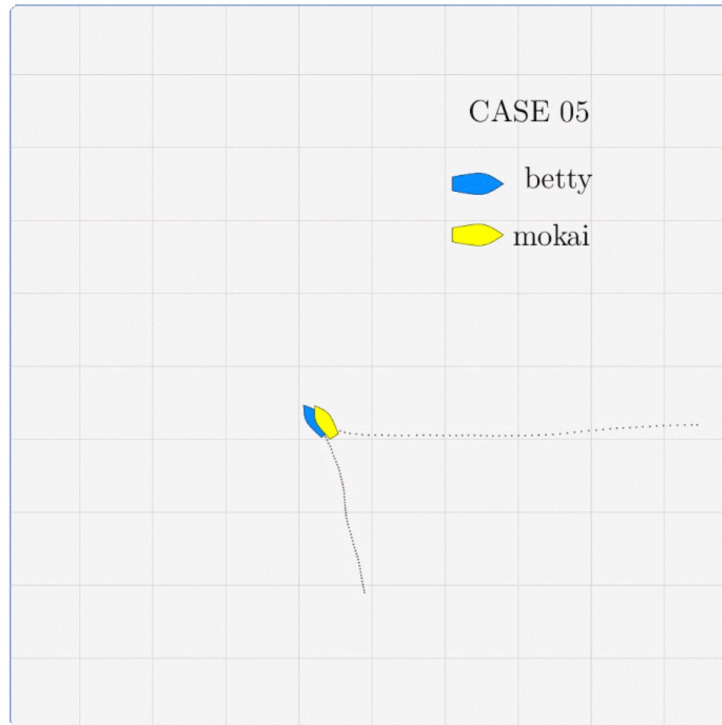


Figure D-5 This still image represents the most meaningful part of Scenario 5 as presented to the respondent. The actual survey included a moving image (Graphics Interchange Format) from time of detection to just pass time of CPA.

- evan (yellow)
- 75% to charlie (blue), 25% to evan (yellow)
- 25% to charlie (blue), 75% to evan (yellow)

D.2.7 Scenario 7

1. What rule is required of these vessels? (Assume nearly reciprocal courses at the time of detection.)
 - overtaking
 - head-on
 - crossing
2. To which vessel would you assign majority blame in the event of a collision?

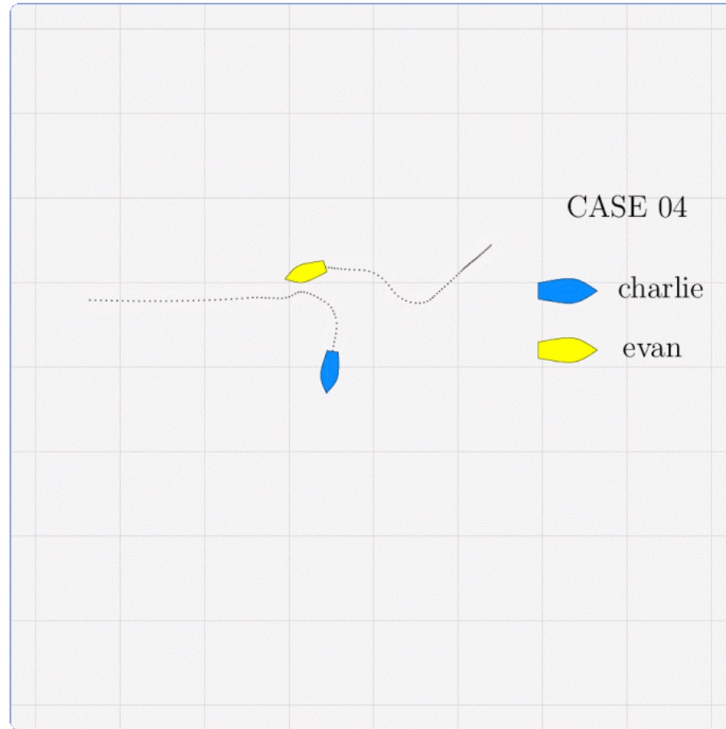


Figure D-6 This still image represents the most meaningful part of Scenario 6 as presented to the respondent. The actual survey included a moving image (Graphics Interchange Format) from time of detection to just pass time of CPA.

- archie (blue)
- betty (yellow)
- 50% to archie (blue) and 50% to charlie (yellow)

D.2.8 Scenario 8

1. What rule is required of the yellow and pink vessels? (Assume all vessels were detectable to each other from the beginning of this scenario.)
 - overtaking
 - head-on
 - crossing
2. To which vessel would you assign blame in the event of a collision.

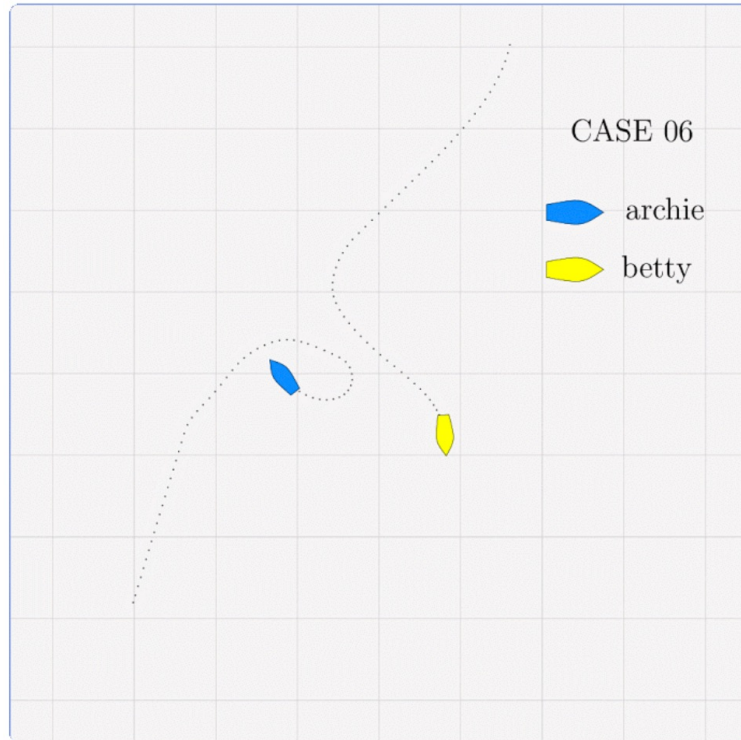


Figure D-7 This still image represents the most meaningful part of Scenario 7 as presented to the respondent. The actual survey included a moving image (Graphics Interchange Format) from time of detection to just pass time of CPA.

- betty (yellow)
 - davis (pink)
 - 75% to betty (yellow) and 25% to davis (pink)
3. Comparing blue and yellow, which vessel best maneuvered for the possible collision with pink and green?
- betty (yellow)
 - archie (blue)
 - neither vessel maneuvered correctly

D.2.9 Scenario 9

1. Assume all vessels are detectable to each other once on an initial constant course. What rule is required of the yellow vessel with respect to the blue vessel?

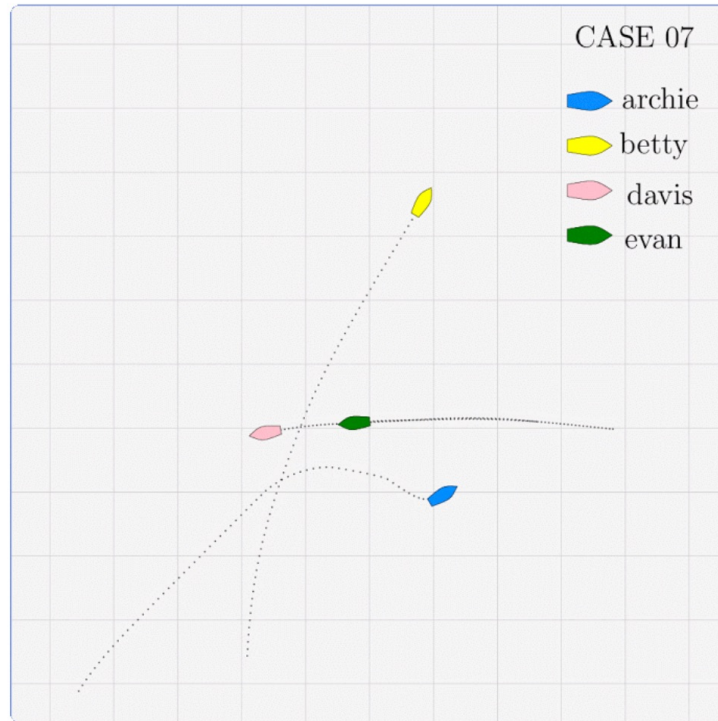


Figure D-8 This still image represents the most meaningful part of Scenario 8 as presented to the respondent. The actual survey included a moving image (Graphics Interchange Format) from time of detection to just pass time of CPA.

- overtaking
- head-on
- crossing

2. To which vessel would you assign blame in the event of a collision?

- charlie (yellow)
- evan (green)
- archie (blue)

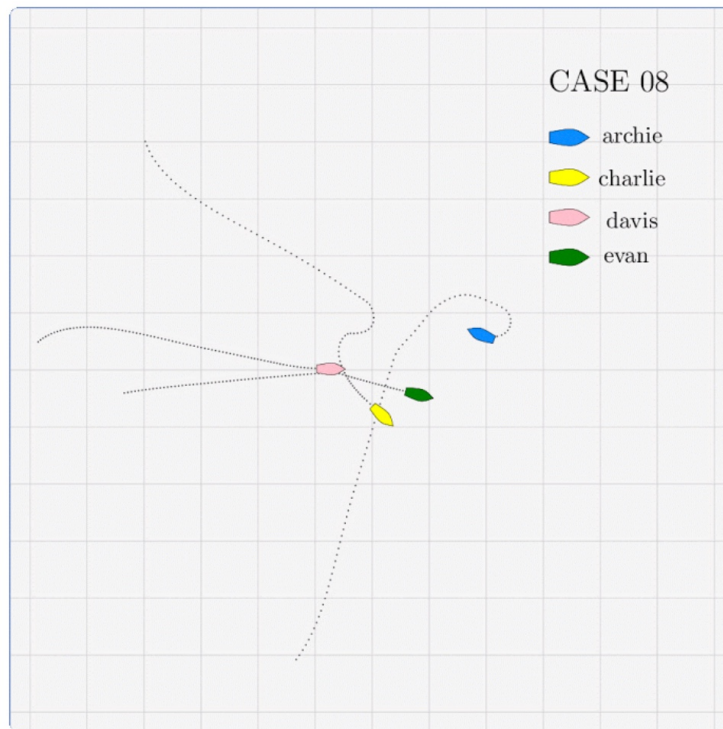


Figure D-9 This still image represents the most meaningful part of Scenario 9 as presented to the respondent. The actual survey included a moving image (Graphics Interchange Format) from time of detection to just pass time of CPA.

Table D.1 *Individual Respondent Data Before Controlling for Percent of Blame*

	Respondent											
Question	1	2	3	4	5	6	7	8	9	10	11	12
1	A	A	A	A	A	A	A	A	A	A	A	A
2	A	A	A	A	A	A	A	A	A	A	A	A
3	B	B	B	B	B	B	B	C	C	B	B	B
4	B	B	B	B	B	B	B	B	B	B	B	B
5	B	B	A	B	C	B	B	A	A	B	C	B
6	B	B	B	B	B	A	B	B	B	B	B	B
7	B	B	C	B	B	B	B	C	B	B	C	B
8	B	B	B	B	B	B	B	C	B	B	B	B
9	A	A	A	A	C	A	A	A	A	A	A	A
10	C	C	C	C	C	C	C	C	C	C	C	C
11	C	C	A	C	C	C	C	B	C	D	C	C
12	C	C	C	C	C	C	C	C	C	C	C	C
13	C	C	B	C	C	A	B	B	C	C	C	C
14	B	B	B	B	B	B	B	B	B	B	B	B
15	B	B	A	B	C	B	B	C	B	B	B	B
16	C	C	C	C	C	C	C	C	C	C	C	C
17	A	C	A	A	A	C	A	B	A	A	A	A
18	B	B	B	B	B	A	B	A	B	B	B	B
19	C	C	C	C	C	C	C	C	C	C	C	C
20	A	A	A	A	A	B	A	A	A	A	A	A

D.3 Studies Conducted in the Literature

Figures D-12, D-12, and D-12 present literature that offer insight into some of the poor scores seen in human testing of protocol requirements. They further identify competency, ignorance, and disregard as the most likely causes of collisions and non-compliant maneuvers. By adapting an objective means of quantification, more detailed assessment of the degree of contradiction is possible for real-world encounters.

Source: Zekić, 2015

Table 1 The percentage of correct answers

Rule number	Correct answers (%)
1	63
3	59
5	96
6	44
7	81
8	93
9	48
10	63
13	26
14	67
15	70
17	41
18	33
19	48
Average percentage	59

Figure D-10 This table displays the percentage of correct answers to COLREGS rule numbers as first reported by Zekic in [99]. Image is Table 1 from [99].

Source: Maritime Accident Investigation Branch, 2004

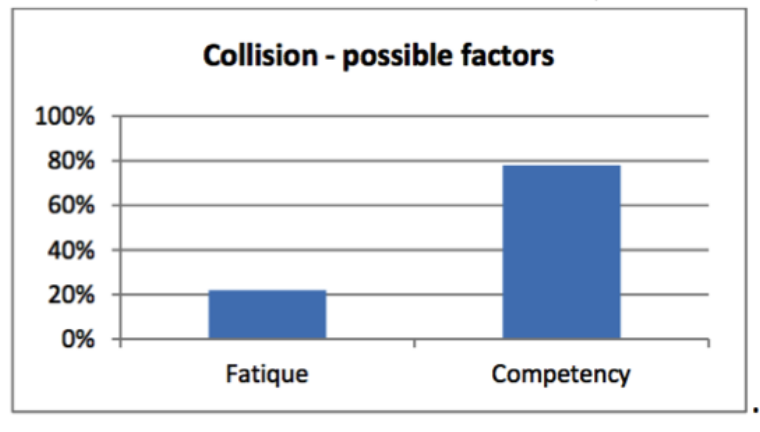


Figure D-11 This chart shows the reasons for collisions with competency of the rules prevailing. Having a set of objective and standard evaluation metrics and algorithms may promote improved competency through more standardized at-sea or in-simulator testing. Image is originally from Maritime Accident Investigation Branch Report of 2004 and reproduced as Figure 5 in [102].

Source: Syms, R.J, 2002

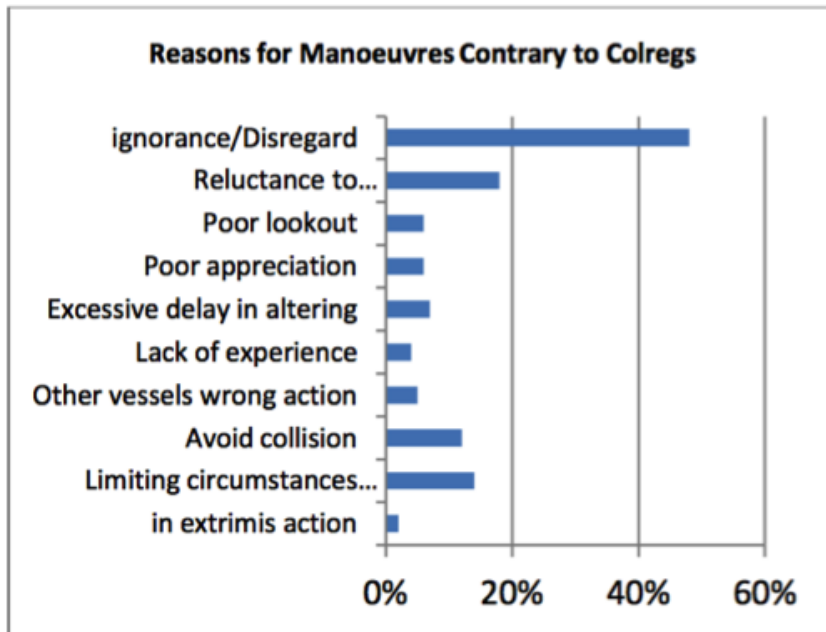


Figure D-12 This chart shows ignorance and disregard were the prevailing reasons that drivers failed to obey COLREGS. Image is from Syms 2002 and reproduced as Figure 6 in [102].

Bibliography

- [1] C. Allen. *Farwell's Rules of the Nautical Road*. Blue and gold professional library series. Naval Institute Press, 2005.
- [2] G. S. Aoude et al. “Probabilistically Safe Motion Planning To Avoid Dynamic Obstacles With Uncertain Motion Patterns”. In: *Autonomous Robots* 35.1 (2013), pp. 51–76.
- [3] M. R. Benjamin. “The Interval Programming Model for Multi-Objective Decision Making”. In: *MIT CSAIL AI Memo* 2004.021 (Sept. 2004).
- [4] M. R. Benjamin, J. A. Curcio, and P. M. Newman. “Navigation of Unmanned Marine Vehicles In Accordance With The Rules of The Road”. In: *IEEE International Conference on Robotics & Automation* (2006), p. 3581.
- [5] M. R. Benjamin et al. “A Method for Protocol-based Collision Avoidance Between Autonomous Marine Surface Craft”. In: *Journal of Field Robotics* 23.5 (2006), pp. 333 –346.
- [6] M. R. Benjamin et al. *An Overview of MOOS-IvP and a Users Guide to the IvP Helm - Release 13.2*. Tech. rep. MIT Computer Science and Artificial Intelligence Lab, Feb. 2013.
- [7] M. R. Benjamin et al. *Extending MOOS-IvP and Users Guide to the IvPBuild Toolbox*. Tech. rep. MIT Computer Science and Artificial Intelligence Lab, 2009.
- [8] M. R. Benjamin and L. P. Adviser-Kaelbling. “Interval Programming: A Multi-Objective Optimization Model for Autonomous Vehicle Control”. PhD thesis. Brown University, 2002.
- [9] I. R. Bertaska et al. “ExperimentAl Evaluation of Approach Behavior for Autonomous Surface Vehicles”. In: *ASME 2013 Dynamic Systems and Control Conference*. American Society of Mechanical Engineers. 2013.
- [10] N. Bowditch. *The American Practical Navigator*. 2002 Bicentennial Edition. Paradise Cay Publications; 2015.
- [11] M. Breivik, V. E. Hovstein, and T. I. Fossen. “Straight-line target tracking for unmanned surface vehicles”. In: *Modeling, Identification and Control* 29.4 (2008), pp. 131–149.

- [12] S. Campbell, W. Naeem, and G. Irwin. “A Review on Improving The Autonomy of Unmanned Surface Vehicles Through Intelligent Collision Avoidance Manoeuvres”. In: *Annual Reviews in Control* 36.2 (Dec. 2012), pp. 267–283.
- [13] K.-Y. Chang, G. E. Jan, and I. Parberry. “A Method for Searching Optimal Routes With Collision Avoidance on Raster Charts”. In: *The Journal of Navigation* 56.03 (2003), pp. 371–384.
- [14] H. Choi et al. “A Reactive Collision Avoidance Algorithm for Multiple Midair Unmanned Aerial Vehicles”. In: *Transactions of the Japan Society for Aeronautical and Space Sciences* 56.1 (2013), pp. 15–24.
- [15] A. S. Clare, M. L. Cummings, and N. P. Repenning. “Influencing Trust for Human–Automation Collaborative Scheduling of Multiple Unmanned Vehicles”. In: *Human Factors: The Journal of the Human Factors and Ergonomics Society* 57.7 (2015), pp. 1208–1218.
- [16] A. S. Clare et al. “Operator object function guidance for a real-time unmanned vehicle scheduling algorithm”. In: *Journal of Aerospace Computing, Information, and Communication* 9.4 (2012), pp. 161–173.
- [17] A. N. Cockcroft and J. N. F. Lameijer. *Guide to the Collision Avoidance Rules*. Butterworth-Heinemann, 2012.
- [18] Commonwealth of Massachusetts. *Right-of-way at Intersecting Ways; Turning on Red Signals*. Part 1 Title XIV Chapter 89 Section 8.
- [19] A. R. Dahl. “Path Planning and Guidance for Marine Surface Vessels”. MA thesis. 2013.
- [20] C. D’Este et al. “Avoiding Marine Vehicles with Passive Acoustics”. In: *Journal of Field Robotics* 32.1 (2015), pp. 152–166.
- [21] I. S. Dolinskaya. “Dynamic Navigation in Direction-Dependent Environments”. In: *Advances in Dynamic Network Modeling in Complex Transportation Systems*. Springer, 2013, pp. 245–263.
- [22] I. S. Dolinskaya and A. Maggiar. “Time-optimal Trajectories With Bounded Curvature In Anisotropic Media”. In: *The International Journal of Robotics Research* 31.14 (2012), pp. 1761–1793.
- [23] L. E. Dubins. “On Curves of Minimal Length with a Constraint on Average Curvature, and with Prescribed Initial and Terminal Positions and Tangents”. In: *American Journal of Mathematics* 79.3 (1957), pp. 497–516.
- [24] M. A. Filimon. “Site Planning and On-Board Collision Avoidance Software to Optimize Autonomous Surface Craft Surveys”. MA thesis. University of Rhode Island, 2013.
- [25] W. Fillingane. *Lookout Training Handbook*. Naval Education and Training Program Management Support Activity (U.S. Navy), 1991.
- [26] P. Fiorini and Z. Shiller. “Motion Planning In Dynamic Environments Using The Relative Velocity Paradigm”. In: *IEEE Proceedings of Robotics and Automation*. May 1993, 560–565 vol.1.

- [27] P. Fiorini and Z. Shiller. “Motion Planning in Dynamic Environments Using Velocity Obstacles”. In: *International Journal of Robotics Research* 17.7 (July 1998), pp. 760–772.
- [28] M. Fisher. *Evaluation of The Vertical Sector Light Requirements for Unmanned Barges; Final Rept.* Tech. rep. US Coast Guard, 1991.
- [29] Y. Fujii and K. Tanaka. “Traffic Capacity”. In: *Journal of Navigation* 24.04 (1971), pp. 543–552.
- [30] J.-M. Godhavn. “Nonlinear Tracking of Underactuated Surface Vessels”. In: *Proceedings on Decision and Control*. Vol. 1. IEEE. 1996, pp. 975–980.
- [31] M. Greytak. “Integrated Motion Planning and Model Learning for Mobile Robots With Application To Marine Vehicles”. PhD thesis. Massachusetts Institute of Technology, 2009.
- [32] K. Hasegawa and A. Kouzuki. “Automatic Collision Avoidance System for Ships Using Fuzzy Control”. In: *Journal of the Kansai Society of Naval Architects* 205 (1987).
- [33] A. Henderson. “Murky Waters: The Legal Status of Unmanned Undersea Vehicles”. In: *Naval Law Review* (2006), pp. 55–72.
- [34] M. J. Hirsch et al. “Multi-depot Vessel Routing Problem In A Direction Dependent Wavefield”. In: *Journal of Combinatorial Optimization* 28.1 (2014), pp. 38–57.
- [35] R. R. Hoffman et al. “Trust in automation”. In: *Intelligent Systems, IEEE* 28.1 (2013), pp. 84–88.
- [36] X. Hong, C. Harris, and P. Wilson. “Autonomous Ship Collision Free Trajectory Navigation and Control Algorithms”. In: *Proceedings on Emerging Technologies and Factory Automation*. Vol. 2. 1999, 923–929 vol.2.
- [37] T. Hussain et al. “Genetic Algorithms for Ugv Navigation, Sniper Fire Localization and Unit of Action Fuel Distribution”. In: *Workshop on Military and Security Applications of Evolutionary Computation (MSAEC-2004) at GECCO-2004*. 2004.
- [38] C.-N. Hwang, J.-M. Yang, and C.-Y. Chiang. “The Design of Fuzzy Collision-Avoidance Expert System Implemented by H-Autopilot”. In: *Journal of Marine Science and Technology* 9.1 (2001), pp. 25–37.
- [39] Y. Iijima, H. Hagiwara, and H. Kasai. “Results of Collision Avoidance Manoeuvre Experiments Using A Knowledge-Based Autonomous Piloting System”. In: *Journal of Navigation* 44.02 (1991), pp. 194–204.
- [40] International Civil Aviation Organization. *Rules of the Air*. Ed. by International Civil Aviation Organization. Convention on International Civil Aviation, 2005.
- [41] M. Ito, F. Zhnng, and N. Yoshida. “Collision Avoidance Control of Ship With Genetic Algorithm”. In: *Proceedings of Control Applications*. Vol. 2. IEEE. 1999, pp. 1791–1796.

- [42] J. Jouffroy. “A Control Strategy for Steering An Autonomous Surface Sailing Vehicle In A Tacking Maneuver”. In: *IEEE International Conference on Systems, Man and Cybernetics*. IEEE. 2009, pp. 2391–2396.
- [43] D. H. Kim et al. “A New Criterion Pose and Shape of Objects for Collision Risk Estimation”. In: *International Journal of Electrical, Computer, Electronics and Communication Engineering* 7.12 (2013), pp. 1221–1225.
- [44] A. Kreutzmann et al. “Towards Safe Navigation by Formalizing Navigation Rules”. In: *TransNav: International Journal on Marine Navigation and Safety of Sea Transportation* 7.2 (2013).
- [45] Y. Kuwata et al. “Safe Maritime Autonomous Navigation With COLREGS, Using Velocity Obstacles”. In: *Oceanic Engineering, IEEE Journal of* 39.1 (2014), pp. 110–119.
- [46] Y. Kuwata et al. “Safe Maritime Navigation with COLREGS Using Velocity Obstacles”. In: *IEEE Conference on Intelligent Robots and Systems* (2011), pp. 4728–4734.
- [47] J. Larson, M. Bruch, and J. Ebken. “Autonomous Navigation and Obstacle Avoidance for Unmanned Surface Vehicles”. In: *Defense and Security Symposium*. International Society for Optics and Photonics. 2006, pp. 623007–623007.
- [48] S. M. LaValle. “Rapidly-Exploring Random Trees A New Tool for Path Planning”. In: (1998).
- [49] H.-J. Lee and K. P. Rhee. “Development of Collision Avoidance System by Using Expert System and Search Algorithm”. In: *International Shipbuilding Progress* 48.3 (2001), pp. 197–212.
- [50] Y.-i. Lee and Y.-G. Kim. “A Collision Avoidance System for Autonomous Ship Using Fuzzy Relational Products and COLREGs”. In: *Intelligent Data Engineering and Automated Learning*. Springer, 2004, pp. 247–252.
- [51] A. M. Lekkas. “Guidance and Path-Planning Systems for Autonomous Vehicles”. PhD thesis. Norwegian University of Science and Technology, 2014.
- [52] A. M. Lekkas and T. I. Fossen. “Integral LOS Path Following for Curved Paths Based on a Monotone Cubic Hermite Spline Parametrization”. In: *IEEE Transactions on Control Systems Technology* (2014).
- [53] A. M. Lekkas et al. “Continuous-Curvature Path Generation Using Fermat”. In: *Modeling, Identification and Control* (2013).
- [54] J. Leng, J. Liu, and H. Xu. “Online Path Planning Based on MILP for Unmanned Surface Vehicles”. In: *Oceans*. 2013, pp. 1–7.
- [55] Ø. A. G. Loe. “Collision Avoidance for Unmanned Surface Vehicles”. MA thesis. Norwegian University of Science and Technology, 2008.
- [56] A. Madrigal. *By The Time Your Car Goes Driverless, You Won’t Know The Difference*. npr.com. Mar. 2014.

- [57] A Miele et al. “Optimal Control of A Ship for Collision Avoidance Maneuvers”. In: *Journal of Optimization Theory and Applications* 103.3 (1999), pp. 495–519.
- [58] K. Miettinen. *Nonlinear Multiobjective Optimization*. 1st ed. Vol. 12. Springer US, 1998.
- [59] W. Naeem, G. W. Irwin, and A. Yang. “COLREGs-based Collision Avoidance Strategies for Unmanned Surface Vehicles”. English. In: *Mechatronics* 22.6, SI (2012), 669–678.
- [60] L. P. Perera, J. Carvalho, and C. Soares. “Fuzzy Logic Based Decision Making System for Collision Avoidance of Ocean Navigation Under Critical Collision Conditions”. In: *Journal of Marine Science and Technology* 16.1 (Aug. 2010), pp. 84–99.
- [61] L. P. Perera, J. Carvalho, and C. Soares. “Intelligent Ocean Navigation and Fuzzy-Bayesian Decision/Action Formulation”. In: *IEEE Journal of Oceanic Engineering* 37.2 (2012), pp. 204–219.
- [62] L. P. Perera et al. “Experimental Evaluations on Ship Autonomous Navigation and Collision Avoidance by Intelligent Guidance”. In: (2014).
- [63] A. Perez et al. “LQR-RRT*: Optimal Sampling-Based Motion Planning With Automatically Derived Extension Heuristics”. In: *IEEE International Conference on Robotics and Automation*. May 2012, pp. 2537–2542.
- [64] C. Petres et al. “Path Planning for Autonomous Underwater Vehicles”. In: *Robotics, IEEE Transactions on* 23.2 (Apr. 2007), pp. 331–341.
- [65] M. Schuster, M. Blaich, and J. Reuter. “Collision Avoidance for Vessels using a Low-Cost Radar Sensor”. In: (2014).
- [66] B. C. Shah. “Trajectory Planning with Adaptive Control Primitives for Autonomous Surface Vehicles Operating in Congested Civilian Traffic”. In: *IEEE International Conference on Intelligent Robots and Systems* (2014).
- [67] B. C. Shah et al. “Resolution-adaptive risk-aware trajectory planning for surface vehicles operating in congested civilian traffic”. English. In: *Autonomous Robots* (2015), pp. 1–25.
- [68] Z. Shiller, F. Large, and S. Sekhavat. “Motion Planning In Dynamic Environments: Obstacles Moving Along Arbitrary Trajectories”. In: *IEEE International Conference on Robotics and Automation*. Vol. 4. 2001, 3716–3721 vol.4.
- [69] R. Smierzchalski. “EvolutiOnary Trajectory Planning of Ships In Navigation Traffic Areas”. In: *Journal of Marine Science and Technology* 4.1 (1999), pp. 1–6.
- [70] J. Snape et al. “The Hybrid Reciprocal Velocity Obstacle”. English. In: *IEEE Transactions on Robotics* 27.4 (2011), 696–706.
- [71] P. Švec et al. “Dynamics-Aware Target Following for An Autonomous Surface Vehicle Operating Under COLREGs In Civilian Traffic”. In: *International Conference on Intelligent Robots and Systems*. 2013, pp. 3871–3878.

- [72] P. Švec et al. “A Simulation Based Framework for Discovering Planning Logic for Autonomous Unmanned Surface Vehicles”. In: *Conference on Engineering Systems Design and Analysis*. American Society of Mechanical Engineers. 2010, pp. 711–720.
- [73] P. Švec et al. “Target Following With Motion Prediction for Unmanned Surface Vehicle Operating In Cluttered Environments”. In: *Autonomous Robots* (2013), pp. 1–23.
- [74] P. Švec et al. “USV Trajectory Planning for Time Varying Motion Goals in an Environment With Obstacles”. In: *ASME 2012 International Design Engineering Technical Conferences and Computers and Information in Engineering Conference*. American Society of Mechanical Engineers. 2012, pp. 1297–1306.
- [75] R. Szlapczynski. “A New Method of Ship Routing on Raster Grids, With Turn Penalties and Collision Avoidance”. In: *Journal of Navigation* 59.01 (2006), pp. 27–42.
- [76] R. Szlapczynski. “Evolutionary Planning of Safe Ship Tracks in Restricted Visibility”. In: *Journal of Navigation* 68 (01 Jan. 2015), pp. 39–51.
- [77] C. Tam and R. Bucknall. “Collision Risk Assessment for Ships”. In: *Journal of Marine Science and Technology* 15.3 (2010), pp. 257–270.
- [78] C. Tam, R. Bucknall, and A. Greig. “Review of Collision Avoidance and Path Planning Methods for Ships In Close Range Encounters”. In: *Journal of Navigation* 62.03 (2009), pp. 455–476.
- [79] C. Tam et al. “Towards an Autonomous Surface Vessel”. 2014.
- [80] C. Tan, R. Sutton, and J. Chudley. “An Integrated Collision Avoidance System for Autonomous Underwater Vehicles”. In: *International Journal of Control* 80.7 (2007), pp. 1027–1049.
- [81] *Technical Characteristics for An Automatic Identification System Using Time Division Multiple Access In The VHF Maritime Mobile Band*. ITU-R M.1371-4. International Telecommunication Union (Radiocommunication Sector). Apr. 2010.
- [82] D. Thomas. *The Fatal Flaw: Collision at Sea and the Failure of the Rules*. Carmarthenshire, United Kingdom: Phaiacia, 2001.
- [83] A. Tsourdos, B. White, and M. Shanmugavel. *Cooperative Path Planning of Unmanned Aerial Vehicles*. Vol. 32. John Wiley & Sons, 2011.
- [84] United States Coast Guard. *Navigation Rules, International-Inland*. 1977-19. United States Department of Transportation, 1999.
- [85] United States Coast Guard. *Standing Orders for The Officers of The Deck (Freedom of Information Act)*. USCGC HEALY Instruction M1603.1C. June 2006.
- [86] United States Navy. *Standing Orders for USS Greeneville (Freedom of Information Act)*. USS Greeneville Instruction C3120.25. Dec. 1999.

- [87] United States Navy. *Submarine Torpedo Fire Control Manual*. Commander, Submarine Force United States Atlantic Fleet, May 1950.
- [88] U.S. Supreme Court. *Lozman v. City of Riviera Beach, Fla.* 2013.
- [89] U.S. Supreme Court. *Stewart v. Dutra Construction Co.* 543 U.S. 481. 2005.
- [90] J. Van den Berg, M. Lin, and D. Manocha. “Reciprocal Velocity Obstacles for Real-Time Multi-Agent Navigation”. English. In: *International Conference on Robotics and Automation*. IEEE, 2008, 1928–1935.
- [91] J. Wakefield. *Rolls-Royce Imagines A Future of Unmanned Ships*. BBC.com. Mar. 2014.
- [92] D. Wilkie, J. Van den Berg, and D. Manocha. “Generalized Velocity Obstacles”. In: *International Conference on Intelligent Robots and Systems*. IEEE. 2009, pp. 5573–5578.
- [93] K. L. Woerner. “COLREGS-Compliant Autonomous Collision Avoidance Using Multi-Objective Optimization with Interval Programming”. MA thesis. 77 Massachusetts Avenue, Cambridge, MA 02139: Massachusetts Institute of Technology, June 2014.
- [94] K. L. Woerner and M. R. Benjamin. “Autonomous Collision Avoidance Tradespace Analysis for High-Speed Vessels”. In: *13th International Conference on Fast Sea Transportation*. Society of Naval Architects and Marine Engineers. 2015.
- [95] K. L. Woerner and M. R. Benjamin. “Safety and Efficiency Analysis of Autonomous Collision Avoidance Using Multi-Objective Optimization with Interval Programming”. In: *Naval Engineers Journal* 126.4 (Dec. 2014), pp. 163–167.
- [96] A. Wu and J. P. How. “Guaranteed Infinite Horizon Avoidance of Unpredictable, Dynamically Constrained Obstacles”. In: *Autonomous Robots* 32.3 (2012), pp. 227–242.
- [97] Y. Xue et al. “Automatic Simulation of Ship Navigation”. In: *Ocean Engineering* 38.17–18 (2011), pp. 2290–2305.
- [98] L. Yu-Hong and S. Chao-Jian. “A Fuzzy-Neural Inference Network for Ship Collision Avoidance”. In: vol. 8. Merchant Marine Coll., Shanghai Maritime Univ., China, 2005.
- [99] A. Zekić, Đ. Mohović, and R. Mohović. “Analysis of the level of knowledge and understanding of regulations for preventing collisions at sea”. In: *Pomorstvo: Scientific Journal of Maritime Research* 29.2 (2015), pp. 143–149.
- [100] J. Zhao. “The Legal Interpretation of Keeping Course and Speed”. In: *Journal of Maritime Law & Commerce* 41 (2010), p. 85.
- [101] Y. Zhuo and K. Hasegawa. “Intelligent Collision Avoidance Control for Large Ships”. In: *International Conference on Information Science, Electronics and Electrical Engineering*. Vol. 3. IEEE. 2014, pp. 1887–1891.

- [102] R. Ziarati, C. H. Lahiry, and M. Ziarati. “Avoiding Collisions At Sea–Pareto Analysis”. In: *Marifuture* (2015).